

---

---

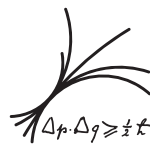
Applications of Sum-Rule Techniques in  
Quantum Chromodynamics for the  
Search of New Physics at Low Energies

Amando Hala

---

---

MAX-PLANCK-INSTITUT  
FÜR PHYSIK



München 2021





---

# Applications of Sum-Rule Techniques in Quantum Chromodynamics for the Search of New Physics at Low Energies

Amando Hala

---

Vollständiger Abdruck der von der Fakultät für Physik der Technischen Universität München zur Erlangung des akademischen Grades eines

**Doktors der Naturwissenschaften (Dr. rer. nat.)**

genehmigten Dissertation.

**Vorsitzender:**

Prof. Dr. Bastian Märkisch

**Prüfende der Dissertation:**

1. Prof. Dr. Andreas Weiler
2. TUM Junior Fellow Dr. Danny van Dyk

Die Dissertation wurde am 23.08.2021 bei der Technischen Universität München eingereicht und durch die Fakultät für Physik am 27.09.2021 angenommen.



# Abstract

Potential interactions of new physics, which violate CP- and baryon-number conservation, are investigated within an effective field theory approach. In particular, CP-violating interactions involving the Higgs boson and gluons are studied, focusing on new-physics scenarios with vanishing or strongly suppressed light-quark Yukawa couplings. The CP-violating interactions lead to three- and four-gluon operators of Weinberg type at low energies, which contribute to the electric dipole moment of the neutron. The corresponding hadronic matrix elements are calculated with the help of sum-rule techniques in QCD. Moreover, baryon-number-violating interactions that involve gravity are studied in this thesis. In this context, the sensitivity of existing and next-generation neutrino experiments in detecting a proton-decay signature with a pion, a positron and a graviton in the final state is examined. The hadronic form factors that parametrise the corresponding proton-to-pion transition are calculated by means of light-cone sum rules. The validity of the sum-rule approach is verified on the basis of a matrix element for a related but simpler decay channel which is known from lattice QCD.

# Zusammenfassung

Im Rahmen einer effektiven Feldtheorie werden potenzielle Wechselwirkungen (WW) neuer Physik untersucht, welche CP- und Baryonenzahlerhaltung verletzen. Im Fokus stehen CP-verletzende WW zwischen dem Higgsboson und Gluonen, wobei insbesondere Modelle mit sehr kleinen oder verschwindenden Yukawa-Kopplungen für leichte Quarks untersucht werden. Die CP-verletzenden WW führen bei niedrigen Energien zu Weinberg-Operatoren mit drei oder vier Gluonen, welche zum elektrischen Dipolmoment des Neutrons beitragen. Die zugehörigen hadronischen Matrixelemente werden mithilfe von Summenregeln in der QCD berechnet. Außerdem werden in dieser Arbeit gravitative WW untersucht, welche die Baryonenzahlerhaltung verletzen. Dabei wird die Sensitivität von existierenden und zukünftigen Neutrino-Experimenten bezüglich Signaturen von Protonzerfällen mit einem Pion, einem Positron und einem Graviton im Endzustand untersucht. Die hadronischen Formfaktoren, welche den Übergang vom Proton zum Pion parametrisieren, werden mithilfe von Light-Cone-Summenregeln berechnet. Die Gültigkeit des Summenregelansatzes wird anhand eines ähnlichen, aber einfacheren Matrixelements verifiziert, welches bereits in der Gittereichtheorie berechnet wurde.



# Contents

<b>Abstract</b>	<b>iii</b>
<b>Zusammenfassung</b>	<b>iii</b>
<b>List of Figures</b>	<b>vii</b>
<b>Acronyms</b>	<b>ix</b>
<b>1 Introduction</b>	<b>1</b>
<b>2 An EFT perspective on fundamental symmetries</b>	<b>7</b>
2.1 The idea of the SMEFT . . . . .	10
2.2 CP violation in the SM and beyond . . . . .	11
2.3 Baryon-number violation and proton decay . . . . .	14
2.4 EFT of gravity . . . . .	17
<b>3 QCD at hadronic scales: sum-rule techniques</b>	<b>21</b>
3.1 QCD sum rules for baryons: Ioffe's formula . . . . .	22
3.2 Sum rules for CP-violating operators of Weinberg type . . . . .	28
3.2.1 Phenomenological side of the sum rules . . . . .	29
3.2.1.1 Hadronic representation . . . . .	29
3.2.1.2 Phenomenological parametrisation . . . . .	31
3.2.2 OPE calculation for the dimension-six operator . . . . .	33
3.2.2.1 Interpolating current . . . . .	34
3.2.2.2 Weinberg contribution to the quark propagator . . . . .	34
3.2.2.3 OPE including the Weinberg operator . . . . .	38
3.2.2.4 Matching and discussion . . . . .	39
3.2.3 OPE calculation for the dimension-eight operators . . . . .	40
3.2.3.1 Weinberg contribution to the quark propagator . . . . .	41
3.2.3.2 OPE correlator, matching and discussion . . . . .	44
3.2.4 Numerical analysis . . . . .	45
3.2.4.1 Dimension-six contribution . . . . .	45
3.2.4.2 Dimension-eight contributions . . . . .	46
<b>4 LCSRs for proton decay</b>	<b>49</b>
4.1 Semi-leptonic two-body proton decay modes . . . . .	50
4.1.1 Phenomenological parametrisation . . . . .	51

## Contents

4.1.2	LCSR calculation . . . . .	53
4.1.3	Numerical analysis . . . . .	61
4.2	Semi-leptonic three-body proton decay modes . . . . .	69
4.2.1	Hadronic form factors . . . . .	69
4.2.2	Structure of the LCSRs . . . . .	72
4.2.3	Numerical analysis . . . . .	74
4.2.4	GUT-like form factors . . . . .	78
<b>5</b>	<b>Low-energy probes of CP and baryon-number violation</b>	<b>81</b>
5.1	CP-violating Higgs-gluon interactions in the limit of vanishing light-quark Yukawa couplings . . . . .	82
5.1.1	Calculation . . . . .	84
5.1.1.1	Dimension-six contribution . . . . .	85
5.1.1.2	Dimension-eight contribution . . . . .	87
5.1.2	Discussion . . . . .	88
5.2	Proton decay in the GRSMEFT . . . . .	92
<b>6</b>	<b>Conclusions</b>	<b>99</b>
<b>A</b>	<b>Fixed-point gauge</b>	<b>105</b>
<b>B</b>	<b>OPE for the quark propagator</b>	<b>107</b>
<b>C</b>	<b>Fourier transforms</b>	<b>109</b>
<b>D</b>	<b>Pion DAs</b>	<b>111</b>
<b>E</b>	<b>Analytic results of the LCSRs for two-body proton decay</b>	<b>113</b>
<b>F</b>	<b>Analytic results of the LCSRs for three-body proton decay</b>	<b>117</b>
	<b>Bibliography</b>	<b>121</b>

# List of Figures

3.1	Contributions to the neutron EDM induced by CP-violating Weinberg-type operators . . . . .	33
3.2	Contribution of the dimension-six Weinberg operator to the quark propagator . . . . .	35
3.3	One- and two-loop QCD contributions to the correlation function of the neutron EDM . . . . .	39
3.4	Contribution of the dimension-eight Weinberg operator to the quark propagator . . . . .	42
4.1	Feynman diagrams contributing to the light-cone expansion of the proton-to-pion transition matrix element . . . . .	56
4.2	Proton-to-pion transition form factor $W_{RR}^{0,S+T}(s_0, Q^2)$ as a function of the Borel mass $M$ for three values of the continuum threshold $s_0$ . . . .	63
4.3	Proton-to-pion transition form factor $W_{LR}^{1,Q}(s_0, Q^2)$ as a function of the Borel mass $M$ for three values of the continuum threshold $s_0$ . . . . .	64
4.4	Proton-to-pion transition form factors $W_{RR}^{n,\gamma}(Q^2)$ as functions of the momentum transfer $Q^2$ . . . . .	66
4.5	Proton-to-pion transition form factors $W_{LR}^{n,\gamma}(Q^2)$ as functions of the momentum transfer $Q^2$ . . . . .	67
4.6	Comparison between the results of LCSRs and an LQCD calculation for the form factors of the decay $p \rightarrow \pi^0 e^+$ . . . . .	68
4.7	Proton-to-pion transition form factors $w_n(s_0, Q^2)$ as functions of the Borel mass $M$ for three different values of the continuum threshold $s_0$ .	75
4.8	Proton-to-pion transition form factors $w_n(Q^2)$ as functions of the momentum transfer $Q^2$ . . . . .	76
4.9	Comparison of the form factors $W_{RR}^0(Q^2)$ and $W_{RR}^1(Q^2)$ of GUT-like proton decay obtained by direct calculation and indirectly through combinations of the form factors $w_n(Q^2)$ . . . . .	79

## List of Figures

5.1	Feynman diagrams with an insertion of an effective Higgs-gluon coupling giving rise to $pp \rightarrow h + 2j$ production at the LHC and an example graph contributing to the nEDM . . . . .	84
5.2	Example one- and two-loop contributions to Weinberg-type operators from dimension-six Higgs-gluon interactions . . . . .	87
5.3	Acceptance for the selection criteria imposed in searches for proton decay with final states involving a neutral pion $\pi^0$ and a positron $e^+$ as a function of the relevant phase space cut on the invariant mass of the $e^+\pi^0$ system . . . . .	96

# Acronyms

AD	Anomalous dimension
BSM	Beyond the Standard Model
CEDM	Chromo-electric dipole moment
CKM	Cabibbo–Kobayashi–Maskawa
CL	Confidence level
DA	Distribution amplitude
EDM	Electric dipole moment
eEDM	Electron EDM
EFT	Effective field theory
EM	Electromagnetic
EWSB	Electroweak symmetry breaking
GR	General relativity
GRSMEFT	EFT of gravitons and SM particles
HK	Hyper-Kamiokande
HL-LHC	High-luminosity LHC
IR	Infrared
LCSR	Light-cone sum rule
LHC	Large hadron collider
LO	Leading order
LQCD	Lattice QCD
NDA	Naive dimensional analysis
nEDM	Neutron EDM
OPE	Operator product expansion
QCD	Quantum chromodynamics
QFT	Quantum field theory
RG	Renormalisation group
RGE	Renormalisation group equation

## *Acronyms*

SK	Super-Kamiokande
SM	Standard Model
SMEFT	Standard Model effective field theory
UV	Ultraviolet
VIA	Vacuum insertion approximation

# 1 Introduction

The formulation of the Standard Model (SM) has been ground-breaking for modern particle physics. The theory is celebrated for its grand success in describing the fundamental forces in nature (in combination with general relativity (GR)) and many of its predictions have been verified ever since its proposal. In particular, collider experiments of the pre-large hadron collider (LHC) era tested the electroweak interactions of the SM at a very high degree of precision [1]. But it was not until the time of LHC physics that the Higgs boson was directly measured [2, 3] and the Yukawa interactions of the Higgs field with the heavy generations of quarks and leptons in the SM could be established experimentally [4].<sup>1</sup>

There is however ample of both theoretical and empirical motivation to hypothesise the existence of new physics beyond the SM (BSM). For instance, it is well known that gravity as described by GR, or rather the Einstein-Hilbert action, has to be augmented at sufficiently high energies, at the latest at the Planck scale. Another issue that arises in this context is the Hierarchy problem. The problem is given by the observation that the physical Higgs mass is around the electroweak scale even though quantum corrections would lead to contributions proportional to the scale of new physics, which might be as high as the Planck scale if indeed no new dynamics arises at lower energies [5–8].

But also empirical evidence points towards new physics; well-known examples are the lack of a dark matter candidate in the SM and the absence of neutrino masses which are however required to explain neutrino oscillations [9, 10]. The latter observation provides evidence of lepton-flavour violation, which cannot occur in the SM due to a global symmetry of the Lagrangian. Other symmetries of this kind exist in the SM, and they also forbid or strongly suppress processes that violate lepton- or baryon-number conservation. However, all these global symmetries arise accidentally, i.e. they are not required to obtain a consistent model, so one might naturally expect that they are broken by BSM physics at some level. But there is an even stronger motivation to look for new physics that violates fundamental symmetries in the SM than is provided by the mere possibility of its existence. In particular, baryon-number conservation and

---

<sup>1</sup>Details and references on the current experimental status of research on the Yukawa couplings of lighter quark generations are provided in Section 5.1.

## 1 Introduction

discrete symmetries like parity (P) and charge conjugation (C) play an important role in the discussion on the matter-antimatter asymmetry in the observable universe.

Today's great dominance of baryons over anti-baryons is most likely a remnant of a small imbalance in the early universe [11]. Models of baryogenesis describe a dynamical mechanism that can explain the asymmetry at present. Sakharov established three conditions that are required for successful baryogenesis [12]: First, baryon-number symmetry must be violated because otherwise the transition from a state with a net baryon number of zero to a state with a non-zero baryon number is forbidden. Second, the discrete symmetry C and the combination CP must be violated. If C and CP were exactly preserved, the relevant processes of particles *and* anti-particles would occur at the same rate, so no asymmetry could emerge if the initial state was C- or CP-symmetric. Third, the system has to depart from thermal equilibrium because otherwise, the state of the system would not change in time. These qualitative arguments are examined more rigorously in the articles [11–13]. All three conditions are actually satisfied in the SM and generic models of cosmology, but a quantitative analysis in this setup shows that the observed asymmetry cannot be fully accounted for [13, 14]. This is considered yet another proof of the existence of BSM physics. Moreover, it can be concluded that searches for new sources of CP and baryon-number violation are well motivated by the observation of the matter-antimatter asymmetry.

While strong and electromagnetic (EM) interactions separately preserve P and C, the electroweak theory violates both symmetries. But it turns out that the flavour structure of quarks in the SM, as encoded in the Cabibbo–Kobayashi–Maskawa (CKM) matrix, includes a single physical complex phase which leads to CP violation in flavour-changing interactions. The Jarlskog invariant [15] is constructed from the complex phase and other parameters of the CKM matrix, and it quantifies CP violation in a basis-independent manner. The observable turns out to be suppressed by off-diagonal CKM elements, so the amount of CP violation in the weak sector of the SM is actually small. The only other possibility of CP violation in the SM may be given by a so-called  $\theta$  term in the strong sector; however, it was experimentally established that this too would have to be a small effect (cf. Section 2.2).

Since measurable effects of CP and baryon-number violation are strongly suppressed, both symmetries can be considered to be approximately preserved in the SM. This offers a great opportunity to search for BSM physics in rare or forbidden processes: No detailed knowledge of the SM contributions is required because they are often negligible. This means that even small contributions due to new physics can be detected if the sensitivity of the experiment is high enough. In particular, low-energy experiments searching for rare and forbidden processes are known to provide powerful constraints on related BSM models [16]. Typical examples are searches for electric dipole mo-

ments (EDMs), sensitive to CP violation, and proton decay, which tests baryon-number violation. In these experiments, however, only indirect effects of new physics are probed by searching for deviations from the SM prediction in the properties of known particles. So the details of the underlying physics may not be fully revealed. Hence, by searching for such indirect effects often a wide range of BSM scenarios is tested instead of a particular model. The observation of the matter-antimatter asymmetry also provides little information on the details of the new physics since it is parametrised by only a single parameter. It is therefore very convenient to employ a model-independent approach to parametrise the effects of new physics so that no strong assumptions on the details of the underlying BSM theory are required.

A framework to study the effects of CP- and baryon-number-violating new physics at low energies necessarily involves new interactions among the SM particles, i.e. new operators, to capture virtual effects. The underlying assumption is that all new particles that could be relevant are too heavy to be produced on-shell in the experiment and they can be effectively decoupled from the particle spectrum. Then new physics either modifies the SM parameters or leads to higher-dimensional operators in the Lagrangian, i.e. operators of mass dimension larger than four, which are built from the SM fields [17]. If operators with arbitrarily high mass dimension are permitted in the Lagrangian, the theory is called an effective field theory (EFT).

Since the scattering amplitudes obtained from operators of mass dimension  $n > 4$  contain contributions that scale with energy to the power of  $n - 4$ , it is immediately clear that a theory with higher-dimensional operators can only be valid up to a certain cutoff scale. So the theory works effectively in a certain energy regime and requires ultraviolet (UV) completion above this cutoff. A typical example is the 4-Fermi theory or  $V - A$  theory of weak interactions, where four-fermion interactions are described by dimension-six operators multiplied by inverse powers of the masses of the weak gauge fields. The effective theory requires a UV completion (i.e. the theory of electroweak interactions) as the energy approaches the mass of the  $W$  boson. In contrast, the strong and electroweak interactions in the SM are renormalisable (cf. Chapter 2), and in principle, they can be employed to derive predictions at any energy scale. In practice however other subtleties may arise, e.g. at low energies where the strong interactions of quantum chromodynamics (QCD) lead to confinement.

Another interesting example of an EFT is GR. Any field in the SM interacts gravitationally, and in this work, gravity in terms of GR as an EFT will be considered to be part of the SM. It is well known that the effective quantum field theory (QFT) of gravity is non-renormalisable and requires a UV completion at the Planck scale or below. Therefore, the Planck mass naturally sets an upper limit on the validity of the SM as a theory of fundamental interactions in nature. To date, no deviations from the

## 1 Introduction

predictions of GR have been observed; on the other hand, if the theory indeed holds for energies up to the Planck scale one would not even expect to see large departures from GR at low energies because all interactions due to BSM physics would be Planck-mass suppressed. In other words, a very high experimental sensitivity would be required to probe gravitational interactions at the particle level. Various constraints on the interactions of gravitons and SM particles due to BSM physics can be derived in an EFT framework [18], but proton decay searches are expected to set the nominally strongest bounds on the associated new-physics couplings.

In order to probe new physics by means of e.g. the neutron EDM (nEDM) or proton decay searches, theory predictions for the associated low-energy observables are required. But the coupling of partons in QCD becomes strong at hadronic scales, and the parameters that can be measured are related to properties of hadrons rather than elementary fields. The scale where the perturbative expansion in powers of the strong coupling breaks down is called the QCD or confinement scale, which lies in the vicinity of 300 MeV. Predictions for the nEDM or proton decay, which are probed at energies close to the nucleon mass of about 1 GeV, rely on the knowledge of the associated hadronic matrix elements of partonic operators. However, it is not possible to calculate these matrix elements perturbatively because of large radiative corrections, i.e. non-perturbative effects are important at energies close to the QCD scale. For many of the scenarios discussed in this thesis, even numerical evaluations by means of lattice QCD (LQCD) are not available at present. Thus, other methods to derive at least estimates for the hadronic matrix elements are needed to study the effects of BSM physics on the relevant low-energy observables. Sum-rule techniques in QCD can be employed for this purpose. They permit a systematic separation of the leading perturbative and non-perturbative effects so that eventually the form factors that parametrise the hadronic matrix elements can be calculated approximately.

This work focuses on model-independent studies on new physics related to CP and baryon-number violation. In particular, the hadronic matrix elements that parametrise the BSM contributions to the nEDM as well as two- and three-body proton decay rates are studied with the help of sum-rule techniques in QCD. The thesis is structured as follows. The basics of EFTs are discussed in Chapter 2. Here, a suitable operator basis for the analyses of the subsequent chapters is identified, and an overview of the experimental probes of EDMs and proton decay modes is provided.

In Chapter 3, the methods of QCD sum rules are introduced. A simple example is studied in Section 3.1 in order to illustrate important features of the sum-rule techniques. Section 3.2 contains a more involved application. Here, the QCD sum rules are presented that describe the contributions of CP-violating dimension-six and dimension-

eight gluon operators to the nEDM. The corresponding hadronic matrix elements represent one of the leading contributions to the nEDM in models that contain new sources of CP violation in the strongly interacting sector. In Chapter 4, the hadronic matrix elements of semi-leptonic two- and three-body proton decay modes are calculated with the help of light-cone sum rules (LCSRs) in QCD. The focus is on transitions with a neutral pion and a positron in the final state since the associated decay channels are expected to be dominant in many BSM scenarios and they typically set the strongest constraints on new-physics models. Section 4.1 is about a simple two-body proton decay. The hadronic form factors that parametrise the matrix element of the corresponding proton-to-pion transition have been extensively studied in literature by means of LQCD. The LCSR predictions can thus be verified by LQCD results. Then, the same techniques are employed in Section 4.2 to estimate the form factors that parametrise semi-leptonic proton decay involving an additional graviton in the final state. These predictions are required to probe gravitational interactions of partons that violate baryon-number conservation.

Eventually, phenomenological applications of the sum-rule results are discussed in Chapter 5. In Section 5.1, CP-violating interactions of the Higgs boson and gluons induced by a dimension-six operator are examined. The Higgs-gluon couplings generate self-interactions for gluons at low energies when the Higgs particle is integrated out.<sup>2</sup> These gluonic interactions contribute to the nEDM through the hadronic matrix elements that are calculated in Section 3.2. An example of baryon-number violation due to BSM physics is discussed in Section 5.2. In particular, an effective interaction is studied, which involves gravity and leads to semi-leptonic proton decay with a graviton in the final state. Here, the LCSR results of Section 4.2 are needed to calculate the relevant hadronic matrix element. A summary and discussion of the results of Chapters 3, 4 and 5 are provided in Chapter 6.

---

<sup>2</sup>The role of other partonic operators, which are typically generated in this context, is also discussed in Section 5.1.

## 1 Introduction

This thesis is based on the following publications by the author

- [19] U. Haisch and A. Hala, *Sum rules for CP-violating operators of Weinberg type*, *JHEP* **11** (2019) 154 [1909.08955],
- [20] U. Haisch and A. Hala, *Bounds on CP-violating Higgs-gluon interactions: the case of vanishing light-quark Yukawa couplings*, *JHEP* **11** (2019) 117 [1909.09373],
- [21] U. Haisch and A. Hala, *Light-cone sum rules for proton decay*, *JHEP* **05** (2021) 258 [2103.13928],
- [22] U. Haisch and A. Hala, *Semi-leptonic three-body proton decay modes from light-cone sum rules, prepared for submission to JHEP* (2021) [2108.06111].

In particular, the results of Chapters 3, 4 and 5 were originally published in the above references, which is also indicated at the beginning of the respective sections.

## 2 An EFT perspective on fundamental symmetries

At the heart of EFTs in particle physics is the idea of describing a physical phenomenon that involves two or more scales with the help of a simple, effective theory by utilising the ratio of well-separated scales as an expansion parameter. The intuitive idea is that physical effects at very small length scales should not affect the dynamics at large distances — at least at a certain level of accuracy. Following this reasoning, an effective theory can be considered an approximation of an exact theory at a given scale, and in this sense, any theory can be regarded as an effective theory. Moreover, EFTs can even be employed if not all the details of an underlying theory are known. The lack of information about the exact theory then is reflected in the fact that free, unknown parameters occur in the expansion of the effective theory. The EFT method is particularly convenient for studying the effects of BSM physics in a bottom-up approach. The SM is then considered to be an approximation to a more fundamental theory which additionally includes new particles or new interactions or both.

All of the strong and electroweak interactions in the SM are given by renormalisable operators, i.e. operators with mass dimension smaller than or equal to four. In a renormalisable QFT, only a finite number of counterterms are needed to cure all UV divergences of loop effects. What seems to be a technical remark has, however, profound implications on the applicability of the theory. In a renormalisable theory, in principle, infinitely many predictions can be derived from a finite number of measurements, which fix the coefficients of the operators. If the Lagrangian contained non-renormalisable interactions, then all higher-dimensional operators that are allowed by the specified symmetries and field content need to be included in the theory to cancel all UV divergences (see e.g. Refs. [23, 24] for details). An EFT in particle physics by definition allows for terms of arbitrarily high mass dimension, so it contains infinitely many coefficients (parameters). Under certain conditions however, only a finite number of operators, i.e. also a finite number of coefficients, are ever relevant to obtain a prediction at the desired level of accuracy.

As an example, consider the  $V - A$  theory mentioned in Chapter 1, where the massive  $W$  boson is integrated out. Here, the dimension-six four-fermion operators of the theory

## 2 An EFT perspective on fundamental symmetries

are only the leading-order (LO) low-energy approximation to an expansion in powers of momenta divided by the heavy  $W$  mass. Similarly, the effects of BSM physics on an experimental observable, which is measured at some energy  $E$ , can typically be incorporated in terms of an expansion in powers of the ratio  $E/m_*$  or possibly  $v/m_*$  for experiments performed below the electroweak scale  $v \simeq 246$  GeV. Here,  $m_*$  is the energy scale where the dynamics of the theory change due to new physics, e.g. the mass of a heavy new particle. Hence, a separation between the new physics scale and the other relevant energy scales is required to ensure the convergence of the expansion. In other words, if the energy scale of the experiment is well below the new physics scale, only a finite number of operators is required to obtain a prediction at finite accuracy. Often, only the leading terms of the operator expansion are needed. If the EFT is obtained by integrating out heavy resonances from the particle spectrum, the theory is only valid up to energies of the lowest-lying mass scale where new particles can be produced on-shell in the experiment (see Refs. [23–25] and references therein for further reading).

An EFT description of new physics crucially relies on the concept of locality, which matches the intuition that long-distance effects can be separated from the short-range dynamics of the UV completion of the theory. Namely, the effects of heavy new physics are incorporated in the infrared (IR) regime by augmenting the Lagrangian by a series of local, higher-dimensional operators that are built from the field content of the low-energy theory. The coefficients of these higher-dimensional operators, which are referred to as Wilson coefficients, encode the short-distance effects and are a priori unknown unless they are measured or specified by the details of the underlying UV completion. In the  $V - A$  theory these can be computed from the parameters of the electroweak sector of the SM, which is the UV completion of the theory. The higher-dimensional operators themselves, or rather the scattering amplitudes computed from them, describe the long-range dynamics since they are constructed from the field content of the low energy theory.

Often, the scale dependence of amplitudes related to higher-dimensional operators is made explicit by factoring out inverse powers of an energy scale  $\Lambda$  such that the Wilson coefficients are dimensionless. Note that only the product of the dimensionless Wilson coefficient and  $1/\Lambda^n$  with an appropriate power  $n$  can be extracted from experimental data, i.e. only the coefficients of the operators as a whole can be measured. The scale  $\Lambda$  is then proportional to the new physics scale  $m_*$ , but additional factors of SM coupling constants as well as new couplings and possibly loop factors may be hidden in the Wilson coefficients and the scale  $\Lambda$ .

The EFT approach also allows the systematic treatment of problems that involve multiple scales. Many of the observables studied in this thesis are extracted from

low-energy measurements performed at hadronic scales, i.e. around the nucleon mass  $m_N \sim 1$  GeV. So between the scale of new physics  $m_*$  and the energy scale of the experiment many thresholds might occur, below which a certain particle cannot be produced on-shell. Starting from a suitable operator basis at high energies that captures the effects of new physics and contains unknown Wilson coefficients, an EFT of light fields at low energies can be obtained by making successive use of a matching procedure at each mass threshold [25]. Here, the Wilson coefficients of a low-energy theory that excludes a certain heavy particle are expressed in terms of the coefficients of the respective high-energy EFT that includes this particle. The matching is performed at the renormalisation group (RG) scale  $\mu$ , which is usually chosen near the respective mass threshold, and with the help of the RG equations (RGEs) the coefficients can be evolved down to lower energies. Hence, this approach enables us to study the effects of physics beyond the SM within the EFT framework at low energies — without detailed knowledge of the underlying UV-complete theory.

The SM EFT (SMEFT) includes all operators that can be constructed from the SM field content and that preserve the SM gauge symmetries as well as Lorentz symmetry. The main focus of this thesis concerns low-energy probes of rare and forbidden processes related to CP and baryon-number violation, where only a small subset of SMEFT operators is relevant. The experiments that test the corresponding conservation laws are sensitive enough to probe even strongly suppressed contributions of BSM scenarios. In particular, the non-conservation of baryon number is strongly constrained by state-of-the-art proton decay searches provided by the Super-Kamiokande (SK) experiment [26, 27]. Therefore, even the highly suppressed contributions of operators involving gravity can be probed in principle [18]. Although gravity can be considered to be part of the SM, gravitational effects are typically not taken into account in the construction of the SMEFT because they are suppressed by powers of the gravitational coupling and therefore often negligible. Studying gravity-associated proton decay, therefore, requires an extension of the SMEFT with couplings involving the graviton, which leads to the so-called GRSMEFT [28, 29]. The latter theory includes possible departures from GR, which can be systematically studied in the EFT approach. The EFT of gravity breaks down at the Planck mass  $M_{\text{Pl}} = 1/\sqrt{G_N} \simeq 1.22 \cdot 10^{19}$  GeV, where  $G_N \simeq 6.71 \cdot 10^{-39}$  GeV<sup>-2</sup> [30] denotes the gravitational constant; however, modifications of gravity may arise well below the Planck mass.

The goal of this chapter is to establish a systematic framework for model-independent studies of new physics related to CP violation in Higgs-gauge boson interactions on the one hand and baryon-number-violating new physics on the other hand. The chapter is structured as follows. The general idea behind the SMEFT is presented in Section 2.1. Section 2.2 is devoted to the basics of low-energy probes of CP violation and the nEDM

in particular. In Section 2.3, baryon-number violation and proton decay are discussed. In particular, the set of operators in the SMEFT that is needed to study the possible effects of new physics is identified in these sections. Finally, the basic features of the EFT of GR as well as the GRSMEFT are outlined in Section 2.4.

## 2.1 The idea of the SMEFT

The most general EFT constructed out of the SM fields that preserves the gauge symmetries  $SU(3)_C \times SU(2)_L \times U(1)_Y$  is provided by the SMEFT, where effects of BSM physics are described by higher-dimensional operators while the four-dimensional part corresponds to the SM Lagrangian. Schematically, the Lagrangian reads

$$\mathcal{L}_{\text{SMEFT}} = \mathcal{L}_{\text{SM}} + \mathcal{L}^{(5)} + \mathcal{L}^{(6)} + \dots, \quad (2.1)$$

where the ellipsis denotes operators of mass dimension higher than six. Each of the higher-dimensional parts of the Lagrangian is composed of a finite set of operators  $O_i$  and powers of the expansion parameter  $\Lambda$  according to the mass dimension  $n$ ,

$$\mathcal{L}^{(n)} = \sum_i \frac{\bar{C}_i}{\Lambda^{n-4}} O_i, \quad (2.2)$$

where the  $\bar{C}_i$  denote dimensionless Wilson coefficients. Note that only the combinations  $\bar{C}_i/\Lambda^{n-4}$  can be measured, and hence the parameters may be combined into Wilson coefficients with negative mass dimension,

$$C_i \equiv \frac{\bar{C}_i}{\Lambda^{n-4}}. \quad (2.3)$$

This notation will be employed in later chapters of this thesis. By limiting the field content to that of the SM, electroweak symmetry breaking (EWSB) by the SM Higgs mechanism is assumed; possible relaxations of this assumption are not discussed in this thesis (for further reading see Ref. [31] and references therein). At the dimension-five level only two operators exist in the SMEFT [32], which consist of two lepton doublets and two insertions of the Higgs doublet and which generate a Majorana mass for neutrinos.<sup>1</sup> Most scenarios of BSM physics discussed in this thesis rely on the dimension-six basis of the SMEFT, which already comprises 84 independent operators [32–36] (a discussion on the systematic construction of the operator basis is provided in the Refs. [37, 38]).<sup>2</sup> However, only a subset of the operators in the SMEFT is relevant

---

<sup>1</sup>Note that equivalent operators for different fermion generations are counted as one here. However, operators that are related by hermitian conjugation are counted separately. In parts of the literature, fewer operators are quoted at the various levels of mass dimension because hermitian conjugates of operators are not counted separately.

<sup>2</sup>Note that the list provided in Ref. [35] contains redundant operators, which are removed in Ref. [36].

for a specific process. The power of the SMEFT lies in the fact that it systematically encodes the effects of new physics on observables in terms of the Wilson coefficients. As the EFT works without detailed knowledge of the new physics, a large number of new theories can be explored by studying once the effects of those operators that contain the relevant field content and have appropriate symmetry properties. Moreover, the relative significance of different experimental probes for the underlying new-physics model can be efficiently assessed with the help of the SMEFT.

Some of the Wilson coefficients in the EFT may however contribute to the same observable. Then only a combination of the coefficients can be constrained by measuring the observable but not each of them individually. The parameter space is said to have a flat or weakly bound direction in this case, and certain details of the UV physics cannot be resolved. This happens for instance when studying CP-violating interactions between the SM Higgs and gauge fields with the help of an EFT approach. As a solution in this particular case, low-energy probes can be combined with collider searches [39], which respectively probe different combinations of the relevant Wilson coefficients. A more detailed discussion on this topic is provided in Section 5.1 of this thesis.

## 2.2 CP violation in the SM and beyond

The CPT theorem states that any operator in a local and Lorentz invariant QFT is invariant under the combined transformation of charge conjugation C, parity P and time reversal T [40, 41]; see Section 4.3 of Ref. [42] for a proof. The theorem agrees with all observations at present, and it directly follows that CP is actually equivalent to time reversal, since  $CPT = 1$ . In the SM, CP is violated by the complex phase of the CKM matrix, which also parametrises non-diagonal, i.e. flavour-changing, weak interactions among the quarks after EWSB. But there is another source of CP violation that is permitted by the SM symmetries, which is the strong CP phase  $\bar{\theta}$  in QCD. In particular, the SM Lagrangian admits a bare  $\theta$  term,

$$\mathcal{L}_\theta = \theta \frac{g_s^2}{32\pi^2} \epsilon^{\mu\nu\rho\sigma} G_{\mu\nu}^A G_{\rho\sigma}^A, \quad (2.4)$$

where  $G_{\mu\nu}^A$  denotes the gluon field-strength tensor,  $g_s$  is the strong coupling constant and  $\epsilon^{\mu\nu\rho\sigma}$  is the Levi-Civita symbol with  $\epsilon^{0123} = +1$ . The bare  $\theta$  term can however receive an additional contribution from the phase of chiral rotations in the up- and down-quark Yukawa sector due to the axial anomaly. Only a combination of the latter phase and the bare  $\theta$  parameter that is invariant under chiral rotations can be physical; such a combination is provided by

$$\bar{\theta} = \theta + \text{Arg det}(Y_d Y_u), \quad (2.5)$$

## 2 An EFT perspective on fundamental symmetries

where  $Y_u$  and  $Y_d$  denote the up- and down-quark Yukawa matrices. It should be noted at this point that one can also write down bare  $\theta$ -like terms for the electroweak gauge fields. These, however, can be removed by chiral rotations, and thus they are basis-dependent and therefore unphysical. The strong CP phase is severely constrained by searches for the nEDM  $d_n$ . By naive dimensional analysis (NDA) one obtains the estimate [43]

$$\frac{d_n}{e} \sim \bar{\theta} \frac{m_{\text{red}}}{\Lambda_{\text{had}}^2}, \quad (2.6)$$

where  $e$  is the elementary charge,  $\Lambda_{\text{had}} \sim 1$  GeV denotes the hadronic scale and  $m_{\text{red}} = m_u m_d / (m_u + m_d)$  is the reduced quark mass with  $m_u$  and  $m_d$  the up- and down-quark masses. By employing the numerical values for the light-quark masses evaluated at 1 GeV in the  $\overline{\text{MS}}$ -scheme provided in Ref. [30], the reduced mass is given by  $m_{\text{red}} \simeq 2$  MeV.

Experimentally, the strongest bounds on the magnitude of the nEDM come from measurements with ultracold neutrons, which are exposed to an electric and a magnetic field [44–47]. While the magnetic field is fixed, the electric field is alternated between a parallel and an anti-parallel orientation compared to the magnetic field. The shift in the frequency of the Larmor precession of the neutron spin polarisation about the direction of the external fields is proportional to the EDM and can be determined experimentally. This yields an upper bound on the magnitude of the nEDM of [44–46]

$$\frac{|d_n|}{e} < 2.2 \cdot 10^{-26} \text{ cm} \quad (2.7)$$

at 95% confidence level (CL). The SM prediction for the nEDM due to the complex phase in the Yukawa sector is CKM and loop suppressed, which yields a tiny value of about  $d_n^{\text{CKM}}/e \sim 10^{-32}$  cm [48]. This contribution can be neglected and thus the experimental constraint can be readily translated into a bound on the strong CP phase of  $|\bar{\theta}| \lesssim 6 \cdot 10^{-10}$ . This requires a strong tuning in the combination (2.5), which is surprising — even more so if potentially large corrections due to yet unknown additional sources of CP violation at high scales are taken into consideration. This constitutes the strong CP problem. The tuning in  $\bar{\theta}$  may arise accidentally, but one might expect a more natural explanation where this parameter is dynamically turned to zero, e.g. by a mechanism of the Peccei–Quinn type [49–51] (for further reading see Refs. [43, 52] and references therein).

The discussion on the strong CP phase nicely illustrates the power of experimental low-energy searches for EDMs in testing flavour-diagonal CP violation. In general, together with the nEDM constraint (2.7), the strongest EDM limits at present are set by measurements of the electron spin precession in thorium monoxide [53, 54] and the mercury atom [55, 56]. These searches are known to place stringent constraints on a

wide range of BSM scenarios with additional sources of CP violation (see also [39, 43, 52, 57–76] for reviews and recent discussions). For systematic, model-independent studies the EFT approach can be employed.

The largest contributions to the EDMs from higher-dimensional operators in the SMEFT are expected to arise at the dimension-six level (before EWSB). But EDMs are typically measured at low energies so that it is often more convenient to work with an EFT where also the massive gauge fields, the Higgs field and the heavy fermions of the SM have been integrated out. In this case one can distinguish between operators including and excluding fermions; the former read [43]

$$\mathcal{L}_{\text{CP-odd}} \supset -\frac{i}{2} \sum_{\psi=u,d,s,e,\mu} d_\psi \bar{\psi} \sigma_{\mu\nu} \gamma_5 \psi F^{\mu\nu} - \frac{i}{2} \sum_{\psi=u,d,s} \tilde{d}_\psi \bar{\psi} \sigma_{\mu\nu} \gamma_5 \psi G^{\mu\nu} + \mathcal{L}_{4F}, \quad (2.8)$$

where  $\sigma^{\mu\nu} = i/2(\gamma^\mu \gamma^\nu - \gamma^\nu \gamma^\mu)$ ,  $F^{\mu\nu}$  denotes the EM field strength tensor and  $G_{\mu\nu} = G_{\mu\nu}^A T^A$  with  $T^A$  the  $SU(3)$  generators. The parameters  $d_\psi$  with  $\psi = u, d, s, e, \mu$  respectively denote the EDMs of the up-quark  $u$ , down-quark  $d$ , strange-quark  $s$ , the electron  $e$  and the muon  $\mu$ . The chromo-electric dipole moments (CEDMs) of the light quarks are given by  $\tilde{d}_\psi$ , and  $\mathcal{L}_{4F}$  denotes numerous four-fermion operators of mass dimension six constructed out of the light fermions. The latter operators are often neglected because they require two flips of chirality which typically originates from dimension-eight operators [43]. At the dimension-six level, also a pure gauge operator exists, the so-called Weinberg operator, and even dimension-eight operators of Weinberg type may be relevant in certain applications (cf. Sections 3.2 and 5.1 as well as Refs. [19, 20]). The relevant interactions are [77–82]

$$\begin{aligned} \mathcal{L}_{\text{CP-odd}} \supset & -\frac{g_s}{3} C_{3\tilde{G}} f^{ABC} \tilde{G}_{\mu\nu}^A G^{B\nu\rho} G_\rho^C{}^\mu \\ & -\frac{g_s^2}{12} \sum_{m=1}^3 C_{4\tilde{G},m} c_m^{ABCD} \tilde{G}_{\mu\nu}^A G^{B\mu\nu} G_{\rho\lambda}^C G^{D\rho\lambda}, \end{aligned} \quad (2.9)$$

where  $\tilde{G}^{A\mu\nu} = 1/2 \epsilon^{\mu\nu\rho\lambda} G_{\rho\lambda}^A$  denotes the dual of the gluon field strength tensor and  $f^{ABC}$  are the fully anti-symmetric structure constants of  $SU(3)_C$ . The colour structure of the dimension-eight operators is given by

$$c_m^{ABCD} = \{ \delta^{AB} \delta^{CD}, \delta^{AC} \delta^{BD}, d^{ABE} d^{CDE} \}, \quad (2.10)$$

where

$$d^{ABC} = 2 \text{Tr} [T^A \{T^B, T^C\}] \quad (2.11)$$

denotes totally symmetric constants.

At energies close to the QCD scale  $\Lambda_{\text{QCD}} \sim 300$  MeV, hadrons populate the particle spectrum. When studying the EDMs of atoms or molecules, atomic and nuclear interactions need to be taken into account in addition to partonic EDM contributions; see

Refs. [70, 83, 84] for reviews. The nEDM however allows direct access to CP violation at the parton level. One of the main goals of this thesis is to explore the contributions of pure-gluon operators to the nEDM,

$$\mathcal{L}_{\text{hadronic}} \supset -\frac{i}{2} d_n \bar{n} \sigma_{\mu\nu} \gamma_5 n F^{\mu\nu}, \quad (2.12)$$

where  $n$  is the neutron field. The contributions of pure-gluon as well as quark-gluon operators to the nEDM involve non-perturbative physics because the typical energy scale of the problem is given by the neutron mass of about 1 GeV. While the thorium monoxide measurements can be interpreted as a probe of the electron EDM (eEDM) with small theoretical uncertainties [85, 86], nucleon, nuclear and diamagnetic EDMs receive contributions from several effective operators that are plagued by theoretical uncertainties of different sizes. For instance, the EDM contributions from down and up quarks to the nEDM have been calculated with an accuracy of  $\mathcal{O}(5\%)$  using LQCD [87–89], while sum-rule calculations [90–92] can be used to determine the nEDM contributions from the down-quark and up-quark CEDMs with uncertainties of  $\mathcal{O}(50\%)$ . To date, only estimates of the hadronic matrix element of the leading operator of Weinberg type exist. These rely on either NDA [77], the vacuum insertion approximation (VIA) [93] or sum rules [94]. The resulting uncertainties are hard to quantify but are commonly said to be of  $\mathcal{O}(100\%)$ . LQCD computations of the contributions of the CEDMs and the leading Weinberg operator have gained significant momentum in recent years [95–102], and considering the ongoing efforts by several LQCD groups, calculations with uncertainties similar to those of the sum-rule estimates may be achievable within the next five years [103, 104]. To fully exploit the expected increase in sensitivity of future EDM searches (see for instance [105–107] for discussions), improved calculations of the hadronic matrix elements of CEDMs and Weinberg-type operators are direly needed. This is the subject of Section 3.2.

## 2.3 Baryon-number violation and proton decay

The idea of a symmetry that ensures the stability of the proton has a rather long history, and it was referenced already in the first half of the 20th century [108, 109]. Baryon number is preserved at the classical level in the SM, where baryon-number conservation accidentally arises in the form a global symmetry. Baryon number as well as lepton number are however anomalous, and they are broken by non-perturbative effects [110]. While instanton-like transitions between degenerate vacua are suppressed by the tunnelling amplitude, which is proportional to  $\exp(-8\pi^2/g^2) \sim 10^{-84}$  with  $g \simeq 0.64$  the  $SU(2)_L$  gauge coupling constant, sphaleron processes may have occurred frequently in the early universe, and they play an important role in models of baryogenesis [11–13].

### 2.3 Baryon-number violation and proton decay

Baryon and lepton number both change by three units in anomaly-related processes in the SM [110] so that the proton is stable (and the difference between baryon and lepton number is preserved).

Considering baryon-number violation at the perturbative level, however, is well motivated by theories of grand unification (GUTs) [111, 112], supersymmetric theories [113–115], models of baryogenesis [11, 12] and more generally in theories of quantum gravity, where the global symmetries of the SM are expected to be broken at some level [116, 117]. In the case of GUTs, baryon number is typically violated by tree-level interactions, and proton decay is mediated by the massive gauge fields of the spontaneously broken unified gauge group [118–121]. On the experimental side, searches for simple proton decay channels, such as decays into a pseudoscalar meson and an anti-lepton, provide very strong constraints on the proton lifetime of  $\tau_p \gtrsim 10^{34}$  years [122]. These bounds can be used to probe theories that predict proton decay up to extremely high energy scales, thereby putting severe constraints on the scale of unification.

The discussion of proton decay can be put on a more systematic footing in a model-independent manner by using the relevant set of lowest-dimensional operators of the SMEFT. There are four types of operators at the dimension-six level that violate baryon number and lead to proton decay [32–34]. GUTs provide a variety of predictions for decay widths that involve flavour-changing interactions, but the following discussion is restricted to the first generation of quarks and leptons because the decay channel of a proton ( $p$ ) into a neutral pion ( $\pi^0$ ) and a positron ( $e^+$ ) is expected to be dominant in many scenarios (compared to processes involving heavier mesons and neutrinos) [118–121], and the most stringent bounds on the proton lifetime arise from probes of this channel [123–125]. The relevant low-energy effective Lagrangian reads

$$\mathcal{L}_{\mathcal{B}}^{(6)} = \sum_{\Gamma, \Gamma'} c_{\Gamma\Gamma'} \mathcal{O}_{\Gamma\Gamma'} = \sum_{\Gamma, \Gamma'} c_{\Gamma\Gamma'} \epsilon^{abc} (d_a^T C P_{\Gamma} u_b) (e^T C P_{\Gamma'} u_c) , \quad (2.13)$$

where  $C$  is the charge conjugation matrix,  $T$  denotes the transpose of the Dirac or spinor index, the symbols  $P_{\Gamma, \Gamma'}$  denote the left- and right-chiral projectors  $P_L$  and  $P_R$  such that  $\Gamma$  ( $\Gamma'$ ) denotes the chirality of the first (second) fermion bilinear,  $\epsilon^{abc}$  is the fully antisymmetric Levi-Civita symbol and  $a, b, c$  are colour indices. We consider all possible chirality combinations of the interaction (2.13) in order to provide a model-independent analysis. Note that the Wilson coefficients  $c_{\Gamma\Gamma'}$ , which encode short-distance physics, have a mass dimension of  $-2$ .

The strongest bound on the proton lifetime  $\tau_p$  is set by the SK experiment [26, 27] for the decay channel  $p \rightarrow \pi^0 e^+$  which is given by [122]

$$\frac{\tau_p}{B(p \rightarrow \pi^0 e^+)} > 2.4 \cdot 10^{34} \text{ yr} \quad (2.14)$$

at the 90% CL, where  $B(p \rightarrow \pi^0 e^+)$  denotes the branching ratio of the channel. The SK water Cherenkov detector is located underground in Japan for shielding against cosmic ray muons. The water tank of SK is covered with inward- and outward-facing arrays of photomultiplier tubes. The inner detector can measure the Cherenkov light produced within the detector, and events from particles entering the detector from the outside can be discriminated with the help of the outer detector; for details see Ref. [26]. The most dominant source of background for the pion-positron channel comes from interactions of atmospheric neutrinos with the water molecules inside the detector [126]. Information on the underlying event is extracted from the size, shape and orientation of the Cherenkov light pattern. The Cherenkov light-cone of highly energetic particles produces a signal of ring-like shape on the array of photomultiplier tubes of the inner detector. Low-mass particles like electrons and photons produce EM showers while heavier particles like the muon do not so that all of the detected Cherenkov light comes from the original particle in the latter case. Therefore, muons produce sharper rings which allows us to distinguish between  $e$ -like and  $\mu$ -like events [126, 127]. The final state pion decays into two photons in about 99% of the cases [30] and hence can be measured by the same means.

Deriving constraints on models that predict proton decay induced by the operators (2.13) requires a theoretical prediction for the widths of semi-leptonic proton decay channels such as  $p \rightarrow \pi^0 e^+$ , which in turn relies on the knowledge of the hadronic matrix element of the underlying proton-to-meson transition. Experiments such as SK attempt to measure the decay products of protons that are approximately at rest, and thus the relevant energy scale for the hadronic transition is given by the proton mass. A perturbative description of the relevant hadronic matrix elements in QCD is not possible at this energy scale because of large radiative corrections due to the exchange of soft gluons. A prediction for the hadronic matrix elements by other means is therefore required to probe baryon-number-violating new physics with the help of experimental data from proton decay searches.

Moreover, experimental bounds are today available for a broad range of baryon-number-violating processes [123–125]. In particular, inclusive proton decay searches for processes like  $p \rightarrow \pi^0 \ell^+ + X$  might be of interest if baryon-number violation does not become manifest in a simple two-body decay. For example, the case where  $X$  is a graviton may provide relevant constraints on theories where baryon-number violation occurs in connection with gravity such as in the GRSMEFT. LQCD results are not available for processes of this kind, which raises the question: how can one obtain estimates of the proton lifetime in such cases? This issue is addressed in Chapter 4 with the help of LCSR techniques. A short description of an EFT framework including gravitational effects is provided in the following section.

## 2.4 EFT of gravity

An effective description of the classical phenomena as well as the quantum effects of gravity at low energies is naturally provided by the EFT framework [128]. Gravity as an EFT should reproduce GR in the classical limit, and therefore a convenient way to construct such an EFT is by quantising GR for weak gravitational fields. This topic has been reviewed many times, see e.g. [129–133], so only some key features will be presented in the following in order to clarify the terminology and conventions. Possible extensions due to BSM physics are discussed later on in this section.

The starting point for the EFT of gravity is the action of GR, that is the Einstein-Hilbert term augmented by a matter Lagrangian  $\mathcal{L}_m$ ,

$$S_g = \frac{2}{\kappa^2} \int d^4x \sqrt{-g} [R + \mathcal{L}_m] \quad (2.15)$$

where  $g$  is the determinant of the metric tensor  $g_{\mu\nu}$ ,  $R$  is the Ricci scalar and  $\kappa = 2/\bar{M}_{\text{Pl}}$  with  $\bar{M}_{\text{Pl}} = 1/\sqrt{8\pi G_N} \simeq 2.435 \cdot 10^{18}$  GeV the reduced Planck mass. Here and in the following, the cosmological constant term is neglected. The equations of motion for this choice of the action correspond to the Einstein field equations,

$$R_{\mu\nu} - \frac{1}{2}g_{\mu\nu}R = -8\pi G_N T_{\mu\nu}, \quad (2.16)$$

where  $R_{\mu\nu}$  is the Ricci tensor and the energy-momentum tensor  $T_{\mu\nu}$  is defined by the variation of the matter action  $S_m = 2/\kappa^2 \int d^4x \sqrt{-g} \mathcal{L}_m$ ,

$$\delta S_m = -\frac{1}{2} \int d^4x \sqrt{-g(x)} T^{\mu\nu}(x) \delta g_{\mu\nu}(x). \quad (2.17)$$

The graviton field operator  $h_{\mu\nu}(x)$  is obtained by quantising linear perturbations around Minkowski spacetime  $\eta = \text{diag}(+1, -1, -1, -1)$  for a weak gravitational field,

$$g_{\mu\nu}(x) = \eta_{\mu\nu} + \kappa h_{\mu\nu}(x), \quad g^{\mu\nu}(x) = \eta^{\mu\nu} - \kappa h^{\mu\nu} + \mathcal{O}(\kappa^2 h^2). \quad (2.18)$$

The hence obtained EFT of gravity has a gauge symmetry under which the graviton field in the weak field limit transforms as

$$h_{\mu\nu}(x) \rightarrow h'_{\mu\nu}(x') = h_{\mu\nu}(x) - \partial_\mu \xi_\nu - \partial_\nu \xi_\mu, \quad (2.19)$$

with  $x'^\mu = x^\mu + \kappa \xi^\mu(x)$  and  $\xi^\mu(x)$  infinitesimal. The gauge is fixed in the following by choosing the de Donder or harmonic gauge,

$$\partial_\mu h^\mu_\nu = \frac{1}{2} \partial_\nu h, \quad (2.20)$$

where  $h \equiv h^\mu_\mu$ . Quantising GR leads to a non-renormalisable theory because quantum corrections give rise to higher-dimensional operators in pure gravity [134–137] but also

for gravity-matter couplings [134, 135, 138–140]. Hence it is a natural example of an EFT, which breaks down at  $1/\kappa$ , so a UV completion of GR is required to describe gravity at and beyond the Planck scale.

But departures from GR may arise at energies well below the Planck mass; in particular, little is known about gravitational interactions at the particle level because direct experimental probes are typically not sensitive enough to measure Planck-mass suppressed interactions. In order to study the imprints of possible deviations from GR due to new physics, the LO terms in the Einstein-Hilbert action (2.15) need to be augmented by higher-dimensional interactions in the EFT. The most general EFT of gravitons and SM fields including pure gravity terms as well as all potential matter couplings, which can be generated by BSM physics, is called GRSMEFT [28, 29]. It can be used to systematically study departures from GR in a bottom-up approach, i.e. in a model-independent fashion. In order to construct the GRSMEFT, it suffices to consider higher-dimensional operators that involve the Weyl tensor, which transforms in an irreducible representation of the Lorentz group (in contrast to the Riemann tensor  $R_{\mu\nu\rho\sigma}$  which is reducible). All occurrences of the Ricci scalar and the Ricci tensor can be removed by field redefinitions of the metric [28]. Corrections to the Lagrangian (2.15) due to higher-dimensional operators arise at mass dimension six and higher. The phenomenology of all matter interactions at the dimension-six level as well some dimension-eight operators in the GRSMEFT is studied in Ref. [18].

A promising attempt to probe some of the gravitational interactions at the particle level is to study rare and forbidden processes. Particularly strong experimental constraints on the new-physics couplings of the GRSMEFT come from proton decay searches [18, 22]. The most relevant proton decay channel that involves a graviton  $G$  is  $p \rightarrow \pi^0 e^+ G$ .<sup>3</sup> Phenomenologically, this decay mode would lead to a final state with a positron, two photons from the decaying pion and missing energy because the graviton escapes undetected, but no experimental searches for this kind of signature exist. Nevertheless, constraints for related signatures can be employed to test the relevant operator in the GRSMEFT; and a detailed discussion of the corresponding experimental searches is postponed to Section 5.2.

Considering the case of one generation of fermions, baryon-number violation is induced by only a single dimension-eight operator in the GRSMEFT [28, 29]. We write this operator in the following way

$$\mathcal{L}_{\mathcal{B}}^{(8)} = c_{\mathcal{B}} \epsilon^{abc} (d_a^T C \sigma^{\mu\nu} P_R u_b) (e^T C \sigma^{\rho\sigma} P_R u_c) C_{\mu\nu\rho\sigma} + \text{h.c.}, \quad (2.21)$$

---

<sup>3</sup>Note that the two-body transition  $p \rightarrow e^+ G$  is forbidden by angular momentum conservation.

where the notation is similar to the previous sections. Here,  $C_{\mu\nu\rho\sigma}$  represents the Weyl tensor which is the traceless part of the Riemann tensor  $R_{\mu\nu\rho\sigma}$ . It takes the form

$$C_{\mu\nu\rho\sigma} = R_{\mu\nu\rho\sigma} - (g_{\mu[\rho}R_{\sigma]\nu} - g_{\nu[\rho}R_{\sigma]\mu}) + \frac{1}{3}g_{\mu[\rho}g_{\sigma]\nu}R, \quad (2.22)$$

where the brackets denote index anti-symmetrisation, i.e.  $X_{[\mu}Y_{\nu]} = (X_{\mu}Y_{\nu} - X_{\nu}Y_{\mu})/2$ . Notice that the Wilson coefficient  $c_{\mathcal{B}}$  entering (2.21) carries mass dimension  $-4$ .

The challenge when computing decay rates due to the interaction (2.21) is once again given by the fact that the hadronic transition for the semi-leptonic decay involves non-perturbative effects. As mentioned at the end of the previous section, LCSR techniques can be employed to derive estimates on the form factors that parametrise the matrix element. The computation follows the procedure that is employed for the two-body proton decay, and the details are spelled out in Chapter 4 and in particular Section 4.2. Eventually, these results are applied in Section 5.2 for studying the phenomenology of proton decay in the GRSMEFT.



### 3 QCD at hadronic scales: sum-rule techniques

The effects of new physics on hadronic properties in low-energy experiments can be systematically studied with the help of the EFT approach. But how do the new interactions, that are introduced in Chapter 2 in terms of higher-dimensional operators, contribute to observables at hadronic energy scales? The problem is that non-perturbative effects become important in QCD at energies of a few GeV, i.e. close to the confinement scale  $\Lambda_{\text{QCD}}$ . Sum-rule techniques in QCD address this issue, and they enable us to encode a systematic separation of the short-range quark-gluon interactions and soft, non-perturbative effects. The former can be calculated perturbatively in QCD while the latter have to be determined by other means.

The central objects in sum-rule calculations are correlation functions of hadronic currents. These currents interpolate between the asymptotic incoming and outgoing states of the hadrons. The correlation functions or correlators are chosen such that they can be related to the relevant hadronic matrix element of a physical process, but they are evaluated at large virtualities. Formally the separation of long- and short-distance effects is implemented with the help of an operator product expansion (OPE). The short-range interactions are computed in QCD while the long-range interactions are captured in terms of vacuum condensates or light-cone distribution amplitudes (DAs). These non-perturbative objects must be provided as external input to the sum rules, which typically comes from either other sum-rule calculations, LQCD computations or experimental results. The hence obtained QCD result is then matched on a sum over hadronic states that provides an alternative description of the correlation function. This matching leads to sum rules that relate the contributions of partonic operators to hadronic properties.

The advantage of the sum rules is that the non-perturbative interactions inside the hadrons do not need to be modelled explicitly because the OPE systematically encodes them in terms of known objects (at large virtualities). The accuracy of the sum-rule approach is however limited because of two reasons. First, the sum rules can be computed only up to a finite order in the OPE as well as in the  $\alpha_s$  expansion. Radiative corrections may be particularly significant in applications for the nucleon

### 3 QCD at hadronic scales: sum-rule techniques

where the renormalisation scale is often close to the confinement scale. Second, the sum over hadronic states contains not just the ground state of a hadronic resonance but also heavier excited and multiparticle states with the same quantum numbers as the ground state. The sum rules are constructed such that heavier states are typically suppressed, but their contributions can be modelled only approximately. These two sources of uncertainty are typically reflected in the fact that the sum rules depend on certain unphysical parameters that are introduced in the calculation. Therefore, one usually tries to minimise the dependence on such parameters as described in the following sections, but in general this constitutes a source of systematic uncertainty, and the size of the corresponding error can only be estimated.

Despite these restrictions, many fruitful applications exist which employ one of the two common versions of the sum rules: QCD sum rules (aka SVZ sum rules), which were introduced by Shifman, Vainshtein and Zakharov [141], and LCSRs [142–147] which also incorporate the concepts of hard exclusive processes [148–154]. In the following section, basic concepts of QCD sum rules are introduced, and a more involved application is discussed in Section 3.2 where the contributions of pure-gluon operators to the nEDM are discussed. The results that are presented in Section 3.2 were originally published in the article [19]. Applications of the LCSR approach are discussed separately in Chapter 4.

#### 3.1 QCD sum rules for baryons: Ioffe’s formula

Before discussing a more involved application in the following section, Ioffe’s formula for the nucleon mass [155] is derived in order to illustrate some of the basic features of sum-rule techniques. The nucleon mass  $m_N$  can be extracted from the propagator, which is related to the two-point correlation function  $\Pi_{2\text{-pt}}$ ,

$$\Pi_{2\text{-pt}} = i \int d^4x e^{ipx} \langle 0 | T [\eta_N(x) \bar{\eta}_N(0)] | 0 \rangle . \quad (3.1)$$

Here  $T$  denotes the time-ordering operator,  $\eta_N(x)$  denotes an interpolating current for the nucleon evaluated at the spacetime point  $x$ ,  $p$  is the nucleon’s momentum and  $|0\rangle$  represents the QCD vacuum. The exact partonic structure of the nucleon is not known, but the current  $\eta_N$  is chosen such that it overlaps with the physical nucleon state  $|N(p)\rangle$ ,

$$\langle 0 | \eta_N(x) | N(p) \rangle = \lambda_N u_N(p) e^{-ipx} . \quad (3.2)$$

where  $\lambda_N$  quantifies the coupling strength between the current and the physical state,  $u_N(p)$  is the polarisation spinor of the nucleon and the spin of the nucleon is left implicit. Next, a complete set of intermediate states is inserted into the correlator by making

use of the completeness relation

$$\mathbb{1} = \sum_{N'} |N'\rangle \langle N'|, \quad (3.3)$$

where the sum extends over all single and multi-particle states that have the quantum numbers of the nucleon  $N$  including a summation over their spin and the integration is over the momenta  $k$  of the particles. Factors of the integration measure,  $d^3k/(2k^0(2\pi)^3)$ , are not denoted explicitly in the above formula. Note that excitations of the nucleon with both positive and negative parity occur in the sum. By separating the ground state from contributions of the heavier excited states and the continuum one obtains

$$\begin{aligned} \Pi_{2\text{-pt}} &= i\lambda_N^2 \int d^4x \frac{\bar{d}^3k}{2k^0} e^{ipx} \\ &\times \left[ \theta(x^0) (\not{k} + m_N) e^{-ikx} - \theta(-x^0) (\not{k} - m_N) e^{ikx} \right] + \dots, \end{aligned} \quad (3.4)$$

where  $\bar{d}k \equiv dk/(2\pi)$  and the ellipsis denotes the contributions of heavier states. The Heaviside step functions  $\theta(x^0)$  and  $\theta(-x^0)$  arise due to time ordering; the standard treatment of these functions is outlined e.g. in Section 10.2 of Ref. [156] or Section 3.6 of [157]. The procedure is nevertheless summarised in the following because it can be applied to the non-standard applications in the following sections, as well. The basic idea is to use the integral representation of the Heaviside function,

$$\theta(x^0) = \lim_{\epsilon \rightarrow 0^+} \int_{-\infty}^{\infty} \frac{d\tau}{2\pi i} \frac{e^{i\tau x^0}}{\tau - i\epsilon}, \quad (3.5)$$

and to use  $\bar{d}^3k/(2k^0) \exp(ikx) = 2\pi \bar{d}^4k \delta(k^2 - m_N^2) \theta(k^0) \exp(ikx)$ . For a function  $f(k^0, \vec{k})$  of the momentum  $k = (k^0, \vec{k})^T$  one obtains

$$\begin{aligned} \int \frac{\bar{d}^3k}{2k^0} e^{-ikx} \theta(x^0) f(k^0, \vec{k}) &= \\ &= -i \int \bar{d}^4k d\tau \delta((k^0 + \tau)^2 - \vec{k}^2 - m_N^2) \theta(k^0 + m_N) \frac{e^{-ikx}}{\tau - i\epsilon} f(k^0 + \tau, \vec{k}) \\ &= i \int \bar{d}^4k f(E_k, \vec{k}) \frac{e^{-ikx}}{2E_k(k^0 - E_k + i\epsilon)} \end{aligned} \quad (3.6)$$

where the shift  $k^0 \rightarrow k^0 + \tau$  is applied to remove  $\tau$  from the exponent in the first step, the Dirac delta function and the remaining Heaviside function are used to perform the  $\tau$  integration in the second step and  $E_k = (\vec{k}^2 + m_N^2)^{1/2}$ . Similarly, the second term is written as

$$\int \frac{\bar{d}^3k}{2k^0} e^{ikx} \theta(-x^0) f(k^0, \vec{k}) = -i \int \bar{d}^4k f(-E_k, -\vec{k}) \frac{e^{-ikx}}{2E_k(k^0 + E_k + i\epsilon)}. \quad (3.7)$$

### 3 QCD at hadronic scales: sum-rule techniques

Hence one arrives at

$$\Pi_{2\text{-pt}} = -\lambda_N^2 \frac{\not{p} + m_N}{p^2 - m_N^2 + i\epsilon} + \dots, \quad (3.8)$$

where the pole of the ground state is now explicit. Excited and multi-particle states, which are denoted by the ellipsis, lead to additional poles and branch cuts at larger values of  $p^2$ . Ideally, the sum rules are constructed such that the contributions of heavier states are small compared to the contribution of the ground state. This topic will be addressed later.

When studying correlators related to proton decay in the context of LCSRs in Chapter 4, only the positive energy solutions contribute to the hadronic representation. In this case, the ground-state contribution can be parametrised by employing the fact that the momentum integral in equation (3.6) is dominated by the pole contribution at  $k^0 = E_k$  where the following replacement holds

$$\frac{1}{k^0 - E_k + i\epsilon} = \frac{k^0 + E_k - i\epsilon}{k^{02} - E_k^2 + i\epsilon} \xrightarrow{k^0=E_k} \frac{2E_k}{k^2 - m_N^2 + i\epsilon}, \quad (3.9)$$

so that the pole of the ground-state contribution is recovered.

Equation (3.8) constitutes the hadronic or phenomenological side of the sum rules. The next step is to derive a result for the correlation function (3.8) in QCD. To this end an explicit form of the interpolating current  $\eta_N(x)$  is required. The current of a proton can be parametrised by the following two independent terms

$$\eta_1(x) = 2\epsilon^{abc} (u_a^T(x) C \gamma_5 d_b(x)) u_c(x), \quad \eta_2(x) = 2\epsilon^{abc} (u_a^T(x) C d_b(x)) \gamma_5 u_c(x). \quad (3.10)$$

The corresponding currents for a neutron are obtained from that of the proton by the replacement  $u \leftrightarrow d$ . In literature, often an alternative set of currents is employed,  $\eta_V(x)$  and  $\eta_T(x)$ , which can be obtained from the two above ones by means of Fierz transformations as follows (see for instance [158, 159])

$$\begin{aligned} \eta_V(x) &= \eta_2(x) - \eta_1(x) = \epsilon^{abc} (u_a^T(x) C \gamma_\mu u_b(x)) \gamma_5 \gamma^\mu u_c(x), \\ \eta_T(x) &= \eta_2(x) + \eta_1(x) = \epsilon^{abc} (u_a^T(x) C \sigma_{\mu\nu} u_b(x)) \gamma_5 \sigma^{\mu\nu} u_c(x). \end{aligned} \quad (3.11)$$

The combination  $\eta_V(x)$  is sometimes referred to as Ioffe's current, which was used in his original work [155]. Moreover, it can be argued that from these two currents,  $\eta_V(x)$  is more pertinent than  $\eta_T(x)$  as the sum rules derived for the latter choice are plagued by large contributions from heavier states [155, 160]. The ideal choice of the current depends on the application; while physical predictions must be independent of this choice (to a certain extent), technical features like the convergence of the OPE and the size of the contributions of heavier states typically depend on the choice of the current. Consider the linear combination  $\eta_2 + \beta\eta_1$  with some real-valued number  $\beta$ .

The parameter  $\beta$  is unphysical and the less a prediction for an observable depends on this parameter the closer it should be to the true, physical result. For a certain regime of values for  $\beta$  the prediction may be approximately independent of  $\beta$ , i.e. a flat function of the parameter. In this regime, the accuracy of the sum rules is expected to be better than if the dependence was strong. So by finding the right regime for  $\beta$  the accuracy can be improved. In the following though the sum rules are presented for the historical choice  $\eta_N(x) = \eta_V(x)$ , i.e.  $\beta = -1$ , for simplicity.

The time-ordered product in the correlator (3.1) can be expanded in terms of composite, local operators  $O_n(0)$  with increasing mass dimension which are built from the quark fields,

$$iT[\eta_V(x)\bar{\eta}_V(0)] = \sum_n C_n(x)O_n(0), \quad (3.12)$$

where the  $C_n$  denote Wilson coefficients, which contain the information on the  $x$ -dependence. The OPE converges for space-like and small  $x$ ,  $x^2 < 0$  and  $x \sim 0$  [161]. By taking the vacuum expectation value and the Fourier transform, an expansion in terms of local condensates and momentum-dependent functions  $C_n(p)$  is obtained. The operators and coefficients of the OPE are defined at a specific scale  $\mu$  — the renormalisation scale. Long- and short-range interactions are characterised by energies below and above  $\mu$ , respectively. While the condensates capture the long-distance (or IR) physics in terms of condensates, the Wilson coefficients are determined by short-range (or UV) interactions. Thus, the integration over momenta of radiative corrections should in principle be divided into the domains of  $k < \mu$  and  $k > \mu$ , which then respectively contribute to the condensates and the Wilson coefficients. In practice, it is however assumed that perturbative corrections are subtracted from the condensates, which are thus considered to be purely non-perturbative objects, so that loop-integrals for corrections to the Wilson coefficients extend over the whole domain of momenta [162,163]. Hence, the OPE systematically separates long- and short-range interactions, where the factorisation scale is given by the renormalisation scale  $\mu$ .

Since radiative corrections are computed only up to a finite order, the terms of the OPE depend on the renormalisation scale  $\mu$  even though physical quantities are of course independent of this scale. The UV divergences that occur in the calculation of the perturbative part can be handled by applying a Borel transformation with respect to  $P^2 \equiv -p^2$  on both sides of the sum rules, which for a function  $F(P^2)$  is defined by

$$\mathcal{B}[F(P^2)] = \lim_{\substack{P^2, n \rightarrow \infty \\ P^2/n = M^2 = \text{const.}}} \frac{(P^2)^n}{(n-1)!} \left(-\frac{d}{dP^2}\right)^n F(P^2), \quad (3.13)$$

### 3 QCD at hadronic scales: sum-rule techniques

where  $M$  denotes the so-called Borel mass.<sup>1</sup> All poles and constants from the regularisation occur as factors of polynomials in  $P^2$ , so they vanish after taking the Borel transform. Furthermore, the Borel transformation eventually turns the OPE into an expansion in powers of the QCD scale  $\Lambda_{\text{QCD}} \simeq 300$  MeV over the Borel mass  $M$ , or rather  $(\Lambda_{\text{QCD}}^2/M^2)^n$  with  $n \geq 0$ , because the condensates are expected to scale like some power of  $\Lambda_{\text{QCD}}$ . Radiative corrections are typically evaluated at the Borel mass as well, i.e.  $\mu \sim M$ , because it is related to the momentum flow through the correlator.

On the hadronic side of the sum rules, the Borel transform effectively exponentiates the denominators, e.g. the masses of the resonances. A collection of useful Borel transforms can be found for instance in [164–166] and reads

$$\begin{aligned}
\mathcal{B} \left[ (P^2)^k \right] &= 0, \\
\mathcal{B} \left[ \left( \frac{1}{P^2} \right)^k \right] &= \frac{1}{(k-1)!} \left( \frac{1}{M^2} \right)^k, \\
\mathcal{B} \left[ \left( \frac{1}{s+P^2} \right)^k \right] &= \frac{1}{(k-1)!} \left( \frac{1}{M^2} \right)^k e^{-\frac{s}{M^2}}, \\
\mathcal{B} \left[ (P^2)^k \ln(P^2) \right] &= (-1)^{k+1} \Gamma(k+1) (M^2)^k, \\
\mathcal{B} \left[ \left( \frac{1}{P^2} \right)^k \left( \ln \left( \frac{P^2}{\mu^2} \right) \right)^{-\epsilon} \right] &= \frac{1}{\Gamma(k)} \left( \frac{1}{M^2} \right)^k \left( \ln \left( \frac{P^2}{\mu^2} \right) \right)^{-\epsilon} \\
&\quad \times \left[ 1 + \mathcal{O} \left( \left( \ln \left( \frac{P^2}{\mu^2} \right) \right)^{-1} \right) \right].
\end{aligned} \tag{3.14}$$

Here  $k \in \mathbb{N}_+$  and  $\Gamma(z)$  denotes the Euler gamma function. From (3.14) it is clear that heavier states exhibit a stronger suppression than the ground state after Borel transformation, which is another advantage of this approach.

Section 3.2 contains many details on the calculation of local OPEs, so for the correlation function (3.1) with the current  $\eta_V(x)$  in (3.11) only the results, which can be found in the Refs. [155, 167, 168], are presented here. In particular, there are two sum rules that can be extracted from this correlator, one for each of the structures in (3.8), i.e. for  $\not{p}$  and  $\mathbb{1}$ . By matching the QCD result on the hadronic expression (3.8), the following result is obtained after Borel transformation

$$\begin{aligned}
\lambda_N^2 e^{-m_N^2/M^2} + \dots &= M^6 + \dots, \\
\lambda_N^2 m_N e^{-m_N^2/M^2} + \dots &= -8\pi^2 \langle \bar{q}q \rangle M^4 + \dots,
\end{aligned} \tag{3.15}$$

---

<sup>1</sup>Note that the OPE converges only if  $P^2 > 0$  and in particular  $P^2 \gg \Lambda_{\text{QCD}}^2$ .

### 3.1 QCD sum rules for baryons: Ioffe's formula

where condensates of mass dimension higher than 3, radiative corrections and contributions from heavier states are neglected as indicated by the ellipses. The Borel mass  $M$  is expected to be in the ballpark of the nucleon mass, which is well above  $\Lambda_{\text{QCD}}$  and well below the lightest excitation in the nucleon spectrum with a mass of approximately 1.44 GeV [30]. A crude estimate for the nucleon mass is hence obtained by taking the ratio of the two sum rules and setting the Borel mass to  $M \simeq 1$  GeV,

$$m_N \simeq -8\pi \frac{\langle \bar{q}q \rangle}{M^2} \simeq 1.2 \text{ GeV}, \quad (3.16)$$

where the numerical value  $\langle \bar{q}q \rangle \simeq -(0.25 \text{ GeV})^3$  has been used. This estimate reproduces the physical value of the nucleon mass within a deviation of about 30%. This result is however accidental to some extent, because large radiative corrections at the order  $\alpha_s$  occur in the first sum rule which are then partially cancelled by  $\alpha_s$ -corrections for the second sum rule. For a more rigorous analysis of QCD sum rules for the nucleon mass see Section 6.7 of Ref. [169] and references therein.

The above discussion clearly illustrates the limitations of the sum-rule techniques for nucleons. Working at the LO in the OPE and in the  $\alpha_s$  expansion often leads to large uncertainties due to the occurrence of unphysical parameters, and often it is difficult to determine the size of the related uncertainty. One way to fix the Borel mass and to estimate part of the uncertainties is to determine a window, where  $M$  is large enough so that the OPE converges sufficiently fast and small enough so that heavier states are sufficiently suppressed. Then  $M$  can be varied within the Borel window to assess how strongly the final prediction for a physical parameter depends on the choice of this parameter. In addition, one can try to model the contributions of heavier states explicitly so that their contribution can be subtracted from the sum rules. The most common model approximates the sum over hadronic states (3.8) by the pole of the ground state plus a continuous distribution covering smeared heavier resonances and multi-particle states, or in short: pole + continuum. The continuum part is then estimated by the QCD result of the sum rules, which should hold at sufficiently large virtualities because the OPE becomes exact in the limit  $P^2 \rightarrow \infty$ . This approximation is known as quark-hadron duality [170] (see also [171] for a review). The method will be applied in Chapter 4 in the context of LCSRs, where technical details are explained.

With these improvements, the systematic uncertainties that are intrinsic to all sum rules can be somewhat reduced. The applications that are discussed in Sections 3.2 and Chapter 4 are technically more involved and the uncertainties range from 25% to 100%; however, in typical applications of these results, as for instance presented in Chapter 5, estimates at the correct order of magnitude are desirable.

### 3.2 Sum rules for CP-violating operators of Weinberg type

The goal of this section is to determine the contributions of the hadronic matrix elements of effective operators of Weinberg type defined in (2.9) to the nEDM from (2.12). The operators of interest are dubbed  $O_6$  and  $O_8$ ,

$$O_6 = f^{ABC} \tilde{G}_{\mu\nu}^A G^{B\nu\rho} G_{\rho}^{C\mu}, \quad O_8 = c^{ABCD} \tilde{G}_{\mu\nu}^A G^{B\mu\nu} G_{\rho\lambda}^C G^{D\rho\lambda}. \quad (3.17)$$

In the case of the dimension-six contribution  $O_6$  such a calculation has already been performed in [94], but this publication does not provide details on the actual computation making an independent re-evaluation worthwhile. The determination of the hadronic matrix elements of the dimension-eight term  $O_8$  is instead new. Both results are used in Section 5.1, where model-independent bounds on CP-violating Higgs-gluon interactions in BSM scenarios with vanishing or highly suppressed light-quark Yukawa couplings are derived.

The central object for the derivation of the sum-rule estimates for the hadronic matrix elements is the following correlation function

$$\Pi(q^2) = i \int d^4x e^{iqx} \langle 0 | T [\eta_n(x) \bar{\eta}_n(0)] | 0 \rangle_{\text{EM}, O_k}, \quad (3.18)$$

where  $\eta_n(x)$  is the interpolating field of the neutron,  $|0\rangle$  represents the vacuum on a CP-conserving background and the subscripts EM and  $O_k$  imply that the correlator is evaluated in the presence of a constant external EM source and one of the operators introduced in (3.17). The basic idea is to calculate (3.18) using two different approaches (as outlined in the introduction of this chapter) and to match the results to obtain an analytic expression for the nEDM. In the first approach, one defines a phenomenological form  $\Pi_{\text{phen}}$  of the correlator, which incorporates the wave function of the neutron, its EDM and other parameters. The second approach relies instead on an OPE of the correlator leading to the object  $\Pi_{\text{OPE}}$  that depends on the expectation values of effective operators, such as the three-gluon and four-gluon interactions introduced in (3.17). Matching the expressions for  $\Pi_{\text{phen}}$  and  $\Pi_{\text{OPE}}$  then yields the contribution of the effective operators of interest to the nEDM. To improve the accuracy of the sum rules, the correlators are, however, not matched themselves but their Borel transforms are considered in order to remove higher-order polynomial terms and to suppress excited states.

The analysis is structured as follows. In Section 3.2.1 the phenomenological side of the sum rules is derived. The OPE computation of the dimension-six and dimension-eight contributions is described in Section 3.2.2 and Section 3.2.3, respectively. The matching and the numerical analysis of the sum rules are performed in Section 3.2.4. Technical details are relegated to the appendices.

### 3.2.1 Phenomenological side of the sum rules

The parametrisation of the correlation function (3.18) is derived in two steps. Since we are eventually interested in the electric dipole interactions of the neutron with the background, first the relevant EM interactions of the correlator are decomposed in Section 3.2.1.1. After the structures of the EM dipole interactions are identified, a representation suitable for the sum-rule calculations is derived in Section 3.2.1.2.

#### 3.2.1.1 Hadronic representation

In this section, the phenomenological form  $\Pi_{\text{phen}}$  of the correlator (3.18) is derived following the argument presented in [90, 92, 172, 173]. An often considered approach for the phenomenological side of two-point correlators is the use of dispersion relations [141, 164, 165, 168, 174–176]. Since we are interested in the correlator of two nucleon currents  $\eta_n$  in an external EM field, we are, however, effectively dealing with a three-point correlation function. Dispersion relations for three-point correlators are less constraining than those of two-point correlators due to the lack of positivity constraints [173]. Therefore, we relate the correlator (3.18) to a perturbative expansion of the nucleon propagator in a non-zero and constant EM background. We write

$$\Pi_N(q^2) = \Pi_N^{(0)}(q^2) + e\Pi_N^{(1)}(q^2) + \dots, \quad (3.19)$$

where  $e$  is the electron charge magnitude that serves as the expansion parameter. The first non-trivial term in (3.19) describes the response of the nucleon states to the weak external perturbation and arises from a single insertion of the EM interactions

$$\mathcal{L}_{\text{EM}}(x) = J_\mu(x) A^\mu(x), \quad J_\mu(x) = e \sum_{q=d,u} Q_q \bar{q}(x) \gamma_\mu q(x). \quad (3.20)$$

It takes the form

$$e\Pi_N^{(1)}(q^2) = i \int d^4x d^4y e^{iqx} \langle 0 | T [\eta_n(x) \bar{\eta}_n(0) i\mathcal{L}_{\text{EM}}(y)] | 0 \rangle. \quad (3.21)$$

Here  $J_\mu$  denotes the EM current,  $A^\mu$  is the photon field and  $Q_q$  is the fractional electric charge of the relevant quark. Note that the EM field is a non-dynamical, classical field in this approach.

In order to evaluate the first-order contribution to (3.19), we insert a complete set of hadronic states  $N'$  and  $N''$  with the quantum numbers of the neutron into (3.21), i.e. we make use of the identity  $\mathbb{1} = \sum_{N'} |N'\rangle \langle N'|$  twice. Working in the so-called fixed-point gauge (see Appendix A), which allows us to express the photon field through the QED field strength tensor employing  $A_\mu(y) = -1/2 y^\nu F_{\mu\nu}(0)$  (cf. (A.5)), one obtains the

### 3 QCD at hadronic scales: sum-rule techniques

following expression for the first non-trivial term in the Taylor expansion (3.19) of the nucleon propagator  $\Pi_N(q^2)$ :

$$e\Pi_N^{(1)}(q^2) = \sum_{N', N''} \int d^4x d^4y e^{iqx} \theta(x_0 - y_0) \theta(y_0) \frac{1}{2} y^\nu F_{\mu\nu}(0) \quad (3.22)$$

$$\times \langle 0 | \eta_n(x) | N' \rangle \langle N' | J_\mu(y) | N'' \rangle \langle N'' | \bar{\eta}_n(0) | 0 \rangle + \dots$$

Here the ellipses represent the different combinations due to time ordering. The double sum in (3.22) involves three types of matrix elements of the EM current. These correspond to nucleon transitions of (i) ground state to ground state, (ii) ground state to excited states and vice versa, and (iii) excited states to excited states.

Let us first focus on the ground-state contributions, i.e. the terms of the hadronic sums that involve only neutron states  $|n\rangle$ . Up to an arbitrary chiral phase  $\chi$  the matrix elements involving  $|n\rangle$  can be parametrised by the coupling  $\lambda_n$  between the physical neutron and the interpolating current  $\eta_n$  as follows

$$\langle 0 | \eta_n(x) | n \rangle = \lambda_n U(\chi) u_n(p, s), \quad U(\chi) = e^{i\frac{\chi}{2}\gamma_5}. \quad (3.23)$$

Here  $u_n$  is the neutron spinor which satisfies

$$(\not{p} - m_n) u_n(p, s) = 0, \quad \sum_s u_n(p, s) \bar{u}_n(p, s) = \not{p} + m_n, \quad (3.24)$$

with  $\not{p} = p_\mu \gamma^\mu$ ,  $m_n$  denoting the neutron mass and  $\bar{u}_n(p, s) = u_n^\dagger(p, s) \gamma_0$ . Notice that for our correlator (3.22) a spin summation is implicit in the sum over all hadronic states.

The product of the matrix element involving the EM current and the photon field can be reduced to a set of four neutron form factors (see for instance [177])

$$\int d^4x e^{iqx} \langle n | J_\mu(x) | n \rangle A^\mu = (2\pi)^4 \delta^{(4)}(q - (p_2 - p_1)) \quad (3.25)$$

$$\times \bar{u}_n(p_2, s_2) \Gamma_\mu(p_1, p_2) u_n(p_1, s_1) A^\mu(q),$$

with

$$\Gamma_\mu(p_1, p_2) A^\mu(q) = F_1(q^2) \gamma_\mu A^\mu - (F_2(q^2) + F_3(q^2) i \gamma_5) \frac{\sigma_{\mu\nu} F^{\mu\nu}}{4m_n} \quad (3.26)$$

$$+ F_4(q^2) \gamma_\mu \gamma_5 \partial_\nu F^{\mu\nu}.$$

Here  $q = p_2 - p_1$  is the outgoing momentum carried by the photon. At  $q^2 = 0$ , the form factors in (3.26) can be identified with the fractional electric charge  $Q_n$ , the magnetic moment  $\mu_n$ , the EDM  $d_n$  and the anapole moment  $a_n$  of the neutron. Since the electric

### 3.2 Sum rules for CP-violating operators of Weinberg type

charge of the neutron is zero and its anapole moment, as a result of the constant EM background, vanishes as well, one has explicitly

$$\mu_n = \frac{F_2(0)}{2m_n}, \quad d_n = \frac{F_3(0)}{2m_n}. \quad (3.27)$$

It then follows that the tensor structures in (3.26) associated with  $\mu_n$  and  $d_n$  only differ by a factor  $i\gamma_5$ , meaning that at zero-momentum transfer one can write

$$\Gamma_\mu(p_1, p_2) A^\mu(q) |_{q^2=0} = -\frac{\mu_n}{2} \left( 1 + \frac{d_n}{\mu_n} i\gamma_5 \right) \sigma \cdot F = -\frac{1}{2} \left( \mu_n \sigma \cdot F - d_n \sigma \cdot \tilde{F} \right), \quad (3.28)$$

with  $\sigma \cdot F = \sigma_{\mu\nu} F^{\mu\nu}$  etc. and we have used that  $\gamma_5 \sigma \cdot F = i\sigma \cdot \tilde{F}$ .

Inserting (3.23), (3.25) and (3.28) into (3.22) and using (3.24), one obtains for the  $|n\rangle$  contributions to the first-order correction (3.22) of the nucleon correlation function the following expression

$$e\Pi_N^{(1)}(q^2) = -\frac{\lambda_n^2}{2(q^2 - m_n^2)^2} U(\chi) P U(\chi) + \dots, \quad (3.29)$$

with

$$P = (\not{q} + m_n) \left( \mu_n \sigma \cdot F - d_n \sigma \cdot \tilde{F} \right) (\not{q} + m_n). \quad (3.30)$$

Here the ellipsis denotes contributions due to excited states and other operators that turn out to be suppressed in the course of our analysis. Up to  $\mathcal{O}(\chi)$  the Lorentz structure in (3.29) behaves under chiral transformations as

$$\begin{aligned} U(\chi) P U(\chi) &= P + \left\{ P, i \frac{\chi}{2} \gamma_5 \right\} + \mathcal{O}(\chi^2) \\ &= m_n \left\{ \mu_n \sigma \cdot F - d_n \sigma \cdot \tilde{F}, \not{q} \right\} + m_n^2 \left[ \mu_n \sigma \cdot F - (d_n + \chi \mu_n) \sigma \cdot \tilde{F} \right] \\ &\quad + \not{q} \left[ \mu_n \sigma \cdot F - (d_n - \chi \mu_n) \sigma \cdot \tilde{F} \right] \not{q} + \mathcal{O}(\chi^2). \end{aligned} \quad (3.31)$$

This result implies that the anti-commutators  $\{\sigma \cdot F, \not{q}\}$  and  $\{\sigma \cdot \tilde{F}, \not{q}\}$  are the only structures that are invariant under chiral rotations.

#### 3.2.1.2 Phenomenological parametrisation

In calculating  $d_n$  it should then be clear from the above discussion that one should study the operator  $\{\sigma \cdot \tilde{F}, \not{q}\}$  as this structure is the unique choice with an unambiguous coefficient for what concerns the EDM. We thus make the following ansatz [90, 92, 172, 173]

$$\Pi_N^{(1)}(q^2) = \frac{1}{2} f(q^2) \left\{ \sigma \cdot \tilde{F}, \not{q} \right\}, \quad (3.32)$$

### 3 QCD at hadronic scales: sum-rule techniques

with

$$f(q^2) = \frac{\lambda_n^2 m_n d_n}{(q^2 - m_n^2)^2} + \sum_{N' \neq n} \frac{f'_{N'}}{(q^2 - m_n^2)(q^2 - m_{N'}^2)} + \sum_{N', N'' \neq n} \frac{f_{N'N''}}{(q^2 - m_{N'}^2)(q^2 - m_{N''}^2)}, \quad (3.33)$$

for the first-order contribution to the nucleon propagator (3.19). The first term in (3.33) corresponds to the ground-state contribution. It matches the result that we have already derived in (3.29). The second and third term describe transitions of the ground state to excited states and vice versa and transitions of excited states to excited states, respectively. The corresponding form factors are called  $f_{N'}$  and  $f_{N'N''}$ . They do not have definite signs due to the lack of positivity constraints of the considered correlator [173].

Applying the Borel transformation defined in Section 3.1, one finds that the numerically leading contributions of the Borel transforms of the three terms in (3.33) are given by

$$c_n = \mathcal{B} \left[ \frac{\lambda_n^2 m_n d_n}{(q^2 - m_n^2)^2} \right] = \frac{\lambda_n^2 m_n d_n}{M^4} e^{-\frac{m_n^2}{M^2}},$$

$$c_{N'} = \mathcal{B} \left[ \frac{f_{N'}}{(q^2 - m_n^2)(q^2 - m_{N'}^2)} \right] \simeq \frac{f_{N'}}{M^2 (m_{N'}^2 - m_n^2)} e^{-\frac{m_n^2}{M^2}}, \quad (3.34)$$

$$c_{N'N''} = \mathcal{B} \left[ \frac{f_{N'N''}}{(q^2 - m_{N'}^2)(q^2 - m_{N''}^2)} \right] \simeq \frac{f_{N'N''}}{M^4} e^{-\frac{m_{N'}^2}{M^2}}.$$

Here we have exploited that empirically  $m_{N'} \gg m_n$  and  $m_{N'} \simeq m_{N''}$ . Compared to the ground-state contribution the mixed ground-state and excited-state contributions and the excited-states only contributions are hence of approximate size

$$\frac{c_{N'}}{c_n} \simeq 0.3 \frac{f_{N'}}{\lambda_n^2 m_n d_n} \left( \frac{M}{0.6 \text{ GeV}} \right)^2, \quad \frac{c_{N'N''}}{c_n} \simeq \frac{f_{N'N''}}{\lambda_n^2 m_n d_n} e^{-\frac{m_{N'}^2 - m_n^2}{M^2}}, \quad (3.35)$$

where we have used the values  $m_n \simeq 0.94 \text{ GeV}$  and  $m_{N'} \simeq 1.44 \text{ GeV}$  [178] for the mass of the neutron and its lightest excitation to obtain the quoted numerical prefactor. Under the assumption that  $|f_{N'}| \simeq |f_{N'N''}| \simeq \lambda_n^2 m_n d_n$  and setting  $M = 2\Lambda_{\text{QCD}} \simeq 0.6 \text{ GeV}$  with  $\Lambda_{\text{QCD}}$  the QCD scale, the mixed ground-state and excited-state (excited-states only) contributions therefore naively amount to relative corrections of the order of 30% (5%). In the following, we only include the ground-state contribution to (3.32) in our sum-rule calculation, and estimate the uncertainties that are associated to this simplification by a variation of the Borel mass  $M$  (cf. Section 3.2.4).

The appropriate form of the phenomenological side of our sum rule can be established by realising that the contributions to the nEDM induced by CP-violating Weinberg-type operators (3.17) have a simple pictorial interpretation [93]. As illustrated in

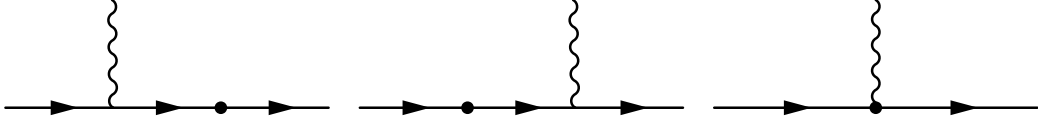


**Figure 3.1:** Contributions to the neutron EDM induced by CP-violating Weinberg-type operators. The dotted vertices indicate operator insertions and the solid lines represent propagators of the neutron  $n$  or the excited states  $N'$  and  $N''$ . See text for further explanations.

Figure 3.1, there are two types of graphs that one needs to consider in general. The first type of diagrams (left and middle) factorises into a propagator with a CP-violating mass insertion proportional to  $i\gamma_5$  and into a part that couples to the external photon field. The effect of Weinberg-type operators in this context is to rotate the nucleon wave function by an amount proportional to  $d_n/\mu_n$  as in (3.28). The second type of diagrams (right) only exists if either an insertion of an operator is considered that couples several gluons to a single photon or if at least one of the external legs corresponds to an excited state [93]. The former possibility is not viable at the dimension-six level, because there is no gauge-invariant operator that couples two gluons to a single photon. In the approximation that neglects the contributions of vertex diagrams and excitations, one can therefore use the following parameterisation

$$\Pi_{\text{phen}}(q^2) = -\frac{\lambda_n^2 m_n^2 \mu_n}{2(q^2 - m_n^2)} (1 + r(q^2) i\gamma_5) , \quad (3.36)$$

where the coefficient function  $r(q^2)$  has to be determined by matching the phenomenological side of the sum rule to the corresponding OPE calculation. Since from (3.28) we know that the EDM and the magnetic moment of the neutron are simply related by a chiral rotation with  $i\gamma_5$  though, the following relation holds

$$d_n = \mu_n r(q^2) . \quad (3.37)$$

In physical terms this result means that the Weinberg-type contributions to  $d_n$  can be approximated by calculating the  $i\gamma_5$  rotation of the nucleon wave function and relating it to the corresponding chiral rotation of  $\mu_n$  [93, 94]. In Section 3.2.2 and Section 3.2.3 we will use (3.36) and (3.37) to extract the hadronic matrix elements of  $O_6$  and  $O_8$ , respectively.

### 3.2.2 OPE calculation for the dimension-six operator

The QCD calculation for the correlation function is carried out in several steps. First, the appropriate choice for the interpolating current of the neutron is discussed in Section 3.2.2.1. In Section 3.2.2.2, the contribution of the dimension-six Weinberg operator

### 3 QCD at hadronic scales: sum-rule techniques

to the quark propagator on a CP-conserving background is described, which directly contributes to the OPE of the correlation function as outlined in Section 3.2.2.3. Eventually, the matching of the QCD result and the phenomenological representation of the correlator is discussed in Section 3.2.2.4.

#### 3.2.2.1 Interpolating current

We parameterise the interpolating current introduced in (3.18) as follows

$$\eta_n(x) = j_1(x) + \beta j_2(x), \quad (3.38)$$

where the real parameter  $\beta$  is kept arbitrary throughout our calculations. The two currents

$$j_1(x) = 2\epsilon_{abc} (d_a^T(x) C \gamma_5 u_b(x)) d_c(x), \quad j_2(x) = 2\epsilon_{abc} (d_a^T(x) C u_b(x)) \gamma_5 d_c(x), \quad (3.39)$$

form a basis for projection onto the neutron state in the case of a CP-conserving background. The current  $j_1(x)$  is often used in LQCD simulations to describe the neutron wave function (see for instance [179–181]). While  $j_2(x)$  vanishes in the non-relativistic limit, it should be included in the interpolating field since we are dealing with light quarks. In (3.39)  $C$  is the charge conjugation matrix, which satisfies  $C = C^* = -C^\dagger = -C^T = -C^{-1}$ ,  $C\gamma_5^T C = -\gamma_5$  and  $C^\dagger \gamma^0 = \gamma^0 C$ .

Notice that in contrast to the publications [90,92,172,173], we do not need to consider the two additional currents  $i_1(x) = \gamma_5 j_2(x)$  and  $i_2(x) = \gamma_5 j_1(x)$ , because in our case the only source of CP violation is provided by the Weinberg-type operators (3.17). The vacuum  $|0\rangle$  appearing in correlators such as (3.18) is instead taken to be CP-conserving, which in particular means that we assume that the QCD  $\theta$  term  $\theta \tilde{G}_{\mu\nu}^A G^{A\mu\nu}$  vanishes either accidentally or dynamically due to a Peccei-Quinn mechanism [49] (cf. Section 2.2).

#### 3.2.2.2 Weinberg contribution to the quark propagator

In the presence of a non-trivial EM background and the dimension-six operator  $O_6$ , the OPE of the correlator (3.18) can be formally written as

$$\Pi_{\text{OPE}}(q^2) = i \int d^4x e^{iqx} \langle 0 | T [\eta_n(x) \bar{\eta}_n(0)] | 0 \rangle_{\text{EM}, O_6} = \sum_k C_k(q^2) \langle O_k \rangle, \quad (3.40)$$

where  $C_k$  are the Wilson coefficients and  $\langle O_k \rangle = \langle 0 | O_k | 0 \rangle$  are vacuum matrix elements or condensates of the operator  $O_k$  (cf. Section 3.1).

One important ingredient to evaluate (3.40) is the quark propagator on the CP-conserving background including insertions of the EM field and  $O_6$ . In position space

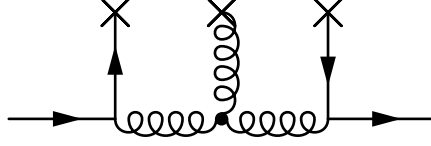


**Figure 3.2:** Contribution of the dimension-six Weinberg operator to the quark propagator. The dotted vertex represents the operator insertion, the crosses indicate interactions with the background and the solid lines depict quark propagators.

and suppressing colour and spinor indices the sought propagator reads

$$S(x) = S^{(0)}(x) + S^q(x) + S^{O_6}(x), \quad (3.41)$$

where the first term is the free propagator for a massless quark and the second term describes non-perturbative interactions with background quark fields. As shown in Appendix B at LO in the OPE these two quantities take the following form

$$S^{(0)}(x) = \frac{i\not{x}}{2\pi^2 x^4}, \quad S^q(x) = -\frac{1}{12} \langle \bar{q}q \rangle, \quad (3.42)$$

with  $\langle \bar{q}q \rangle \simeq -(0.25 \text{ GeV})^3$  [175, 176, 182] the quark condensate.

The effective operator  $O_6$  can be perturbatively inserted into the quark propagator [94]. The corresponding Feynman diagram is shown in Figure 3.2. It follows that the Weinberg-induced contribution to (3.41) can be written as

$$S^{O_6}(x) = \int d^4 z_1 d^4 z_2 S^{(0)}(x - z_1) S_{\text{amp}}^{O_6}(z_1 - z_2) S^{(0)}(z_2), \quad (3.43)$$

where the amputated two-point function  $S_{\text{amp}}^{O_6}(z)$  is given by

$$\begin{aligned} S_{\text{amp}}^{O_6}(z) &= i g_s T_{ac}^A \gamma_{ik}^\mu \left\langle T \left[ q_c^k(x) D_{\mu\nu}^{O_6 AB}(z) \bar{q}_d^l(0) \right] \right\rangle i g_s T_{db}^B \gamma_{lj}^\nu \\ &= -g_s^2 T_{ac}^A T_{db}^B \gamma_{ik}^\mu \gamma_{lj}^\nu \left\langle T \left[ q_c^k(0) D_{\mu\nu}^{O_6 AB}(z) \bar{q}_d^l(0) \right] \right\rangle + \dots \end{aligned} \quad (3.44)$$

Here we have expanded the quark wave function to zeroth order using (A.7) to obtain the final result. The object  $D_{\mu\nu}^{O_6 AB}(z)$  entering (3.44) represents the Weinberg-induced correction of the gluon propagator. Pictorially, one has

$$D_{\mu\nu}^{O_6 AB}(z) = \text{diagram} + \dots, \quad (3.45)$$

where the dotted vertex represents the insertion of the operator  $O_6$  and the cross indicates interactions with the classic background.

### 3 QCD at hadronic scales: sum-rule techniques

In order to determine the form of (3.45) we rely on standard background-field techniques. We start by writing the dimension-six Weinberg operator of (3.17) in a more convenient form, namely as (see for instance [79, 80, 82])

$$O_6 = -\frac{i}{16} f^{ABC} T^{\mu\nu\rho\lambda\sigma\tau} G_{\mu\nu}^A G_{\rho\lambda}^B G_{\sigma\tau}^C, \quad (3.46)$$

where  $T^{\mu\nu\rho\lambda\sigma\tau}$  denotes the following trace

$$T^{\mu\nu\rho\lambda\sigma\tau} = \frac{i}{2} \text{Tr} \left( \sigma^{\mu\nu} \sigma^{\rho\lambda} \sigma^{\sigma\tau} \gamma_5 \right). \quad (3.47)$$

Notice that this tensor is anti-symmetric under  $\mu \leftrightarrow \nu$ , etc. as well as  $\mu\nu \leftrightarrow \rho\lambda$  etc. By splitting the original gluon field  $G_\mu^A = \bar{G}_\mu^A + \hat{G}_\mu^A$  into a classical field  $\bar{G}_\mu^A$  and quantum field  $\hat{G}_\mu^A$ , one can then expand the QCD field strength tensor around its classical configuration to obtain

$$\begin{aligned} G_{\mu\nu}^A &= \bar{G}_{\mu\nu}^A + \bar{D}_\mu \hat{G}_\nu^A - \bar{D}_\nu \hat{G}_\mu^A + g_s f^{ABC} \bar{G}_\mu^B \hat{G}_\nu^C, \\ \bar{D}_\mu \hat{G}_\nu^A &= \partial_\mu \hat{G}_\nu^A + g_s f^{ABC} \bar{G}_\mu^B \hat{G}_\nu^C. \end{aligned} \quad (3.48)$$

When one now expands (3.46) using (3.48), one is only interested in terms that are linear in  $\bar{G}_\mu^A$  and bilinear in  $\hat{G}_\mu^A$ . Using the anti-symmetric properties of  $f^{ABC}$  and that of (3.47), we find that the relevant terms are

$$O_6 = -\frac{3i}{2} f^{ABC} T^{\mu\nu\rho\lambda\sigma\tau} \partial_\mu \bar{G}_\nu^A \partial_\rho \hat{G}_\lambda^B \partial_\sigma \hat{G}_\tau^C + \dots \quad (3.49)$$

Employing the result (3.49) one can now calculate the Weinberg-induced corrections (3.45) to the gluon propagator. By performing all possible contractions of the time-ordered product, we obtain the expression

$$\begin{aligned} D_{\mu\nu}^{O_6 AB}(z) &= \int d^4y \left\langle T \left[ \hat{G}_\mu^A(z) \hat{G}_\nu^B(0) iO_6(y) \right] \right\rangle \\ &= \frac{3}{2} f^{CDE} T^{\alpha\beta\gamma\delta\varphi\pi} \int d^4y \left\{ \partial_\alpha^y \bar{G}_\beta^C(y) \left[ \partial_\gamma^y D_{\mu\delta}^{(0)AD}(z-y) \partial_\varphi^y D_{\nu\pi}^{(0)BE}(y) \right. \right. \\ &\quad \left. \left. + \partial_\varphi^y D_{\mu\pi}^{(0)AE}(z-y) \partial_\gamma^y D_{\nu\delta}^{(0)BD}(y) \right] \right\}, \end{aligned} \quad (3.50)$$

where  $D_{\mu\nu}^{(0)AB}(x)$  denotes the free gluon propagator in position space. In Feynman gauge it takes the following simple form

$$D_{\mu\nu}^{(0)AB}(x) = \int d^4p e^{-ipx} \left[ -i\delta^{AB} \frac{\eta_{\mu\nu}}{p^2} \right] = \frac{1}{4\pi^2 x^2} \delta^{AB} \eta_{\mu\nu}, \quad (3.51)$$

a result that can be gleaned by inspection of (C.3).

### 3.2 Sum rules for CP-violating operators of Weinberg type

In order to simplify (3.50) we use the following two relations

$$\partial_\mu \bar{G}_\nu^A(x) = \frac{1}{2} G_{\mu\nu}^A(0) + \dots, \quad \partial_\mu D_{\nu\rho}^{(0)AB}(x) = -\delta^{AB} \eta_{\nu\rho} \int d^4p e^{-ipx} \frac{p_\mu}{p^2}, \quad (3.52)$$

which follow from the expansion (A.6) and the explicit form (3.51) of the free gluon propagator in momentum space, respectively. Using (3.52) yields

$$\begin{aligned} D_{\mu\nu}^{O_6 AB}(z) &= -\frac{3}{4} f^{ABC} G_{\alpha\beta}^C(0) \\ &\quad \times \int d^4y d^4p d^4q e^{-ip(z-y)} e^{-iqy} \left[ T^{\alpha\beta\gamma\mu\varphi\nu} \frac{p_\gamma q_\varphi}{p^2 q^2} - T^{\alpha\beta\gamma\nu\varphi\mu} \frac{p_\varphi q_\gamma}{p^2 q^2} \right] \\ &= -\frac{3}{2} f^{ABC} G_{\alpha\beta}^C(0) T^{\alpha\beta\gamma\mu\varphi\nu} \int d^4p e^{-ipz} \frac{p_\gamma p_\varphi}{p^4} \\ &= \frac{3i}{8\pi^2} f^{ABC} G_{\alpha\beta}^C(0) T^{\alpha\beta\gamma\mu\varphi\nu} \frac{1}{z^4} \left[ z_\gamma z_\varphi - \frac{\eta_{\gamma\varphi}}{2} z^2 \right], \end{aligned} \quad (3.53)$$

where in the last step we have employed the Fourier integral given in (C.6).

Plugging this into (3.44) we find

$$\begin{aligned} S_{\text{amp}}^{O_6}(z) &= -\frac{3ig_s}{8\pi^2} f^{ABC} T_{ac}^A T_{db}^B \gamma_{ik}^\mu \gamma_{lj}^\nu \langle q_c^k(0) g_s \bar{G}_{\alpha\beta}^C(0) \bar{q}_d^l(0) \rangle T^{\alpha\beta\gamma\mu\varphi\nu} \frac{1}{z^4} \left[ z_\gamma z_\varphi - \frac{\eta_{\gamma\varphi}}{2} z^2 \right] \\ &= \frac{ig_s}{512\pi^2} f^{ABC} (T^A T^C T^B)_{ab} (\gamma^\mu \sigma_{\alpha\beta} \gamma^\nu)_{ij} T^{\alpha\beta\gamma\mu\varphi\nu} \\ &\quad \times \frac{1}{z^4} \left[ z_\gamma z_\varphi - \frac{\eta_{\gamma\varphi}}{2} z^2 \right] \langle \bar{q} g_s \sigma \cdot G q \rangle \\ &= \frac{3ig_s \delta_{ab}}{32\pi^2 z^2} \gamma_{ij}^5 \langle \bar{q} g_s \sigma \cdot G q \rangle. \end{aligned} \quad (3.54)$$

Here we have used that the non-perturbative quark-gluon condensate appearing in the first line simplifies as follows (see for instance [166, 181])

$$\langle q_c^k(0) g_s \bar{G}_{\alpha\beta}^C(0) \bar{q}_d^l(0) \rangle = -\frac{1}{192} \sigma_{\alpha\beta}^{kl} T_{cd}^C \langle \bar{q} g_s \sigma \cdot G q \rangle, \quad (3.55)$$

with  $\sigma \cdot G = \sigma_{\mu\nu} G^{\mu\nu} T^A$ . Furthermore, the colour factor in the second line evaluates to

$$f^{ABC} (T^A T^C T^B)_{ab} = -\frac{i}{2} C_A C_F \delta_{ab}, \quad (3.56)$$

with the Casimir operators given by  $C_A = 3$  and  $C_F = 4/3$  for  $SU(3)$ .

From (C.9) one sees that the Fourier transform of (3.54) reads

$$S_{\text{amp}}^{O_6}(p) = \frac{3g_s}{8p^2} \gamma_5 \langle \bar{q} g_s \sigma \cdot G q \rangle, \quad (3.57)$$

### 3 QCD at hadronic scales: sum-rule techniques

where we have dropped colour and spinor indices. Inserting this result into (3.43) leads to

$$\begin{aligned} S^{O_6}(x) &= \frac{3g_s}{8} \langle \bar{q} g_s \sigma \cdot G q \rangle \int d^4 z_1 d^4 z_2 d^4 p d^4 q d^4 r e^{i(q-p)z_1} e^{i(p-r)z_2} e^{-iqx} \frac{\not{q} \gamma_5 \not{r}}{q^2 p^2 r^2} \\ &= -\frac{3g_s}{8} \gamma_5 \langle \bar{q} g_s \sigma \cdot G q \rangle \int d^4 p e^{-ipx} \frac{1}{p^4} = \frac{3g_s}{128\pi^2} i \gamma_5 \langle \bar{q} g_s \sigma \cdot G q \rangle \ln \left( -\frac{\mu_{\text{IR}}^2 x^2}{4} \right). \end{aligned} \quad (3.58)$$

To arrive at the final result we have made use of the Fourier integral (C.4) dropping infrared (IR) poles and constant pieces, because such terms vanish after Borel transformation. The appearance of the scale  $\mu_{\text{IR}}$  signals that the  $O_6$  contribution to (3.40) will depend logarithmically on an IR cut-off. Notice finally that the second result in (3.58) implies that the Weinberg-induced correction to the quark propagator takes the following form in momentum space

$$S^{O_6}(p) = -\frac{3g_s}{8p^4} \gamma_5 \langle \bar{q} g_s \sigma \cdot G q \rangle. \quad (3.59)$$

This result agrees up to a factor of  $i$  with the corresponding expression reported in [94] after taking into account that the definition of  $O_6$  used in this paper differs from the one employed in (3.17) by a factor of  $1/3$ .

#### 3.2.2.3 OPE including the Weinberg operator

In terms of (3.41) and

$$S^c(x) = C S^T(x) C = S^{(0)}(x) - S^q(x) - S^{O_6}(x), \quad (3.60)$$

the general form of the correlator (3.40) can be written as

$$\begin{aligned} \Pi_{\text{OPE}}(q^2) &= 24i \int d^4 x e^{iqx} \left\{ \text{Tr} (S^c \gamma_5 S \gamma_5) S + S \gamma_5 S^c \gamma_5 S \right. \\ &\quad + \beta [\text{Tr} (S^c S \gamma_5) \gamma_5 S + \gamma_5 S \gamma_5 S^c S + \text{Tr} (S^c \gamma_5 S) S \gamma_5 + S S^c \gamma_5 S \gamma_5] \\ &\quad \left. + \beta^2 [\text{Tr} (S^c S) \gamma_5 S \gamma_5 + \gamma_5 S S^c S \gamma_5] \right\}, \end{aligned} \quad (3.61)$$

where we have performed all possible Wick contractions. Here  $\beta$  is the real parameter that appears in our definition (3.38) of the interpolating current for the neutron.

We are only interested in the LO result of the OPE, in other words in terms that are linear either in the quark condensate (3.42) or the Weinberg-induced correction (3.58) to the quark propagator. The relevant contributions are given by the following expression

$$\Pi_{\text{OPE}}(q^2) = -24i \int d^4 x e^{iqx} \left[ S^{(0)}(x) \right]^2 \left[ f_q(\beta) S^q(x) + f_O(\beta) S^{O_6}(x) \right], \quad (3.62)$$

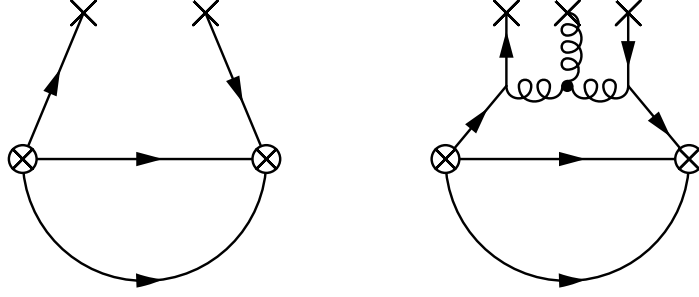


**Figure 3.3:** One-loop and two-loop contributions to the OPE correlation function (3.62). Insertions of the interpolating currents  $\eta_n(x)$  or  $\bar{\eta}_n(0)$  are denoted by circled crosses. The lower quark lines correspond to the free propagator  $S^{(0)}(x)$  of a massless quark, while the crosses indicate interactions with either quark or gluon background fields. In the right graph the dotted vertex represents the insertion of the Weinberg-type operator  $O_6$ .

with

$$f_q(\beta) = 7 - 2\beta - 5\beta^2, \quad f_O(\beta) = 5 + 2\beta - 7\beta^2. \quad (3.63)$$

This result can be interpreted in terms of the two Feynman diagrams depicted in Figure 3.3. The left graph shows the  $S^q(x)$  part of (3.62) which corresponds to a one-loop diagram because the background quark fields are non-dynamical. The right diagram has instead a dynamical and perturbative gluon that closes the second loop. In the case of the  $S^{O_6}(x)$  correction one therefore has to deal with a two-loop contribution.

To evaluate (3.62) we now parameterise the mixed quark-gluon condensate as [167]

$$\langle \bar{q} g_s \sigma \cdot G q \rangle = m_0^2 \langle \bar{q} q \rangle, \quad (3.64)$$

where  $m_0^2 \simeq 0.8 \text{ GeV}^2$  is a QCD parameter. Inserting (3.42) and (3.58) into (3.62), we then find

$$\begin{aligned} \Pi_{\text{OPE}}(q^2) &= \frac{6i \langle \bar{q} q \rangle}{\pi^4} \int d^4x e^{iqx} \frac{1}{x^6} \left[ -\frac{f_q(\beta)}{12} + \frac{3g_s m_0^2 f_O(\beta)}{128\pi^2} \ln \left( -\frac{\mu_{\text{IR}}^2 x^2}{4} \right) i\gamma_5 \right] \\ &= \frac{q^2}{16\pi^2} f_q(\beta) \ln \left( -\frac{\mu_{\text{UV}}^2}{q^2} \right) \langle \bar{q} q \rangle \left[ 1 - \frac{9g_s m_0^2}{32\pi^2} \frac{f_O(\beta)}{f_q(\beta)} \ln \left( -\frac{\mu_{\text{IR}}^2}{q^2} \right) i\gamma_5 \right]. \end{aligned} \quad (3.65)$$

Here we have used the Fourier integrals given in (C.10) and (C.12), respectively, to obtain the second line.

#### 3.2.2.4 Matching and discussion

In order to derive the sum rules for the  $O_6$  contribution to the nEDM, we match the phenomenological and the OPE correlators, i.e. we set (3.36) and (3.65) equal and

### 3 QCD at hadronic scales: sum-rule techniques

determine the coefficient  $r(q^2)$  that appears in front of the  $i\gamma_5$  term in  $\Pi_{\text{phen}}(q^2)$ . After Borel transformation and identifying the IR cut-off with the QCD scale, we obtain

$$r_6(\beta) = \frac{9g_s m_0^2}{32\pi^2} \frac{f_O(\beta)}{f_q(\beta)} \ln \left( \frac{M^2}{\Lambda_{\text{QCD}}^2} \right). \quad (3.66)$$

With this result at hand, we now discuss the appropriate choice for the mixing parameter  $\beta$  introduced in (3.38) for our sum rule. There are two commonly used ways for fixing this parameter: (i) at a value where the leading terms of the OPE are stationary under variations of  $\beta$  or (ii) at a point that maintains a balance between OPE convergence and contributions of excited states (cf. the discussion presented in Section 3.1). Both methods are not applicable in our case, because (i) the result (3.66) does not possess an extremum and (ii) contributions of excited states have been ignored in our sum rule (cf. Section 3.2.1.1). The procedure advocated in [90,92,172,173] where  $\beta$  is chosen such that subleading IR logarithms are cancelled in the QCD  $\theta$  term and CEDM contributions to the nEDM is also not useful, since on the OPE side (3.65) of our sum rule IR logarithms appear already at LO.

Our choice of  $\beta$  is instead based on the observation that the function  $f_q(\beta)$  introduced in (3.63) appears in the numerator of Ioffe's formula [155], which for arbitrary  $\beta$  takes the following form [181]

$$m_n = -\frac{7 - 2\beta - 5\beta^2}{5 + 2\beta + 5\beta^2} \frac{4(2\pi)^2}{M^2} \langle \bar{q}q \rangle. \quad (3.67)$$

This relation connects the neutron mass  $m_n$  to the quark condensate  $\langle \bar{q}q \rangle$ . While it is not an exact relationship, one observes that for  $\beta = 1$ , Ioffe's formula (3.67) predicts  $m_n = 0$  in gross disagreement with observation. For the second standard choice of the mixing parameter, i.e. the Ioffe interpolating current with  $\beta = -1$ , one instead has  $m_n \simeq 1.2 \text{ GeV}^3/M^2$  if the numerical value  $\langle \bar{q}q \rangle \simeq -(0.25 \text{ GeV})^3$  for the quark condensate is used (cf. Section 3.1). For  $\beta = -1$  and a Borel mass of  $M \simeq 1 \text{ GeV}$ , the formula (3.67) thus predicts a neutron mass that is in the ballpark of the experimental value  $m_n \simeq 0.94 \text{ GeV}$ . We conclude from this that the appropriate choice for the mixing parameter in the case of our sum rule (3.65) is  $\beta = -1$ . In fact, this choice is the one that has been employed in essentially all CP-even sum rules [155, 160, 167], including the sum-rule calculations of the anomalous magnetic moment  $\mu_n$  of the neutron [168, 174, 183, 184]. We believe that the Ioffe interpolating current has also been used in [94].

#### 3.2.3 OPE calculation for the dimension-eight operators

The procedure for the dimension-eight Weinberg-type operators follows the steps taken for the dimension-six operator, which was outlined in Section 3.2.2. After the con-

tributions of the gluonic self-interactions to the quark-propagator are determined in Section 3.2.3.1, the OPE derived in the previous section is employed to perform the matching on the hadronic form of the correlation function in Section 3.2.3.2.

### 3.2.3.1 Weinberg contribution to the quark propagator

In this section, we derive the contribution to the nEDM from the dimension-eight Weinberg operator  $O_8$  introduced in (3.17). Like in Section 3.2.2.2 we will treat the CP-violating four-gluon operator as a perturbative insertion into the quark propagator. The corresponding Feynman graph is shown in Figure 3.4. In analogy to (3.41), (3.43) and (3.44) we write

$$S(x) = S^{(0)}(x) + S^q(x) + S^{O_8}(x), \quad (3.68)$$

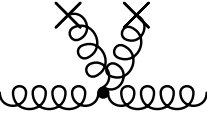
and

$$S^{O_8}(x) = \int d^4 z_1 d^4 z_2 S^{(0)}(x - z_1) S_{\text{amp}}^{O_8}(z_1 - z_2) S^{(0)}(z_2), \quad (3.69)$$

with

$$S_{\text{amp}}^{O_8}(z) = -g_s^2 T_{ac}^A T_{db}^B \gamma_{ik}^\mu \gamma_{lj}^\nu \left\langle T \left[ q_c^k(0) D_{\mu\nu}^{O_8 AB}(z) \bar{q}_d^l(0) \right] \right\rangle + \dots \quad (3.70)$$

The explicit LO expressions for  $S^{(0)}(x)$  and  $S^q(x)$  can be found in (3.42). The function  $D_{\mu\nu}^{O_8 AB}(z)$  in (3.70) corresponds to the correction of the gluon propagator due to an insertion of  $O_8$ , namely

$$D_{\mu\nu}^{O_8 AB}(z) = \text{diagram} + \dots \quad (3.71)$$


To determine the analytic expression corresponding to (3.71), we proceed as in Section 3.2.2.2 and write the operator  $O_8$  in the more convenient form

$$O_8 = \frac{i}{16} c^{ABCD} T_1^{\mu\nu\lambda\rho} T_2^{\alpha\beta\gamma\delta} G_{\mu\nu}^A G_{\lambda\rho}^B G_{\alpha\beta}^C G_{\gamma\delta}^D, \quad (3.72)$$

with

$$T_1^{\mu\nu\lambda\rho} = \frac{i}{2} \text{Tr} \left( \sigma^{\mu\nu} \sigma^{\lambda\rho} \right), \quad T_2^{\alpha\beta\gamma\delta} = \frac{i}{2} \text{Tr} \left( \sigma^{\alpha\beta} \sigma^{\gamma\delta} \gamma_5 \right). \quad (3.73)$$

These traces are anti-symmetric under the exchanges  $\mu \leftrightarrow \nu$  etc. but symmetric under the exchanges  $\mu\nu \leftrightarrow \lambda\rho$  etc. The effective operator  $O_8$  is then expanded in terms of partial derivatives and gluon fields using (3.48). Picking out the terms that are bilinear in both the background field  $\bar{G}_\mu^A$  and the quantum field  $\hat{G}_\mu^A$ , we obtain

$$O_8 = i c^{ABCD} T_1^{\mu\nu\lambda\rho} T_2^{\alpha\beta\gamma\delta} \left[ \partial_\mu \bar{G}_\nu^A \partial_\lambda \bar{G}_\rho^B \partial_\alpha \hat{G}_\beta^C \partial_\gamma \hat{G}_\delta^D + \partial_\mu \bar{G}_\nu^A \partial_\lambda \hat{G}_\rho^B \partial_\alpha \bar{G}_\beta^C \partial_\gamma \hat{G}_\delta^D \right. \\ \left. + \dots + \partial_\mu \hat{G}_\nu^A \partial_\lambda \hat{G}_\rho^B \partial_\alpha \bar{G}_\beta^C \partial_\gamma \bar{G}_\delta^D \right] + \dots, \quad (3.74)$$

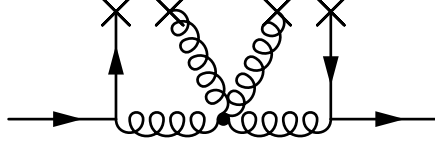


**Figure 3.4:** Contribution of the dimension-eight Weinberg operator to the quark propagator. The operator insertion corresponds to the dotted vertex, interactions with the background are represented by crosses and quark propagators are depicted by solid lines.

where the ellipsis in the bracket represents the other three terms that are quadratic in  $\tilde{G}_\mu^A$  and  $\hat{G}_\mu^A$ .

With the expression (3.74) at hand it is a matter of simple algebra to calculate (3.71). Using the relations in (3.52) we find

$$\begin{aligned}
 D_{\mu\nu}^{O_8 AB}(z) &= \int d^4y \left\langle T \left[ \hat{G}_\mu^A(z) \hat{G}_\nu^B(0) iO_8(y) \right] \right\rangle \\
 &= -4i c^{CDEF} \int d^4p e^{-ipz} \frac{1}{p^4} \\
 &\quad \times \left[ \left( \delta^{AD} \delta^{BF} \tilde{G}_{\nu\lambda}^E G_{\mu\rho}^C + \delta^{AF} \delta^{BD} \tilde{G}_{\mu\lambda}^E G_{\nu\rho}^C \right) p^\lambda p^\rho + \dots \right. \\
 &\quad \left. - \frac{1}{2} (\delta^{AC} \delta^{BD} + \delta^{AD} \delta^{BC}) \tilde{G}^E \cdot G^F (p_\mu p_\nu - \eta_{\mu\nu} p^2) \right].
 \end{aligned} \tag{3.75}$$

Here we have used the shorthand notation  $\tilde{G}^A \cdot G^B = \tilde{G}_{\mu\nu}^A G^{B\mu\nu}$  and all field strength tensors and duals are evaluated at 0. The ellipsis represents three additional terms that have a structure that is similar to that of the contribution proportional to  $p^\lambda p^\rho$ .

Inserting (3.75) into (3.70) it then turns out that to obtain the amputated two-point function  $S_{\text{amp}}^{O_8}(z)$ , one has to calculate objects of the form

$$\begin{aligned}
 M_{\lambda\rho}^{AB} &= T_{ac}^A T_{db}^B \gamma_{ik}^\mu \gamma_{lj}^\nu X^{CD} \left\langle q_c^k(0) g_s^2 \tilde{G}_{\mu\lambda}^C(0) G_{\nu\rho}^D(0) \bar{q}_d^l(0) \right\rangle, \\
 N_{\mu\nu}^{AB} &= T_{ac}^A T_{db}^B \gamma_{ik}^\mu \gamma_{lj}^\nu X^{CD} \left\langle q_c^k(0) g_s^2 \tilde{G}^C(0) \cdot G^D(0) \bar{q}_d^l(0) \right\rangle,
 \end{aligned} \tag{3.76}$$

where  $X^{CD}$  is a symmetric matrix in colour space. To achieve this we expand the quark current in terms of the set of basis matrices,

$$\Gamma_n = \left\{ \mathbb{1}, \gamma_5, \gamma_\alpha, i\gamma_5 \gamma_\alpha, \frac{1}{\sqrt{2}} \sigma_{\alpha\beta} \right\}, \tag{3.77}$$

using the Fierz identity (see for instance [158, 159])

$$q_a^i \bar{q}_d^l = -\frac{\delta_{ad}}{12} \Gamma_n^{il} (\bar{q} \Gamma_n q) - \frac{T_{ad}^C}{2} \Gamma_n^{il} (\bar{q} T^C \Gamma_n q). \tag{3.78}$$

### 3.2 Sum rules for CP-violating operators of Weinberg type

In the case of the structure  $M_{\lambda\rho}^{AB}$ , we obtain

$$M_{\lambda\rho}^{AB} = \gamma^\mu \Gamma_n \gamma^\nu \left[ -\frac{T^A T^B}{12} X^{CD} \left\langle \bar{q} \Gamma_n q g_s^2 \tilde{G}_{\mu\lambda}^C G_{\nu\rho}^D \right\rangle - \frac{T^A T^E T^B}{2} X^{CD} \left\langle \bar{q} T^E \Gamma_n q g_s^2 \tilde{G}_{\mu\lambda}^C G_{\nu\rho}^D \right\rangle \right], \quad (3.79)$$

where a sum over the five different Lorentz structures in (3.77) is implicit.

Recalling from (3.54) that we are only interested in the pieces of  $S_{\text{amp}}^{O_8}(z)$  that are proportional to  $i\gamma_5$  it is readily seen that these contributions all arise from the term

$$\gamma^\mu \gamma_5 \gamma^\nu = -\eta^{\mu\nu} \gamma_5 + \frac{1}{2} \epsilon^{\mu\nu\lambda\rho} \sigma_{\lambda\rho} \quad (3.80)$$

in the above expression for  $M_{\lambda\rho}^{AB}$ . The colour factors appearing in (3.79) can be decomposed in the following way

$$\begin{aligned} T^A T^B &= \frac{1}{6} \delta^{AB} + \frac{1}{2} d^{ABC} T^C + \frac{i}{2} f^{ABC} T^C, \\ T^A T^C T^B &= \frac{1}{12} d^{ABC} - \frac{i}{12} f^{ABC} + \frac{1}{6} \delta^{BC} T^A \\ &\quad + \frac{1}{4} (d^{BCD} - i f^{BCD}) (d^{ADE} + i f^{ADE}) T^E. \end{aligned} \quad (3.81)$$

Realising that only the structures that are proportional to  $\delta^{AB}$  and  $d^{ABC}$  in (3.81) can lead to  $SU(3)$  invariant condensates, we find that the terms relevant for our sum-rule calculation of the  $O_8$  contributions are

$$\begin{aligned} M_{\lambda\rho}^{AB} &= -\eta^{\mu\nu} \gamma_5 \left[ -\frac{\delta^{AB}}{72} X^{CD} \left\langle \bar{q} \gamma_5 q g_s^2 \tilde{G}_{\mu\lambda}^C G_{\nu\rho}^D \right\rangle - \frac{d^{ABE}}{24} X^{CD} \left\langle \bar{q} T^E \gamma_5 q g_s^2 \tilde{G}_{\mu\lambda}^C G_{\nu\rho}^D \right\rangle \right] + \dots \\ &= \eta_{\lambda\rho} \gamma_5 \left[ \frac{\delta^{AB}}{288} X^{CD} \langle Q^{CD} \rangle + \frac{d^{ABE}}{96} X^{CD} \langle Q^{ECD} \rangle \right] + \dots \end{aligned} \quad (3.82)$$

Here we have used the identity

$$X^{AB} \tilde{G}_{\mu\lambda}^A G^{B\mu}{}_\rho = \frac{1}{4} \eta_{\lambda\rho} X^{AB} \tilde{G}^A \cdot G^B, \quad (3.83)$$

that holds for any symmetric  $X^{AB}$  and introduced the following shorthand notation

$$\langle Q^{AB} \rangle = \left\langle \bar{q} \gamma_5 q g_s^2 \tilde{G}^A \cdot G^B \right\rangle, \quad \langle Q^{ABC} \rangle = \left\langle \bar{q} T^A \gamma_5 q g_s^2 \tilde{G}^B \cdot G^C \right\rangle \quad (3.84)$$

for the two types of condensates appearing in (3.82). A calculation similar to the one detailed above leads to

$$N_{\mu\nu}^{AB} = \eta^{\mu\nu} \gamma_5 \left[ \frac{\delta^{AB}}{72} X^{CD} \langle Q^{CD} \rangle + \frac{d^{ABE}}{24} X^{CD} \langle Q^{ECD} \rangle \right] + \dots \quad (3.85)$$

### 3 QCD at hadronic scales: sum-rule techniques

To determine the expression (3.70), we employ colour structures  $c^{ABCD}$  defined in (2.10), which appear in the definition (3.17) of  $O_8$ . Notice that these coefficients are symmetric under the simultaneous exchange of  $A \leftrightarrow B$  and  $C \leftrightarrow D$  and the pairwise exchange  $AB \leftrightarrow CD$ . Using (3.82), (3.85) and the properties of  $c^{ABCD}$ , we find that (3.70) can be written as follows

$$S_{\text{amp}}^{O_8}(z) = -\frac{1}{72\pi^2 z^2} \gamma_5 \left[ c^{AB} \langle Q^{AB} \rangle + c^{ABC} \langle Q^{ABC} \rangle \right], \quad (3.86)$$

with the new colour structures

$$\begin{aligned} c^{AB} &= c^{ACBC} + c^{ACCB} + 3c^{ABCC}, \\ c^{ABC} &= 3d_{CDE} (c^{ADBE} + c^{ADEB} + 3c^{ABDE}). \end{aligned} \quad (3.87)$$

In fact, using the identities (see for instance [185])

$$d_{ACD}d_{BCD} = \frac{C_A^2 - 4}{C_A} \delta_{AB}, \quad d_{ADE}d_{BDF}d_{CEF} = \frac{C_A^2 - 12}{2C_A} d_{ABC}, \quad (3.88)$$

it is a matter of simple algebra to show that for the three colour structures in (2.10) the coefficients (3.87) take the explicit form

$$c^{AB} = c_1 \delta^{AB}, \quad c_1^m = \left\{ 26, 12, \frac{10}{3} \right\}, \quad c^{ABC} = c_2 d^{ABC}, \quad c_2^m = \{6, 12, 12\}. \quad (3.89)$$

A comparison of (3.86) with (3.54) and (3.58) then implies that the Weinberg-induced correction (3.69) to the quark propagator in position space can be written as

$$\begin{aligned} S^{O_8}(x) &= \frac{1}{288\pi^2} i\gamma_5 \ln \left( -\frac{\mu_{\text{IR}}^2 x^2}{4} \right) \\ &\times \left[ c_1 \left\langle \bar{q} i\gamma_5 q g_s^2 \tilde{G} \cdot G \right\rangle + c_2 \left\langle \bar{q} T^A i\gamma_5 q g_s^2 d_{ABC} \tilde{G}^B \cdot G^C \right\rangle \right], \end{aligned} \quad (3.90)$$

with the coefficients  $c_1$  and  $c_2$  given in (3.89). Notice that the dimension-seven condensates appearing in (3.90) are the only non-zero matrix elements that can be constructed out of two quark fields, a QCD field strength tensor and its dual [186, 187]. This finding provides a sanity check of the calculations leading to  $S^{O_8}(x)$ .

#### 3.2.3.2 OPE correlator, matching and discussion

To determine the OPE correlator (3.40) which corresponds to the dimension-eight Weinberg-type operator  $O_8$ , we also need values for the two condensates in (3.90). The only estimates that exist at present are based on the instanton liquid model [176, 188–191]. One obtains [187]

$$\left\langle \bar{q} i\gamma_5 q g_s^2 \tilde{G} \cdot G \right\rangle = \frac{64}{5\bar{\rho}^4} \langle \bar{q}q \rangle, \quad \left\langle \bar{q} T^A i\gamma_5 q g_s^2 d_{ABC} \tilde{G}^B \cdot G^C \right\rangle = \frac{32}{15\bar{\rho}^4} \langle \bar{q}q \rangle. \quad (3.91)$$

### 3.2 Sum rules for CP-violating operators of Weinberg type

In the diluted instanton gas model, the quark condensate is given by

$$\langle \bar{q}q \rangle = -\frac{3m_q}{2\pi^2 \bar{\rho}^2}, \quad (3.92)$$

where  $m_q \simeq \Lambda_{\text{QCD}} \simeq 0.3 \text{ GeV}$  denotes the constituent quark mass and  $\bar{\rho} \simeq 1/(0.6 \text{ GeV})$  is the average instanton size. Notice that for the quoted values of  $m_q$  and  $\bar{\rho}$  one finds  $\langle \bar{q}q \rangle \simeq -(0.25 \text{ GeV})^3$  in agreement with the standard value for the quark condensate [175, 176, 182].

Noticing that after employing the relations (3.91) the structures of (3.90) and (3.58) are precisely the same, the derivation of  $\Pi_{\text{OPE}}(q^2)$  and the matching of the phenomenological and the OPE correlators for  $O_8$  proceeds as in Sections 3.2.2.3 and 3.2.2.4, respectively. In particular, for the coefficient  $r(q^2)$  that multiplies the  $i\gamma_5$  term in (3.36), we obtain

$$r_8(\beta) = \frac{4(6c_1 + c_2)}{45\pi^2 \bar{\rho}^4} \frac{f_O(\beta)}{f_q(\beta)} \ln \left( \frac{M^2}{\Lambda_{\text{QCD}}^2} \right), \quad (3.93)$$

with the functions  $f_q(\beta)$  and  $f_O(\beta)$  defined in (3.63). Like in the case of  $O_6$ , we will employ  $\beta = -1$  in our numerical analysis of the  $O_8$  matrix elements, since this is the appropriate choice for our sum-rule calculations (cf. the discussion at the end of Section 3.2.2.4).

#### 3.2.4 Numerical analysis

In this section, the final numerical results of the sum-rule calculations are presented, which are then used in the phenomenological application that is discussed in Section 5.1.

##### 3.2.4.1 Dimension-six contribution

Using  $\beta = -1$  and inserting (3.66) into (3.37), we obtain the following expression for the contribution of the dimension-six Weinberg operator to the nEDM

$$(d_n)_{O_6} = -\mu_n \frac{9g_s m_0^2}{32\pi^2} \ln \left( \frac{M^2}{\Lambda_{\text{QCD}}^2} \right), \quad (3.94)$$

which differs from the analytic result given in [94] by a sign.

In our numerical analysis we use

$$\begin{aligned} \mu_n &= -1.91 \frac{e}{2m_p} = -1.02 \frac{e}{\text{GeV}}, & g_s &= \sqrt{4\pi\alpha_s} = 2.13 \pm 0.03, \\ m_0^2 &= (0.8 \pm 0.2) \text{ GeV}^2, & \frac{M}{\Lambda_{\text{QCD}}} &\in \sqrt{2} [1, 2], \end{aligned} \quad (3.95)$$

### 3 QCD at hadronic scales: sum-rule techniques

where the input values and errors of  $\mu_n$ ,  $m_p$ ,  $g_s$  and  $m_0^2$  are taken from [175,176,178,182] and the strong coupling constant corresponds to a LO  $\alpha_s$  evaluated at a renormalisation scale of 1 GeV. We note that our choice  $M \in \sqrt{2} [1, 2] \Lambda_{\text{QCD}} \simeq [0.42, 0.85] \text{ GeV}$  covers the full range of Borel masses that has been considered in the related sum-rule calculations of the QCD  $\theta$  term and CEDM contributions to the nEDM [90,92,172,173].

With the input given in (3.95) we find from (3.94) the following numerical result

$$\left(\frac{d_n}{e}\right)_{O_6} = 74 (1 \pm 0.5) \text{ MeV}, \quad (3.96)$$

where the individual uncertainties have been added in quadrature to obtain the final relative error of 50%. The dominant source of uncertainty in our prediction for  $(d_n/e)_{O_6}$  arises from the variation of the scale ratio  $M/\Lambda_{\text{QCD}}$  and amounts to almost 90% of the total error given above. We add that the quoted total uncertainty in (3.94) is larger than the naive expectation of the size of the sum-rule contributions due to excited states (cf. the discussion at the end of Section 3.2.1.2) and that the sum-rule predictions for the down-quark and up-quark CEDMs [90, 92] are also accurate to about 50%. Notice that the central value of our prediction (3.94) differs by a factor of roughly 1/3 from the numerical result presented in [94]. Here a factor of 1/3 is accounted for by the different normalisation of the effective operator  $O_6$ , while the flipped overall sign in (3.94) is compensated by the fact that in the latter article the incorrect relation  $\mu_n = 1.91 e/(2m_p)$  has been used to obtain a numerical result.

#### 3.2.4.2 Dimension-eight contributions

Inserting (3.93) into (3.37), we find for the Ioffe interpolating current, i.e.  $\beta = -1$ , the following expression for the nEDM contribution of the dimension-eight Weinberg operators

$$(d_n)_{O_8}^m = -\mu_n \frac{72}{5\pi^2 \bar{\rho}^4} \ln \left( \frac{M^2}{\Lambda_{\text{QCD}}^2} \right) \left\{ 1, \frac{14}{27}, \frac{16}{81} \right\}, \quad (3.97)$$

where the numbers in the curly bracket correspond to the three different colour structures in (2.10).

The average instanton size that enters (3.97) can be determined in various ways. Including the value of  $\bar{\rho}$  that allows us to reproduce the phenomenological values of the quark and gluon condensates [188], that is obtained through variational techniques and the mean field approximation [189] and that is found in LQCD calculations [192–197], we arrive at the combination

$$\bar{\rho} = \frac{1}{(0.58 \pm 0.09) \text{ GeV}}. \quad (3.98)$$

This prediction has an uncertainty of 15%, which we believe to be a rather conservative error in view of the results given in [188,189,192–197].

### 3.2 Sum rules for $CP$ -violating operators of Weinberg type

In order to obtain a numerical result for the  $O_8$  contribution to the nEDM, we use the input given in (3.95) and (3.98). Adding individual uncertainties in quadrature we find

$$\left(\frac{d_n}{e}\right)_{O_8}^m = 2.5 \cdot 10^{-1} (1 \pm 0.8) \text{ GeV}^3 \left\{1, 0.5, 0.2\right\}. \quad (3.99)$$

Here the dominant source of uncertainty stems again from the variation of  $M/\Lambda_{\text{QCD}}$  and amounts close to 60% of the quoted total error of 80%.



## 4 LCSRs for proton decay

Many concepts of QCD sum rules that were presented in Chapter 3 and in particular in Section 3.1 can be found again in LCSR calculations [142–147] for proton decay channels of the type  $p \rightarrow \pi^0 \ell^+ + X$ , where  $\ell^+$  denotes an anti-lepton and  $X$  can be anything. The main difference compared to SVZ sum rules is that instead of employing an expansion around short distances, LCSRs utilise an expansion in small transverse separations among partons in the infinite momentum frame [198]. The approach effectively combines the methods of QCD sum rules and the theory of hard exclusive processes [148–154]. Eventually, this enables the separation of the hard scattering from soft interactions. While the hard-scattering kernel can be computed perturbatively in QCD, the soft contributions are parametrised in terms of DAs of the final-state pion.<sup>1</sup> Moreover, the approximate conformal symmetry of QCD permits a decomposition of the DAs in terms of partial waves or conformal spin so that transverse and longitudinal variables in the pion wave function can be separated [199, 200]. This leads to an expansion of the DAs in terms of a converging series of orthogonal polynomials of the momentum fraction carried by one of the partons in the pion (cf. Appendix D). The coefficients of the expansion are hadronic parameters which enter the LCSRs as input.

In Sections 4.1 and 4.2, the LCSR approach is employed to estimate the form factors that parametrise the hadronic matrix elements of proton-to-pion transitions which are relevant for semi-leptonic proton decay channels. The framework for this endeavour is developed in Section 4.1 where a simple two-body decay is studied. The contents of this section were originally published in the article [21], and the results could be verified by comparing them to recent lattice computations. By employing the same methods, the hadronic form factors for proton decay in GRSMEFT can be calculated, which is shown in Section 4.2; this part is based on the contents of Ref. [22].

---

<sup>1</sup>Some of the condensates that were introduced in Chapter 3 also occur in the LCSRs when a naive factorisation approach is used for higher-order DAs; see Section 4.1.2 for details.

## 4.1 Semi-leptonic two-body proton decay modes

Early attempts to compute the hadronic matrix elements of semi-leptonic proton decays date back to the '80s and employed non-relativistic quark models, often based on the approximate  $SU(6)$  flavour-spin symmetry of the partons [201–205], bag models which allow for relativistic partons [206–211], or QCD sum rules [212]. An effective chiral theory was also proposed in the articles [213–216], which can be used to derive relations among the various two-body decay widths but still contains a priori unknown low-energy constants. As a result, the latter approach cannot predict the absolute value of the proton decay width without further input. The methods mentioned above have also been applied to estimate these low-energy constants, in which case the final predictions for the hadronic matrix elements suffer from additional systematic uncertainties due to the approximate nature of the effective chiral theory. Moreover, the results of these model calculations differ by up to an order of magnitude from each other (see Table VI in [217] for a summary and comparison). On the other hand, LQCD groups have by now achieved to directly compute the needed hadronic matrix elements within uncertainties of  $(10 - 15)\%$  [217–224]. These results cover all two-body decays into pseudoscalar mesons and light anti-leptons, which are relevant for GUTs.

In this section, a method to estimate the hadronic matrix elements that enter processes of the type  $p \rightarrow \pi^0 \ell^+ (+X)$  is established. As a proof-of-principle the general approach is applied to the simple two-body case  $p \rightarrow \pi^0 e^+$  with  $e^+$  a positron, while the application to three-body proton decay processes such as transitions involving an additional graviton is discussed in Section 4.2. In fact, studying the simple decay mode  $p \rightarrow \pi^0 e^+$  allows us to make a thorough comparison with the latest LQCD results [223]. In this way, we are not only able to validate our method but can also assess the systematic uncertainties that plague our estimates. Our method employs the techniques of LCSRs in QCD. The light-cone expansion works well if the momentum transfer  $q$  from the proton to the pion is large in magnitude and space-like, i.e.  $q^2 < 0$ . We therefore cannot directly compute the hadronic matrix elements at the physical point of the two-body decay kinematics, where  $q^2$  is fixed and equal to the square of the positron mass. However, we are able to find values in the space-like regime at  $q^2 \simeq -0.5 \text{ GeV}^2$ , which are close enough to the physical regime to provide an estimate of the hadronic matrix elements at the physical point by means of suitable extrapolations. Albeit this approach does not achieve the same level of accuracy as the state-of-the-art LQCD calculation [223], the results of this work are promising, because the obtained precision is better than the methods that have been developed in the '80s to estimate proton decay rates. Furthermore, the LCSR approach developed in this section should be able to at least provide order-of-magnitude estimates for hadronic matrix elements that

enter certain three-body proton decay processes. Such decays could be phenomenologically relevant (see for instance [124]) but only model estimations exist for selected modes [225], making three-body final-state proton decay processes an interesting target of future LQCD studies [104].

This section is organised as follows. In Section 4.1.1 the framework for studying hadronic matrix elements for the  $p \rightarrow \pi^0 e^+$  decay is explained. In particular, all of the dimension-six operators in the SMEFT that are relevant for this decay, which are presented in (2.13), are considered so that the analysis is model-independent. These operators are typically generated by baryon-number-violating new physics that can be integrated out below a certain (large) energy scale. As a next step, the hadronic matrix elements are decomposed into form factors. These form factors enter a correlation function that is computed with the help of LCSR techniques in Section 4.1.2, which allows us to derive the LCSRs for the form factors relevant for proton decay in GUTs. In Section 4.1.3 we turn to the numerical evaluation of the LCSRs and compute the form factors in the regime of virtual momentum transfer. Eventually, these findings are compared to the results of the latest LQCD computation [223] and the uncertainties that enter the final estimates are discussed in detail. Technical details are relegated to the appendices.

#### 4.1.1 Phenomenological parametrisation

The transition matrix element of the proton decay  $p \rightarrow \pi^0 e^+$  induced by an insertion of an operator entering (2.13) can be factorised into a hadronic and leptonic part (up to electroweak corrections),

$$\langle \pi^0(p_\pi) e^+(q) | \mathcal{O}_{\Gamma\Gamma'} | p(p_p) \rangle = \bar{v}_e^c(q) H_{\Gamma\Gamma'}(p_p, q) u_p(p_p). \quad (4.1)$$

Here  $u_p(p_p)$  denotes the spinor of the proton with momentum  $p_p$  and  $\bar{v}_e^c(q)$  is the charge conjugate anti-spinor of the electron with momentum  $q \equiv p_p - p_\pi$ . The main goal of the following analysis is to calculate the hadronic matrix element  $H_{\Gamma\Gamma'}(p_p, q)$  of the  $p \rightarrow \pi^0$  transition,

$$H_{\Gamma\Gamma'}(p_p, q) u_p(p_p) \equiv \langle \pi^0(p_\pi) | \epsilon^{abc} (d_a^T C P_\Gamma u_b) P_{\Gamma'} u_c | p(p_p) \rangle, \quad (4.2)$$

where all the quark fields are evaluated at the space-time point  $x = 0$ . For an on-shell proton the above matrix element can be decomposed into two form factors as follows,

$$H_{\Gamma\Gamma'}(p_p, q) u_p(p_p) = i P_{\Gamma'} \left( W_{\Gamma\Gamma'}^0(q^2) + \frac{\not{q}}{m_p} W_{\Gamma\Gamma'}^1(q^2) \right) u_p(p_p), \quad (4.3)$$

with  $m_p = 938 \text{ MeV}$  the proton mass. Notice that the form factors are related due to parity, which is conserved in QCD. Specifically, one has

$$W_{RR}^n(q^2) = W_{LL}^n(q^2), \quad W_{LR}^n(q^2) = W_{RL}^n(q^2), \quad (4.4)$$

with  $n = 0, 1$ . In this work we calculate the combinations  $\Gamma\Gamma' = RR, LR$  explicitly, which covers all chirality combinations due to the above relations.

The starting point for evaluating the form factors  $W_{\Gamma\Gamma'}^n(q^2)$  in LCSRs is the correlation function

$$\Pi_{\Gamma\Gamma'}(p_p, q) = i \int d^4x e^{iqx} \langle \pi^0(p_\pi) | T [Q_{\Gamma\Gamma'}(x) \bar{\eta}_p(0)] | 0 \rangle, \quad (4.5)$$

where the current  $\eta_p$  ( $\bar{\eta}_p \equiv \eta_p^\dagger \gamma^0$ ) is a combination of three quark fields that interpolates the proton,

$$\langle 0 | \eta_p(0) | p(p_p) \rangle = m_p \lambda_p u_p(p_p). \quad (4.6)$$

Here  $\lambda_p$  denotes the couplings strength of the current  $\eta_p$  to the physical proton state.<sup>2</sup> The strongly-interacting parts of the dimension-six operators (2.13) are represented by

$$Q_{\Gamma\Gamma'}(x) \equiv \epsilon^{abc} (d_a^T(x) C P_\Gamma u_b(x)) P_{\Gamma'} u_c(x). \quad (4.7)$$

In order to derive a parametrisation of the hadronic matrix elements  $H_{\Gamma\Gamma'}(p_p, q)$  we insert a complete set of intermediate states that have the same quantum numbers as the proton into (4.5) (cf. equation (3.3)) and isolate the pole contribution of the ground state to obtain the hadronic representation of the correlation function:

$$\begin{aligned} \Pi_{\Gamma\Gamma'}^{\text{had}}(p_p, q) &= -\frac{m_p}{p_p^2 - m_p^2 + i\epsilon} \lambda_p H_{\Gamma\Gamma'}(p_p, q) (\not{p}_p + m_p) + \dots \\ &= P_{\Gamma'} \left( \Pi_{\Gamma\Gamma'}^{\text{had},S} + \frac{\not{p}_p}{m_p} \Pi_{\Gamma\Gamma'}^{\text{had},P} + \frac{\not{q}}{m_p} \Pi_{\Gamma\Gamma'}^{\text{had},Q} + \frac{i\sigma^{pq}}{m_p^2} \Pi_{\Gamma\Gamma'}^{\text{had},T} \right), \end{aligned} \quad (4.8)$$

with  $\epsilon > 0$  and infinitesimal,  $\sigma^{pq} \equiv \sigma_{\mu\nu} p^\mu q^\nu$ , and the ellipsis denotes contributions from heavier states, i.e. excited states and the continuum. The four independent Dirac structures in (4.8) can be used to derive LCSRs for the form factors  $W_{\Gamma\Gamma'}^n(q^2)$  or combinations of them. The corresponding scalar functions  $\Pi_{\Gamma\Gamma'}^{\text{had},\gamma}$  depend only on the square of the proton momentum  $p_p^2$  and on the square of the momentum transfer  $Q^2 \equiv -q^2$ . They are conveniently parametrised in terms of dispersion integrals,

$$\Pi_{\Gamma\Gamma'}^{\text{had},\gamma}(p_p^2, Q^2) = \int_{m_p^2}^{\infty} ds \frac{\rho_{\Gamma\Gamma'}^{\text{had},\gamma}(s, Q^2)}{s - p_p^2}, \quad (4.9)$$

where  $\gamma = S, P, Q, T$  and we have introduced the spectral densities

$$\rho_{\Gamma\Gamma'}^{\text{had},\gamma}(s, Q^2) \equiv \frac{1}{\pi} \text{Im} \Pi_{\Gamma\Gamma'}^{\text{had},\gamma}(s + i\epsilon, Q^2). \quad (4.10)$$

---

<sup>2</sup>Note the difference in the normalisation compared to the conventions used in the previous sections, i.e. equations (3.2) and (3.23).

Separating the ground-state contribution from the contribution of heavy states denoted by  $\rho_{\Gamma\Gamma'}^{\text{cont},\gamma}(s, Q^2)$ , the four spectral densities appearing in (4.8) can be cast into the form

$$\rho_{\Gamma\Gamma'}^{\text{had},\gamma}(s, Q^2) = i\lambda_p m_p^2 \delta(s - m_p^2) W_{\Gamma\Gamma'}^\gamma(s, Q^2) + \rho_{\Gamma\Gamma'}^{\text{cont},\gamma}(s, Q^2), \quad (4.11)$$

where

$$W_{\Gamma\Gamma'}^S(s, Q^2) = W_{\Gamma\Gamma'}^0(s, Q^2) + \frac{s - Q^2 - m_\pi^2}{2m_p^2} W_{\Gamma\Gamma'}^1(s, Q^2), \quad (4.12)$$

$$W_{\Gamma\Gamma'}^P(s, Q^2) = W_{\Gamma\Gamma'}^0(s, Q^2), \quad W_{\Gamma\Gamma'}^Q(s, Q^2) = W_{\Gamma\Gamma'}^T(s, Q^2) = W_{\Gamma\Gamma'}^1(s, Q^2),$$

and  $m_\pi = 135 \text{ MeV}$  is the pion mass. We stress that the relations (4.12) only hold on-shell, i.e. if  $s = m_p^2$ . This is however guaranteed by the  $\delta(s - m_p^2)$  function appearing in (4.11). Under the assumption of a global quark-hadron duality [170] (see also [171] for a review) the contributions of heavy states can be approximated by

$$\int_{s_0}^{\infty} ds \frac{\rho_{\Gamma\Gamma'}^{\text{cont},\gamma}(s, Q^2)}{s - p_p^2} \simeq \int_{s_0}^{\infty} ds \frac{\rho_{\Gamma\Gamma'}^{\text{QCD},\gamma}(s, Q^2)}{s - p_p^2}, \quad (4.13)$$

where  $\rho_{\Gamma\Gamma'}^{\text{QCD},\gamma}(s, Q^2)$  are the spectral densities in QCD and we will explain how to compute them in the next section. The approximation (4.13) is expected to work well for a sufficiently large continuum threshold  $s_0$ , which is a free parameter and has to be determined within the LCSR calculation. A more detailed discussion on how to fix  $s_0$  is provided in Section 4.1.3, but ideally it is chosen low enough to cover even the lightest excitation, which is the Roper resonance with a mass of  $1.44 \text{ GeV}$ .

### 4.1.2 LCSR calculation

The basic idea of the LCSRs is to derive a result for  $\Pi_{\Gamma\Gamma'}(p, q)$  in QCD while parametrisising unknown soft contributions in terms of quantities that can be determined by other means. It can be shown that for large virtualities  $Q^2 \gg \Lambda_{\text{QCD}}^2$  and  $P_p^2 \equiv -p_p^2 \gg \Lambda_{\text{QCD}}^2$  with  $\Lambda_{\text{QCD}} \simeq 300 \text{ MeV}$  the QCD scale, the integrand of the correlator (4.5) can be approximated by an expansion on the light-cone  $x^2 \sim 1/Q^2 \simeq 0$  (see [175] and references therein). Schematically, this light-cone expansion takes the form

$$T[Q_{\Gamma\Gamma'}(x)\bar{\eta}_p(0)] = \sum_k C_k(x) \mathcal{O}_k(0), \quad (4.14)$$

where the Wilson coefficients  $C_k$  encode the hard scattering process and the objects  $\mathcal{O}_k$  are composite operators of twist  $k$ . The matrix elements of these composite operators correspond to the light-cone DAs of the pion which are non-perturbative objects. Performing a Borel transformation with respect to  $P_p^2$  then yields an expansion in inverse

powers of the two scales that enter our calculation, i.e. it leads to a power expansion in  $\Lambda_{\text{QCD}}^2/M^2$  and  $\Lambda_{\text{QCD}}^2/Q^2$ , where  $M$  denotes the Borel mass associated to  $P_p^2$  (cf. (3.13)). In the following analysis we will provide explicit LCSR expressions that include the leading contributions in this expansion, namely the twist-2 and twist-3 DAs. We will however also comment on the possible impact of twist-4 contributions in all cases where such terms could be phenomenologically relevant (cf. Section 4.1.3).

In order to carry out the light-cone expansion, we need to choose an explicit form for the proton current  $\eta_p$ . The most general choice with the appropriate quantum numbers (at lowest order in derivatives and spin) can be written as a linear combination of the two currents introduced in equation (3.10) [160]:

$$\eta_1(x) = 2\epsilon^{abc} (u_a^T(x) C \gamma_5 d_b(x)) u_c(x), \quad \eta_2(x) = 2\epsilon^{abc} (u_a^T(x) C d_b(x)) \gamma_5 u_c(x). \quad (4.15)$$

The current  $\eta_1$  excites the ground state as well as heavier states, while  $\eta_2$  almost exclusively excites heavier states [180]. As a result the coupling strength of  $\eta_1$  (cf. (4.6)) to the proton state is larger by a factor of about 100 than that of  $\eta_2$ . Due to its weak coupling to the proton state, the contribution of the current  $\eta_2$  is expected to be very small in the case at hand, and we therefore choose for simplicity

$$\eta_p(x) \equiv \eta_1(x), \quad (4.16)$$

neglecting a possible admixture of  $\eta_2$ . This choice of the proton current also corresponds to the interpolator usually used in LQCD calculations. Note that the proton current enters the correlator linearly in the case at hand. In contrast to that, the applications discussed in Sections 3.1 and 3.2 rely on correlation functions with two powers of the current, so that also mixed contributions of the form  $\eta_1 \times \eta_2$  contribute there (see also the discussion of Section 3.2.2.4).

The expansion of the time-ordered product that occurs in the twist expansion (4.14) is carried out by partially contracting the quark fields,

$$\begin{aligned} T [Q_{\Gamma\Gamma'}(x) \bar{\eta}_p(0)] = & -\frac{1}{2} \epsilon_{ijk} \epsilon_{abc} P_{\Gamma'} \left\{ (\bar{u}^a(0) \Gamma_A u^i(x)) \right. \\ & \times \left[ S_u^{kc}(x) \gamma_5 \tilde{S}_d^{jb}(x) P_\Gamma \Gamma^A + S_u^{kc}(x) \text{Tr} \left( \Gamma^A \gamma_5 \tilde{S}_d^{jb}(x) P_\Gamma \right) \right. \\ & \left. \left. + \Gamma^A \gamma_5 \tilde{S}_d^{jb}(x) P_\Gamma S_u^{kc}(x) + \Gamma^A \text{Tr} \left( S_u^{kc}(x) \gamma_5 \tilde{S}_d^{jb}(x) P_\Gamma \right) \right] \right. \\ & \left. + (\bar{d}^a(0) \Gamma_A d^i(x)) \left[ S_u^{kc}(x) \gamma_5 \tilde{\Gamma}^A P_\Gamma S_u^{jb}(x) + S_u^{kc}(x) \text{Tr} \left( S_u^{jb}(x) \gamma_5 \tilde{\Gamma}^A P_\Gamma \right) \right] \right\}. \end{aligned} \quad (4.17)$$

Here we have employed the following basis of gamma matrices

$$\Gamma_A = \left\{ \mathbb{1}, \gamma_5, \gamma^\rho, i\gamma^\rho \gamma_5, \frac{1}{\sqrt{2}} \sigma^{\rho\sigma} \right\}, \quad (4.18)$$

and we use the notation  $\tilde{\Gamma}_A \equiv C\Gamma_A^T C$  with  $C = i\gamma^2\gamma^0$  and a summation over the index  $A$  is implicit. The pairwise contraction of up (down) quark fields is denoted by  $S_u^{ij}(x)$  ( $S_d^{ij}(x)$ ),  $i, j, k$  are colour indices and  $\text{Tr}$  denotes a trace over Dirac matrices. Hereafter we will work in the isospin limit and will therefore drop the flavour index of the contraction.

With the help of (4.18) it is possible to derive the following completeness relation:

$$u(x)\bar{u}(0) = -\frac{1}{4}(\bar{u}(0)\Gamma_A u(x))\Gamma^A. \quad (4.19)$$

The contracted fields need to be expanded for light-like distances (including single-gluon emission), which reads [226]

$$S^{ij}(x) = \frac{i\not{x}}{2\pi^2 x^4} \delta^{ij} - \frac{ig_s}{16\pi^2 x^2} \int_0^1 du G_{\mu\nu}^{ij}(ux) [\bar{u}\not{x}\sigma^{\mu\nu} + u\sigma^{\mu\nu}\not{x}] + \dots, \quad (4.20)$$

where the ellipsis represents terms that lead to contributions of twist higher than three, we have employed the short-hand notation  $G_{\mu\nu}^{ij} \equiv G_{\mu\nu}^A T_A^{ij}$  for the gluon field strength tensor and defined  $\bar{u} \equiv 1-u$ . We neglect contributions proportional to the quark masses because they are numerically negligible. In the following we consider only single-gluon interactions which is consistent with truncating the expansion (4.14) after the leading-twist contribution [199]. This leads to the two types of one-loop diagrams that are displayed in the top row of Figure 4.1.

In addition to these LO terms factorised contributions of higher twist and multiplicity turn out to be numerically relevant in the case at hand. Such contributions originate from operators with four quark fields or four quark fields and one gluon, such that only one pair of quarks is contracted in the time-ordered product. Part of the respective amplitudes can be approximated by a factorisation into two- or three-particle DAs (of twist two and three) and vacuum condensates of the remaining quark and gluon fields. Such contributions scale with a smaller power of  $1/Q^2$  than genuine, non-factorisable terms of higher twist (as one might naively expect from the light-cone expansion (4.14)) and instead are suppressed by powers of  $1/M^2$  [227, 228]. Effectively, these factorised contributions can be taken into account by replacing one of the contractions  $S^{ij}(x)$  in the expression (4.17) by the appropriate local terms and condensates as encoded by [181]

$$\Delta S^{ij}(x) = -\frac{\langle\bar{q}q\rangle}{12} \delta^{ij} \left(1 + \frac{m_0^2 x^2}{16}\right) - \frac{ig_s}{32\pi^2 x^2} G_{\mu\nu}^{ij}(0) [\not{x}\sigma^{\mu\nu} + \sigma^{\mu\nu}\not{x}] + \dots \quad (4.21)$$

The ellipsis denotes higher-dimensional condensates and terms with additional gluons, which are neglected in our work because they are numerically small. The parameter  $m_0$  entering (4.21) is associated with the mixed condensate

$$\langle\bar{q}g_s G \cdot \sigma q\rangle = m_0^2 \langle\bar{q}q\rangle, \quad (4.22)$$

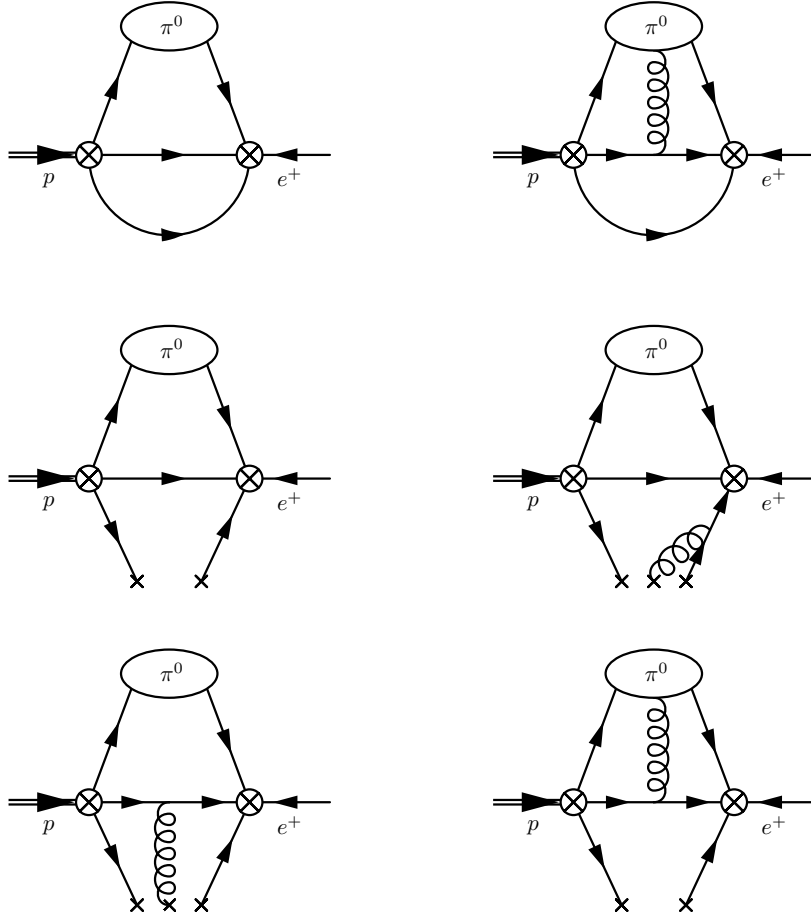


**Figure 4.1:** Feynman diagrams contributing to the light-cone expansion of (4.14) at the twist-2 and twist-3 level including factorised higher-twist contributions. The two vertices with a circled cross denote insertions of the currents  $Q_{\Gamma\Gamma'}(x)$  and  $\eta_p(0)$ . The external proton and positron lines are attached for illustration even though they do not enter the LCSR computation. The diagrams shown in the top row result from the light-cone expansion (4.20). The diagrams in the middle and bottom row instead originate from factorised higher-twist contributions, which involve the condensates  $\langle \bar{q}q \rangle$  and  $\langle \bar{q}g_s G \cdot \sigma q \rangle$  of (4.21) and (4.22) (crosses on the bottom of the diagram). See text for further details.

where  $G \cdot \sigma \equiv G_{\mu\nu} \sigma^{\mu\nu}$ . The diagrams resulting from the local expansion (4.21) of the contraction are displayed in the middle and bottom row of Figure 4.1.

The uncontracted quark bilinears in (4.17) form a pion and still need to be expanded around light-like distances to obtain the light-cone DAs. The pion DAs have been extensively studied in the literature (see [229] for a state-of-the-art discussion), and they have definite twist. The only twist-2 pion DA is given by (cf. for instance [200, 230])

$$\langle \pi^0(p_\pi) | \bar{q}(0) \gamma^\mu \gamma_5 \tau^3 q(x) | 0 \rangle = -\frac{i f_\pi}{\sqrt{2}} p_\pi^\mu \int_0^1 du e^{i\bar{u} p_\pi x} \phi^{(2)}(u, \mu), \quad (4.23)$$

#### 4.1 Semi-leptonic two-body proton decay modes

where  $q \equiv (u \ d)^T$  and  $\tau^3 \equiv \sigma^3/2$  with  $\sigma^3 = \text{diag}(1, -1)$  the third Pauli matrix, while  $f_\pi$  denotes the pion decay constant given by  $f_\pi = (130.2 \pm 0.8) \text{ MeV}$  [231].<sup>3</sup> The parameters  $u$  and  $\bar{u}$  correspond to the momentum fractions of the two quarks that form the pion. The renormalisation scale  $\mu$  that appears in the twist-2 pion DA  $\phi^{(2)}(u, \mu)$  is set equal to 1 GeV for most of this work. Higher-order contributions to the matrix element (4.23) arise at the twist-4 level. There are two two-particle twist-3 DAs called  $\phi_p^{(3)}(u, \mu)$  and  $\phi_\sigma^{(3)}(u, \mu)$ . These are defined by [200, 230]

$$\langle \pi^0(p_\pi) | \bar{q}(0) i\gamma_5 \tau^3 q(x) | 0 \rangle = \frac{f_\pi \mu_\pi}{\sqrt{2}} \int_0^1 du e^{i\bar{u}p_\pi x} \phi_p^{(3)}(u, \mu), \quad (4.24)$$

$$\begin{aligned} \langle \pi^0(p_\pi) | \bar{q}(0) \sigma^{\mu\nu} \gamma_5 \tau^3 q(x) | 0 \rangle &= -\frac{if_\pi \mu_\pi}{6\sqrt{2}} (1 - \rho_\pi^2) (p_\pi^\mu x^\nu - p_\pi^\nu x^\mu) \\ &\times \int_0^1 du e^{i\bar{u}p_\pi x} \phi_\sigma^{(3)}(u, \mu). \end{aligned} \quad (4.25)$$

We also include the only twist-3 three-particle DA called  $\mathcal{T}^{(3)}(\alpha_d, \alpha_u, \alpha_g, \mu)$ , which depends on the momentum fractions  $\alpha_d$ ,  $\alpha_u$  and  $\alpha_g$  of the down quark, up quark and gluon, respectively, as well as on  $\mu$ . This object is defined as follows [200, 230]

$$\begin{aligned} \langle \pi^0(p_\pi) | \bar{q}(0) \sigma^{\mu\nu} \gamma_5 g_s G^{\alpha\beta}(ux) \tau^3 q(x) | 0 \rangle &= \\ \frac{if_\pi \mu_\pi}{\sqrt{2}} \left( p_\pi^\alpha p_\pi^\mu \eta^{\nu\beta} - p_\pi^\alpha p_\pi^\nu \eta^{\mu\beta} + p_\pi^\beta p_\pi^\nu \eta^{\alpha\mu} - p_\pi^\beta p_\pi^\mu \eta^{\alpha\nu} \right) \\ \times \int_0^1 d\alpha_d d\alpha_u d\alpha_g \delta(1 - \alpha_d - \alpha_u - \alpha_g) e^{i(\alpha_u + u\alpha_g)p_\pi x} \mathcal{T}^{(3)}(\alpha_d, \alpha_u, \alpha_g, \mu). \end{aligned} \quad (4.26)$$

The normalisation of the twist-3 DAs contains the sum of the up- and down-quark mass, which fixes the values of the parameters  $\mu_\pi$  and  $\rho_\pi$  as well as the quark condensate via the Gell-Mann–Oakes–Renner (GMOR) relation  $m_\pi^2 \simeq -2(m_u + m_d) \langle \bar{q}q \rangle / f_\pi^2$  first derived in the article [232]. One obtains

$$\mu_\pi \equiv \frac{m_\pi^2}{m_u + m_d} \simeq -\frac{2 \langle \bar{q}q \rangle}{f_\pi^2}, \quad \rho_\pi \equiv \frac{m_u + m_d}{m_\pi} \simeq -\frac{f_\pi^2 m_\pi}{2 \langle \bar{q}q \rangle}. \quad (4.27)$$

The DAs can be obtained by a conformal expansion [200]. Explicit formulas for the DAs appearing in our work are provided in Appendix D.

Summing up all the contributions of Figure 4.1, using (4.23) to (4.26) and performing a Fourier integration allows us to derive an analytic expression for the QCD correlation function

$$\Pi_{\Gamma\Gamma'}^{\text{QCD}}(p_p, q) = P_{\Gamma'} \left( \Pi_{\Gamma\Gamma'}^{\text{QCD},S} + \frac{\not{p}_p}{m_p} \Pi_{\Gamma\Gamma'}^{\text{QCD},P} + \frac{\not{q}}{m_p} \Pi_{\Gamma\Gamma'}^{\text{QCD},Q} + \frac{i\sigma^{p_p q}}{m_p^2} \Pi_{\Gamma\Gamma'}^{\text{QCD},T} \right). \quad (4.28)$$

---

<sup>3</sup>We employ the Fock-Schwinger gauge, i.e.  $x^\mu G_\mu^A = 0$  with  $G_\mu^A$  the gluon field, such that the Wilson lines which enter the definition of the DAs are equal to 1.

#### 4 LCSRs for proton decay

The analytic expressions for the results of  $\Pi_{\Gamma\Gamma'}^{\text{QCD},\gamma}(p_p^2, Q^2)$  are somewhat lengthy and therefore provided in Appendix E. In the derivation of these results integrals of the following type are encountered

$$\int d^4x e^{iPx} \frac{x_\mu x_\nu \cdots}{(x^2)^n}, \quad \int d^4x e^{iP_g x} \frac{x_\mu x_\nu \cdots}{(x^2)^n}, \quad (4.29)$$

where the relevant momenta  $P \equiv q + \bar{u}p_\pi$  and  $P_g \equiv q + \alpha p_\pi$  with  $\alpha \equiv \alpha_u + u\alpha_g$  arise from combining the exponential factor in (4.5) with those of (4.23) to (4.26). The momentum dependence can be rewritten in terms of  $Q^2 = -q^2$  and  $P_p^2 = -p_p^2$  using

$$P^2 = (\bar{u}p_p + uq)^2 = -\bar{u}P_p^2 - u(Q^2 + \bar{u}m_\pi^2), \quad (4.30)$$

$$P_g^2 = (\alpha p_p + \bar{\alpha}q)^2 = -\alpha P_p^2 - \bar{\alpha}(Q^2 + \alpha m_\pi^2), \quad (4.31)$$

where we employ the notation  $\bar{z} \equiv 1 - z$  for the momentum fractions  $z = u$  and  $z = \alpha$ . The UV divergent Fourier integrals are carried out in dimensional regularisation (cf. Appendix C). In this step of the sum-rule calculation, the poles and the scheme-dependent constants can be dropped as long as we perform a Borel transformation in the end (cf. Section 3.1). Only inverse powers of the momenta, arising from finite integrals, and logarithms from the divergent integrals contribute to our sum rules.

For the matching with the hadronic representation (4.8), we also introduce QCD spectral densities like it was done in (4.9) and (4.10) for the hadronic case. The matching conditions for the LCSRs ( $\gamma = S, P, Q, T$ ) then read

$$\Pi_{\Gamma\Gamma'}^{\text{had},\gamma}(p_p^2, Q^2) \stackrel{!}{=} \Pi_{\Gamma\Gamma'}^{\text{QCD},\gamma}(p_p^2, Q^2). \quad (4.32)$$

Using the quark-hadron duality in the form (4.13), we can subtract the unknown contributions of heavy states from the LCSRs. Effectively, this procedure cuts off the spectral integral computed in QCD at the continuum threshold  $s_0$ . Applying a Borel transformation with respect to  $P_p^2$  to both sides of the sum rules suppresses heavy contributions exponentially and generically improves the accuracy of the LCSR approach — the accuracy of our LCSRs will be investigated in Section 4.1.3. The Borel transformations also remove all terms that are polynomial in  $P_p^2$ , which sets all divergent contributions of the dispersion integrals as well as the UV divergences of the diagrams in Figure 4.1 to zero; cf. Section 3.1. Moreover, only the imaginary parts of the correlation functions  $\Pi_{\Gamma\Gamma'}^{\text{QCD},\gamma}(s + i\epsilon, Q^2)$  enter the dispersion integrals (4.13), and eventually the  $s$ -integration has to be performed.

All the steps described above can be translated into replacement rules for the integrals over the momentum fraction. For the logarithmic terms we find

$$\int_0^1 du f(u) (P^2)^n \ln\left(\frac{-P^2}{\mu^2}\right) \rightarrow -n! \int_0^\Delta du f(u) (\bar{u}M^2)^n e(\tilde{s}) \tilde{E}_{n+1}(\tilde{s}), \quad (4.33)$$

#### 4.1 Semi-leptonic two-body proton decay modes

with  $\mu$  the renormalisation scale and  $f(u)$  some function which depends on the momentum fraction  $u$ . Here we have introduced

$$\Delta \equiv \frac{s_0 + Q^2 + m_\pi^2}{2m_\pi^2} \left( 1 - \sqrt{1 - \frac{4m_\pi^2 s_0}{(s_0 + Q^2 + m_\pi^2)^2}} \right), \quad (4.34)$$

$$e(s) \equiv e^{-\frac{s}{M^2}}, \quad \tilde{E}_n(s) \equiv E_n \left( \frac{s_0 - s}{M^2} \right), \quad \tilde{s} \equiv \frac{u}{\bar{u}} (Q^2 + \bar{u}m_\pi^2), \quad (4.35)$$

where

$$E_n(x) \equiv 1 - e^{-x} \sum_{k=0}^{n-1} \frac{x^k}{k!}. \quad (4.36)$$

The upper limit of the integration over  $u$  satisfies  $\Delta(Q^2 = 0) = 1 = \Delta(s_0 \rightarrow \infty)$  and  $\Delta \leq 1$ , and it arises because the dispersion integral only has support if  $s_0 \geq \tilde{s}$ .

For terms involving three-particle DAs one furthermore has

$$\begin{aligned} \int_0^1 D\alpha f(u, \alpha_u, \alpha_g) (P_g^2)^n \ln \left( \frac{-P_g^2}{\mu^2} \right) &\rightarrow -n! \int_0^1 D\alpha \theta(\alpha - \Delta_g) f(u, \alpha_u, \alpha_g) \\ &\times (\alpha M^2)^n e(\tilde{s}_g) \tilde{E}_{n+1}(\tilde{s}_g), \end{aligned} \quad (4.37)$$

where  $f(u, \alpha_u, \alpha_g)$  now depends on  $u$ ,  $\alpha_u$  and  $\alpha_g$ , and we have eliminated  $\alpha_d = 1 - \alpha_u - \alpha_g$ . We have furthermore used the abbreviation

$$D\alpha \equiv du d\alpha_u d\alpha_g \theta(1 - \alpha_u - \alpha_g) \quad (4.38)$$

for the integration measure. The integration boundaries are now modified by the Heaviside step function  $\theta(x)$ ,

$$\Delta_g \equiv \frac{s_0 + Q^2 - m_\pi^2}{2m_\pi^2} \left( \sqrt{1 + \frac{4m_\pi^2 Q^2}{(s_0 + Q^2 - m_\pi^2)^2}} - 1 \right), \quad \tilde{s}_g \equiv \frac{\bar{\alpha}}{\alpha} (Q^2 + \alpha m_\pi^2), \quad (4.39)$$

where  $\Delta_g(Q^2 = 0) = 0 = \Delta(s_0 \rightarrow \infty)$  and  $\Delta_g \geq 0$ . For the non-divergent contributions appearing in our LCSRs, we find

$$\int_0^1 du f(u) \frac{1}{P^2} \rightarrow -\frac{1}{M^2} \int_0^\Delta du \frac{f(u)}{\bar{u}} e(\tilde{s}), \quad (4.40)$$

$$\int_0^1 du f(u) \frac{1}{P^4} \rightarrow \frac{1}{M^4} \int_0^\Delta du \frac{f(u)}{\bar{u}^2} e(\tilde{s}) + \frac{f(\Delta)}{M^2 (Q^2 + \bar{\Delta}^2 m_\pi^2)} e(s_0), \quad (4.41)$$

$$\begin{aligned} \int_0^1 du f(u) \frac{1}{P^6} &\rightarrow -\frac{1}{2M^6} \int_0^\Delta du \frac{f(u)}{\bar{u}^3} e(\tilde{s}) - \frac{f(\Delta)}{2M^4 \bar{\Delta} (Q^2 + \bar{\Delta}^2 m_\pi^2)} e(s_0) \\ &- \frac{\bar{\Delta}^2}{2M^2 (Q^2 + \bar{\Delta}^2 m_\pi^2)} e(s_0) \frac{\partial}{\partial \Delta} \frac{f(\Delta)}{\bar{\Delta} (Q^2 + \bar{\Delta}^2 m_\pi^2)}, \end{aligned} \quad (4.42)$$

and for the three-particle integrals:

$$\int_0^1 D\alpha f(u, \alpha_u, \alpha_g) \frac{1}{P_g^2} \rightarrow -\frac{1}{M^2} \int_0^1 \frac{D\alpha}{\alpha} \theta(\alpha - \Delta_g) f(u, \alpha_u, \alpha_g) e(\tilde{s}_g), \quad (4.43)$$

$$\begin{aligned} \int_0^1 D\alpha f(u, \alpha_u, \alpha_g) \frac{1}{P_g^4} &\rightarrow \frac{1}{M^4} \int_0^1 \frac{D\alpha}{\alpha^2} \theta(\alpha - \Delta_g) f(u, \alpha_u, \alpha_g) e(\tilde{s}_g) \\ &+ \frac{1}{M^2} \int_0^1 du d\alpha_g \theta(1 - \bar{u}\alpha_g - \Delta_g) e(s_0) \\ &\times \frac{f(u, \Delta_g - u\alpha_g, \alpha_g)}{Q^2 + \Delta_g^2 m_\pi^2}. \end{aligned} \quad (4.44)$$

Finally, the matching conditions (4.32) take the form

$$i\lambda_p m_p^2 e^{-\frac{m_p^2}{M^2}} W_{\Gamma\Gamma'}^\gamma(s_0, Q^2) = \int_0^{s_0} ds e^{-\frac{s}{M^2}} \rho_{\Gamma\Gamma'}^{\text{QCD},\gamma}(s, Q^2), \quad (4.45)$$

where the expressions for the form factors  $W_{\Gamma\Gamma'}^\gamma(s_0, Q^2)$  can be found in (4.12) and the right-hand sides are given by the expressions of Appendix E when the replacement rules as described above are employed. By an appropriate combination of the four independent relations (4.45) one can derive two LCSRs for each of the two form factors appearing in (4.3). Hereafter we will refer to these combinations as  $W_{\Gamma\Gamma'}^{0,P}(s_0, Q^2)$ ,  $W_{\Gamma\Gamma'}^{0,S+T}(s_0, Q^2)$ ,  $W_{\Gamma\Gamma'}^{1,Q}(s_0, Q^2)$  and  $W_{\Gamma\Gamma'}^{1,T}(s_0, Q^2)$ . Notice that the LCSRs (4.45) depend on two unphysical parameters, namely the continuum threshold  $s_0$  and the Borel mass  $M$ . However, the results of a LCSR calculation can only be trusted if the final predictions are to a certain extent independent of the exact choice of  $s_0$  and  $M$ . In Section 4.1.3 we will provide criteria that allow us to assess the convergence properties of (4.45), which we will then use to estimate the uncertainties that plague our LCSR results for the form factors  $W_{\Gamma\Gamma'}^{n,\gamma}(Q^2)$ .

The coupling  $\lambda_p$  in (4.45) is in principle known from LQCD calculations (see [181] and references therein), but it can as well be extracted from local QCD sum rules of the two-point correlator

$$i \int d^4x e^{ipx} \langle 0 | T [\eta_p(x) \bar{\eta}_p(0)] | 0 \rangle = -\lambda_p^2 \frac{\not{p} + m_p}{p^2 - m_p^2 + i\epsilon} + \dots, \quad (4.46)$$

where the ellipsis denotes the contributions of heavier states. Using  $\lambda_p$  from sum rules has the salient advantage that in this way the uncertainties of the form factors due to the input parameters such as the quark condensate  $\langle \bar{q}q \rangle$  or  $m_0^2$  are reduced.<sup>4</sup> We therefore choose to fix  $\lambda_p$  with the help of sum-rule techniques rather than to take  $\lambda_p$  from LQCD

---

<sup>4</sup>In  $B$ -meson to light-meson transitions this procedure even leads to a partial cancellation of perturbative corrections, which improves the convergence of the sum rules [230].

computations. The sum rule derived from the structure  $\not{p}$  of the correlator (4.46) is typically disregarded due to uncontrollably large radiative corrections as well as large contributions from heavier states [181]; see also the discussion in Section 3.1 and references provided there for details. We thus extract  $\lambda_p$  from the sum rule for the mass term. As outlined in Section 3.1, the QCD result for the correlator (4.46) can be expressed in terms of an expansion in condensates with increasing mass dimension. In the following, contributions including condensates up to dimension seven are included but no perturbative QCD corrections. Using the proton current (4.16) yields [181]

$$\lambda_p^2 = -\frac{\langle \bar{q}q \rangle}{16\pi^2 m_p^3} e^{\frac{m_p^2}{\bar{M}^2}} \left[ 7\bar{M}^4 E_2\left(\frac{\bar{s}_0}{\bar{M}^2}\right) - 3m_0^2 \bar{M}^2 E_1\left(\frac{\bar{s}_0}{\bar{M}^2}\right) + \frac{19\pi^2}{18} \left\langle \frac{\alpha_s}{\pi} G^2 \right\rangle \right] \quad (4.47)$$

with  $\alpha_s \equiv g_s^2/(4\pi)$ ,  $G^2 \equiv G_{\mu\nu}^A G^{A,\mu\nu}$ , where the definition of  $E_n(x)$  can be found in (4.36). The parameters  $\bar{s}_0$  and  $\bar{M}$  denote the continuum threshold and the Borel mass of the local sum rule (4.47). These parameters can be related to the corresponding parameters of the LCSRs, because the Borel mass is connected to the momentum flow through the proton current. However, we assume for simplicity that  $\bar{s}_0$  and  $\bar{M}$  are independent parameters and determine them such that the value of  $\lambda_p$  does not depend too strongly on the specific choice.

Notice finally that the sign of  $\lambda_p$  is not fixed by (4.47). More generally, the sign of  $\lambda_p$  depends on the (unphysical) phase of the nucleon wave function. The same holds for the overall sign of the form factors  $W_{\Gamma\Gamma'}^{n,\gamma}(s_0, Q^2)$  that are determined from (4.45). The relative sign between  $W_{\Gamma\Gamma'}^0(Q^2)$  and  $W_{\Gamma\Gamma'}^1(Q^2)$  is however fixed by our sum rules. In the following, we will choose a negative sign for the coupling strength of the proton current, i.e. we will use  $\lambda_p < 0$ .

### 4.1.3 Numerical analysis

To derive physical predictions from (4.45), we need to find regions where the LCSRs converge sufficiently fast as an expansion in  $\Lambda_{\text{QCD}}^2/Q^2$  and  $\Lambda_{\text{QCD}}^2/M^2$  and where the sum rules are to a certain extent insensitive to the choice of the continuum threshold  $s_0$  and the Borel mass  $M$ . Therefore, the Borel mass  $M$  has to be chosen well above the QCD scale  $\Lambda_{\text{QCD}}$  but at the same time below the mass of the lightest excitation. These conditions are formulated more precisely in the following, and they lead to a set of requirements which are then applied to each of the four LCSRs (4.45) as well as the local sum rule (4.47).

In order to eliminate contributions other than the proton in our sum-rule calculations [141], we use  $s_0 = \bar{s}_0 = (1.44 \text{ GeV})^2$  as a central value in all cases. This value of the continuum threshold  $s_0$  corresponds to the mass of the lightest excited state in the nucleon spectrum, i.e. the Roper resonance. We then vary  $s_0$  (and  $\bar{s}_0$ ) between

$(1.4 \text{ GeV})^2$  and  $(1.5 \text{ GeV})^2$  to estimate the uncertainty related to the choice of the continuum threshold. A similar procedure has been adopted in [233, 234], and our choice can be further motivated by the observation that for values in this interval, the sum rule (4.47) leads to a good agreement with the LQCD results for  $\lambda_p$  (see for instance [218, 235–237]).

A lower bound on  $M$  is determined by demanding sufficient suppression of higher powers in the OPE. In particular, we require that the contribution of the highest dimensional condensate in each LCSR does not amount to more than approximately 30% of the total QCD result. An upper limit on  $M$  is instead obtained by demanding that the ground-state contribution in the hadronic representation constitutes at least 50% of the dispersion integral. In other words the contributions of the heavy states, which we model by the QCD result, are smaller or equal than approximately 50% of the total result,

$$\frac{\left| P_{\Gamma\Gamma'}^{\text{QCD},\gamma}(s_0, \infty) \right|}{\left| P_{\Gamma\Gamma'}^{\text{QCD},\gamma}(0, \infty) \right|} \lesssim 0.5, \quad (4.48)$$

with

$$P_{\Gamma\Gamma'}^{\text{QCD},\gamma}(s_1, s_2) = \int_{s_1}^{s_2} ds \frac{\rho_{\Gamma\Gamma'}^{\text{QCD},\gamma}(s, Q^2)}{s - p_p^2}. \quad (4.49)$$

We then vary the Borel mass  $M$  in this so obtained Borel window to estimate the systematic uncertainty related to the variation of this unphysical parameter.

The physical values of the form factors do not depend on the choice of the continuum threshold  $s_0$  or the Borel mass  $M$ . The residual dependence of the form factors extracted from the LCSRs on these parameters originates from the truncation of the expansion in  $\Lambda_{\text{QCD}}^2/M^2$  at a finite order and the effective description of the a priori unknown contributions of heavy states. Therefore, the predictions of the sum rules are reliable if the dependence on the unphysical parameters is weak, and thus the uncertainties related to the variation of these parameters also quantifies the validity of the predictions.

In order to illustrate the latter statements we show in Figure 4.2 and Figure 4.3 the dependence of the form factors  $W_{RR}^{0,S+T}(s_0, Q^2)$  and  $W_{LR}^{1,Q}(s_0, Q^2)$  on the Borel mass  $M$ , respectively. In each panel predictions are displayed for the following three different values of the continuum threshold  $s_0 = (1.4 \text{ GeV})^2$  (dashed lines),  $s_0 = (1.44 \text{ GeV})^2$  (solid lines) and  $s_0 = (1.5 \text{ GeV})^2$  (dotted lines), and each figure contains results where the form factors are evaluated at  $Q^2 = 0.5 \text{ GeV}^2$  (left panels) and  $Q^2 = 2 \text{ GeV}^2$  (right panels). The shown predictions have been obtained for the central values of the input parameters as given in (4.50) to (4.52) and (D.5) to (D.7). One sees that for very small values of  $M$  the form factors steeply increase because the power suppression in  $1/M^2$  becomes ineffective. On the other hand, for large values of  $M$  the exponential suppres-

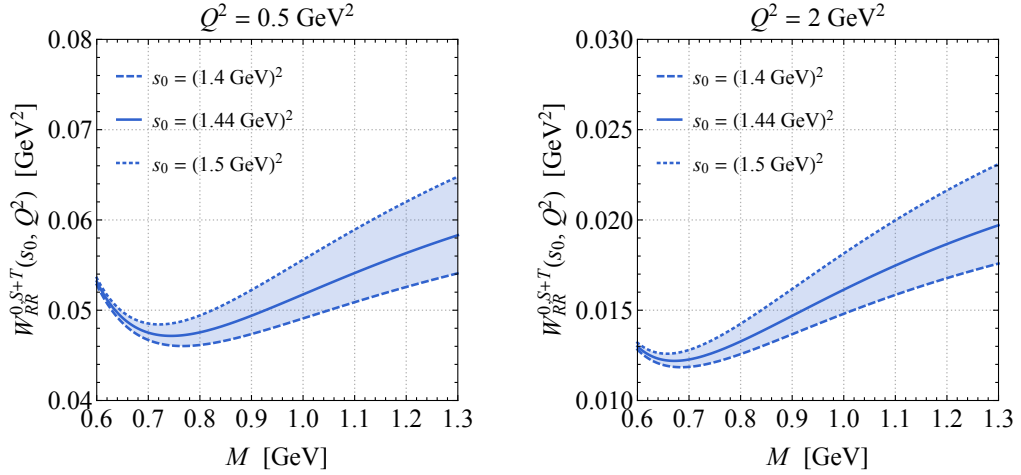


**Figure 4.2:** Form factor  $W_{RR}^{0,S+T}(s_0, Q^2)$  as a function of the Borel mass  $M$  for three values of the continuum threshold  $s_0$ . The left (right) plot shows the results at  $Q^2 = 0.5 \text{ GeV}^2$  ( $Q^2 = 2 \text{ GeV}^2$ ).

sion of heavier states due to the factor  $e^{-s/M^2}$  in the dispersion integrals (4.45) is not present. This in turn leads to a stronger sensitivity on  $M$  such that the form factors increase again for larger Borel masses. The sensitivity to the continuum threshold is also more pronounced if  $M$  gets closer to  $s_0$ , as indicated by the widening of the coloured bands in Figures 4.2 and 4.3. One can furthermore observe that the sensitivity on the unphysical parameters becomes stronger for larger values of  $Q^2$ . We remark that for  $Q^2 \gtrsim 2 \text{ GeV}^2$  this effect saturates such that the plots on the right-hand side of Figures 4.2 and 4.3 represent in a sense worst-case scenarios. The results of the other LCSRs behave similarly to  $W_{RR}^{0,S+T}(s_0, Q^2)$  and  $W_{LR}^{1,Q}(s_0, Q^2)$ , so we do not show their dependence on  $M$  explicitly.

By considering the momentum range  $0.5 \text{ GeV}^2 \leq Q^2 \leq 2.5 \text{ GeV}^2$ , we find the Borel windows  $0.7 \text{ GeV} \leq M \leq 1.1 \text{ GeV}$  for the LCSRs with  $\gamma = S, Q, T$  and  $\Gamma\Gamma' = RR$  and  $0.7 \text{ GeV} \leq M \leq 1 \text{ GeV}$  for the LCSRs with  $\gamma = S, Q, T$  and  $\Gamma\Gamma' = LR$ . The LCSRs for the structure  $\gamma = P$  do not meet the above requirements in the  $Q^2$  region of interest, because the contributions of heavy states are large and even dominate the sum rules for certain values of  $Q^2$ . In order to have one common Borel window for each chirality combination, we also choose in the case  $\gamma = P$  either  $0.7 \text{ GeV} \leq M \leq 1.1 \text{ GeV}$  or  $0.7 \text{ GeV} \leq M \leq 1 \text{ GeV}$  as our Borel window when studying the  $Q^2$  dependence of  $W_{\Gamma\Gamma'}^{0,P}(Q^2)$ .

In our numerical analysis of the LCSRs we make use of  $(m_u + m_d)/2 = (3.410 \pm 0.043) \text{ MeV}$  [231] which corresponds to the  $\overline{\text{MS}}$  value at  $2 \text{ GeV}$ . Using the two-loop RG

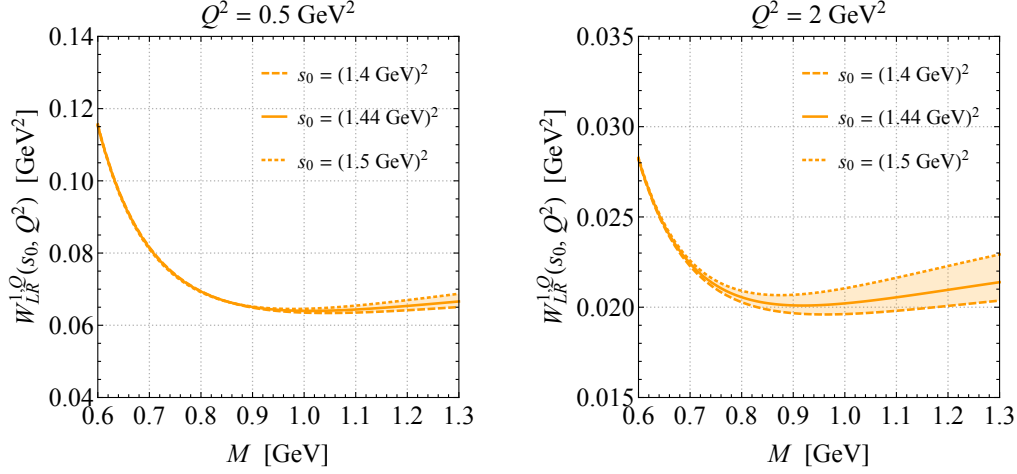


**Figure 4.3:** As Figure 4.2 but for the form factor  $W_{LR}^{1,Q}(s_0, Q^2)$ .

running and the one-loop threshold corrections as implemented in `RunDec` [238, 239], we obtain at 1 GeV the value  $m_u + m_d = (8.60 \pm 0.11)$  MeV. Employing the GMOR relation this value leads to

$$\langle \bar{q}q \rangle = -((256 \pm 2) \text{ MeV})^3, \quad (4.50)$$

if the LO chiral corrections of [240] are included and uncertainties are added in quadrature. For the non-perturbative parameters defined in (4.27) we then find

$$\mu_\pi = (1.98 \pm 0.05) \text{ GeV}, \quad \rho_\pi = 0.068 \pm 0.002. \quad (4.51)$$

The parameter  $m_0$  for the mixed condensate as well as the pure-gluon condensate are known from sum-rule estimates evaluated at 1 GeV. We will use the values and uncertainties from [241] which are widely accepted. The relevant numbers read

$$m_0^2 = (0.8 \pm 0.2) \text{ GeV}^2, \quad \left\langle \frac{\alpha_s}{\pi} G^2 \right\rangle = (0.009 \pm 0.009) \text{ GeV}^4. \quad (4.52)$$

We remark that using (4.52) the local QCD sum rule (4.47) agrees with the LQCD results for  $\lambda_p$  within uncertainties (cf. Table I of [181]). The corresponding Borel window is  $0.7 \text{ GeV} \leq \bar{M} \leq 1 \text{ GeV}$ . The central values and uncertainties of the parameters that enter the definitions of the twist-2 and twist-3 pion DAs can be found in (D.5), (D.6) and (D.7).

After having explained how we choose the continuum thresholds and the Borel mass windows and having specified the numerical values of the input parameters, we are in a position to present the results of our LCSR analysis. Our results for the form factors  $W_{RR}^{n,\gamma}(Q^2)$  and  $W_{LR}^{n,\gamma}(Q^2)$  are shown in Figure 4.4 and Figure 4.5 as coloured

lines and bands, respectively. The predictions in the range  $0.5 \text{ GeV}^2 \leq Q^2 \leq 2.5 \text{ GeV}^2$  result from a direct evaluation of (4.45). The solid curves correspond to the results obtained for the central values of the unphysical and physical parameters, while the bands represent the corresponding theoretical uncertainties. The latter are determined by varying all input parameters independently within their allowed ranges and adding individual uncertainties in quadrature.<sup>5</sup> For  $Q^2 \leq 0.5 \text{ GeV}^2$  we instead rely on an extrapolation. Specifically, we consider both a linear and a quadratic fit in  $Q^2$  to the LCSR form factors  $W_{\Gamma\Gamma'}^{n,\gamma}(Q^2)$  evaluated in the vicinity of  $Q^2 = 0.6 \text{ GeV}^2$ , and take the smallest and largest values of the fits at each  $Q^2$  to obtain the displayed uncertainty bands. The results of the quadratic fit to our central form-factor predictions are indicated as dashed lines. For comparison we also show the values of  $W_{\Gamma\Gamma'}^n(Q^2)$  determined in the recent LQCD study [223]. The numbers given in this article correspond to the  $\overline{\text{MS}}$  form factors evaluated at  $2 \text{ GeV}$  and we use the two-loop RG running (cf. [217, 242]) of (2.13) to evolve the form factors down to  $1 \text{ GeV}$ . The shown single (double) error bars represent the statistical (total) uncertainties of the LQCD predictions. Notice that the LQCD uncertainties at the physical point, i.e.  $Q^2 \simeq 0$ , are dominantly of systematic origin.

As explained before, based on our study of the Borel windows we expect the LCSR prediction for  $W_{\Gamma\Gamma'}^{0,P}(Q^2)$  to be less reliable than the other results because of the large contributions of heavy states. Indeed, when comparing the results of  $W_{\Gamma\Gamma'}^{0,P}(Q^2)$  and  $W_{\Gamma\Gamma'}^{0,S+T}(Q^2)$  as shown in Figures 4.4 and 4.5, one finds that  $W_{\Gamma\Gamma'}^{0,S+T}(Q^2)$  is closer to the LQCD predictions than  $W_{\Gamma\Gamma'}^{0,P}(Q^2)$  for both chirality combinations, and that  $W_{LR}^{0,S+T}(Q^2)$  itself agrees well with the LQCD calculation within uncertainties. One also observes from Figure 4.4 that the LCSR predictions for the modulus of  $W_{RR}^{n,\gamma}(Q^2)$  tend to undershoot the LQCD results. An exhaustive comparison to the shown LQCD results for  $Q^2 \gtrsim 0.5 \text{ GeV}^2$  would require knowledge about the systematic uncertainties of the LQCD calculations for non-zero  $Q^2$ . A full error budget is in Tables 4 and 5 of the work [223] however provided only for  $Q^2 \simeq 0$ . Notice that if the systematic uncertainties at  $Q^2 \gtrsim 0.5 \text{ GeV}^2$  were comparable to the systematic uncertainties at  $Q^2 \simeq 0$ , our LCSR results might in fact overlap with the displayed LQCD predictions for  $Q^2 \gtrsim 0.5 \text{ GeV}^2$ .

The observed differences between the LCSR and the LQCD results may be related to higher-twist effects. In order to examine this issue, we have calculated the twist-4 corrections to (4.23), which is the only two-particle twist-4 correction [199], using the hadronic input parameters provided in [243]. We find that for  $Q^2 = 0.5 \text{ GeV}^2$  the relative corrections to the values of the form factors shown in Figure 4.4 amount

---

<sup>5</sup>Since we use the pion decay constant  $f_\pi$  and the condensate  $\langle \bar{q}q \rangle$  as input parameters the uncertainties of  $\mu_\pi$  and  $\rho_\pi$  (cf. (4.51)) are not separately included when calculating the total uncertainties.

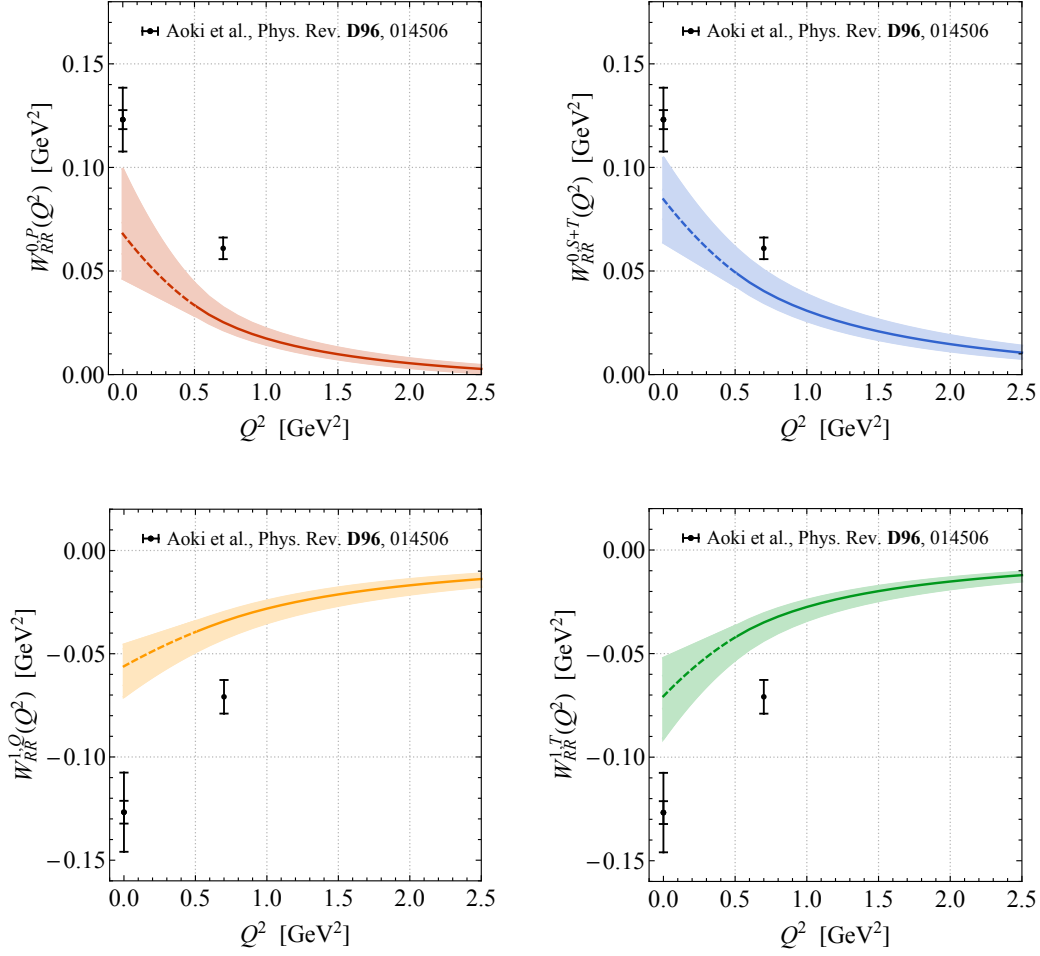


**Figure 4.4:** Form factors  $W_{RR}^{n,\gamma}(Q^2)$  as a function of  $Q^2$ . The coloured curves and bands correspond to the central values and uncertainties of the four independent LCSRs (4.45). The predictions for  $0.5 \text{ GeV}^2 \leq Q^2 \leq 2.5 \text{ GeV}^2$  are obtained by a direct calculation (solid lines), while the predictions for  $Q^2 \leq 0.5 \text{ GeV}^2$  are obtained by an extrapolation (dashed lines). The black dots display the central values of the form factors calculated in LQCD [223]. The associated single (double) error bars represent statistical (total) uncertainties. Consult the main text for further information.

to 38% for  $W_{RR}^{0,P}$ , 5% for  $W_{RR}^{0,S+T}$ , 51% for  $W_{RR}^{1,Q}$  and 26% for  $W_{RR}^{1,T}$ . Other twist-4 corrections to the LCSRs arise from additional three-particle DAs (see [200, 230] for details), and depending on their size and sign the actual effect of twist-4 corrections may be notably different from the numbers quoted here. Nevertheless, the corrections we have computed are larger for the vectorial structures than for the scalar and tensor structure. This could explain why our LCSR calculation of  $W_{RR}^{n,\gamma}(Q^2)$  seems to work better for  $\gamma = S + T, T$  than for  $\gamma = P, Q$ . As a comparison, the two-particle twist-4

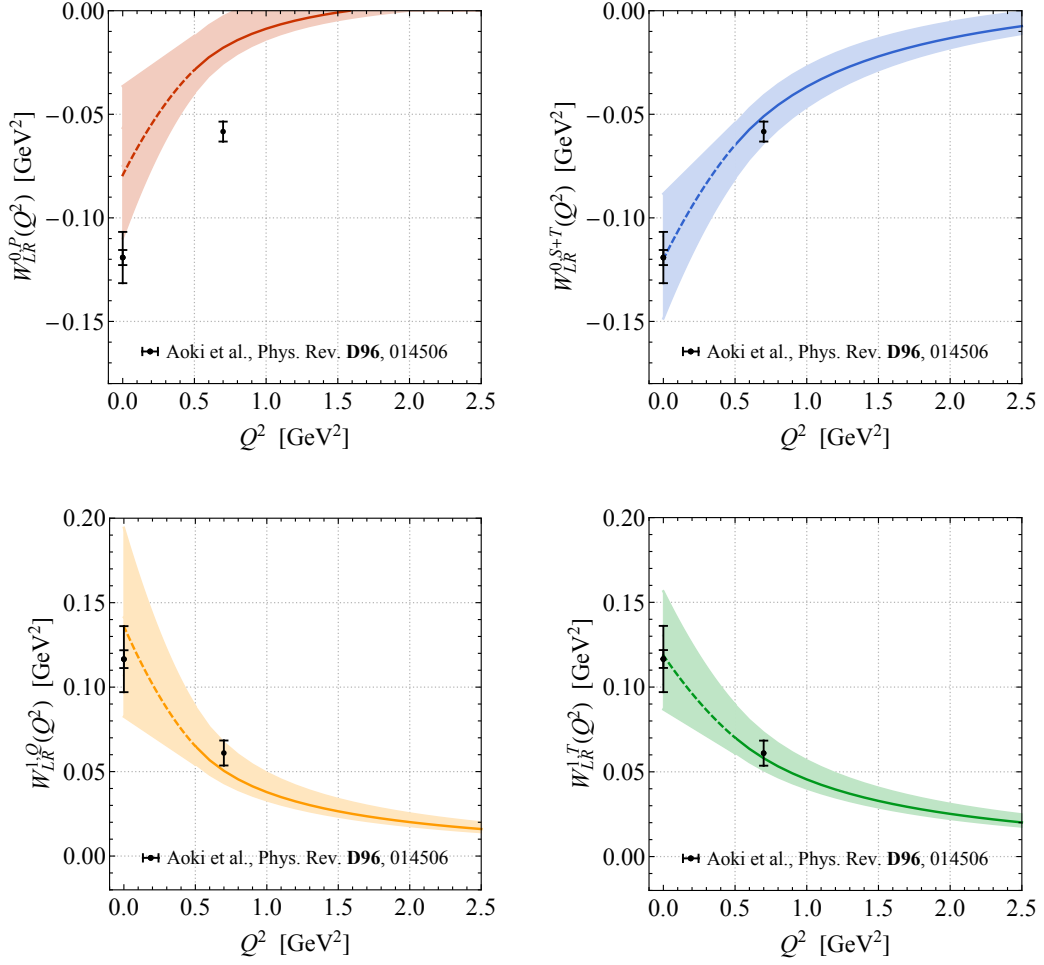


**Figure 4.5:** As Figure 4.4 but for the form factors  $W_{LR}^{n,\gamma}(Q^2)$ .

contributions to the form factor values shown in Figure 4.5 amount to 22% for  $W_{LR}^{0,P}$ , 7% for  $W_{LR}^{0,S+T}$ , 12% for  $W_{LR}^{1,Q}$  and 31% for  $W_{LR}^{1,T}$  at  $Q^2 = 0.5 \text{ GeV}^2$ . In this case the tensor structure receives a larger correction than the vectorial structures, but overall the twist-4 corrections seem to be better under control for  $\Gamma\Gamma' = LR$  than for  $\Gamma\Gamma' = RR$ . This may explain why the LCSR predictions for  $W_{LR}^{n,\gamma}(Q^2)$  are in general in good agreement with the LQCD results. In conclusion, we expect that uncertainties due to higher twist are minor for  $Q^2 \gtrsim 1 \text{ GeV}^2$ , while in the range  $0.5 \text{ GeV}^2 \lesssim Q^2 \lesssim 1 \text{ GeV}^2$ , twist-4 corrections may in the case  $\Gamma\Gamma' = RR$  account for the differences between our LCSR predictions and the corresponding LQCD results. Notice that on general grounds one would expect that the total uncertainties of the LCSRs become larger for decreasing values of  $Q^2$ , because the power suppression in  $\Lambda_{\text{QCD}}^2/Q^2$  of the light-cone expansion (4.14) starts to become ineffective. In the plots of Figures 4.4 and 4.5 this

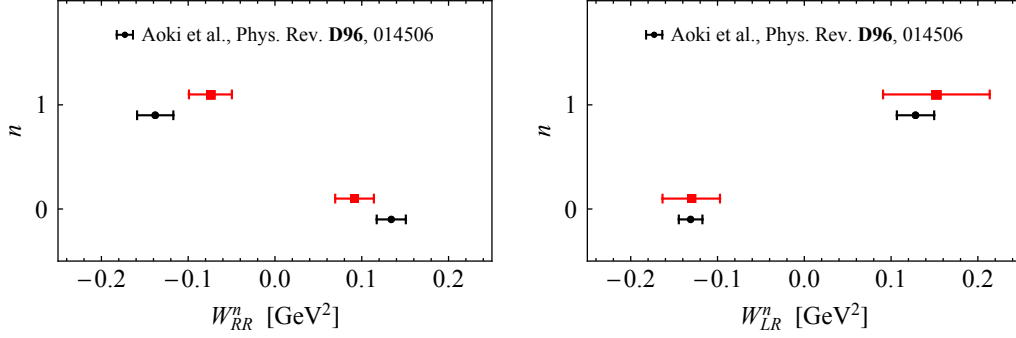


**Figure 4.6:** Comparison between the physical form factors  $W_{RR}^n$  (left) and  $W_{LR}^n$  (right) obtained by our LCSRs (red squares and error bars) and the state-of-the-art LQCD calculation (black dots and error bars) [223]. The shown results correspond to the  $\overline{\text{MS}}$  scheme renormalised at 2 GeV. See main text for additional details.

effect is mimicked by our extrapolation procedure that leads to larger total uncertainties for  $Q^2 \lesssim 0.5 \text{ GeV}^2$ .

The physical form factors  $W_{\Gamma\Gamma'}^0 \equiv W_{\Gamma\Gamma'}^0(Q^2 \simeq 0)$  can be extracted from both the LCSRs for  $W_{\Gamma\Gamma'}^{0,P}(Q^2)$  and  $W_{\Gamma\Gamma'}^{0,S+T}(Q^2)$ , while in the case of  $W_{\Gamma\Gamma'}^1 \equiv W_{\Gamma\Gamma'}^1(Q^2 \simeq 0)$  one can consider the two independent combinations  $W_{\Gamma\Gamma'}^{1,Q}(Q^2)$  and  $W_{\Gamma\Gamma'}^{1,T}(Q^2)$ . Since we believe that the LCSR for  $W_{\Gamma\Gamma'}^{0,P}(Q^2)$  is unreliable, we determine  $W_{\Gamma\Gamma'}^0$  from the full range of solutions for  $W_{\Gamma\Gamma'}^{0,S+T}(0)$ . The prediction for the form factor  $W_{\Gamma\Gamma'}^1$  is instead obtained from the extrapolations leading to  $W_{\Gamma\Gamma'}^{1,Q}(0)$  and  $W_{\Gamma\Gamma'}^{1,T}(0)$ , because in this case the different LCSR estimates result in quite similar numerical predictions (see Figures 4.4 and 4.5). At a renormalisation scale of 1 GeV, we obtain in this way the following central values and uncertainties:

$$W_{RR}^0 = (0.084 \pm 0.021) \text{ GeV}^2, \quad W_{RR}^1 = (-0.068 \pm 0.023) \text{ GeV}^2, \quad (4.53)$$

$$W_{LR}^0 = (-0.118 \pm 0.030) \text{ GeV}^2, \quad W_{LR}^1 = (0.14 \pm 0.06) \text{ GeV}^2. \quad (4.54)$$

Our LCSR predictions have total uncertainties of around (25 – 40)%. In Figure 4.6 we compare the results (4.53) and (4.54) evolved to 2 GeV to the corresponding LQCD predictions [223]. Notice that two-loop RG effects (see [217, 242]) lead to an enhancement of the LCSR results by 8.9% and 9.9%, respectively. From the two panels it is evident that while the LCSR approach does not achieve the (10 – 15)% accuracy of the latest LQCD computations of the form factors  $W_{\Gamma\Gamma'}^n$ , the overall agreement between our LCSR predictions and the latest LQCD results is quite compelling.

## 4.2 Semi-leptonic three-body proton decay modes

While for all two-body proton decays into anti-leptons and pseudoscalar mesons, LQCD techniques nowadays enable direct computations of the relevant hadronic matrix elements within uncertainties of  $(10 - 15)\%$  [217–224], LQCD calculations of three-body decay modes do not exist at present although the formalism and methodologies are in principle known [104]. Model estimates of three-body final-state proton decay rates are therefore available only for selected modes [225] or rely on NDA and phase-space arguments [124, 125]. In Section 4.1 it was shown that by employing LCSRs it is possible to reproduce the LQCD results for the hadronic matrix elements relevant for GUT-like proton decay. The goal of this Section is to extend the LCSR formalism developed in the previous Section to the case of semi-leptonic three-body proton decay processes. In particular, we will describe in detail the calculation of all form factors needed to compute the differential decay rate for the process  $p \rightarrow e^+ \pi^0 G$  with  $G$  denoting a graviton. This decay mode is the leading proton decay channel in the effective theory that describes the interactions of gravitons and SM particles aka GRSMEFT [28, 29]. Of all possible laboratory probes of the GRSMEFT proton decay measurements are expected to set the nominally strongest bound on the effective mass scale that suppresses the GRSMEFT interactions. While this work focuses on obtaining predictions for  $p \rightarrow e^+ \pi^0 G$ , the provided analytic expressions and numerical results allow computations of the differential decay rates of other semi-leptonic three-body proton decay modes as well.

This Section is structured as follows. In Section 4.2.1 the calculation of the relevant hadronic matrix elements using LCSR techniques is outlined, while the structure of the resulting LCSRs is discussed in Section 4.2.2. We turn to the numerical evaluation of the LCSRs in Section 4.2.3, providing predictions and uncertainty estimates for the proton-to-pion form factors in the physical region. Section 4.2.4 provides a cross-check on the LCSR results for the form factors; the hadronic form factors derived for the matrix element of the semi-leptonic three-body decay  $p \rightarrow e^+ \pi^0 G$  can actually be related to the two form factors that parametrise the two-body decay  $p \rightarrow e^+ \pi^0$  if only right-handed fields are considered at the partonic level. Since the results for the latter channel agreed with state-of-the-art lattice computations (cf. Section 4.1.3), the comparison presented in Section 4.2.4 validates the LCSR results presented in the following. Analytical expressions for the LCSRs are displayed in Appendix F.

### 4.2.1 Hadronic form factors

In what follows we discuss the necessary steps to calculate the hadronic part of the  $p \rightarrow \pi^0 e^+ G$  amplitude with the help of LCSRs in QCD. We employ the notation and

#### 4 LCSRs for proton decay

conventions introduced in Section 4.1. The starting point for the sum rules is the correlation function

$$\Pi_{\mu\nu}(p_p, q) = i \int d^4x e^{iqx} \langle \pi^0(p_\pi) | T [Q_{\mu\nu}(x) \bar{\eta}_p(0)] | 0 \rangle, \quad (4.55)$$

where the proton current  $\eta_p$  and the coupling strength  $\lambda_p$  of the current to the physical proton state are defined in equation (4.6). The strongly-interacting part of the dimension-eight operator (2.21) is encoded by

$$Q_{\mu\nu}(x) \equiv \epsilon^{abc} (d_a^T(x) C \sigma_{\mu\nu} P_R u_b(x)) P_R u_c(x). \quad (4.56)$$

By following the standard procedure the hadronic representation of the sum rules can be cast into the form

$$\Pi_{\mu\nu}^{\text{had}}(p_p, q) = -\frac{m_p}{p_p^2 - m_p^2 + i\epsilon} \lambda_p H_{\mu\nu}(p_p, q) (\not{p}_p + m_p) + \dots, \quad (4.57)$$

with  $\epsilon > 0$  and infinitesimal, and the ellipsis denotes contributions from heavier states, i.e. excited states and the continuum. The hadronic tensor  $H_{\mu\nu}(p_p, q)$  that characterises the  $p \rightarrow \pi^0$  transition can be parameterised by four independent form factors  $w_n$  with  $n = 1, 2, 3, 4$  in the following way

$$\begin{aligned} H^{\mu\nu}(p_p, q) u_p(p_p) &\equiv \langle \pi^0(p_\pi) | \epsilon^{abc} (d_a^T C \sigma^{\mu\nu} P_R u_b) P_R u_c | p(p_p) \rangle \\ &= P_R \left[ \left( i\epsilon^{\mu\nu p_p q} + 2p_p^{[\mu} q^{\nu]} \right) \frac{w_1}{m_p^2} + i\sigma^{p_p q} \left( i\epsilon^{\mu\nu p_p q} + 2p_p^{[\mu} q^{\nu]} \right) \frac{w_2}{m_p^4} \right. \\ &\quad \left. + 2i \left( p_p^{[\mu} \sigma^{\nu]q} - q^{[\mu} \sigma^{\nu]p_p} \right) \frac{w_3}{m_p^2} + i\sigma^{\mu\nu} w_4 \right] u_p(p_p). \end{aligned} \quad (4.58)$$

Here the proton spinor is understood to be on-shell, the fully antisymmetric Levi-Civita tensor is defined with the convention  $\epsilon^{0123} = +1$  and we have introduced the abbreviations  $\sigma^{\mu p} \equiv \sigma^{\mu\nu} p_\nu$ ,  $\sigma^{pq} \equiv \sigma^{\mu\nu} p_\mu q_\nu$  and  $\epsilon^{\mu\nu pq} \equiv \epsilon^{\mu\nu\rho\sigma} p_\rho q_\sigma$ .

The decomposition (4.58) can be derived in the following way. One first notices that only three types of Lorentz structures can occur in the square brackets of (4.58), namely scalar, vector and tensor structures which are proportional to the Dirac matrices  $\mathbb{1}$ ,  $\gamma^\rho$  and  $\sigma^{\rho\sigma}$ . With the help of the Dirac equation all vector structures can be turned into scalar or tensor ones because one can always insert a factor of  $\not{p}_p/m_p$  in front of the on-shell spinor  $u_p(p_p)$ . The only available objects for constructing Lorentz tensors which are antisymmetric under the exchange of  $\mu$  and  $\nu$  are therefore  $\eta^{\rho\sigma}$ ,  $p_p^\rho$ ,  $q^\rho$ ,  $\epsilon^{\rho\sigma\alpha\beta}$  and  $\sigma^{\rho\sigma}$ , where the metric tensor  $\eta^{\rho\sigma}$  here is only used to contract the indices of the other building blocks. The hadronic tensor furthermore has to fulfil the duality relation

$$\tilde{H}^{\mu\nu} \equiv \frac{i}{2} \epsilon^{\mu\nu\rho\sigma} H_{\rho\sigma} = H^{\mu\nu}, \quad (4.59)$$

## 4.2 Semi-leptonic three-body proton decay modes

which the first line of (4.58) satisfies because

$$\gamma_5 \sigma^{\mu\nu} = \frac{i}{2} \epsilon^{\mu\nu\rho\sigma} \sigma_{\rho\sigma}. \quad (4.60)$$

Regarding the scalar structures, the only combination of  $p_p^\rho$ ,  $q^\sigma$  and  $\epsilon^{\rho\sigma\alpha\beta}$  that satisfies the constraint (4.59) is the one in (4.58) that is multiplied by the form factor  $w_1$ . Notice that for constructing all possible tensor structures one can remove any occurrence of the Levi-Civita tensor because with the help of (4.60) one can always generate a second Levi-Civita tensor. The product of the two Levi-Civita tensors furthermore can be reduced to factors of the metric tensor. This implies that all possible tensor structures can be constructed entirely from  $\sigma^{\rho\sigma}$  and the two four-momenta  $p_p^\rho$  and  $q^\sigma$ . Exhausting all possibilities, one finds six Lorentz structures with the appropriate transformation property under the exchange of the two Lorentz indices:

$$\{X_m^{\mu\nu}\} \equiv \left\{ q^{[\mu} \sigma^{\nu]q}, \quad p_p^{[\mu} \sigma^{\nu]p_p}, \quad q^{[\mu} \sigma^{\nu]p_p}, \quad p_p^{[\mu} \sigma^{\nu]q}, \quad p_p^{[\mu} q^{\nu]} \sigma^{p_p q}, \quad \sigma^{\mu\nu} \right\}, \quad (4.61)$$

where the square brackets around the Lorentz indices denote anti-symmetrisation (cf. Section 2.4). The last of the above structures satisfies  $P_R \tilde{X}_6^{\mu\nu} = P_R X_6^{\mu\nu}$  and thus it can be chosen as one of the basis elements in the tensor decomposition (4.58). This leads to the form factor  $w_4$ . Now, the only remaining task is to find a linear combination

$$X^{\mu\nu} \equiv \sum_{m=1}^5 a_m X_m^{\mu\nu}, \quad (4.62)$$

of the first five structures of (4.61) that satisfies the duality condition (4.59). This leads to relations among the coefficients  $a_m$  but leaves two linear combinations unconstrained, implying the existence of two more independent form factors. The actual expressions are somewhat lengthy, but a much more compact form can be obtained by noting that  $X_1^{\mu\nu}$  and  $X_2^{\mu\nu}$  occur as a combination that can be replaced by a sum of  $\epsilon^{\mu\nu p_p q} \sigma^{p_p q}$  and the structures  $X_m^{\mu\nu}$  with  $m \neq 1, 2$ . In this way one ends up with two more independent Lorentz structures in (4.58) which define the form factors  $w_2$  and  $w_3$ . We add that after making use of the Dirac equation and algebraic identities the result (4.58) matches the decomposition provided in [244, 245].

With the help of the decomposition (4.58) the hadronic representation of the correlation function (4.57) can be written as

$$\begin{aligned} \Pi_{\mu\nu}^{\text{had}}(p_p, q) = & P_R \left[ \frac{1}{m_p^2} \left( i \epsilon^{\mu\nu p_p q} + 2 p_p^{[\mu} q^{\nu]} \right) \Pi_S^{\text{had}} + \frac{\not{q}}{m_p^3} \left( i \epsilon^{\mu\nu p_p q} + 2 p_p^{[\mu} q^{\nu]} \right) \Pi_{A_1}^{\text{had}} \right. \\ & + \frac{\not{p}_p}{m_p^3} \left( i \epsilon^{\mu\nu p_p q} + 2 p_p^{[\mu} q^{\nu]} \right) \Pi_{A_2}^{\text{had}} + \frac{1}{m_p} \left( i \gamma_\rho \epsilon^{\mu\nu \rho q} + 2 \gamma^{[\mu} q^{\nu]} \right) \Pi_{A_3}^{\text{had}} \\ & \left. + \frac{1}{m_p} \left( i \gamma_\rho \epsilon^{\mu\nu \rho p_p} + 2 \gamma^{[\mu} p_p^{\nu]} \right) \Pi_{A_4}^{\text{had}} + i \sigma^{\mu\nu} \Pi_{T_1}^{\text{had}} \right] \end{aligned}$$

$$+ \frac{2i}{m_p^2} \left( p_p^{[\mu} \sigma^{\nu]q} - q^{[\mu} \sigma^{\nu]p_p} \right) \Pi_{T_2}^{\text{had}} + \frac{i\sigma^{p_p q}}{m_p^4} \left( i\epsilon^{\mu\nu p_p q} + 2p_p^{[\mu} q^{\nu]} \right) \Pi_{T_3}^{\text{had}} \Big], \quad (4.63)$$

where  $\epsilon^{\mu\nu\rho p} \equiv \epsilon^{\mu\nu\rho\sigma} p_\sigma$ . The eight Dirac structures in (4.63) can be used to derive LCSRs for the four form factors  $w_n$  or combinations of them. The corresponding scalar functions  $\Pi_\alpha^{\text{had}}$  with  $\alpha = S, A_1, A_2, A_3, A_4, T_1, T_2, T_3$  depend only on the square  $p_p^2$  of the proton four-momentum and on the square  $Q^2 \equiv -q^2$  of the four-momentum transfer between the proton and the neutral pion. They can be expressed as dispersive integrals as follows

$$\Pi_\alpha^{\text{had}}(p_p^2, Q^2) = \int_{m_p^2}^{\infty} ds \frac{\rho_\alpha^{\text{had}}(s, Q^2)}{s - p_p^2}, \quad (4.64)$$

where

$$\rho_\alpha^{\text{had}}(s, Q^2) \equiv \frac{1}{\pi} \text{Im} \Pi_\alpha^{\text{had}}(s + i\epsilon, Q^2) \quad (4.65)$$

are spectral densities. In this way the ground-state contribution can be separated from the contributions due to heavier states collectively denoted by  $\rho_\alpha^{\text{cont}}(s, Q^2)$ :

$$\rho_\alpha^{\text{had}}(s, Q^2) = \lambda_p m_p^2 \delta(s - m_p^2) W_\alpha(s, Q^2) + \rho_\alpha^{\text{cont}}(s, Q^2). \quad (4.66)$$

On-shell, i.e. for  $s = m_p^2$ , the functions  $W_\alpha(Q^2) \equiv W_\alpha(m_p^2, Q^2)$  take the following form

$$\begin{aligned} W_S(Q^2) &= w_1, & W_{A_1}(Q^2) &= w_2, & W_{A_2}(Q^2) &= w_1 + w_3 - \frac{w_2}{2m_p^2} (m_p^2 - Q^2 - m_\pi^2), \\ W_{A_3}(Q^2) &= -w_3, & W_{A_4}(Q^2) &= -w_4 + \frac{w_3}{2m_p^2} (m_p^2 - Q^2 - m_\pi^2), \\ W_{T_1}(Q^2) &= w_4, & W_{T_2}(Q^2) &= w_3, & W_{T_3}(Q^2) &= w_2, \end{aligned} \quad (4.67)$$

with  $m_\pi \simeq 135 \text{ MeV}$  denoting the mass of the neutral pion.

## 4.2.2 Structure of the LCSRs

The derivation of the QCD results for the LCSRs proceeds in full analogy to Section 4.1.2, which contains many technical details. The analytic expressions for the QCD correlation functions relevant for this section can be found in Appendix F. Rather than repeating the necessary steps to derive them, let us discuss the structure of the  $\Pi_\alpha^{\text{QCD}}$  functions. A striking feature of the results for the QCD correlation function is that

$$\Pi_{T_3}^{\text{QCD}} = 0 \quad (4.68)$$

at the lowest order in the twist expansion. The first non-zero correction to the QCD function  $\Pi_{T_3}^{\text{QCD}}$  schematically takes the form

$$\Pi_{T_3}^{\text{QCD}} \sim \langle \bar{q}q \rangle \cdot \langle \pi^0 | \bar{q}(0) \gamma^\mu i g_s \tilde{G}^{\alpha\beta}(ux) \tau^3 q(x) | 0 \rangle. \quad (4.69)$$

Here we have defined  $\tilde{G}^{\alpha\beta} \equiv \epsilon^{\alpha\beta\mu\nu} G_{\mu\nu}^A T^A/2$ . The contribution (4.69) corresponds to a three-particle pion distribution amplitude (DA) of twist 4 with the fields evaluated at 0,  $ux$  and  $x$ . See for instance [200, 230] for details. Being of higher twist the correction (4.69) is expected to be small compared to the values predicted for the form factor  $w_2$  by the LCSRs for  $\Pi_{A_1}$  and  $\Pi_{A_2}$  — cf. (4.67). This implies that there has to be a cancellation among the contributions of the ground state and that of heavier states in the hadronic sum leading to  $\Pi_{T_3}^{\text{had}} \simeq 0$ . Similar cancellations are also observed in certain QCD sum rules for the nucleon mass [155, 160]. In this case, for a specific choice of the nucleon interpolating current, one of the sum rules starts at higher order in the OPE, which numerically yields a very small value for the QCD side of the sum rule. In this example, on the hadronic side excitations of the nucleon with even and odd parity contribute with opposite signs leading to a cancellation. In the case of (4.68) the contributions of excited states are not sign-definite, but in principle cancellations may occur if the contributions from heavier states are sizeable. Sum rules that have this feature cannot be used to extract the form factors related to the ground state because the corrections of excited states are just as important as the formally leading ground-state contributions. The LCSR for the correlation function  $\Pi_{T_3}$  is thus disregarded in our work.

Convergence criteria are now applied to the remaining LCSRs in order to determine the Borel window for each  $\Pi_\alpha$ . Notice that compared to the correlator studied for GUT-like proton decay in Section 4.1 the hadronic representation of the correlation function (4.63) comprises a larger number of independent Lorentz structures. This feature leads to simpler analytic LCSR expressions for the correlation functions  $\Pi_\alpha$ , but it also renders the numerical impact of the dimension-five condensate  $\langle \bar{q}g_s G \cdot \sigma q \rangle$  with  $G \cdot \sigma \equiv G_{\mu\nu} \sigma^{\mu\nu}$  larger than in the GUT case. As a result the LCSRs analysed below will have larger uncertainties than those that have been studied in Section 4.1. In the following, we will use the LCSRs for  $\Pi_S$ ,  $\Pi_{A_1}$ ,  $\Pi_{A_2}$  and  $\Pi_{T_1}$  to extract the form factors  $w_n$  because they are the most well behaved with regard to the power suppression of higher-dimensional condensates and the dominance of the ground-state contributions. We add that the LCSR for  $\Pi_{A_4}$  also fulfils the convergence criteria but one would need to combine it with the result for  $\Pi_{T_1}$  to extract the form factor  $w_3$  and it turns out that the Borel windows of these two LCSRs do not overlap.

In the case of the LCSRs for  $\Pi_S$  and  $\Pi_{A_2}$  we find the window  $1.1 \text{ GeV} \lesssim M \lesssim 1.5 \text{ GeV}$  with  $M$  the Borel mass, while for  $\Pi_{T_1}$  we obtain  $0.7 \text{ GeV} \lesssim M \lesssim 1.1 \text{ GeV}$ . In all three cases the Borel analysis has been restricted to  $0.6 \text{ GeV}^2 \lesssim Q^2 \lesssim 2.5 \text{ GeV}^2$ . The lower limits are obtained by demanding that the mixed condensate  $\langle \bar{q}g_s G \cdot \sigma q \rangle$  does not account for more than 50% of the total QCD result and as an absolute minimum of the Borel mass we choose  $0.7 \text{ GeV}$ . The upper limits arise from the requirement

that heavier states constitute less than 50% of the total dispersion integrals (4.64) and that the Borel mass should not considerably exceed the continuum threshold  $s_0 = 1.44 \text{ GeV}^2$ . The latter is chosen as the square of the mass of the Roper resonance [30] which is the lightest excitation in the nucleon spectrum. The Borel transformation ensures that heavier states with a mass  $m_{N'}$  are exponentially suppressed by a factor of  $\exp(-(m_{N'}^2 - m_p^2)/M^2)$ , but the dispersion integral over heavier states, which starts at  $s_0$ , can be modelled as an integral over the QCD result assuming quark-hadron duality [170, 171].

In order to determine all four form factors  $w_n$  one also needs to evaluate  $\Pi_{A_1}$ , where the power suppression turns out to be less effective than in the other cases. Therefore the use of this LCSR is restricted to  $Q^2 \gtrsim 0.9 \text{ GeV}^2$  because the power suppression becomes more effective for larger values of  $Q^2$ . For Borel masses of  $1.1 \text{ GeV} \lesssim M \lesssim 1.5 \text{ GeV}$  the relative contribution of the dimension-five condensate  $\langle \bar{q}g_s G \cdot \sigma q \rangle$  to the LCSR lies between 60% and 100%. The form factor  $w_2$  can therefore only be estimated within systematic uncertainties of the order of 100%. The result of  $w_2$  also enters the prediction for  $w_3$  through the LCSR for  $\Pi_{A_2}$  but the contribution is suppressed by a kinematical factor of about 0.1 for  $Q^2 \simeq 1 \text{ GeV}^2$  (cf. (4.67)). As a result the uncertainties plaguing  $w_2$  represent only a subleading part of the uncertainty in  $w_3$ . In fact, it turns out that the differential decay width of  $p \rightarrow e^+ \pi^0 G$  receives the dominant contributions from the form factors  $w_1$  and  $w_3$ , meaning that the uncertainty due to  $w_2$  plays only a minor role in the proton decay phenomenology in the GRSMEFT.

If one could resum the expansion of the QCD side to all orders and exactly model the contributions of heavier states on the hadronic side, the dependence on  $M$  and  $s_0$  of the form factors would vanish. Truncating the expansion at some finite order leaves a residual dependence on these parameters, but ideally the results for the form factors  $w_n$  do not depend too strongly on the exact choice of these unphysical parameters. Figure 4.7 displays the dependence of the form factors on the Borel mass  $M$  and the continuum threshold  $s_0$ , where  $s_0$  is varied between  $(1.4 \text{ GeV})^2$  and  $(1.5 \text{ GeV})^2$ . The broader the obtained band the stronger is the dependence of the form factor on  $s_0$ , and the steeper the curves the stronger is the dependence on  $M$ . By varying the Borel mass within the corresponding window and the continuum threshold between  $(1.4 \text{ GeV})^2$  and  $(1.5 \text{ GeV})^2$  one can obtain an uncertainty estimate for the relevant form factor  $w_n$ .

### 4.2.3 Numerical analysis

Using the numerical input and the definitions of the pion DAs of Sections 4.1.2 and 4.1.3 and Appendix D we obtain the results for the form factors  $w_n$  shown in Figure 4.8. The displayed central values of  $w_n$  correspond to  $M = 1.3 \text{ GeV}$  for  $\Pi_S$ ,  $\Pi_{A_1}$  and  $\Pi_{A_2}$ , while in the case of  $\Pi_{T_1}$  we use  $M = 0.9 \text{ GeV}$ . All central predictions employ  $s_0 =$

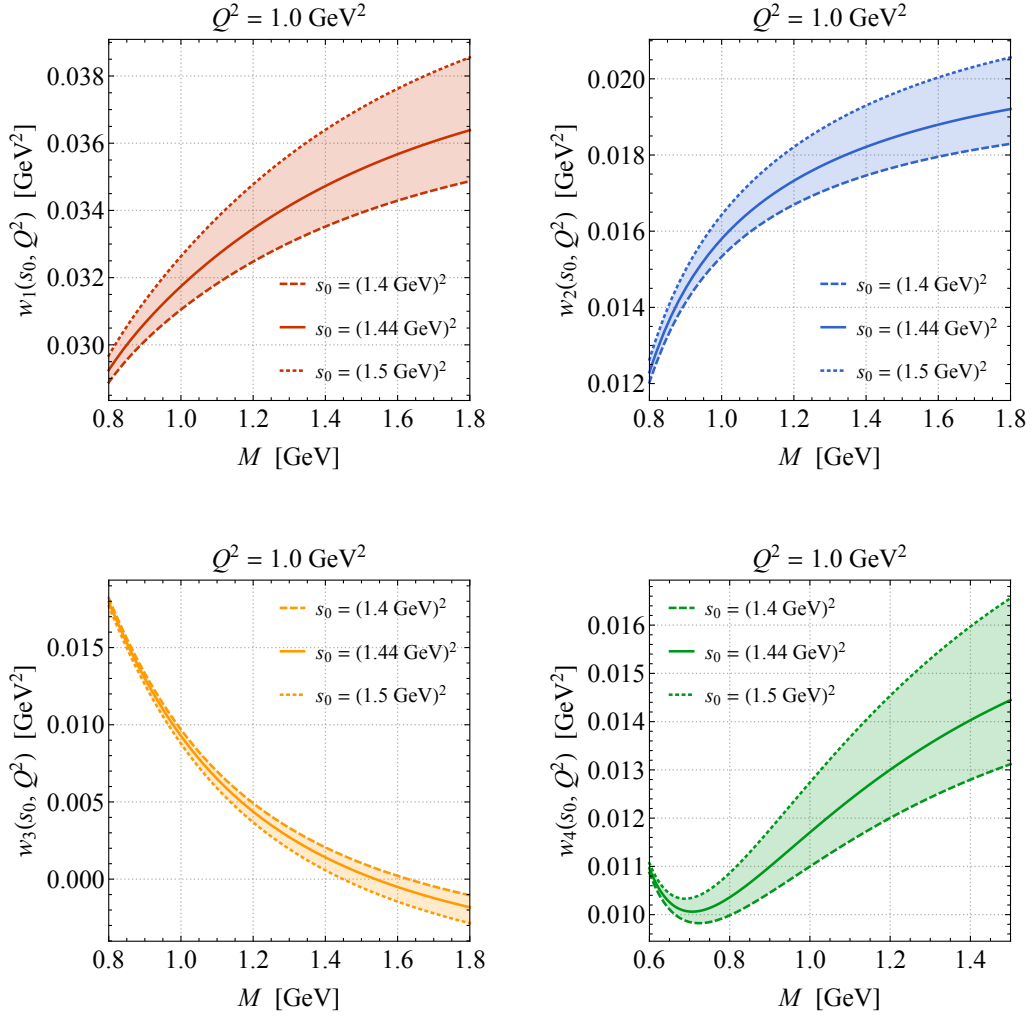


**Figure 4.7:** Form factors  $w_n(s_0, Q^2)$  as a function of the Borel mass  $M$  for three different values of the continuum threshold  $s_0$ . All plots show the results at  $Q^2 = 1 \text{ GeV}^2$ .

$(1.44 \text{ GeV})^2$ . The total theoretical uncertainties receive contributions from variations of  $M$  and  $s_0$  as described above but also from variations of the numerical input parameters within their uncertainties. Each parameter is varied independently while the remaining parameters are kept fixed at their central values. The total uncertainty is then obtained by adding individual uncertainties in quadrature. The values of the form factors  $w_1(Q^2)$  and  $w_4(Q^2)$  are computed with the help of the LCSRs for  $Q^2 \geq 0.6 \text{ GeV}^2$  while for  $Q^2 \leq 0.6 \text{ GeV}^2$  the values are obtained by a naive extrapolation. Similarly, the form factors  $w_2(Q^2)$  and  $w_3(Q^2)$  are predicted by the LCSRs for  $Q^2 \geq 0.9 \text{ GeV}^2$  and by the extrapolation for  $Q^2 \leq 0.9 \text{ GeV}^2$ . A linear and a quadratic function in  $Q^2$  is taken to extrapolate the form factors which are then fitted to the results of the values

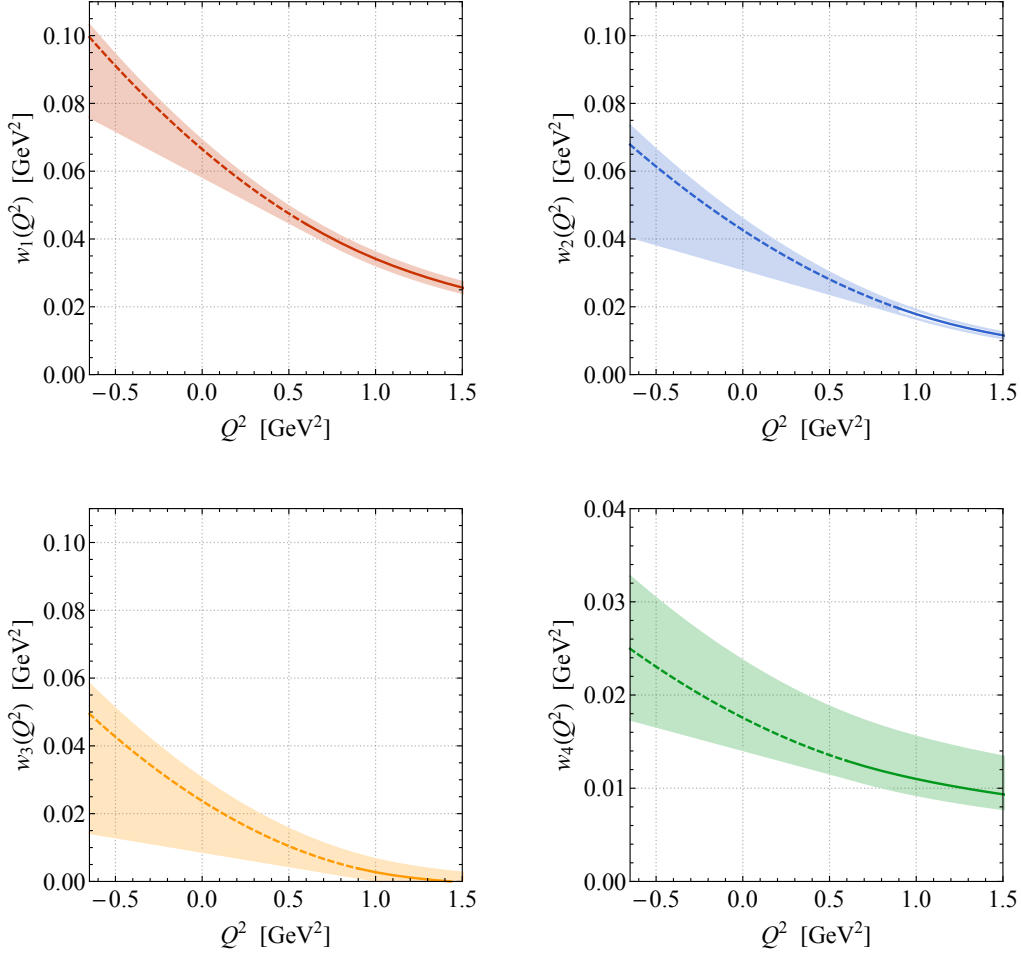


**Figure 4.8:** Form factors  $w_n(Q^2)$  as a function of  $Q^2$ . The coloured curves and bands correspond to the central values and uncertainties of the LCSRs. In the case of  $w_1(Q^2)$  and  $w_4(Q^2)$  ( $w_2(Q^2)$  and  $w_3(Q^2)$ ) the predictions for  $0.6 \text{ GeV}^2 \leq Q^2 \leq 1.5 \text{ GeV}^2$  ( $0.9 \text{ GeV}^2 \leq Q^2 \leq 1.5 \text{ GeV}^2$ ) are obtained by a direct calculation (solid lines), while the predictions for  $Q^2 \leq 0.6 \text{ GeV}^2$  ( $Q^2 \leq 0.9 \text{ GeV}^2$ ) are obtained by an extrapolation (dashed lines). Consult the main text for further explanations.

obtained from the LCSRs in the vicinity of  $Q^2 = 0.6 \text{ GeV}^2$  for  $w_1(Q^2)$  and  $w_4(Q^2)$  and  $Q^2 = 0.9 \text{ GeV}^2$  for  $w_2(Q^2)$  and  $w_3(Q^2)$ . For a given form factor the quadratic fit is chosen to obtain the central value for  $w_n$ , while the maximum and minimum of all extrapolations determine the uncertainty band. We remark that the same fitting approach has been successfully used in the LCSR calculation of Section 4.1 to reproduce the results from LQCD in the case of a GUT-like proton decay.

The fit formulas for the form factors  $w_n$  that we obtain in the physical region, i.e. in the four-momentum range  $-0.65 \text{ GeV}^2 \simeq -(m_p - m_\pi)^2 \leq Q^2 \leq 0$ , take the following

form

$$w_1(Q^2) = \begin{cases} \left[ 0.012 \left( \frac{Q^2}{\text{GeV}^2} \right)^2 - 0.045 \left( \frac{Q^2}{\text{GeV}^2} \right) + 0.069 \right] \text{GeV}^2, \\ \left[ 0.011 \left( \frac{Q^2}{\text{GeV}^2} \right)^2 - 0.044 \left( \frac{Q^2}{\text{GeV}^2} \right) + 0.066 \right] \text{GeV}^2, \\ \left[ 0.058 - 0.027 \left( \frac{Q^2}{\text{GeV}^2} \right) \right] \text{GeV}^2, \end{cases} \quad (4.70)$$

$$w_2(Q^2) = \begin{cases} \left[ 0.009 \left( \frac{Q^2}{\text{GeV}^2} \right)^2 - 0.036 \left( \frac{Q^2}{\text{GeV}^2} \right) + 0.046 \right] \text{GeV}^2, \\ \left[ 0.008 \left( \frac{Q^2}{\text{GeV}^2} \right)^2 - 0.033 \left( \frac{Q^2}{\text{GeV}^2} \right) + 0.043 \right] \text{GeV}^2, \\ \left[ 0.031 - 0.015 \left( \frac{Q^2}{\text{GeV}^2} \right) \right] \text{GeV}^2, \end{cases} \quad (4.71)$$

$$w_3(Q^2) = \begin{cases} \left[ 0.012 \left( \frac{Q^2}{\text{GeV}^2} \right)^2 - 0.035 \left( \frac{Q^2}{\text{GeV}^2} \right) + 0.030 \right] \text{GeV}^2, \\ \left[ 0.011 \left( \frac{Q^2}{\text{GeV}^2} \right)^2 - 0.032 \left( \frac{Q^2}{\text{GeV}^2} \right) + 0.024 \right] \text{GeV}^2, \\ \left[ 0.009 - 0.009 \left( \frac{Q^2}{\text{GeV}^2} \right) \right] \text{GeV}^2, \end{cases} \quad (4.72)$$

$$w_4(Q^2) = \begin{cases} \left[ 0.004 \left( \frac{Q^2}{\text{GeV}^2} \right)^2 - 0.012 \left( \frac{Q^2}{\text{GeV}^2} \right) + 0.024 \right] \text{GeV}^2, \\ \left[ 0.003 \left( \frac{Q^2}{\text{GeV}^2} \right)^2 - 0.009 \left( \frac{Q^2}{\text{GeV}^2} \right) + 0.018 \right] \text{GeV}^2, \\ \left[ 0.014 - 0.005 \left( \frac{Q^2}{\text{GeV}^2} \right) \right] \text{GeV}^2. \end{cases} \quad (4.73)$$

Here the upper (lower) line in each formula corresponds to the upper (lower) border of the corresponding envelope shown in Figure 4.8, while the middle line represents the central value of our LCSR form factor prediction. We add that the form factors  $w_n$  are related to the off-shell form factors of the decomposition of the more general matrix element  $\langle \pi^0 | \epsilon^{abc} d_a^\alpha u_b^\beta u_c^\gamma | p \rangle$  [244, 245], where  $\alpha$ ,  $\beta$  and  $\gamma$  are Dirac indices. Certain combinations of the form factors  $w_n$  therefore yield the form factors  $W_{RR}^k$  with  $k = 0, 1$  that are relevant for GUT-like proton decay. In Section 4.2.4 we show that using the results (4.70) to (4.73) allows reproducing the physical values of the form factors  $W_{RR}^k$ .

calculated in Section 4.1 within uncertainties. This gives reason to believe that the naive extrapolation used to obtain the above expressions for  $w_n$  approximates the true scaling in the relevant four-momentum regime.

#### 4.2.4 GUT-like form factors

The hadronic form factors  $w_n$  with  $n = 1, 2, 3, 4$  of the process  $p \rightarrow e^+ \pi^0 G$  are related to the form factors  $W_{RR}^k$  with  $k = 0, 1$  of the GUT-like decay  $p \rightarrow e^+ \pi^0$ . The subscript  $RR$  for the latter process denotes the chiralities of the quark fields in the associated dimension-six operator (2.13), which leads to the hadronic transition  $H_{RR}(p_p, q)$  defined in equations (4.2) and (4.3). Other transitions due to operators of the type (2.13) with different chiralities for the quark fields exist and contribute to GUT-like proton decay. But only the matrix element  $H_{RR}(p_p, q)$ , where all quarks are right-handed, is related to the decay induced by the GRSMEFT operator (2.21).

The hadronic matrix elements of both scenarios of proton decay, mediated by either the dimension-six term (2.13) or the dimension-eight term (2.21), are related to the more general matrix element

$$H^{\alpha\beta\gamma}(p_p, q) \equiv \langle \pi^0(p_\pi) | \epsilon^{abc} d_a^\alpha u_b^\beta u_c^\gamma | p(p_p) \rangle , \quad (4.74)$$

where all fields are evaluated at zero. In particular, the following relations hold

$$(CP_R)_{\alpha\beta} (P_R)_{\delta\gamma} H^{\alpha\beta\gamma}(p_p, q) = [H_{RR}(p_p, q) u_p(p_p)]_\delta , \quad (4.75)$$

$$(C\sigma^{\mu\nu} P_R)_{\alpha\beta} (P_R)_{\delta\gamma} H^{\alpha\beta\gamma}(p_p, q) = [H^{\mu\nu}(p_p, q) u_p(p_p)]_\delta , \quad (4.76)$$

where  $H^{\mu\nu}(p_p, q)$  is defined in (4.58).

The most general decomposition of  $H^{\alpha\beta\gamma}(p_p, q)$  in terms of a set of form factors for an off-shell proton is provided in [244, 245] — see in particular (4.64) of the first arXiv version of [245]. Hence, both sets of on-shell form factors  $w_n$  and  $W_{RR}^k$  can be related to these off-shell form factors upon using the equations of motion for the proton. In this way it is possible to relate the on-shell form factors for both scenarios of proton decay among each other. We find

$$\begin{aligned} W_{RR}^0(Q^2) &= 3w_4(Q^2) - \frac{m_p^2 - Q^2 - m_\pi^2}{2m_p^2} (2w_3(Q^2) - w_1(Q^2)) \\ &\quad - \left[ \frac{Q^2}{m_p^2} + \frac{(m_p^2 - Q^2 - m_\pi^2)^2}{4m_p^4} \right] w_2(Q^2) , \end{aligned} \quad (4.77)$$

$$W_{RR}^1(Q^2) = 2w_3(Q^2) - w_1(Q^2) . \quad (4.78)$$

Numerical results for  $W_{RR}^k(Q^2)$  were computed in Section 4.1.3, where our findings were also shown to be in agreement with the results of the state-of-the-art LQCD

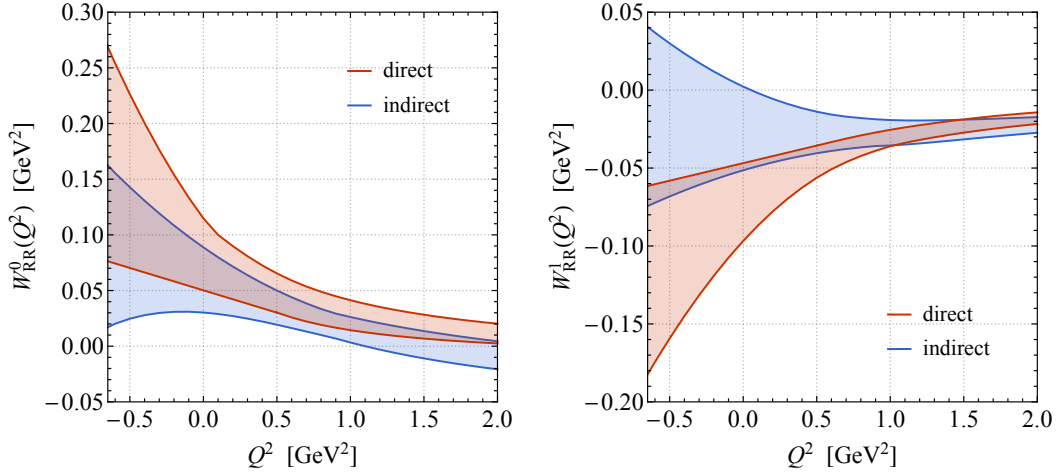


**Figure 4.9:** Comparison of the form factors  $W_{RR}^0(Q^2)$  (left panel) and  $W_{RR}^1(Q^2)$  (right panel) obtained by the direct calculation and the indirect method based on the relations (4.77) and (4.78). The results of the direct (indirect) computation are indicated in red (blue) and the coloured envelopes include all possible solutions found in [21] and (4.70) to (4.73), respectively. Further explanations can be found in the main text.

calculation [223] at  $Q^2 = 0$ . The form factors  $w_n(Q^2)$  are derived in the same way in this work. One can therefore employ the relations (4.77) and (4.78) to directly assess the validity of first the numerical results presented in Figure 4.8 for large virtualities ( $Q^2 \gg \Lambda_{\text{QCD}}^2$  with  $\Lambda_{\text{QCD}} \simeq 300$  MeV the QCD scale) and second the extrapolations (4.70) to (4.73) for physical momenta ( $Q^2 \lesssim 0$ ). We find that the relations (4.77) and (4.78) hold numerically within uncertainties in the relevant regime  $-(m_p - m_\pi)^2 \leq Q^2 \leq (2 \text{ GeV})^2$ , even though the uncertainties of the combinations on the right-hand sides of (4.77) and (4.78) are rather large and the results tend to undershoot the more accurate results for  $W_{RR}^0(Q^2)$  and  $W_{RR}^1(Q^2)$  obtained by a direct calculation of the corresponding left-hand sides. This feature is illustrated by the two panels in Figure 4.9. Although the agreement is not perfect, the shown results validate to a certain extent the LCSR approach employed in this section as well as the extrapolation procedure used to obtain (4.70) to (4.73).



## 5 Low-energy probes of CP and baryon-number violation

Indirect probes of new-physics contributions to processes that are rare or forbidden in the SM provide an excellent opportunity to search for physics beyond the SM [16] (see also Chapter 1 for more details). However, it was established in the previous chapters that the theory predictions for the corresponding BSM effects often rely on the knowledge of the associated hadronic transition matrix elements. Estimates for various matrix elements related to the nEDM and proton decay are derived in Chapters 3 and 4 with the help of sum-rule techniques in QCD. These results are applied in the following for the purpose of studying certain aspects of the associated BSM phenomenology. As advertised in Chapter 2, the following discussions are model-independent to a large extent; nevertheless, references on practical scenarios are provided in the following sections.

Section 5.1 is about BSM theories that generate effective, CP-violating Higgs-gluon interactions. Experimentally, the CP structure of Higgs-gauge boson interactions can be probed by measurements of the kinematic properties of the Higgs boson and the associated jet spectra [246,247]. In the context of the SMEFT (cf. Section 2.1) one CP-violating dimension-six operator, that has been constrained using LHC data [248–251], is

$$\mathcal{L}_{\phi\tilde{G}} = -g_s^2 \phi^\dagger \phi \tilde{G}_{\mu\nu}^A G^{A\mu\nu} C_{\phi\tilde{G}}. \quad (5.1)$$

Here,  $\phi$  is the SM Higgs doublet and  $G_{\mu\nu}^A$  the QCD field strength tensor, where the conventions of the previous chapters are employed. Notice that the Wilson coefficient  $C_{\phi\tilde{G}}$  introduced in (5.1) carries mass dimension  $-2$ . Higgs-gauge boson interactions of the type (5.1) have been studied in Ref. [39], where also operators involving electroweak gauge fields are considered. This reference provides a global picture of high- and low-energy constraints on Higgs-gauge boson interactions and the authors discuss how different probes can be interfaced to constrain the parameter space spanned by the relevant Wilson coefficients. The purpose of the analysis presented in Section 5.1 is to extend the study [39] with regard to Higgs-gluon interactions as given by (5.1) and in particular to examine those contributions to the nEDM that are independent of the light-quark Yukawa interactions. The Yukawa couplings of light quarks are ex-

perimentally unknown, raising the question, which effects on the nEDM remain if the Higgs boson does not couple to the light quarks inside the neutron in an SM-like fashion. This issue is explained in more detail in Section 5.1. The results of this section were originally published in Ref. [20].

Section 5.2 is dedicated to a particular scenario of proton decay, namely  $p \rightarrow e^+ \pi^0 G$ , which is described by the effective interactions of the GRSMEFT introduced in Section 2.4. Such a transition is induced by the operator (2.21) which constitutes a source of baryon-number violation beyond the SM and a possible departure from GR — both effects are to some extent required by theoretical and empirical observations as discussed in Chapter 1 (see also Sections 2.3 and 2.4 for related discussions). The content of Section 5.2 is largely based on the article [22].

## 5.1 CP-violating Higgs-gluon interactions in the limit of vanishing light-quark Yukawa couplings

Searches for EDMs are known to place stringent constraints on many new-physics scenario with additional sources of CP violation (see [43, 52, 57, 60, 62–65, 67–72, 75, 76] for reviews and recent discussions). In particular, the low-energy constraints on effective operators of the form (5.1) have been considered in Refs. [39, 58, 59, 61, 66, 73, 74]. In fact, the recent article [39] performed a comprehensive study of the relative strengths and complementarity of collider and low-energy measurements in probing CP violation in Higgs-gauge boson interactions. Employing a SMEFT description and working in the context of so-called universal theories [252–254], i.e. theories in which mainly the couplings between the SM Higgs and gauge bosons are modified by new dynamics, it was found that in a single-operator analysis the existing EDM limits leave very little room for observing CP violation in the Higgs sector at the LHC. Including all relevant dimension-six CP-violating operators, it was furthermore established that the EDM searches enforce strong correlations among Higgs-gauge boson couplings, which barring intricate cancellations lead again to stringent bounds on the individual Wilson coefficients. Similar conclusions were drawn in [74] where only the limits arising from the eEDM have been studied.

In the following a simple way of how-to relax the constraints obtained in [39, 74] is pointed out. In contrast to the these articles, it is not assumed here that the new-physics modifications are confined to the Higgs-gauge boson sector, but also allow for effects in the Yukawa sector. Specifically, we will consider the following dimension-six SMEFT terms

$$\mathcal{L}_{\phi q} = -Y_d \phi^\dagger \phi \bar{Q}_L \phi d_R C_{\phi d} - Y_u \phi^\dagger \phi \bar{Q}_L \tilde{\phi} u_R C_{\phi u} + \text{h.c.} , \quad (5.2)$$

where we have employed the shorthand notation  $\tilde{\phi}^i = \epsilon_{ij} (\phi^j)^*$  with  $\epsilon_{ij}$  totally antisymmetric and  $\epsilon_{12} = +1$ . The Yukawa couplings  $Y_d$  and  $Y_u$  are matrices in flavour space and a sum over flavour indices is implicit in (5.2). Finally,  $Q_L$  denote left-handed quark doublets, while  $d_R$  and  $u_R$  are right-handed fermion singlets of down-quark and up-quark type, respectively.

After EWSB the dimension-six operators in (5.2) modify the couplings of the Higgs boson to quarks. Assuming that new-physics is minimally flavour violating [255] and that the Wilson coefficients  $C_{\phi u}$  and  $C_{\phi d}$  are real,<sup>1</sup> each SM quark Yukawa coupling gets rescaled by an independent factor

$$\kappa_q \simeq 1 + v^2 C_{\phi q}, \quad (5.3)$$

where  $q = t, b, c, s, d, u$  and  $v \simeq 246$  GeV denotes the electroweak vacuum expectation value. The coupling modifiers  $\kappa_q$  or equivalently the Wilson coefficients  $C_{\phi q}$  can be constrained by LHC Higgs physics. In the case of the top and bottom quark, our knowledge of Yukawa interactions has undergone a revolution in recent years, since the ATLAS and CMS collaborations have independently observed  $pp \rightarrow t\bar{t}h$  production [256, 257] and the  $h \rightarrow b\bar{b}$  decay [258, 259]. Combining direct and indirect information on the Higgs properties into a global fit ATLAS [260] finds the following 68% CL limits<sup>2</sup>

$$\kappa_t = 1.02^{+0.11}_{-0.10}, \quad \kappa_b = 1.06^{+0.19}_{-0.18}. \quad (5.4)$$

The quoted results are in full agreement with the bounds obtained by CMS [261], and yield clear and model-independent evidence for the existence of non-zero top-quark and bottom-quark Yukawa couplings in nature. Despite significant experimental and theoretical effort [262–282] only very weak (no relevant) bounds exist at present in the case of the second-generation (first-generation) quarks. Whether the Higgs mechanism is responsible for the generation of the masses of the charm, strange, down and up quark is thus an open question, and new-physics scenarios (see e.g. [283]) that predict a significant reduction of the couplings of the observed Higgs boson to the first two generation of quarks, i.e.  $\kappa_{c,s,d,u} \simeq 0$ , are from the phenomenological point of view a viable option.

A question that one therefore may want to ask is how sensitively the LHC limits [248–251] and the EDM constraints [39, 74] depend on the assumption that the observed Higgs boson has couplings to the light fermions. In the case of the operator (5.1) this question can be answered immediately by looking at the Feynman diagrams depicted in

<sup>1</sup>CP-violating diagonal [62, 75] and flavour-changing Higgs-fermion [64] couplings involving the third generation would be subject to stringent EDM constraints.

<sup>2</sup>In the considered benchmark model no new-physics contributions to Higgs-boson decays are assumed to exist and Higgs-boson vertices involving loops are resolved in terms of their SM content.

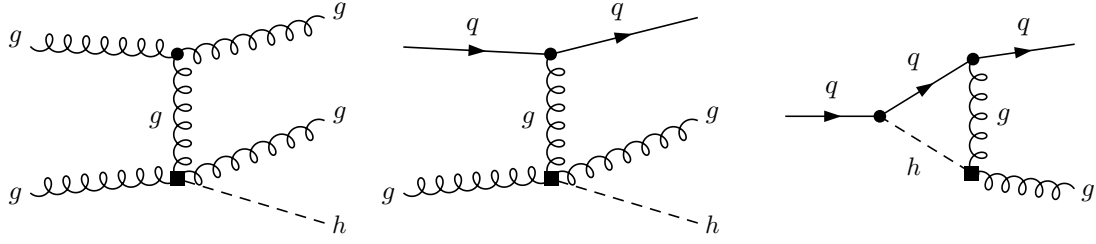


**Figure 5.1:** Left: Tree-level graphs that give rise to  $pp \rightarrow h + 2j$  production at the LHC. Right: Example one-loop diagram that contributes to the nEDM. The black squares indicate insertions of the CP-violating dimension-six operator (5.1).

Figure 5.1. The two tree-level diagrams on the left-hand side give a correction to Higgs plus two jet production  $pp \rightarrow h + 2j$ , while the one-loop graph shown on the right induces CEDMs for light quarks, which in turn generate non-zero contributions to the nEDM and all other hadronic EDMs. Since the diagrams that lead to the LHC signal do not involve a vertex where the Higgs couples to a light quark, the constraints on  $C_{\phi\tilde{G}}$  that can be obtained from kinematic properties of  $pp \rightarrow h + 2j$  are obviously independent of the size of the  $\kappa_q$  parameters. The amplitude of the chromoelectric dipole transition  $q \rightarrow qg$  instead depends linearly on  $\kappa_q$ , and hence tends to zero in the limit of vanishing light-quark Yukawa couplings. In consequence, if the down-quark and up-quark Yukawa couplings are identical to zero, no bound on the Wilson coefficient  $C_{\phi\tilde{G}}$  can be obtained from hadronic EDM searches at the one-loop level. The same statement can be shown to hold for the Wilson coefficients of the dimension-six operators which encode the CP-violating couplings between the Higgs and electroweak gauge bosons and contribute to the eEDM. Since in [39, 74] it is assumed that the Yukawa couplings of light fermions are exactly SM-like, it follows that the limits derived in these papers do not directly apply in the case that the light-fermion Yukawa couplings vanish exactly or are strongly suppressed.

Motivated by the above observation, the leading contributions to the nEDM that involve an insertion of (5.1) and that survive in the limit of vanishing light-quark Yukawa couplings are computed in Section 5.1.1. Based on these results, the bounds on the Wilson coefficient of the CP-violating dimension-six operator (5.1) from current and future nEDM searches are then derived in Section 5.1.2 and compared to existing LHC limits as well as their projections.

### 5.1.1 Calculation

Before describing the basic steps of the calculation, it should be mentioned that after EWSB the operator (5.1) shifts the QCD  $\theta$  term (2.4) by a finite amount, i.e.  $\theta \rightarrow$

$\theta - 8\pi^2 v^2 C_{\phi\tilde{G}}$ . Since based on the current experimental nEDM results the (physical)  $\theta$  parameter has to be tiny (cf. equations (2.6) and (2.7)), it is assumed in the following that the total  $\theta$  term vanishes dynamically due to a Peccei-Quinn mechanism [49]. Under this assumption there is no direct bound on (5.1), and the Wilson coefficient  $C_{\phi\tilde{G}}$  can be treated as a free parameter in the SMEFT as done in the analyses [39, 248–251].

As explained previously, the goal of this work is it to calculate the numerically most relevant contributions to the nEDM that are proportional to the Wilson coefficient  $C_{\phi\tilde{G}}$  and that involve the Yukawa couplings of the third-generation quarks. It turns out that at the matching scale the relevant loop graphs give rise to two CP-violating higher-dimensional operators of Weinberg type, namely the terms associated to the Wilson coefficients  $C_{3\tilde{G}}$  and  $C_{4\tilde{G},1}$  of (2.9). Since the bottom-quark contributions can be shown to be suppressed relative to the top-quark effects by a factor of  $m_b^2/m_h^2 \ln^2(m_b^2/m_h^2) \simeq 5\%$ , we neglect corrections that are proportional to the bottom-quark Yukawa coupling in what follows. The top-quark effects are all linearly dependent on the coupling modifier  $\kappa_t$ . In view of the observed SM-like nature (5.4) of the top-quark Yukawa coupling, we will simply employ  $\kappa_t = 1$  in our calculations. Allowing for  $\mathcal{O}(10\%)$  variations of  $\kappa_t$  would, however, not qualitatively change the results of the numerical analysis performed in Section 5.1.2.

### 5.1.1.1 Dimension-six contribution

The LO matching correction to the Wilson coefficient  $C_{3\tilde{G}}$  proportional to  $C_{\phi\tilde{G}}$  arises from two-loop Feynman diagrams like the ones displayed on the left-hand side in Figure 5.2. Employing a hard mass procedure (see [284] for a review) to obtain systematic expansions of the relevant two-loop diagrams in powers of the external momenta and the ratio  $x = m_t^2/m_h^2$  with  $m_t \simeq 163 \text{ GeV}$  and  $m_h \simeq 125 \text{ GeV}$  the top-quark and Higgs-boson mass, we find the following analytic result

$$C_{3\tilde{G}}(m_h) = \frac{\alpha_s^2(m_h)}{8\pi^2} \left[ \frac{65}{6} + 2 \ln x + \frac{1}{x} \left( \frac{383}{900} + \frac{2}{15} \ln x \right) \right] C_{\phi\tilde{G}}(m_h), \quad (5.5)$$

where  $\alpha_s = g_s^2/(4\pi)$ . The expression given above corresponds to the  $\overline{\text{MS}}$  scheme with the renormalisation scale set to  $\mu = m_h$ .<sup>3</sup> The actual calculation was performed in a  $R_\xi$  background field gauge for the gluon [286, 287] keeping an arbitrary gauge parameter. The Levi-Civita tensor  $\epsilon_{\mu\nu\rho\lambda}$  was treated as an external four-dimensional object. Our computations made use of the in-house codes that were developed in the context of [288, 289], except for the tensor reduction of two-point and three-point one-loop integrals

<sup>3</sup>The sum of the bare two-loop Feynman diagrams that contributes to (5.5) is not UV finite. The remaining UV pole is cancelled by taking into account the one-loop mixing of the operator  $\phi^\dagger \phi G_{\mu\nu}^A \tilde{G}^{A\mu\nu}$  into  $\bar{Q}_L \sigma^{\mu\nu} T^A u_R \tilde{\phi} G_{\mu\nu}^A + \text{h.c.}$ . We have calculated the relevant one-loop mixing finding agreement with the result given in [285].

which relied on **Package-X** [290]. We add that we have calculated higher-order terms in the  $1/x$  expansion of  $C_{3\tilde{G}}(m_h)$  and found that these corrections shift the numerical value of the matching correction (5.5) by less than a permille.<sup>4</sup> Such an accuracy is more than sufficient for our purpose.

The RG flow from the electroweak to the hadronic scale  $\mu_H = 1 \text{ GeV}$  does not only change the value of the Wilson coefficient  $C_{3\tilde{G}}$ , but also induces non-zero contributions for the EDMs  $d_q$  and the CEDMs  $\tilde{d}_q$  of the down and up quarks defined in equation (2.8) with  $q = d, u$ . In the basis  $\vec{C}_6 = (d_q, \tilde{d}_q, C_{3\tilde{G}})^T$ , the one-loop anomalous dimension (AD) matrix takes the following form [79, 80, 291]

$$\hat{\gamma}_6 = \begin{pmatrix} \frac{32}{3} & 0 & 0 \\ \frac{32}{3} & \frac{28}{3} & 0 \\ 0 & -6 & 3 + 2N_F + 2\beta_0 \end{pmatrix}, \quad (5.6)$$

where  $\beta_0 = 11 - 2/3N_F$  is the LO QCD beta function and  $N_F$  denotes the number of active quark flavours. Resumming leading-logarithmic corrections in the five-flavour, four-flavour and three-flavour theory, we obtain

$$\begin{aligned} d_q(\mu_H) &\simeq -5.6 \cdot 10^{-2} e Q_q m_q(\mu_H) C_{3\tilde{G}}(m_h), \\ \tilde{d}_q(\mu_H) &\simeq 1.2 \cdot 10^{-1} m_q(\mu_H) C_{3\tilde{G}}(m_h), \\ C_{3\tilde{G}}(\mu_H) &\simeq 1.3 \cdot 10^{-1} C_{3\tilde{G}}(m_h). \end{aligned} \quad (5.7)$$

Here  $Q_q$  is the fractional electric charge of the relevant quark and  $m_q(\mu_H)$  is its  $\overline{\text{MS}}$  mass at the hadronic scale. The numerical factors in (5.7) correspond to the values  $\alpha_s(m_h) \simeq 0.11$ ,  $\alpha_s(m_b) \simeq 0.21$ ,  $\alpha_s(m_c) \simeq 0.32$  and  $\alpha_s(\mu_H) \simeq 0.36$  of the QCD coupling constant. Notice that the Wilson coefficient  $C_{3\tilde{G}}$  of the dimension-six Weinberg operator gets strongly suppressed by one-loop RG running in QCD.<sup>5</sup>

The hadronic matrix elements of the dimension-six operators corresponding to the Wilson coefficients  $d_q$ ,  $\tilde{d}_q$  and  $C_{3\tilde{G}}$  in (5.7) are known with varying levels of theoretical uncertainties. The EDM contributions from down and up quarks have been calculated

<sup>4</sup>The analytic expressions for the  $\mathcal{O}(1/x^2)$  and  $\mathcal{O}(1/x^3)$  terms can be found in the L<sup>A</sup>T<sub>E</sub>X source code of the article [20].

<sup>5</sup>The two-loop and three-loop  $N_F$ -independent contributions to the AD of the dimension-six Weinberg operator have been calculated very recently [292]. Due to cancellations between the next-to-leading-logarithmic and the next-to-next-to-leading-logarithmic QCD corrections, the total three-loop result is numerically close to the one-loop result for  $C_{3\tilde{G}}(\mu_H)$  reported in (5.7). In view of this and given the sizeable uncertainties of the hadronic matrix element of the dimension-six Weinberg operator (cf. (5.8)) using only the leading-logarithmic RG evolution is fully justified. In the same spirit, the two-loop and three-loop mixing of the quark EDMs and CEDMs [291, 293–295] is also neglected in (5.7).

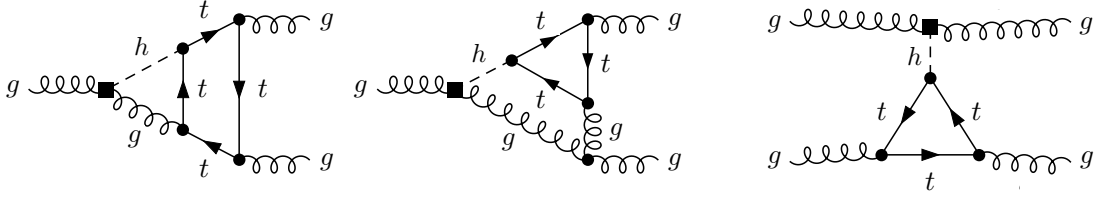


**Figure 5.2:** Left: Example diagrams of two-loop corrections to  $C_{3\tilde{G}}$  arising from the insertion of  $C_{\phi\tilde{G}}$ . Right: A one-loop correction to  $C_{4\tilde{G},1}$  arising from the insertion of  $C_{\phi\tilde{G}}$ . The operator insertions are indicated by black squares.

with an accuracy of 5% using LQCD [87–89], while QCD sum-rule calculations [43, 90–92] can be used to determine the contributions from the down-quark and up-quark CEDMs with uncertainties of 50%. At present only estimates of the hadronic matrix element of the dimension-six Weinberg operator exist that rely on either QCD sum rules [19,94], the VIA [93] or NDA [77]. Since only the QCD sum-rule calculations allow the systematic analysis of theoretical uncertainties, we will in the following rely on them. Adopting the QCD sum-rule estimate of Section 3.2, which is plagued by an uncertainty of 50%, and employing  $m_d(\mu_H) = 5.4 \cdot 10^{-3} \text{ GeV}$  and  $m_u(\mu_H) = 2.5 \cdot 10^{-3} \text{ GeV}$  [178], we obtain

$$\frac{(d_n)_{3\tilde{G}}}{e} = \left[ 1.0 (1 \pm 0.05) + 8.8 (1 \pm 0.5) - 66.6 (1 \pm 0.5) \right] C_{3\tilde{G}}(m_h) \cdot 10^{-4} \text{ GeV}, \quad (5.8)$$

where the first, second and third term corresponds to the  $d_q$ ,  $\tilde{d}_q$  and  $C_{3\tilde{G}}$  contribution in (5.7), respectively. It should be emphasised that in the case that new physics enters only through the matching correction  $C_{3\tilde{G}}(m_h)$  the relative signs in (5.8) are all fixed, meaning that the contribution from the dimension-six Weinberg operator necessarily interferes destructively with both the EDM and CEDM contribution.

### 5.1.1.2 Dimension-eight contribution

At LO the matching correction to the Wilson coefficient  $C_{4\tilde{G},1}$  proportional to  $C_{\phi\tilde{G}}$  arises from one-loop graphs of the type shown on the right in Figure 5.2. A straightforward calculation gives

$$C_{4\tilde{G},1}(m_h) = \frac{\alpha_s(m_h)}{\pi} \frac{1}{m_h^2} \left[ 1 + \frac{7}{120x} + \frac{1}{168x^2} \right] C_{\phi\tilde{G}}(m_h), \quad (5.9)$$

at the matching scale  $\mu = m_h$ . Higher-order terms in the  $1/x$  expansion change the matching correction  $C_{4\tilde{G},1}(m_h)$  by less than a permille, and they are therefore not included in (5.9).<sup>6</sup>

<sup>6</sup>The results for the  $\mathcal{O}(1/x^3)$  and  $\mathcal{O}(1/x^4)$  terms of (5.9) can be found in the L<sup>A</sup>T<sub>E</sub>X source code of the paper [20].

At the dimension-eight level there are three independent CP-violating operators that can be built from QCD field strength tensors (see equations (2.9) and (2.10) as well as Refs. [78, 81, 82] for details). While only the operator associated with  $C_{4\tilde{G},1}$  receives a one-loop matching correction proportional to  $C_{\phi\tilde{G}}$  all three dimension-eight operators mix under QCD. The two additional CP-violating four-gluon operators correspond to the Wilson coefficients  $C_{4\tilde{G},2}$  and  $C_{4\tilde{G},3}$  in (2.9). In the basis  $\vec{C}_8 = (C_{4\tilde{G},1}, C_{4\tilde{G},2}, C_{4\tilde{G},3})^T$  the one-loop AD matrix then reads [78, 81, 82]

$$\hat{\gamma}_8 = \begin{pmatrix} -56 + \frac{8}{3}N_F + 2\beta_0 & 24 & -36 \\ -38 & 56 + \frac{8}{3}N_F + 2\beta_0 & -42 \\ -14 & 12 & -14 + \frac{8}{3}N_F + 2\beta_0 \end{pmatrix}. \quad (5.10)$$

Working in the five, four and three flavour theory and using the values of the QCD coupling constant given earlier leads to the leading-logarithmic approximations

$$\begin{aligned} C_{4\tilde{G},1}(\mu_H) &\simeq 6.6 C_{4\tilde{G},1}(m_h), \\ C_{4\tilde{G},2}(\mu_H) &\simeq -1.9 C_{4\tilde{G},1}(m_h), \\ C_{4\tilde{G},3}(\mu_H) &\simeq 3.9 C_{4\tilde{G},1}(m_h). \end{aligned} \quad (5.11)$$

Notice that in contrast to (5.7) the Wilson coefficient  $C_{4\tilde{G},1}$  of the dimension-eight Weinberg operator that is generated at the matching scale gets enhanced by RG running.

Estimates of the hadronic matrix elements of the dimension-eight CP-violating four-gluon operators were obtained in Section 3.2 with the help of QCD sum rules. Employing these results we find

$$\frac{(d_n)_{4\tilde{G}}}{e} = -6.1 (1 \pm 0.8) C_{4\tilde{G},1}(m_h) \cdot 10^{-1} \text{ GeV}^3, \quad (5.12)$$

which has a theoretical uncertainty of 80%. Note that the sign in  $(d_n)_{4\tilde{G}}/e$  is predicted in the QCD sum-rule approach and that neglecting all contributions from the two additional dimension-eight operators in (2.9) would lead to a numerical result that deviates from (5.12) by less than 5%.

### 5.1.2 Discussion

To discuss the constraints that nEDM measurements can impose on the CP-violating dimension-six Higgs-gluon interactions appearing in (2.9), we introduce the dimensionless Wilson coefficient

$$\bar{C}_{\phi\tilde{G}}(m_h) = v^2 C_{\phi\tilde{G}}(m_h). \quad (5.13)$$

Combining (5.8) and (5.12) we then find in terms of the new Wilson coefficient the following expression

$$\left| \frac{d_n}{e} \right| = \left| (1 \pm 0.05) + 8.6 (1 \pm 0.5) - 65.1 (1 \pm 0.5) - 7.5 (1 \pm 0.8) \right| \times 6.2 \left| \bar{C}_{\phi\tilde{G}}(m_h) \right| \cdot 10^{-26} \text{ cm}, \quad (5.14)$$

where the contributions associated to the terms  $d_q$ ,  $\tilde{d}_q$ ,  $C_{3\tilde{G}}$  and the dimension-eight Weinberg operators have been kept distinct.

In view of the sizeable hadronic uncertainties of the matrix elements of the operators of CEDM and Weinberg type and the relative overall sign of the Weinberg-type contributions, we combine the errors in (5.14) in such a way that our prediction

$$\left| \frac{d_n}{e} \right| = 1.3 \left| \bar{C}_{\phi\tilde{G}}(m_h) \right| \cdot 10^{-24} \text{ cm} \quad (5.15)$$

provides a lower absolute limit on the actual size of the  $\bar{C}_{\phi\tilde{G}}$  corrections to  $d_n$ . Because our error treatment assumes a cancellation among the numerically dominant contributions associated to  $C_{3\tilde{G}}$ ,  $\tilde{d}_q$  and the dimension-eight terms, it is conservative. Notice that if such a cancellation is not at work in practice, predictions for  $|d_n/e|$  can be obtained that are larger by a factor of about 5 than the upper limit (5.15) but still consistent within the individual uncertainties quoted in (5.14).

The experimental result presented in equation (2.7) imposes a 95% CL bound on the magnitude of the nEDM, which, using the lower limit of the only quark EDMs case in (5.15) translates into

$$\left| \bar{C}_{\phi\tilde{G}}(m_h) \right| < 1.8 \cdot 10^{-2}. \quad (5.16)$$

This result should be compared to the bounds obtained in the case of universal theories which assume that the light-quark Yukawa couplings are SM-like [39] (i.e.  $\kappa_q = 1$ ). For such theories the one-loop diagram on the right-hand side in Figure 5.1 induces a CEDM for the down and up quark. In agreement with [39], we find the following expression for the one-loop correction to the CEDMs

$$\tilde{d}_q(m_h)|_{\kappa_q=1} = \frac{3\alpha_s(m_h)}{2\pi} C_{\phi\tilde{G}}(m_h), \quad (5.17)$$

at the matching scale  $\mu = m_h$ . Including the contribution (5.17) in the evaluation of the nEDM, the formula (5.8) turns into

$$\begin{aligned} \left. \frac{(d_n)_{\tilde{d}_q, 3\tilde{G}}}{e} \right|_{\kappa_q=1} &= \left[ \left( 6.9 \tilde{d}_q(m_h) + 1.0 C_{3\tilde{G}}(m_h) \right) (1 \pm 0.05) \right. \\ &\quad + \left( 36.7 \tilde{d}_q(m_h) + 8.8 C_{3\tilde{G}}(m_h) \right) (1 \pm 0.5) \\ &\quad \left. - 66.6 C_{3\tilde{G}}(m_h) (1 \pm 0.5) \right] \cdot 10^{-4} \text{ GeV}. \end{aligned} \quad (5.18)$$

## 5 Low-energy probes of CP and baryon-number violation

Adding the new dimension-six contribution (5.18) to the dimension-eight piece (5.12) we then obtain the formula

$$\begin{aligned} \left| \frac{d_n}{e} \right|_{\kappa_q=1} &= 6.2 \left| 190.6 (1 \pm 0.05) + 1016.6 (1 \pm 0.5) \right. \\ &\quad \left. - 65.1 (1 \pm 0.5) - 7.5 (1 \pm 0.8) \right| \left| \bar{C}_{\phi\tilde{G}}(m_h) \right| \cdot 10^{-26} \text{ cm}, \end{aligned} \quad (5.19)$$

In view of the sizeable hadronic uncertainties of the matrix elements in (5.19) and the relative overall sign of the Weinberg-type contributions, we again combine the errors in  $|d_n/e|$  in such a way that the final prediction provides a lower absolute limit on the actual size of the  $\bar{C}_{\phi\tilde{G}}$  corrections to the nEDM. We find

$$\left| \frac{d_n}{e} \right|_{\kappa_q=1} = 3.6 \left| \bar{C}_{\phi\tilde{G}}(m_h) \right| \cdot 10^{-23} \text{ cm}. \quad (5.20)$$

Numerically, the result (5.20) implies that

$$\left| \bar{C}_{\phi\tilde{G}}(m_h) \right|_{\kappa_q=1} < 6.1 \cdot 10^{-4}. \quad (5.21)$$

Notice that the constraint on  $|\bar{C}_{\phi\tilde{G}}(m_h)|$  for  $\kappa_q = 1$  as given in (5.21) is comparable to the bounds that have been derived in [39] by using the so-called Rfit strategy, in which all hadronic matrix elements entering the prediction for the nEDM are varied within their allowed ranges. This shows that the bound (5.16) obtained in the limit of vanishing light-quark Yukawa couplings is weaker by a factor of almost 30 than the 95% CL exclusion limit in universal theories with SM-like Yukawa couplings of the light quarks.

The constraint (5.16) can also be compared to the 95% CL limit

$$\bar{C}_{\phi\tilde{G}}(m_h) \in [-0.13, 0.83] \cdot 10^{-2} \quad (5.22)$$

on the dimensionless Wilson coefficient (5.13) that has been obtained in [251] from an analysis of the azimuthal angle difference  $\Delta\phi_{jj}$  between the two jets in  $h + 2j$  LHC events. A comparison of the limits (5.16) and (5.22) on the CP-violating interactions involving the Higgs boson and gluons in the limit of vanishing light-quark Yukawa couplings shows that at present the sensitivity of nEDM searches is by roughly an order of magnitude weaker than the constraining power of the LHC. This is mainly a result of the conservative treatment of the hadronic uncertainties in (5.14) that led to (5.15).

In order to obtain an idea of the prospects of the low-energy constraints, one can assume that a lower bound of

$$\left| \frac{d_n}{e} \right| < 1.0 \cdot 10^{-27} \text{ cm} \quad (5.23)$$

can be set at the proposed PSI and LANL nEDM experiments [106, 107]. In such a case, one arrives at the limit

$$\left| \bar{C}_{\phi\tilde{G}}(m_h) \right| < 8.0 \cdot 10^{-4}, \quad (5.24)$$

if one assumes that (5.15) provides a lower absolute limit on the  $\bar{C}_{\phi\tilde{G}}$  corrections to  $d_n$ , and one obtains

$$\left| \bar{C}_{\phi\tilde{G}}(m_h) \right|_{\kappa_q=1} < 2.8 \cdot 10^{-5} \quad (5.25)$$

in the case of SM-like Yukawa couplings, i.e. if (5.20) holds.

The sensitivity study [251] of the  $pp \rightarrow h + 2j$  process finds on the other hand that the high-luminosity LHC (HL-LHC) should be able to set a bound of

$$\left| \bar{C}_{\phi\tilde{G}}(m_h) \right| < 9.2 \cdot 10^{-4}. \quad (5.26)$$

From (5.24), which in a sense represents the worst-case scenario for next-generation EDM bounds, and (5.26) it is evident that in the future the sensitivity of nEDM searches can reach the LHC level even if the accuracy of the hadronic matrix elements is not improved. First-principle calculations of the matrix elements of the CEDMs and the dimension-six Weinberg operator are possible using existing LQCD methodology, and considering the efforts by several LQCD groups [95–102], it seems possible that estimates with uncertainties similar to the current ones can be obtained within the next five years [103, 104]. It remains to be seen which accuracy such computations can achieve in the next 20 years of LHC running, but it seems to be very likely that the bound (5.24) can be improved by the end of the HL-LHC run.

## 5.2 Proton decay in the GRSMEFT

Most of the existing proton decay searches focus on two-body decay channels. However, the null results provided by these experiments (cf. [123–125] for comprehensive summaries of the available experimental results) together with the observation that many higher-dimensional operators violating baryon number by one unit induce multi-body proton decay modes, make proton decay processes with more complicated final states interesting search targets for existing and next-generation neutrino experiments like SK [26], Hyper-Kamiokande (HK) [296], JUNO [297] and DUNE [298]. In this section, the decay mode  $p \rightarrow \pi^0 e^+ G$  with  $G$  a graviton is examined. This proton decay channel is the most relevant mode induced by the dimension-eight interaction (2.21) in the GRSMEFT (cf. Section 2.4). In the following, the differential decay rate of  $p \rightarrow e^+ \pi^0 G$  is computed and the sensitivity of existing and next-generation neutrino experiments to this proton decay mode is discussed.

The amplitude for the decay  $p(p_p) \rightarrow e^+(p_e) \pi^0(p_\pi) G(p)$  can be written as a suitable product of a leptonic and hadronic part,

$$\mathcal{A}(p \rightarrow e^+ \pi^0 G) = -2\kappa c_{\mathcal{B}} \varepsilon_{\mu\rho}^*(p, \lambda) p_\sigma p_\nu \bar{v}_e^c(p_e) P_R \sigma^{\rho\sigma} H^{\mu\nu}(p_p, q) u_p(p_p). \quad (5.27)$$

Here,  $\varepsilon_{\mu\rho}^*(p, \lambda)$  denotes the conjugate of the polarisation tensor of the graviton with four-momentum  $p$  and polarisation  $\lambda$ . The variable  $q \equiv p_p - p_\pi = p + p_e$  denotes the four-momentum transfer from the proton to the neutral pion, and enters  $\mathcal{A}(p \rightarrow e^+ \pi^0 G)$  through the hadronic tensor  $H_{\mu\nu}(p_p, q)$ . Notice that in order to obtain (5.27) the gauge of the graviton is chosen such that the polarisation tensor is transverse and traceless, i.e. the following terms can be omitted in the decomposition of the decay amplitude (5.27)

$$p^\mu \varepsilon_{\mu\rho}^*(p, \lambda) = 0, \quad \varepsilon_\mu^{*\mu}(p, \lambda) = 0. \quad (5.28)$$

The LCSR results for the hadronic form factors, which are defined in (4.58) and parametrise  $H^{\mu\nu}(p_p, q)$ , are presented in Section 4.2.3. With the help of the expressions (4.70) to (4.73) the  $p \rightarrow e^+ \pi^0 G$  decay amplitude (5.27) can be calculated. One first notices that after making use of the on-shell conditions for the graviton (cf. (5.28)) the contribution of  $w_4$  vanishes. This feature can be understood by means of the soft pion theorem [299, 300]. In fact, in the soft pion limit and recalling that  $q = p_p - p_\pi$  one finds that all terms but the contribution of  $w_4$  vanish in the hadronic tensor:

$$\lim_{p_\pi \rightarrow 0} H^{\mu\nu}(p_p, q) = H^{\mu\nu}(p_p, p_p) = i w_4 P_R \sigma^{\mu\nu} u_p(p_p). \quad (5.29)$$

However, in the limit  $p_\pi \rightarrow 0$  the pion can be removed from the decay amplitude giving rise to the following relation

$$\begin{aligned} \lim_{p_\pi \rightarrow 0} \langle e^+ G \pi^0(p_\pi) | \mathcal{L}_{\mathcal{B}}^{(8)}(0) | p \rangle &= - \frac{i}{\sqrt{2} f_\pi} \langle e^+ G | \mathcal{L}_{\mathcal{B}}^{(8)}(0) | p \rangle \\ &+ \lim_{p_\pi \rightarrow 0} \frac{\sqrt{2}}{f_\pi} p_\pi^\mu \int d^4 x e^{i p_\pi x} \langle e^+ G | T [J_\mu^A(x) \mathcal{L}_{\mathcal{B}}^{(8)}(0)] | p \rangle , \end{aligned} \quad (5.30)$$

where  $J_\mu^A(x) \equiv [\bar{u}(x) \gamma_\mu \gamma_5 u(x) - \bar{d}(x) \gamma_\mu \gamma_5 d(x)] / 2$  denotes the axial current and the pion field is related to this current by  $\pi^0(x) = \sqrt{2} \partial^\mu J_\mu^A(x) / (f_\pi m_\pi^2)$ . The second term in (5.30) vanishes unless there are additional poles in the soft pion limit. Such poles occur if the pion is attached to one of the external lines [300] in the  $p \rightarrow e^+ G$  amplitude, which is formally described by inserting a complete set of intermediate states between the operators in the time-ordered product. The pion however can only couple to the external proton line, so pole contributions arise only when the pion is emitted from the incoming proton. This type of correction thus leads again to the matrix element of the  $p \rightarrow e^+ G$  transition, which however satisfies  $\langle e^+ G | \mathcal{L}_{\mathcal{B}}^{(8)}(0) | p \rangle = 0$ , because the transition is forbidden by angular momentum conservation. As a result the right-hand side of (5.30) vanishes identically:

$$\lim_{p_\pi \rightarrow 0} \langle e^+ G \pi^0(p_\pi) | \mathcal{L}_{\mathcal{B}}^{(8)}(0) | p \rangle = 0. \quad (5.31)$$

Since the form factor  $w_4$  itself is non-vanishing it then follows that the associated Lorentz structure (5.29) does not contribute to the proton decay channel  $p \rightarrow e^+ \pi^0 G$  at all.

By squaring the amplitude, summing over spins and polarisations and calculating the phase space integrals the differential decay width can be computed. Note that the transversality of the graviton (see (5.28)) has been used to drop unphysical contributions which violates the gauge symmetry of gravity in the weak field limit as defined by the transformation (2.19). The gauge symmetry ensures that negative-norm states cancel out in the sum over polarisations. Therefore the sum has to be constrained to physical polarisations only by employing [301]

$$\sum_\lambda \varepsilon_{\alpha\beta}^*(p, \lambda) \varepsilon_{\gamma\delta}(p, \lambda) = \frac{1}{2} (\eta'_{\alpha\delta} \eta'_{\beta\gamma} + \eta'_{\alpha\gamma} \eta'_{\beta\delta} - \eta'_{\alpha\beta} \eta'_{\gamma\delta}) , \quad (5.32)$$

with

$$\eta'_{\mu\nu} \equiv \eta_{\mu\nu} - \frac{\bar{p}_\mu p_\nu + p_\mu \bar{p}_\nu}{p \cdot \bar{p}} , \quad (5.33)$$

and  $\bar{p} \equiv (p^0, -\vec{p})$  such that  $\bar{p}^2 = 0$ .

## 5 Low-energy probes of CP and baryon-number violation

Neglecting the mass of the positron but keeping the mass of the neutral pion, the  $p \rightarrow e^+ \pi^0 G$  width corresponding to the fiducial region of the three-particle phase space defined by an upper cut on the graviton energy can be written as

$$\begin{aligned} \Gamma(p \rightarrow e^+ \pi^0 G)_{\text{fid}} &= \frac{m_p^7 |c_{\mathcal{B}}|^2}{128 \pi^3 \overline{M}_{\text{Pl}}^2} \int_0^{y_{\text{fid}}} dy \int_{z_0}^{z_1} dz (x_\pi + y + z - yz - 1) \\ &\quad \times (x_\pi + y + z - 1)^2 \left[ l_1 (w_1 + w_3)^2 + l_2 w_2^2 + l_3 w_2 (w_1 + w_3) \right]. \end{aligned} \quad (5.34)$$

Here we have defined  $y \equiv 2E_G/m_p$  and  $z \equiv 2E_e/m_p$  with  $E_G$  ( $E_e$ ) the graviton (positron) energy in the rest frame of the proton,  $x_\pi \equiv m_\pi^2/m_p^2$ , the boundaries for the integral over  $z$  are given by

$$z_0 = 1 - x_\pi - y, \quad z_1 = \frac{1 - x_\pi - y}{1 - y}, \quad (5.35)$$

and

$$l_1 = -4y, \quad l_2 = y [4x_\pi - (y + z - 2)^2], \quad l_3 = -4 [2x_\pi - (y + z)(y - 2) - 2]. \quad (5.36)$$

When expressed through the integration variables of (5.34) the scale  $Q^2$  that enters the form factors  $w_n$  finally takes the following form

$$Q^2 = -q^2 = -m_p^2 (x_\pi + y + z - 1). \quad (5.37)$$

The GRSMEFT proton decay mode  $p \rightarrow e^+ \pi^0 G$  experimentally leads to events that contain a positron, two photons arising from the decay of the neutral pion and missing energy ( $E^{\text{miss}}$ ) because the graviton escapes the detector undetected. Such a signature has to our knowledge not been searched for directly in experiments that study the possible decays of the proton. As we will show, existing searches that are however sensitive to  $p \rightarrow e^+ \pi^0 G$  are the inclusive search  $p \rightarrow e^+ X$  with  $X$  an arbitrary final state and the exclusive search for  $p \rightarrow e^+ \pi^0$ . The total inclusive rate  $p \rightarrow e^+ X$  can be obtained by employing  $y_{\text{fid}} = 1 - x_\pi$  in (5.34). Numerically, we find that

$$\Gamma(p \rightarrow e^+ \pi^0 G) = \frac{m_p^7 \Lambda_p^4 |c_{\mathcal{B}}|^2}{256 \pi^3 \overline{M}_{\text{Pl}}^2}, \quad \Lambda_p = (99 \pm 13) \text{ MeV}. \quad (5.38)$$

Here we have introduced the hadronic parameter  $\Lambda_p$ , and the normalisation factor  $1/(256 \pi^3)$  takes into account the phase-space suppression for a three-body decay. The uncertainty on  $\Lambda_p$  is obtained by calculating the minimal and maximal decay width that can be achieved by considering all possible combinations of the form factor parameterisations (4.70) to (4.73). Notice that since  $\Lambda_p$  appears in (5.38) to the fourth power the LCSR prediction for  $\Gamma(p \rightarrow e^+ \pi^0 G)$  has an uncertainty of order 50%. The theory uncertainties of  $\Gamma(p \rightarrow e^+ \pi^0 G)$  are therefore significantly larger than those that

plague the GUT predictions for  $\Gamma(p \rightarrow e^+\pi^0)$  obtained in both LQCD [217–224] and LCSRs [21].

Searches for the two-body decay mode  $p \rightarrow e^+\pi^0$  can also be used to set a bound on the GRSMEFT interaction (2.21), because the cuts that experiments such as SK impose do not fully eliminate the contributions that arise from  $p \rightarrow e^+\pi^0 G$ . The relevant requirements in these experiments are selections on the invariant mass  $m_{e\pi}$  and the magnitude of the three-momentum  $p_{e\pi}$  of the  $e^+\pi^0$  system. In the rest frame of the proton these quantities can be expressed in terms of the graviton energy as  $m_{e\pi} = \sqrt{m_p(m_p - 2E_G)}$  and  $p_{e\pi} = E_G$ . In the latest SK search [122] the definition of the signal region involves the requirements  $m_{e\pi} > 800 \text{ MeV}$  and  $p_{e\pi} < 250 \text{ MeV}$ , meaning that all  $p \rightarrow e^+\pi^0 G$  events that satisfy the  $m_{e\pi}$  selection also pass the  $p_{e\pi}$  cut. To quantify by how much a lower cut  $m_{e\pi} > m_{e\pi}^{\text{cut}}$  reduces the observed  $p \rightarrow e^+\pi^0 G$  decay width we introduce the acceptance

$$A(m_{e\pi}^{\text{cut}}) = \frac{\Gamma(p \rightarrow e^+\pi^0 G)_{\text{fid}}}{\Gamma(p \rightarrow e^+\pi^0 G)}, \quad (5.39)$$

where  $\Gamma(p \rightarrow e^+\pi^0 G)_{\text{fid}}$  is the fiducial decay width (5.34) evaluated setting  $y_{\text{fid}} = 1 - (m_{e\pi}^{\text{cut}}/m_p)^2$  and  $\Gamma(p \rightarrow e^+\pi^0 G)$  is the total inclusive width given in (5.38). In Figure 5.3 we show our predictions for  $A(m_{e\pi}^{\text{cut}})$  in the range of  $m_{e\pi}^{\text{cut}}$  that is relevant for searches for the two-body proton decay mode  $p \rightarrow e^+\pi^0$  at existing and next-generation water Cherenkov detectors.

We are now in a position to derive bounds on the Wilson coefficient  $c_{\mathcal{B}}$  that multiplies the dimension-eight operator in (2.21). We begin with the inclusive  $p \rightarrow e^+X$  decay. The currently best proton lifetime limit from  $p \rightarrow e^+X$  is unfortunately more than 40 years old. It reads [302]

$$\tau_p(p \rightarrow e^+X) > 0.6 \cdot 10^{30} \text{ yr}, \quad (5.40)$$

and together with (5.38) leads to

$$|c_{\mathcal{B}}| < (104 \text{ GeV})^{-4} \quad (5.41)$$

at the 90% CL. It has been pointed out in [124] that with existing data from water Cherenkov detectors it should be possible to set a significantly better limit on  $p \rightarrow e^+X$  compared to the proton lifetime limit reported in (5.40). An estimate of such an improved limit can be obtained from the limit of  $1.7 \cdot 10^{32} \text{ yr}$  at 90% CL on the  $p \rightarrow e^+ + E^{\text{miss}}$  channel [303] since the latter decay bears close resemblance to the inclusive  $p \rightarrow e^+X$  mode. In fact, the authors of [124] estimated that with the available SK data it should be possible to improve (5.40) by around two orders of magnitude. Note that a factor of 100 improvement on  $\tau_p(p \rightarrow e^+X)$  would push the bound (5.41) up to  $(186 \text{ GeV})^{-4}$ .

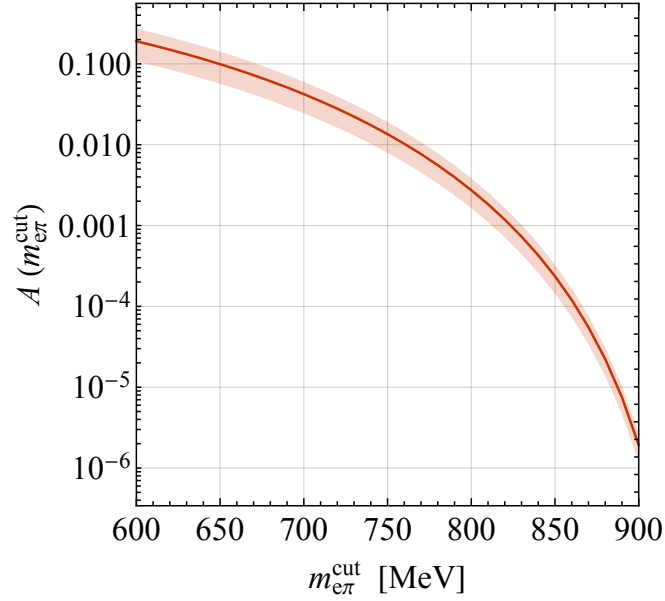


**Figure 5.3:** Acceptance (5.39) as a function of the cut  $m_{e\pi} > m_{e\pi}^{\text{cut}}$  on the invariant mass of the  $e^+\pi^0$  system. The red curve indicates the central prediction, while the red band illustrates the maximal variations that result from considering all possible combinations of the form factor parameterisations (4.70) to (4.73) in the fiducial decay width keeping the inclusive decay width fixed at the central value. See text for further details.

In order to determine the SK sensitivity to the  $p \rightarrow e^+\pi^0 G$  signature that derives from the measurement [303], we need to compute the acceptance (5.39) for  $m_{e\pi}^{\text{cut}} = 800$  MeV. Using the central value of the hadronic parameter  $\Lambda_p$  as given in (5.38) we find

$$A(800 \text{ MeV}) = 2.7 \cdot 10^{-3} (1 \pm 0.40) . \quad (5.42)$$

The smallness of the acceptance is compensated by the fact that the 90% CL lower limit on the lifetime of the proton in  $p \rightarrow e^+\pi^0$  is by more than five orders of magnitude better than (5.40) since one has [122] (cf. also Section 2.3)

$$\tau_p(p \rightarrow e^+\pi^0) > 2.4 \cdot 10^{34} \text{ yr} . \quad (5.43)$$

Combining (5.38) for  $\Lambda_p = 99$  MeV with (5.42) and (5.43) one obtains

$$|c_{\mathcal{B}}| < (185 \text{ GeV})^{-4} \quad (5.44)$$

at the 90% CL. Notice that this bound is very close to the limit that has been quoted above by assuming a factor of 100 improvement of  $\tau_p(p \rightarrow e^+X)$  compared to (5.40) based on the estimate presented in [124].

It is also straightforward to estimate the sensitivity of HK to the Wilson coefficient  $c_{\mathcal{B}}$ . Running HK for eight years it should be possible to set the following 90% CL

bound

$$\tau_p(p \rightarrow e^+ \pi^0) > 1.0 \cdot 10^{35} \text{ yr} . \quad (5.45)$$

This limit has been obtained in [296] by considering the same signal region for  $p \rightarrow e^+ \pi^0$  as the latest SK search [122]. Consequently, we can again use (5.38) and (5.42) as well as (5.45) to arrive at

$$|c_{\cancel{B}}| < (222 \text{ GeV})^{-4} . \quad (5.46)$$

This bound on the Wilson coefficient of the dimension-eight baryon-number violating operator (2.21) is probably the ultimate limit that can be set with the help of data from next-generation neutrino detectors, because both JUNO and DUNE are not expected to reach the HK sensitivity to the  $p \rightarrow e^+ \pi^0$  mode (cf. [297, 298]).



## 6 Conclusions

The matter-antimatter asymmetry of the observable universe implies, under certain assumptions (cf. Chapter 1), the existence of new physics that violates the conservation of CP and baryon number. In fact, many theoretical models for BSM physics admit new sources of CP and baryon-number violation. A wide range of the BSM landscape related to these fundamental symmetries can be constrained by experimental data with the help of a suitable EFT, i.e. in a bottom-up approach. If new particles are too heavy to be produced on-shell in an experiment, their effects on observables at low energies can be systematically taken into account by effective, higher-dimensional operators that augment the SM interactions.

This feature was employed in the work at hand to study the implications of certain CP- and baryon-number-violating interactions in a model-independent way. The observable consequences of these new interactions — contributions to the nEDM and proton decay — can be probed experimentally with high sensitivity. An overview of the relevant operator basis in the EFT approach as well as the corresponding experimental probes was provided in Chapter 2. In particular, it was pointed out that the theory predictions for the relevant observables rely on the knowledge of the associated hadronic matrix elements, which cannot be computed perturbatively in QCD. Thus, predictions for the hadronic parts of the relevant scattering amplitudes by other means are required. This was addressed subsequently in Chapters 3 and 4 where in particular the nEDM and proton-decay searches were examined. The results of these two chapters were used in Chapter 5 to explore the phenomenology of CP-violating Higgs-gluon interactions as well as baryon-number-violating interactions involving gravity. The latter arise in the GRSMEFT and augment not only the strong and electroweak interactions of the SM but also GR. The results of Sections 3.2, 4.1, 4.2, 5.1 and 5.2 represent the main achievements of this work, which were originally presented in [19–22], and they are now discussed in turn.

First, in Section 3.2, the hadronic matrix elements of dimension-six and dimension-eight operators of Weinberg type (3.17) that contribute to the nEDM  $d_n$  were calculated with the help of QCD sum-rule techniques. Calculations along the same line of the dimension-four and dimension-five contributions to the nEDM, i.e. the QCD  $\theta$  term and CEDMs, were performed in [90–92, 172, 173]. A sum-rule estimate of the

dimension-six Weinberg operator  $O_6$  also exists in literature [94], but this article does not provide details on the actual computation, which motivates the independent evaluation presented in this work. The determination of the hadronic matrix elements of the dimension-eight term  $O_8$  is instead new and provides the first systematic study of contributions to  $d_n$  due to CP-violating four-gluon operators. The main results are the numerical expressions (3.96) and (3.99).

The sum-rule estimates are based on the observation [93, 94] that the Weinberg-type contributions to the nEDM can be obtained by calculating the  $i\gamma_5$  rotation of the nucleon wave function induced by (3.17) and relating it to the corresponding rotation of the neutron anomalous magnetic moment  $\mu_n$ . In this approximation only those diagrams are included that factorise into a propagator with a CP-violating mass insertion and into a part that couples to the external photon field, while non-factorisable vertex corrections are neglected (see Figure 3.1). In addition, contributions from excited neutron-like states were neglected. These simplifications lead to uncertainties in the predictions that can be estimated to be of the order of 35% using Borel techniques. The OPE computation of the dimension-six and dimension-eight sum rules is described in detail, and includes a discussion of the matching and the appropriate choice of the neutron-interpolating current. The final analytic expressions for the  $O_6$  and  $O_8$  contributions to  $d_n$  are reported in (3.94) and (3.97), respectively, and the result for  $|(d_n)_{O_6}|$  agrees with the findings given in [94]. The hadronic matrix elements of the Weinberg-type operators turn out to be logarithmically sensitive to the ratio  $M/\Lambda_{\text{QCD}}$  of the Borel mass and the QCD scale. This IR sensitivity provides the dominant theoretical uncertainty of the final predictions. By varying  $M/\Lambda_{\text{QCD}}$  in the range  $\sqrt{2} \cdot [1, 2]$  one finds uncertainties close to 45%, which exceeds the size of the expected effects from vertex diagrams and excited states. Adding individual errors in quadrature the total uncertainties of the numerical predictions for  $(d_n/e)_{O_6}$  and  $(d_n/e)_{O_8}$  are 50% and 80%. Sum-rule studies of the  $\theta$ -term and CEDM contributions to the nEDM [90–92, 172, 173] have found uncertainties of a similar magnitude.

While the sum-rule estimates of the  $d_n$  contributions due to the dimension-six and dimension-eight operators of Weinberg type (3.17) have sizeable uncertainties, they can be considered to be more robust than other existing determinations that are based on NDA [77] or the VIA [93]. In particular, in the sum-rule approach there is no sign ambiguity between the prediction for  $d_n$  and the hadronic matrix elements of  $O_6$  and  $O_8$  — see for instance [60, 67, 69, 72, 75] for EDM studies that allow for both signs of the  $O_6$  contribution. To find out whether the sum-rule estimates are reliable would require first-principle calculations of the nEDM, which are in principle possible using existing LQCD methodology. While such calculations have gained significant momentum [95–102], LQCD simulations involving Weinberg-type operators are challenging [103, 104],

and it remains to be seen which accuracy such computations can achieve in the near future. Till then phenomenological studies of hadronic EDMs have to rely on the predictions (3.96) and (3.99) despite all their limitations.

The sum-rule estimates for the nEDM were employed in Section 5.1 to study the phenomenology of CP-violating Higgs-gluon interactions in BSM scenarios with vanishing light-quark Yukawa couplings. From the discussion presented in Section 5.1.2 it can be concluded that future nEDM searches and LHC measurements are complementary to each other even in the specific class of new-physics models where the Yukawa couplings of light quarks are zero. This is an interesting finding because such new-physics realisations represent in some sense the worst-case scenario for the low-energy constraints considered here. The results show furthermore that in a global SMEFT analysis, EDM constraints can have additional flat or weakly bound directions (cf. Section 2.1) that do not appear in the case of universal theories considered in [39, 74]. As already emphasised in [39], to resolve unbounded directions in the multi-dimensional space of Wilson coefficients, high- $p_T$  and low-energy constraints on CP-violating couplings between the Higgs and gauge bosons should be combined into global fits. The nEDM results presented in this work can be readily used for such a purpose.

Another important result of this work is the prediction for the hadronic matrix elements of the full set of baryon-number violating dimension-six SMEFT operators (2.13) from LCSR techniques, which is presented in Section 4.1. These hadronic matrix elements are needed to predict the rates of the main proton decay modes in GUTs, where a proton decays into a pseudoscalar meson and an anti-lepton. Specifically, the focus in this work lies on the decay  $p \rightarrow \pi^0 e^+$ , and the explicit LCSR expressions for the relevant form factors are presented in Appendix E, which include the leading contributions in the light-cone expansion, namely the twist-2 and twist-3 pion DAs. We performed a detailed study of the dependence of the LCSRs on both the unphysical (i.e. the continuum threshold and the Borel mass) and the physical (i.e. the condensates and the pion DAs) parameters, and discussed the possible impact of twist-4 effects. This can be used to provide results and estimate uncertainties for the form factors in the kinematical regime where the momentum transfer  $q$  from the proton to the pion is space-like, i.e.  $Q^2 = -q^2 > 0$ , and lies in the range  $0.5 \text{ GeV}^2 \leq Q^2 \leq 2.5 \text{ GeV}^2$ . The LCSR results were then extrapolated to the physical point  $Q^2 \simeq 0$  by means of both a linear and a quadratic fit, including the spread of predictions in the uncertainty estimates. The analysis indicates that one of the four sum rules is not reliable, and therefore only the other three are considered when determining the final predictions for the physical form factors  $W_{\Gamma\Gamma'}^n$  with  $n = 0, 1$  and  $\Gamma\Gamma' = RR, LR$  from the range of different solutions shown in Figures 4.4 and 4.5.

## 6 Conclusions

The final results for  $W_{\Gamma\Gamma'}^n$  can be found in (4.53) and (4.54), and the LCSR results are compared to the state-of-the-art LQCD predictions [223] in Figure 4.6. The uncertainties of the LCSR results amount to  $(25 - 40)\%$ , while the total accuracy of the LQCD form factors is  $(10 - 15)\%$ . In view of the inherent systematic uncertainties of LCSRs, it is not clear to which extent possible refinements of the calculations such as including higher-twist contributions or perturbative corrections would increase the precision of (4.53) and (4.54). The observed overall agreement between these results and the latest LQCD form factors demonstrates however that LCSRs can be successfully applied to the calculations of proton decay matrix elements, and that such computations can achieve a precision that is better than the alternative methods to estimate proton decay rates which were developed in the '80s.

Even LQCD calculations of three-body proton decay processes at arbitrary kinematics seem to be in reach in the coming years (see [104] for a discussion), but it remains to be seen which accuracy such computations can initially achieve. Therefore, the LCSR techniques presented in this work are presently the only available tool for calculating the form factors that parametrise the hadronic matrix elements of semi-leptonic three-body proton decays, which is discussed in Section 4.2. While the presented formalism and the obtained results are general, this work specifically focused on the computation of the differential decay rate for the process  $p \rightarrow e^+\pi^0 G$  with  $G$  a graviton. This channel is the dominant proton decay mode in the GRSMEFT, since the two-body transition  $p \rightarrow e^+ G$  is forbidden by angular momentum conservation. Like in Section 4.1 the LCSR study includes the leading contributions in the light-cone expansion, namely the twist-2 and twist-3 pion DAs — the explicit expressions can be found in Appendix F — and a detailed study of the dependence of the obtained LCSRs on all unphysical and physical parameters was performed. In this way, the uncertainties of the final results for the form factors were obtained in the kinematical regime where the momentum transfer  $q$  from the proton to the pion is space-like. The LCSR results were then again extrapolated to the physical regime  $0 \leq q^2 \leq (m_p - m_\pi)^2$  by means of both a linear and a quadratic fit, including the spread of predictions in the uncertainty estimates. The resulting uncertainties turned out to be significantly larger than those that plague the hadronic matrix elements that are relevant in the GUT case (cf. Section 4.1.3).

The LCSR results for the form factors were used in Section 5.2 to study the sensitivity of existing and next-generation water Cherenkov detectors in looking for the  $p \rightarrow e^+\pi^0 G$  signature. To this purpose, the rate for  $p \rightarrow e^+\pi^0 G$  was calculated differentially in the energies of the final state particles. Next, the bounds on the amount of dimension-eight baryon-number violation in the GRSMEFT were derived considering both the inclusive search for  $p \rightarrow e^+ X$  [124, 302] and the exclusive search for  $p \rightarrow e^+\pi^0$ . It turned out that the best constraint arises at the moment from the latest SK search for the two-

body decay mode  $p \rightarrow e^+ \pi^0$  [122]. In fact, this search is able to set a 90% CL lower limit of 185 GeV on the effective mass scale that suppresses the relevant baryon-number violating GRSMEFT interactions. HK measurements are expected to be able to push this limit up to 222 GeV.



## A Fixed-point gauge

In the case of QCD the fixed-point or Fock-Schwinger gauge [304, 305] can be defined without loss of generality for gauge-invariant quantities by

$$x^\mu G_\mu^A(x) = 0, \quad (\text{A.1})$$

where it is sufficient to restrict this choice of gauge to classical gluon fields.

For the gauge choice (A.1) it is easy to show that it is possible to express the gluon field through the QCD field strength tensor  $G_{\mu\nu}^A(x) = \partial_\mu G_\nu^A(x) - \partial_\nu G_\mu^A(x) + g_s f^{ABC} G_\mu^B(x) G_\nu^C(x)$  evaluated at  $x = 0$ . To derive the sought relation, one notices first that

$$\begin{aligned} G_\mu^A(x) &= \partial_\mu (x^\nu G_\nu^A(x)) - x^\nu \partial_\mu G_\nu^A(x) \\ &= -x^\nu (G_{\mu\nu}^A(x) + \partial_\nu G_\mu^A(x) - g_s f^{ABC} G_\mu^B(x) G_\nu^C(x)) \\ &= x^\nu G_{\nu\mu}^A(x) - x^\nu \partial_\nu G_\mu^A(x), \end{aligned} \quad (\text{A.2})$$

where we have employed the gauge condition (A.1) twice and used the anti-symmetry of  $G_{\mu\nu}^A$  to obtain the final result. Setting  $x^\nu = \alpha y^\nu$  with an arbitrary parameter  $\alpha$ , one can then write

$$x^\nu G_{\nu\mu}^A(x) = \alpha y^\nu G_{\nu\mu}^A(\alpha y) = G_\mu^A(\alpha y) + \alpha y^\nu \frac{\partial}{\partial(\alpha y^\nu)} G_\mu^A(\alpha y) = \frac{d}{d\alpha} (\alpha G_\mu^A(\alpha y)). \quad (\text{A.3})$$

Now if one integrates both sides of the above relation over  $\alpha \in [0, 1]$  and assumes that  $G_\mu^A(x)$  is non-singular at  $x = 0$ , one finds

$$\int_0^1 d\alpha \alpha y^\nu G_{\nu\mu}^A(\alpha y) = G_\mu^A(y). \quad (\text{A.4})$$

Using a similar assumption for the QCD field strength, one can Taylor expand  $G_{\nu\mu}^A(\alpha y)$  around  $\alpha y = 0$  and perform the integration on the left-hand side of (A.4). It follows that

$$G_\mu^A(x) = \frac{1}{2} x^\nu G_{\nu\mu}^A(0) + \frac{1}{3} x^\nu x^\rho \partial_\rho G_{\nu\mu}^A(0) + \dots, \quad (\text{A.5})$$

where we have switched back from the variable  $y$  to the variable  $x$ .

## A Fixed-point gauge

The latter expression can be further simplified by noting that as a result of (A.1), the partial derivatives in (A.5) can be promoted to covariant derivatives  $D_\mu = \partial_\mu - ig_s G_\mu^A T^A$ . In consequence, one has

$$G_\mu^A(x) = \frac{1}{2} x^\nu G_{\nu\mu}^A(0) + \frac{1}{3} x^\nu x^\rho D_\rho G_{\nu\mu}^A(0) + \dots, \quad (\text{A.6})$$

in the fixed-point gauge of QCD. The same result also holds in the case of EM fields with  $G_\mu^A$  replaced by  $A_\mu$  and  $G_{\mu\nu}^A$  replaced by  $F_{\mu\nu}$ .

Finally, notice that due to (A.1) the Taylor expansion of the classical quark field  $q$  can also be formulated in terms of covariant rather than partial derivatives. One has

$$q(x) = q(0) + x^\mu D_\mu q(0) + \frac{1}{2} x^\mu x^\nu D_\mu D_\nu q(0) + \dots. \quad (\text{A.7})$$

## B OPE for the quark propagator

The free position-space propagator  $S^{(0)}(x)$  of a massless quark is easily derived by taking the Fourier transform of the well-known momentum-space representation

$$S^{(0)}(x) = \int d^4p e^{-ipx} \frac{i\not{p}}{p^2} = \frac{1}{(2\pi)^4} (-i\not{\phi}_E) \int d^4p_E \frac{e^{ip_E x_E}}{p_E^2}, \quad (\text{B.1})$$

where colour indices are implicit and we have applied a Wick rotation to Euclidean space using  $x^2 \rightarrow -x_E^2$  and  $p^2 \rightarrow -p_E^2$ . The four-dimensional integration measure can be written as  $d^4p_E = \bar{p}^3 d\bar{p} d\Omega_4$ , where the magnitude of the four-dimensional Euclidean momentum vector has been denoted by  $\bar{p} = |p_E|$ . The differential solid angle is given by

$$\int d\Omega_4 = \int_0^{2\pi} d\phi \int_0^\pi d\theta_1 d\theta_2 \sin\theta_1 \sin^2\theta_2. \quad (\text{B.2})$$

It follows that  $d\Omega_4 = d\Omega_3 \sin^2\theta_2$  and (B.1) hence takes the form

$$\begin{aligned} S^{(0)}(x) &= \frac{1}{4\pi^3} (-i\not{\phi}_E) \int_0^\infty d\bar{p} \bar{p} \int_0^\pi d\theta_2 \sin^2\theta_2 e^{i\bar{p}\bar{x} \cos\theta_2} \\ &= \frac{1}{4\pi^3} (-i\not{\phi}_E) \int_0^\infty d\bar{p} \bar{p} \frac{\pi J_1(\bar{p}\bar{x})}{\bar{p}\bar{x}} = \frac{1}{4\pi^2} (-i\not{\phi}_E) \frac{1}{\bar{x}^2} = \frac{i\not{x}}{2\pi^2 x^4}. \end{aligned} \quad (\text{B.3})$$

Here  $\bar{x} = |x_E|$ ,  $J_1(z)$  denotes the Bessel function of first kind with index 1 and in the final step we have rotated back from Euclidean to Minkowski space noting that  $\not{x}_E \rightarrow \not{x}$ .

In order to determine the non-perturbative contributions  $S^q(x)$  to the quark propagator, one needs to evaluate the correlator  $\langle 0|T[q_a^i(x)\bar{q}_b^j(0)]|0\rangle$ . Using the expansion of the classical quark field (A.7), one obtains

$$\langle 0|T[q_a^i(x)\bar{q}_b^j(0)]|0\rangle = \langle q_a^i(0)\bar{q}_b^j(0)\rangle + \dots = -\frac{1}{12} \delta_{ab} \delta^{ij} \langle \bar{q}q \rangle + \dots, \quad (\text{B.4})$$

where the fields of the condensate  $\langle \bar{q}q \rangle$  are evaluated at  $x = 0$ . Notice that the minus sign in the final result comes from the exchange of the fermion fields and the numerical prefactor can be determined by contracting the expression in the middle and on the right with  $\delta^{ab} \delta_{ij}$ . Ignoring colour and spinor indices, the expansion (B.4) thus leads to the expression for  $S^q(x)$  as given in (3.42).



## C Fourier transforms

We define the Fourier transform of a function  $F(p)$  by

$$\mathcal{F}\left[F(p)\right] = \left(\frac{\mu_{\text{IR}}^2}{4\pi e^{\gamma_E}}\right)^{-\epsilon_{\text{IR}}} \int \bar{d}^{4+2\epsilon_{\text{IR}}} p e^{-ipx} F(p), \quad (\text{C.1})$$

where we performed the integration in  $d = 4 + 2\epsilon_{\text{IR}}$  space-time dimensions with  $\epsilon_{\text{IR}} > 0$  to regulate the IR divergences that appear in some of the Fourier integrals that were encountered in Sections 3.2.2.3 and 3.2.3.1. The symbol  $\gamma_E$  denotes Euler's constant and  $\mu_{\text{IR}}$  is a mass scale needed to restore the correct dimensionality of (C.1).

In the case that  $F(p)$  is polynomial in  $1/p^2$ , a simple calculation along the lines of the computation performed in Appendix B leads to

$$\mathcal{F}\left[\frac{1}{(p^2)^k}\right] = \frac{i}{4^k \pi^2} \left(-\frac{\mu_{\text{IR}}^2 x^2}{4e^{\gamma_E}}\right)^{-\epsilon_{\text{IR}}} \frac{\Gamma(2-k+\epsilon_{\text{IR}})}{\Gamma(k)} (x^2)^{k-2}, \quad (\text{C.2})$$

where  $k \in \mathbb{N}_+$ . The Fourier transforms of type (C.2) relevant for this work are

$$\mathcal{F}\left[\frac{1}{p^2}\right] = \frac{i}{4\pi^2 x^2}, \quad (\text{C.3})$$

$$\mathcal{F}\left[\frac{1}{p^4}\right] = \frac{i}{16\pi^2} \left[\frac{1}{\epsilon_{\text{IR}}} - \ln\left(-\frac{\mu_{\text{IR}}^2 x^2}{4}\right)\right]. \quad (\text{C.4})$$

Tensor Fourier integrals with a polynomial denominator of the form  $(p^2)^k$  can be obtained from (C.2) by taking derivatives

$$\mathcal{F}\left[\frac{p_\mu p_\nu \cdots}{(p^2)^k}\right] = (i\partial_\mu)(i\partial_\nu) \cdots \mathcal{F}\left[\frac{1}{(p^2)^k}\right]. \quad (\text{C.5})$$

This procedure allows us to derive for example

$$\mathcal{F}\left[\frac{p_\mu p_\nu}{p^4}\right] = -\frac{i}{4\pi^2 x^4} \left(x_\mu x_\nu - \frac{g_{\mu\nu}}{2} x^2\right), \quad (\text{C.6})$$

a relation that has been used in Sections 3.2.2.3 and 3.2.3.1.

In the sum-rule calculations we also encountered UV divergent Fourier transformations of a function  $F(x)$ . To regulate UV divergences we work in  $d = 4 - 2\epsilon_{\text{UV}}$  space-time dimensions with  $\epsilon_{\text{UV}} > 0$ , introduce the mass scale  $\mu_{\text{UV}}$  and define

$$\mathcal{F}\left[F(x)\right] = \left(\frac{\mu_{\text{UV}}^2 e^{\gamma_E}}{4\pi}\right)^{-\epsilon_{\text{UV}}} \int d^{4-2\epsilon_{\text{UV}}} x e^{ipx} F(x). \quad (\text{C.7})$$

If  $F(x)$  is a polynomial in  $1/x^2$ , it is straightforward to evaluate (C.7). For  $k \in \mathbb{N}_+$  we obtain

$$\mathcal{F} \left[ \frac{1}{(x^2)^k} \right] = -\frac{i\pi^2}{4^{k-2}} \left( -\frac{\mu_{\text{UV}}^2 e^{\gamma_E}}{p^2} \right)^{-\epsilon_{\text{UV}}} \frac{\Gamma(2-k-\epsilon_{\text{UV}})}{\Gamma(k)} (p^2)^{k-2}. \quad (\text{C.8})$$

The Fourier integrals of the form (C.8) that occur in this thesis are

$$\mathcal{F} \left[ \frac{1}{x^2} \right] = -\frac{4i\pi^2}{p^2}, \quad (\text{C.9})$$

$$\mathcal{F} \left[ \frac{1}{x^6} \right] = -\frac{i\pi^2 p^2}{8} \left[ \frac{1}{\epsilon_{\text{UV}}} - \ln \left( -\frac{\mu_{\text{UV}}^2}{p^2} \right) - 1 \right]. \quad (\text{C.10})$$

We also encountered Fourier transforms that are both IR and UV divergent. They are of the type  $\mathcal{F} \left[ 1/((x^2)^l) \mathcal{F} \left[ 1/((p^2)^k) \right] \right]$  with  $k, l \in \mathbb{N}_+$ . Using the result given in (C.2) and (C.8) these double integrals are readily computed. We find

$$\begin{aligned} \mathcal{F} \left[ \frac{1}{(x^2)^l} \mathcal{F} \left[ \frac{1}{(p^2)^k} \right] \right] &= \frac{1}{4^l} \left( -\frac{\mu_{\text{IR}}^2}{p^2 e^{\gamma_E}} \right)^{-\epsilon_{\text{IR}}} \left( -\frac{\mu_{\text{UV}}^2 e^{\gamma_E}}{p^2} \right)^{-\epsilon_{\text{UV}}} \\ &\times \frac{\Gamma(2-k+\epsilon_{\text{IR}}) \Gamma(k-l-\epsilon_{\text{IR}}-\epsilon_{\text{UV}})}{\Gamma(k) \Gamma(2-k+l+\epsilon_{\text{IR}})} (p^2)^{l-k}. \end{aligned} \quad (\text{C.11})$$

The only Fourier integral of the form (C.11) that is necessary to compute the two-loop contributions to the OPE correlation functions considered in this work is

$$\mathcal{F} \left[ \frac{1}{x^6} \mathcal{F} \left[ \frac{1}{p^4} \right] \right] = \frac{p^2}{128} \ln \left( -\frac{\mu_{\text{IR}}^2}{p^2} \right) \ln \left( -\frac{\mu_{\text{UV}}^2}{p^2} \right) + \dots, \quad (\text{C.12})$$

where the ellipsis represents terms that vanish after Borel transformation (cf. Section 3.1), meaning that these contributions do not enter the analytic expressions (3.94) and (3.97).

## D Pion DAs

We use the following expressions for the pion DAs including terms proportional to the pion mass, which have been derived in [200] (and [199] in the chiral limit) with the help of a conformal expansion. One has

$$\phi^{(2)}(u, \mu) = 6u\bar{u} \left[ 1 + a_2(\mu) C_2^{(3/2)}(\zeta) + a_4(\mu) C_4^{(3/2)}(\zeta) \right], \quad (\text{D.1})$$

$$\begin{aligned} \phi_p^{(3)}(u, \mu) = 1 + \left( 30\eta_3(\mu) - \frac{5}{2}\rho_\pi^2 \right) C_2^{(1/2)}(\zeta) \\ + \left( -3\eta_3(\mu)\omega_3(\mu) - \frac{27}{20}\rho_\pi^2 - \frac{81}{10}\rho_\pi^2 a_2(\mu) \right) C_4^{(1/2)}(\zeta), \end{aligned} \quad (\text{D.2})$$

$$\phi_\sigma^{(3)}(u, \mu) = 6u\bar{u} \left[ 1 + \left( 5\eta_3(\mu) - \frac{1}{2}\eta_3(\mu)\omega_3(\mu) - \frac{7}{20}\rho_\pi^2 - \frac{3}{5}\rho_\pi^2 a_2(\mu) \right) \right] C_2^{(3/2)}(\zeta), \quad (\text{D.3})$$

$$\mathcal{T}^{(3)}(\alpha_d, \alpha_u, \alpha_g, \mu) = 360\eta_3(\mu)\alpha_d\alpha_u\alpha_g^2 \left[ 1 + \frac{1}{2}\omega_3(\mu)(7\alpha_g - 3) \right], \quad (\text{D.4})$$

where the expansion in terms of the Gegenbauer polynomials  $C_n^{(m)}(\zeta)$  with  $\zeta \equiv 2u - 1$  is truncated after  $n = 4$ . The hadronic parameters that enter the above definitions depend on the renormalisation scale  $\mu$  which we set equal to 1 GeV in our numerical analysis.

We adopt the numerical values of the two Gegenbauer moments presented in [306],

$$a_2(1 \text{ GeV}) = 0.17 \pm 0.08, \quad a_4(1 \text{ GeV}) = 0.06 \pm 0.10, \quad (\text{D.5})$$

where the moments are obtained by fitting sum rules for the EM pion form factor to the experimental data of [307]. For the numerical values of the other parameters we rely on the sum rules estimates of [243]:

$$f_{3\pi}(1 \text{ GeV}) = (0.45 \pm 0.15) \cdot 10^{-2} \text{ GeV}^2, \quad \omega_3(1 \text{ GeV}) = -1.5 \pm 0.7. \quad (\text{D.6})$$

Using the definition  $f_{3\pi}(\mu) \equiv f_\pi \mu_\pi \eta_3(\mu)$  together with (4.51) we then find

$$\eta_3(1 \text{ GeV}) = 0.017 \pm 0.006, \quad (\text{D.7})$$

where the individual uncertainties are added in quadrature.



## E Analytic results of the LCSRs for two-body proton decay

In this appendix, we provide the analytic expressions for the QCD correlation functions that appear on the right-hand side of the LCSRs (4.45) for the two proton decay  $p \rightarrow \pi^0 e^+$  — the integrations over the momentum fractions have to be calculated numerically. The hat on the functions  $\hat{\Pi}_{\Gamma\Gamma'}^{\text{QCD},\gamma}$  indicates that we have subtracted the contributions of heavy states before taking the Borel transform of the QCD results. We obtain

$$\hat{\Pi}_{RR}^{\text{QCD},S} = \frac{if_\pi}{32\sqrt{2}} \left\{ \frac{m_0^2 \langle \bar{q}q \rangle}{3} \left[ \int_0^\Delta du \frac{\phi^{(2)}(u)}{\bar{u}^3 M^2} e(\tilde{s}) (Q^2 + \bar{u}^2 m_\pi^2 - \bar{u} M^2) + \frac{\phi^{(2)}(\Delta)}{\bar{\Delta}} e(s_0) \right] - \frac{3\mu_\pi M^4}{\pi^2} \int_0^\Delta du \bar{u} \phi_p^{(3)}(u) e(\tilde{s}) \tilde{E}_2(\tilde{s}) \right\}, \quad (\text{E.1})$$

$$\begin{aligned} \hat{\Pi}_{RR}^{\text{QCD},P} = & \frac{if_\pi m_p}{12\sqrt{2}} \left\{ \frac{M^2}{8\pi^2} \int_0^\Delta du \phi^{(2)}(u) e(\tilde{s}) \left[ (Q^2 + \bar{u}^2 m_\pi^2) \tilde{E}_1(\tilde{s}) - 13\bar{u} M^2 \tilde{E}_2(\tilde{s}) \right] \right. \\ & + \frac{\mu_\pi m_0^2 \langle \bar{q}q \rangle}{4M^2} \left[ \int_0^\Delta du \frac{\phi_p^{(3)}(u)}{\bar{u}} e(\tilde{s}) + \frac{\bar{\Delta} M^2 \phi_p^{(3)}(\Delta)}{Q^2 + \bar{\Delta}^2 m_\pi^2} e(s_0) \right] \\ & + \frac{\mu_\pi \langle \bar{q}q \rangle}{3M^2} (1 - \rho_\pi^2) \left\{ \int_0^\Delta du \frac{\phi_\sigma^{(3)}(u)}{\bar{u}^3} e(\tilde{s}) \right. \\ & \quad \times \left[ 2\bar{u}^2 M^2 \left( 1 - \frac{m_0^2}{12\bar{u} M^2} \right) - \bar{u} (Q^2 + \bar{u}^2 m_\pi^2) \left( 1 - \frac{m_0^2}{6\bar{u} M^2} \right) \right] \\ & \quad \left. - M^2 \phi_\sigma^{(3)}(\Delta) e(s_0) \left( 1 - \frac{m_0^2}{6\bar{\Delta} M^2} \right) + \frac{\bar{\Delta} m_0^2 M^2}{6(Q^2 + \bar{\Delta}^2 m_\pi^2)} e(s_0) \frac{\partial}{\partial \Delta} \phi_\sigma^{(3)}(\Delta) \right\} \Bigg\}, \quad (\text{E.2}) \end{aligned}$$

$$\begin{aligned} & - \frac{\mu_\pi \langle \bar{q}q \rangle}{M^2} \left[ \int_0^1 D\alpha \theta(\alpha - \Delta_g) \frac{\mathcal{T}^{(3)}(1 - \alpha_u - \alpha_g, \alpha_u, \alpha_g)}{\alpha^3} e(\tilde{s}_g) \right. \\ & \quad \times [2\bar{u} Q^2 - 2\bar{u} \alpha M^2 + (1 - 4u) \alpha^2 m_\pi^2] \\ & \quad \left. + M^2 e(s_0) \int_0^1 du d\alpha_g \theta(1 - \bar{u} \alpha_g - \Delta_g) \frac{\mathcal{T}^{(3)}(1 - \bar{u} \alpha_g - \Delta_g, \Delta_g - u \alpha_g, \alpha_g)}{\Delta_g (Q^2 + \Delta_g^2 m_\pi^2)} \right] \end{aligned}$$

$$\begin{aligned}
 & \times \left[ 2\bar{u}Q^2 + (1 - 4u)\Delta_g^2 m_\pi^2 \right] \Bigg\}, \\
 \hat{\Pi}_{RR}^{\text{QCD},Q} = & \frac{if_\pi m_p}{12\sqrt{2}} \left\{ \frac{M^2}{8\pi^2} \int_0^\Delta du \frac{\phi^{(2)}(u)}{\bar{u}} e(\tilde{s}) \right. \\
 & \times \left[ u(Q^2 + \bar{u}^2 m_\pi^2) \tilde{E}_1(\tilde{s}) + \bar{u}(14 - 13u)M^2 \tilde{E}_2(\tilde{s}) \right] \\
 & + \frac{\mu_\pi m_0^2 \langle \bar{q}q \rangle}{4M^2} \left[ \int_0^\Delta du \frac{u \phi_p^{(3)}(u)}{\bar{u}^2} e(\tilde{s}) + \frac{\Delta M^2 \phi_p^{(3)}(\Delta)}{Q^2 + \bar{\Delta}^2 m_\pi^2} e(s_0) \right] \\
 & + \frac{\mu_\pi \langle \bar{q}q \rangle}{3M^2} (1 - \rho_\pi^2) \left\{ \int_0^\Delta du \frac{\phi_\sigma^{(3)}(u)}{\bar{u}^4} e(\tilde{s}) \right. \\
 & \times \left[ \zeta \bar{u} M^2 \left( 1 - \frac{m_0^2}{6M^2} \frac{1+u}{\zeta} \right) - u\bar{u} (Q^2 + \bar{u}^2 m_\pi^2) \left( 1 - \frac{m_0^2}{6\bar{u}M^2} \right) \right] \\
 & \left. - \frac{\Delta M^2 \phi_\sigma^{(3)}(\Delta)}{\bar{\Delta}} e(s_0) \left( 1 - \frac{m_0^2}{6\bar{\Delta}M^2} \right) + \frac{\Delta m_0^2 M^2}{6(Q^2 + \bar{\Delta}^2 m_\pi^2)} e(s_0) \frac{\partial}{\partial \Delta} \phi_\sigma^{(3)}(\Delta) \right\} \\
 & \left. + \frac{\mu_\pi \langle \bar{q}q \rangle}{M^2} \left[ \int_0^1 D\alpha \theta(\alpha - \Delta_g) \frac{\mathcal{T}^{(3)}(1 - \alpha_u - \alpha_g, \alpha_u, \alpha_g)}{\alpha^3} e(\tilde{s}_g) \right. \right. \\
 & \times [2\bar{u}Q^2 - 2\bar{u}\alpha M^2 + \alpha(1 + 2u + (1 - 4u)\alpha) m_\pi^2] + \\
 & + M^2 e(s_0) \int_0^1 du d\alpha_g \theta(1 - \bar{u}\alpha_g - \Delta_g) \frac{\mathcal{T}^{(3)}(1 - \bar{u}\alpha_g - \Delta_g, \Delta_g - u\alpha_g, \alpha_g)}{\Delta_g (Q^2 + \Delta_g^2 m_\pi^2)} \\
 & \left. \left. \times [2\bar{u}Q^2 + \Delta_g(1 + 2u + (1 - 4u)\Delta_g) m_\pi^2] \right] \right\}, \\
 \end{aligned} \tag{E.3}$$

$$\begin{aligned}
 \hat{\Pi}_{RR}^{\text{QCD},T} = & \frac{if_\pi m_p^2}{2\sqrt{2}} \left\{ \frac{\langle \bar{q}q \rangle}{3} \left[ - \int_0^\Delta du \frac{\phi^{(2)}(u)}{\bar{u}} e(\tilde{s}) \left( 1 - \frac{m_0^2}{6\bar{u}M^2} \right) \right. \right. \\
 & \left. \left. + \frac{m_0^2 \phi^{(2)}(\Delta)}{6(Q^2 + \bar{\Delta}^2 m_\pi^2)} e(s_0) \right] + \frac{\mu_\pi M^2}{16\pi^2} (1 - \rho_\pi^2) \int_0^\Delta du \phi_\sigma^{(3)}(u) e(\tilde{s}) \tilde{E}_1(\tilde{s}) \right\}, \\
 \end{aligned} \tag{E.4}$$

$$\begin{aligned}
 \hat{\Pi}_{LR}^{\text{QCD},S} = & \frac{if_\pi}{32\sqrt{2}} \left\{ \frac{m_0^2 \langle \bar{q}q \rangle}{3} \left[ \int_0^\Delta du \frac{\phi^{(2)}(u)}{\bar{u}^3 M^2} e(\tilde{s}) (Q^2 + \bar{u}^2 m_\pi^2 - \bar{u}M^2) \right. \right. \\
 & \left. \left. + \frac{\phi^{(2)}(\Delta)}{\bar{\Delta}} e(s_0) \right] + \frac{4\mu_\pi M^4}{\pi^2} \int_0^\Delta du \bar{u} \phi_p^{(3)}(u) e(\tilde{s}) \tilde{E}_2(\tilde{s}) \right\} \\
 \end{aligned} \tag{E.5}$$

$$\begin{aligned}
& + \frac{\mu_\pi M^2}{2\pi^2} \int_0^1 D\alpha \theta(\alpha - \Delta_g) \mathcal{T}^{(3)}(1 - \alpha_u - \alpha_g, \alpha_u, \alpha_g) e(\tilde{s}_g) \\
& \times \left[ \frac{(Q^2 + \alpha^2 m_\pi^2)^2}{\alpha^3 M^2} - 6m_\pi^2 \tilde{E}_1(\tilde{s}_g) \right] \Bigg\},
\end{aligned}$$

$$\begin{aligned}
\hat{\Pi}_{LR}^{\text{QCD},P} = & \frac{if_\pi m_p}{12\sqrt{2}} \left\{ \frac{3M^4}{4\pi^2} \int_0^\Delta du \bar{u} \phi^{(2)}(u) e(\tilde{s}) \tilde{E}_2(\tilde{s}) + \right. \\
& + \frac{\mu_\pi m_0^2 \langle \bar{q}q \rangle}{4M^2} \left[ \int_0^\Delta du \frac{\phi_p^{(3)}(u)}{\bar{u}} e(\tilde{s}) + \frac{\bar{\Delta} M^2 \phi_p^{(3)}(\Delta)}{Q^2 + \bar{\Delta}^2 m_\pi^2} e(s_0) \right] + \\
& - \frac{\mu_\pi \langle \bar{q}q \rangle}{3M^2} (1 - \rho_\pi^2) \left\{ \int_0^\Delta du \frac{\phi_\sigma^{(3)}(u)}{\bar{u}^3} e(\tilde{s}) \right. \\
& \times \left[ 4\bar{u}^2 M^2 \left( 1 - \frac{7m_0^2}{96\bar{u}M^2} \right) - 2\bar{u} (Q^2 + \bar{u}^2 m_\pi^2) \left( 1 - \frac{7m_0^2}{48\bar{u}M^2} \right) \right] \\
& \left. - 2M^2 \phi_\sigma^{(3)}(\Delta) e(s_0) \left( 1 - \frac{7m_0^2}{48\bar{\Delta}M^2} \right) + \frac{7\bar{\Delta}m_0^2 M^2}{24(Q^2 + \bar{\Delta}^2 m_\pi^2)} e(s_0) \frac{\partial}{\partial \Delta} \phi_\sigma^{(3)}(\Delta) \right\} \\
& + \frac{\mu_\pi \langle \bar{q}q \rangle}{M^2} \left[ \int_0^1 D\alpha \theta(\alpha - \Delta_g) \frac{\mathcal{T}^{(3)}(1 - \alpha_u - \alpha_g, \alpha_u, \alpha_g)}{\alpha^3} e(\tilde{s}_g) \right. \\
& \times [(1 - 4u)Q^2 - (1 - 4u)\alpha M^2 + (5 - 8u)\alpha^2 m_\pi^2] \\
& + M^2 e(s_0) \int_0^1 du d\alpha_g \theta(1 - \bar{u}\alpha_g - \Delta_g) \\
& \left. \times \frac{\mathcal{T}^{(3)}(1 - \bar{u}\alpha_g - \Delta_g, \Delta_g - u\alpha_g, \alpha_g)}{\Delta_g (Q^2 + \Delta_g^2 m_\pi^2)} [(1 - 4u)Q^2 + (5 - 8u)\Delta_g^2 m_\pi^2] \right] \Bigg\}, \tag{E.6}
\end{aligned}$$

$$\begin{aligned}
\hat{\Pi}_{LR}^{\text{QCD},Q} = & \frac{if_\pi m_p}{12\sqrt{2}} \left\{ - \frac{3M^4}{4\pi^2} \int_0^\Delta du \bar{u} \phi^{(2)}(u) e(\tilde{s}) \tilde{E}_2(\tilde{s}) \right. \\
& + \frac{\mu_\pi m_0^2 \langle \bar{q}q \rangle}{4M^2} \left[ \int_0^\Delta du \frac{u \phi_p^{(3)}(u)}{\bar{u}^2} e(\tilde{s}) + \frac{\Delta M^2 \phi_p^{(3)}(\Delta)}{Q^2 + \bar{\Delta}^2 m_\pi^2} e(s_0) \right] \\
& - \frac{\mu_\pi \langle \bar{q}q \rangle}{3M^2} (1 - \rho_\pi^2) \left\{ \int_0^\Delta du \frac{\phi_\sigma^{(3)}(u)}{\bar{u}^4} e(\tilde{s}) \right. \\
& \times \left[ 2\zeta \bar{u} M^2 \left( 1 - \frac{7m_0^2}{48M^2} \frac{1+u}{\zeta} \right) - 2u\bar{u} (Q^2 + \bar{u}^2 m_\pi^2) \left( 1 - \frac{7m_0^2}{48\bar{u}M^2} \right) \right] \\
& \left. \left. \right\} \right\}
\end{aligned}$$

$$- \frac{2\Delta M^2 \phi_\sigma^{(3)}(\Delta)}{\bar{\Delta}} e(s_0) \left( 1 - \frac{7m_0^2}{48\bar{\Delta}M^2} \right) + \frac{7\Delta m_0^2 M^2}{24(Q^2 + \bar{\Delta}^2 m_\pi^2)} e(s_0) \frac{\partial}{\partial \Delta} \phi_\sigma^{(3)}(\Delta) \Big\} \quad (\text{E.7})$$

$$\begin{aligned} & - \frac{\mu_\pi \langle \bar{q}q \rangle}{M^2} \left[ \int_0^1 D\alpha \theta(\alpha - \Delta_g) \frac{\mathcal{T}^{(3)}(1 - \alpha_u - \alpha_g, \alpha_u, \alpha_g)}{\alpha^3} e(\tilde{s}_g) \right. \\ & \quad \times [(1 - 4u)Q^2 - (1 - 4u)\alpha M^2 - (4\bar{u} - (5 - 8u)\alpha)\alpha m_\pi^2] \\ & \quad + M^2 e(s_0) \int_0^1 du d\alpha_g \theta(1 - \bar{u}\alpha_g - \Delta_g) \frac{\mathcal{T}^{(3)}(1 - \bar{u}\alpha_g - \Delta_g, \Delta_g - u\alpha_g, \alpha_g)}{\Delta_g(Q^2 + \Delta_g^2 m_\pi^2)} \\ & \quad \left. \times [(1 - 4u)Q^2 - (4\bar{u} - (5 - 8u)\Delta_g)\Delta_g m_\pi^2] \right] \Big\}, \end{aligned}$$

$$\begin{aligned} \hat{\Pi}_{LR}^{\text{QCD},T} = & \frac{if_\pi m_p^2}{2\sqrt{2}} \left\{ \frac{\langle \bar{q}q \rangle}{3} \left[ 2 \int_0^\Delta du \frac{\phi^{(2)}(u)}{\bar{u}} e(\tilde{s}) \left( 1 - \frac{7m_0^2}{48\bar{u}M^2} \right) \right. \right. \\ & \quad \left. \left. - \frac{7m_0^2 \phi^{(2)}(\Delta)}{24(Q^2 + \bar{\Delta}^2 m_\pi^2)} e(s_0) \right] \right. \\ & \quad - \frac{\mu_\pi M^2}{12\pi^2} (1 - \rho_\pi^2) \int_0^\Delta du \phi_\sigma^{(3)}(u) e(\tilde{s}) \tilde{E}_1(\tilde{s}) \\ & \quad - \frac{\mu_\pi}{16\pi^2} \int_0^1 D\alpha \theta(\alpha - \Delta_g) \frac{\mathcal{T}^{(3)}(1 - \alpha_u - \alpha_g, \alpha_u, \alpha_g)}{\alpha^2} e(\tilde{s}_g) \\ & \quad \left. \left. \times \zeta(Q^2 + \alpha^2 m_\pi^2) \right\}. \quad (\text{E.8}) \end{aligned}$$

Recall that  $\zeta = 2u - 1$  and notice that we have used the definitions (4.34), (4.35), (4.38) and (4.39) to write the QCD correlation functions in a compact form. We have furthermore suppressed the renormalisation scale dependence of the pion DAs. The analytic expressions for the DAs are collected in Appendix D. Notice that since we have neglected quark-mass effects in (4.20) and (4.21), it would be consistent to set to zero all terms proportional to  $m_\pi^2$  in the formulas (E.1) to (E.8). While these contributions are in fact numerically small, it turns out that they always improve the agreement between the LCSR form factors calculated here and the LQCD form factors computed in [223]. We therefore included the  $m_\pi^2$  terms in the expressions provided above.

## F Analytic results of the LCSRs for three-body proton decay

The analytic expressions for the QCD correlation functions that are relevant for the process  $p \rightarrow e^+ \pi^0 G$  in the GRSMEFT are provided below. The hat on the functions  $\hat{\Pi}_\alpha^{\text{QCD}}$  indicates that the contributions of heavy states were subtracted before taking the Borel transform of the QCD results. One obtains

$$\hat{\Pi}_S^{\text{QCD}} = \frac{f_\pi m_p^2}{36\sqrt{2}} \left\{ \frac{\langle \bar{q}q \rangle}{M^2} \left[ \int_0^\Delta du \frac{\phi^{(2)}(u)}{\bar{u}^2} e(\tilde{s}) \left( 18\bar{u} - \frac{5m_0^2}{M^2} \right) - \frac{5m_0^2 \phi^{(2)}(\Delta)}{Q^2 + \bar{\Delta}^2 m_\pi^2} e(s_0) \right] \right. \\ \left. - \frac{3\mu_\pi}{8\pi^2} (1 - \rho_\pi^2) \int_0^\Delta du \phi_\sigma^{(3)}(u) e(\tilde{s}) \tilde{E}_1(\tilde{s}) \right\}, \quad (\text{F.1})$$

$$\hat{\Pi}_{A_1}^{\text{QCD}} = \frac{f_\pi m_p^3}{108\sqrt{2}} \left\{ \frac{\langle \bar{q}q \rangle \mu_\pi}{M^2} (1 - \rho_\pi^2) \left[ \int_0^\Delta du \frac{u \phi_\sigma^{(3)}(u)}{\bar{u}^3 M^2} e(\tilde{s}) \left( 24\bar{u} - \frac{7m_0^2}{M^2} \right) \right. \right. \\ \left. \left. + \frac{\phi_\sigma^{(3)}(\Delta)}{\bar{\Delta} (Q^2 + \bar{\Delta}^2 m_\pi^2)} e(s_0) \left( 24\Delta\bar{\Delta} - \frac{7\Delta m_0^2}{M^2} - \frac{((7 + 14\Delta)\bar{\Delta}^3 m_\pi^2 + 7\bar{\Delta} Q^2) m_0^2}{(Q^2 + \bar{\Delta}^2 m_\pi^2)^2} \right) \right. \right. \\ \left. \left. - \frac{7\Delta\bar{\Delta} m_0^2}{(Q^2 + \bar{\Delta}^2 m_\pi^2)^2} e(s_0) \frac{\partial}{\partial \Delta} \phi_\sigma^{(3)}(\Delta) \right] - \frac{9}{\pi^2} \int_0^\Delta du u \phi^{(2)}(u) e(\tilde{s}) \tilde{E}_1(\tilde{s}) \right. \\ \left. + \frac{72 \langle \bar{q}q \rangle \mu_\pi}{M^2} \left[ \int_0^1 D\alpha \theta(\alpha - \Delta_g) \frac{\bar{u} \mathcal{T}^{(3)}(1 - \alpha_u - \alpha_g, \alpha_u, \alpha_g)}{\alpha^2 M^2} e(\tilde{s}_g) \right. \right. \\ \left. \left. + e(s_0) \int_0^1 du d\alpha_g \theta(1 - \bar{u}\alpha_g - \Delta_g) \frac{\bar{u} \mathcal{T}^{(3)}(1 - \bar{u}\alpha_g - \Delta_g, \Delta_g - u\alpha_g, \alpha_g)}{Q^2 + \Delta_g^2 m_\pi^2} \right] \right\}, \quad (\text{F.2})$$

$$\hat{\Pi}_{A_2}^{\text{QCD}} = \frac{f_\pi m_p^3}{108\sqrt{2}} \left\{ \frac{\langle \bar{q}q \rangle \mu_\pi}{M^2} (1 - \rho_\pi^2) \left[ \int_0^\Delta du \frac{\phi_\sigma^{(3)}(u)}{\bar{u}^2 M^2} e(\tilde{s}) \left( 24\bar{u} - \frac{7m_0^2}{M^2} \right) \right. \right. \\ \left. \left. + \frac{\phi_\sigma^{(3)}(\Delta)}{(Q^2 + \bar{\Delta}^2 m_\pi^2)} e(s_0) \left( 24\bar{\Delta} - \frac{7m_0^2}{M^2} - \frac{14\bar{\Delta}^3 m_0^2 m_\pi^2}{(Q^2 + \bar{\Delta}^2 m_\pi^2)^2} \right) \right. \right. \\ \left. \left. - \frac{7\bar{\Delta}^2 m_0^2}{(Q^2 + \bar{\Delta}^2 m_\pi^2)^2} e(s_0) \frac{\partial}{\partial \Delta} \phi_\sigma^{(3)}(\Delta) \right] - \frac{9}{\pi^2} \int_0^\Delta du \bar{u} \phi^{(2)}(u) e(\tilde{s}) \tilde{E}_1(\tilde{s}) \right\} \quad (\text{F.3})$$

$$\begin{aligned}
& + \frac{72 \langle \bar{q}q \rangle \mu_\pi}{M^2} \left[ \int_0^1 D\alpha \theta(\alpha - \Delta_g) \frac{\bar{u} \mathcal{T}^{(3)}(1 - \alpha_u - \alpha_g, \alpha_u, \alpha_g)}{\alpha^2 M^2} e(\tilde{s}_g) \right. \\
& \left. + e(s_0) \int_0^1 du d\alpha_g \theta(1 - \bar{u}\alpha_g - \Delta_g) \frac{\bar{u} \mathcal{T}^{(3)}(1 - \bar{u}\alpha_g - \Delta_g, \Delta_g - u\alpha_g, \alpha_g)}{Q^2 + \Delta_g^2 m_\pi^2} \right] \Bigg\}, \\
\hat{\Pi}_{A_3}^{\text{QCD}} &= \frac{f_\pi m_p}{108\sqrt{2}} \left\{ \frac{\langle \bar{q}q \rangle \mu_\pi}{M^2} \left[ (1 - \rho_\pi^2) \left\{ \int_0^\Delta du \frac{\phi_\sigma^{(3)}(u)}{\bar{u}^4} e(\tilde{s}) \right. \right. \right. \\
& \times \left( \bar{u} (9 - 15u + 6u^2) - \frac{6u\bar{u} (Q^2 + \bar{u}^2 m_\pi^2) + (9 - 14u + 5u^2) m_0^2}{2M^2} \right. \\
& \left. \left. \left. + \frac{um_0^2}{M^4} (Q^2 + \bar{u}^2 m_\pi^2) \right) \right. \right. \\
& - \phi_\sigma^{(3)}(\Delta) e(s_0) \left( \frac{3\Delta}{\bar{\Delta}} - \frac{\Delta m_0^2}{\bar{\Delta}^2 M^2} + \frac{7m_0^2}{2(Q^2 + \bar{\Delta}^2 m_\pi^2)} \right) \\
& \left. + \frac{\Delta m_0^2}{Q^2 + \bar{\Delta}^2 m_\pi^2} e(s_0) \frac{\partial}{\partial \Delta} \phi_\sigma^{(3)}(\Delta) \right\} \\
& - \frac{3m_0^2}{4} \left( \int_0^\Delta du \frac{u \phi_p^{(3)}(u)}{\bar{u}^2 M^2} e(\tilde{s}) + \frac{\Delta \phi_p^{(3)}(\Delta)}{Q^2 + \bar{\Delta}^2 m_\pi^2} e(s_0) \right) \Bigg] \\
& + \frac{9M^2}{8\pi^2} \int_0^\Delta du \frac{\phi^{(2)}(u)}{\bar{u}} e(\tilde{s}) \\
& \times \left[ \frac{u}{M^2} (Q^2 + \bar{u}^2 m_\pi^2) \tilde{E}_1(\tilde{s}) - (2 - 5u + 3u^2) \tilde{E}_2(\tilde{s}) \right] \\
& + \frac{9 \langle \bar{q}q \rangle \mu_\pi}{M^2} \left[ \int_0^1 D\alpha \theta(\alpha - \Delta_g) \frac{\mathcal{T}^{(3)}(1 - \alpha_u - \alpha_g, \alpha_u, \alpha_g)}{\alpha^3} e(\tilde{s}_g) \right. \\
& \times \left( 2\alpha\bar{u} - \frac{2\bar{u}Q^2}{M^2} + \frac{\alpha m_\pi^2}{M^2} (\alpha + 2u - 3) \right) \\
& - e(s_0) \int_0^1 du d\alpha_g \theta(1 - \bar{u}\alpha_g - \Delta_g) \frac{\mathcal{T}^{(3)}(1 - \bar{u}\alpha_g - \Delta_g, \Delta_g - u\alpha_g, \alpha_g)}{Q^2 + \Delta_g^2 m_\pi^2} \\
& \times \left( \frac{2\bar{u}Q^2}{\Delta_g} + m_\pi^2 (3 - 2u - \Delta_g) \right) \Bigg] \Bigg\}, \\
\hat{\Pi}_{A_4}^{\text{QCD}} &= -\frac{f_\pi m_p}{108\sqrt{2}} \left\{ \frac{\langle \bar{q}q \rangle \mu_\pi}{M^2} \left[ (1 - \rho_\pi^2) \left\{ \int_0^\Delta du \frac{\phi_\sigma^{(3)}(u)}{\bar{u}^2} e(\tilde{s}) \right. \right. \right. \\
& \times \left( 6\bar{u} + \frac{6(Q^2 + \bar{u}^2 m_\pi^2) - 5m_0^2}{2\bar{u}M^2} - \frac{m_0^2 (Q^2 + \bar{u}^2 m_\pi^2)}{\bar{u}M^4} \right)
\end{aligned} \tag{F.4}$$

$$\begin{aligned}
& + \phi_\sigma^{(3)}(\Delta) e(s_0) \left( 3 - \frac{m_0^2}{\bar{\Delta} M^2} - \frac{7m_0^2}{2(Q^2 + \bar{\Delta}^2 m_\pi^2)} \right) \\
& - \frac{\bar{\Delta} m_0^2}{Q^2 + \bar{\Delta}^2 m_\pi^2} e(s_0) \frac{\partial}{\partial \Delta} \phi_\sigma^{(3)}(\Delta) \Big\} \\
& + \frac{3m_0^2}{4} \left( \int_0^\Delta du \frac{\phi_p^{(3)}(u)}{\bar{u} M^2} e(\tilde{s}) + \frac{\bar{\Delta} \phi_p^{(3)}(\Delta)}{Q^2 + \bar{\Delta}^2 m_\pi^2} e(s_0) \right) \Big] \\
& - \frac{9}{8\pi^2} \int_0^\Delta du \phi^{(2)}(u) e(\tilde{s}) \left[ (Q^2 + \bar{u}^2 m_\pi^2) \tilde{E}_1(\tilde{s}) + 3\bar{u} M^2 \tilde{E}_2(\tilde{s}) \right] \\
& + \frac{9 \langle \bar{q} q \rangle \mu_\pi}{M^2} \left[ \int_0^1 D\alpha \theta(\alpha - \Delta_g) \frac{\mathcal{T}^{(3)}(1 - \alpha_u - \alpha_g, \alpha_u, \alpha_g)}{\alpha^3} e(\tilde{s}_g) \right. \\
& \quad \times \left( 2\alpha \bar{u} - \frac{2\bar{u} Q^2}{M^2} + \frac{\alpha^2 m_\pi^2}{M^2} \right) \\
& \quad \left. - e(s_0) \int_0^1 du d\alpha_g \theta(1 - \bar{u} \alpha_g - \Delta_g) \frac{\mathcal{T}^{(3)}(1 - \bar{u} \alpha_g - \Delta_g, \Delta_g - u \alpha_g, \alpha_g)}{Q^2 + \bar{\Delta}_g^2 m_\pi^2} \right. \\
& \quad \left. \times \left( \frac{2\bar{u} Q^2}{\Delta_g} - \Delta_g m_\pi^2 \right) \right] \Big\}, \tag{F.5}
\end{aligned}$$

$$\begin{aligned}
\hat{\Pi}_{T_1}^{\text{QCD}} = & -\frac{f_\pi}{288\sqrt{2}} \left\{ \frac{\langle \bar{q} q \rangle m_0^2}{M^2} \left[ \int_0^\Delta du \frac{\phi^{(2)}(u)}{\bar{u}^3} e(\tilde{s}) \left( \bar{u} - \frac{m_0^2}{M^2} \bar{u}^2 - \frac{Q^2}{M^2} \right) \right. \right. \\
& \left. \left. - \frac{\phi^{(2)}(\Delta)}{\bar{\Delta}} e(s_0) \right] + \frac{9\mu_\pi M^2}{\pi^2} \int_0^\Delta du \bar{u} \phi_p^{(3)}(u) e(\tilde{s}) \tilde{E}_2(\tilde{s}) \right\}, \tag{F.6}
\end{aligned}$$

$$\begin{aligned}
\hat{\Pi}_{T_2}^{\text{QCD}} = & \frac{f_\pi m_p^2}{18\sqrt{2}} \left\{ \frac{\langle \bar{q} q \rangle}{M^2} \left[ \int_0^\Delta du \frac{\phi^{(2)}(u)}{\bar{u}^2} e(\tilde{s}) \left( 3\bar{u} - \frac{m_0^2}{M^2} \right) - \frac{m_0^2 \phi^{(2)}(\Delta)}{Q^2 + \bar{\Delta}^2 m_\pi^2} e(s_0) \right] \right. \\
& \left. + \frac{3\mu_\pi}{16\pi^2} (1 - \rho_\pi^2) \int_0^\Delta du \phi_\sigma^{(3)}(u) e(\tilde{s}) \tilde{E}_1(\tilde{s}) \right\}. \tag{F.7}
\end{aligned}$$

Including the leading pion DAs, i.e. the twist-2 and twist-3 contributions, one furthermore finds that  $\hat{\Pi}_{T_3}^{\text{QCD}} = 0$  as already discussed in Section 4.2.2. Furthermore, the same shorthand notations as in Appendix E were employed here.



# Bibliography

- [1] ALEPH, CDF, D0, DELPHI, L3, OPAL, SLD, LEP ELECTROWEAK WORKING GROUP, TEVATRON ELECTROWEAK WORKING GROUP, SLD ELECTROWEAK, HEAVY FLAVOUR GROUPS collaboration, *Precision Electroweak Measurements and Constraints on the Standard Model*, 1012.2367.
- [2] ATLAS collaboration, *Observation of a new particle in the search for the Standard Model Higgs boson with the ATLAS detector at the LHC*, *Phys. Lett. B* **716** (2012) 1 [1207.7214].
- [3] CMS collaboration, *Observation of a New Boson at a Mass of 125 GeV with the CMS Experiment at the LHC*, *Phys. Lett. B* **716** (2012) 30 [1207.7235].
- [4] ATLAS collaboration, *Combined measurements of Higgs boson production and decay using up to 80 fb<sup>-1</sup> of proton-proton collision data at  $\sqrt{s} = 13$  TeV collected with the ATLAS experiment*, *Phys. Rev. D* **101** (2020) 012002 [1909.02845].
- [5] S. Weinberg, *Implications of Dynamical Symmetry Breaking*, *Phys. Rev. D* **13** (1976) 974.
- [6] E. Gildener, *Gauge Symmetry Hierarchies*, *Phys. Rev. D* **14** (1976) 1667.
- [7] L. Susskind, *Dynamics of Spontaneous Symmetry Breaking in the Weinberg-Salam Theory*, *Phys. Rev. D* **20** (1979) 2619.
- [8] G. 't Hooft, *Naturalness, chiral symmetry, and spontaneous chiral symmetry breaking*, *NATO Sci. Ser. B* **59** (1980) 135.
- [9] S.F. King, *Neutrino mass models*, *Rept. Prog. Phys.* **67** (2004) 107 [hep-ph/0310204].
- [10] A. de Gouvêa, *Neutrino Mass Models*, *Ann. Rev. Nucl. Part. Sci.* **66** (2016) 197.
- [11] L. Canetti, M. Drewes and M. Shaposhnikov, *Matter and Antimatter in the Universe*, *New J. Phys.* **14** (2012) 095012 [1204.4186].
- [12] A.D. Sakharov, *Violation of CP Invariance, C asymmetry, and baryon asymmetry of the universe*, *Sov. Phys. Usp.* **34** (1991) 392.
- [13] V.A. Rubakov and M.E. Shaposhnikov, *Electroweak baryon number nonconservation in the early universe and in high-energy collisions*, *Usp. Fiz. Nauk* **166** (1996) 493 [hep-ph/9603208].
- [14] V.A. Kuzmin, V.A. Rubakov and M.E. Shaposhnikov, *On the Anomalous Electroweak Baryon Number Nonconservation in the Early Universe*, *Phys. Lett. B* **155** (1985) 36.

## Bibliography

- [15] C. Jarlskog, *Commutator of the Quark Mass Matrices in the Standard Electroweak Model and a Measure of Maximal CP Violation*, *Phys. Rev. Lett.* **55** (1985) 1039.
- [16] V. Cirigliano and M.J. Ramsey-Musolf, *Low Energy Probes of Physics Beyond the Standard Model*, *Prog. Part. Nucl. Phys.* **71** (2013) 2 [1304.0017].
- [17] T. Appelquist and J. Carazzone, *Infrared Singularities and Massive Fields*, *Phys. Rev. D* **11** (1975) 2856.
- [18] M. Dichtl, U. Haisch, A. Hala, J. Serra and A. Weiler, *in preparation* (2021) .
- [19] U. Haisch and A. Hala, *Sum rules for CP-violating operators of Weinberg type*, *JHEP* **11** (2019) 154 [1909.08955].
- [20] U. Haisch and A. Hala, *Bounds on CP-violating Higgs-gluon interactions: the case of vanishing light-quark Yukawa couplings*, *JHEP* **11** (2019) 117 [1909.09373].
- [21] U. Haisch and A. Hala, *Light-cone sum rules for proton decay*, *JHEP* **05** (2021) 258 [2103.13928].
- [22] U. Haisch and A. Hala, *Semi-leptonic three-body proton decay modes from light-cone sum rules, prepared for submission to JHEP* (2021) [2108.06111].
- [23] A.V. Manohar, *Introduction to Effective Field Theories*, 1804.05863.
- [24] M. Neubert, *Renormalization Theory and Effective Field Theories*, 1901.06573.
- [25] H. Georgi, *Effective field theory*, *Ann. Rev. Nucl. Part. Sci.* **43** (1993) 209.
- [26] SUPER-KAMIOKANDE collaboration, *The Super-Kamiokande detector*, *Nucl. Instrum. Meth. A* **501** (2003) 418.
- [27] K. Abe et al., *Calibration of the Super-Kamiokande Detector*, *Nucl. Instrum. Meth. A* **737** (2014) 253 [1307.0162].
- [28] M. Ruhdorfer, J. Serra and A. Weiler, *Effective Field Theory of Gravity to All Orders*, *JHEP* **05** (2020) 083 [1908.08050].
- [29] G. Durieux and C.S. Machado, *Enumerating higher-dimensional operators with on-shell amplitudes*, *Phys. Rev. D* **101** (2020) 095021 [1912.08827].
- [30] PARTICLE DATA GROUP collaboration, *Review of Particle Physics*, *PTEP* **2020** (2020) 083C01.
- [31] T. Cohen, N. Craig, X. Lu and D. Sutherland, *Is SMEFT Enough?*, *JHEP* **03** (2021) 237 [2008.08597].
- [32] S. Weinberg, *Baryon and Lepton Nonconserving Processes*, *Phys. Rev. Lett.* **43** (1979) 1566.
- [33] F. Wilczek and A. Zee, *Operator Analysis of Nucleon Decay*, *Phys. Rev. Lett.* **43** (1979) 1571.

- [34] L.F. Abbott and M.B. Wise, *The Effective Hamiltonian for Nucleon Decay*, *Phys. Rev. D* **22** (1980) 2208.
- [35] W. Buchmuller and D. Wyler, *Effective Lagrangian Analysis of New Interactions and Flavor Conservation*, *Nucl. Phys. B* **268** (1986) 621.
- [36] B. Grzadkowski, M. Iskrzynski, M. Misiak and J. Rosiek, *Dimension-Six Terms in the Standard Model Lagrangian*, *JHEP* **10** (2010) 085 [[1008.4884](#)].
- [37] B. Henning, X. Lu, T. Melia and H. Murayama, *2, 84, 30, 993, 560, 15456, 11962, 261485, ...: Higher dimension operators in the SM EFT*, *JHEP* **08** (2017) 016 [[1512.03433](#)].
- [38] B. Henning, X. Lu, T. Melia and H. Murayama, *Operator bases, S-matrices, and their partition functions*, *JHEP* **10** (2017) 199 [[1706.08520](#)].
- [39] V. Cirigliano, A. Crivellin, W. Dekens, J. de Vries, M. Hoferichter and E. Mereghetti, *CP Violation in Higgs-Gauge Interactions: From Tabletop Experiments to the LHC*, *Phys. Rev. Lett.* **123** (2019) 051801 [[1903.03625](#)].
- [40] G. Luders, *On the Equivalence of Invariance under Time Reversal and under Particle-Antiparticle Conjugation for Relativistic Field Theories*, *Kong. Dan. Vid. Sel. Mat. Fys. Med.* **28N5** (1954) 1.
- [41] W.E.F. Pauli, L. Rosenfeld and V.F. Weisskopf, *Niels Bohr and the development of physics: essays dedicated to Niels Bohr on the occasion of his seventieth birthday*, Pergamon, London (1955).
- [42] R.F. Streater and A.S. Wightman, *PCT, Spin and Statistics, and All That*, Princeton University Press, Princeton (2016), doi:[10.1515/9781400884230](#).
- [43] M. Pospelov and A. Ritz, *Electric dipole moments as probes of new physics*, *Annals Phys.* **318** (2005) 119 [[hep-ph/0504231](#)].
- [44] nEDM collaboration, *Measurement of the permanent electric dipole moment of the neutron*, *Phys. Rev. Lett.* **124** (2020) 081803 [[2001.11966](#)].
- [45] J.M. Pendlebury et al., *Revised experimental upper limit on the electric dipole moment of the neutron*, *Phys. Rev. D* **92** (2015) 092003 [[1509.04411](#)].
- [46] C.A. Baker et al., *An Improved experimental limit on the electric dipole moment of the neutron*, *Phys. Rev. Lett.* **97** (2006) 131801 [[hep-ex/0602020](#)].
- [47] C.A. Baker et al., *Apparatus for Measurement of the Electric Dipole Moment of the Neutron using a Cohabiting Atomic-Mercury Magnetometer*, *Nucl. Instrum. Meth. A* **736** (2014) 184 [[1305.7336](#)].
- [48] S. Dar, *The Neutron EDM in the SM: A Review*, [hep-ph/0008248](#).
- [49] R.D. Peccei and H.R. Quinn, *CP Conservation in the Presence of Instantons*, *Phys. Rev. Lett.* **38** (1977) 1440.

## Bibliography

- [50] S. Weinberg, *A New Light Boson?*, *Phys. Rev. Lett.* **40** (1978) 223.
- [51] F. Wilczek, *Problem of Strong P and T Invariance in the Presence of Instantons*, *Phys. Rev. Lett.* **40** (1978) 279.
- [52] J. Engel, M.J. Ramsey-Musolf and U. van Kolck, *Electric Dipole Moments of Nucleons, Nuclei, and Atoms: The Standard Model and Beyond*, *Prog. Part. Nucl. Phys.* **71** (2013) 21 [1303.2371].
- [53] ACME collaboration, *Order of Magnitude Smaller Limit on the Electric Dipole Moment of the Electron*, *Science* **343** (2014) 269 [1310.7534].
- [54] ACME collaboration, *Improved limit on the electric dipole moment of the electron*, *Nature* **562** (2018) 355.
- [55] W.C. Griffith, M.D. Swallows, T.H. Loftus, M.V. Romalis, B.R. Heckel and E.N. Fortson, *Improved Limit on the Permanent Electric Dipole Moment of Hg-199*, *Phys. Rev. Lett.* **102** (2009) 101601 [0901.2328].
- [56] B. Graner, Y. Chen, E.G. Lindahl and B.R. Heckel, *Reduced Limit on the Permanent Electric Dipole Moment of Hg199*, *Phys. Rev. Lett.* **116** (2016) 161601 [1601.04339].
- [57] Y. Li, S. Profumo and M. Ramsey-Musolf, *A Comprehensive Analysis of Electric Dipole Moment Constraints on CP-violating Phases in the MSSM*, *JHEP* **08** (2010) 062 [1006.1440].
- [58] D. McKeen, M. Pospelov and A. Ritz, *Modified Higgs branching ratios versus CP and lepton flavor violation*, *Phys. Rev. D* **86** (2012) 113004 [1208.4597].
- [59] W.-F. Chang, W.-P. Pan and F. Xu, *Effective gauge-Higgs operators analysis of new physics associated with the Higgs boson*, *Phys. Rev. D* **88** (2013) 033004 [1303.7035].
- [60] M. Jung and A. Pich, *Electric Dipole Moments in Two-Higgs-Doublet Models*, *JHEP* **04** (2014) 076 [1308.6283].
- [61] B. Gripaios and D. Sutherland, *Searches for CP-violating dimension-6 electroweak gauge boson operators*, *Phys. Rev. D* **89** (2014) 076004 [1309.7822].
- [62] J. Brod, U. Haisch and J. Zupan, *Constraints on CP-violating Higgs couplings to the third generation*, *JHEP* **11** (2013) 180 [1310.1385].
- [63] S. Inoue, M.J. Ramsey-Musolf and Y. Zhang, *CP-violating phenomenology of flavor conserving two Higgs doublet models*, *Phys. Rev. D* **89** (2014) 115023 [1403.4257].
- [64] M. Gorbahn and U. Haisch, *Searching for  $t \rightarrow c(u)h$  with dipole moments*, *JHEP* **06** (2014) 033 [1404.4873].
- [65] W. Altmannshofer, J. Brod and M. Schmaltz, *Experimental constraints on the coupling of the Higgs boson to electrons*, *JHEP* **05** (2015) 125 [1503.04830].
- [66] S. Dwivedi, D.K. Ghosh, B. Mukhopadhyaya and A. Shivaji, *Constraints on CP-violating gauge-Higgs operators*, *Phys. Rev. D* **92** (2015) 095015 [1505.05844].

- [67] Y.T. Chien, V. Cirigliano, W. Dekens, J. de Vries and E. Mereghetti, *Direct and indirect constraints on CP-violating Higgs-quark and Higgs-gluon interactions*, *JHEP* **02** (2016) 011 [1510.00725].
- [68] V. Cirigliano, W. Dekens, J. de Vries and E. Mereghetti, *Is there room for CP violation in the top-Higgs sector?*, *Phys. Rev. D* **94** (2016) 016002 [1603.03049].
- [69] V. Cirigliano, W. Dekens, J. de Vries and E. Mereghetti, *Constraining the top-Higgs sector of the Standard Model Effective Field Theory*, *Phys. Rev. D* **94** (2016) 034031 [1605.04311].
- [70] N. Yamanaka, B.K. Sahoo, N. Yoshinaga, T. Sato, K. Asahi and B.P. Das, *Probing exotic phenomena at the interface of nuclear and particle physics with the electric dipole moments of diamagnetic atoms: A unique window to hadronic and semi-leptonic CP violation*, *Eur. Phys. J. A* **53** (2017) 54 [1703.01570].
- [71] K. Yanase, N. Yoshinaga, K. Higashiyama and N. Yamanaka, *Electric dipole moment of  $^{199}\text{Hg}$  atom from  $P$ , CP-odd electron-nucleon interaction*, *Phys. Rev. D* **99** (2019) 075021 [1805.00419].
- [72] W. Dekens, J. de Vries, M. Jung and K.K. Vos, *The phenomenology of electric dipole moments in models of scalar leptoquarks*, *JHEP* **01** (2019) 069 [1809.09114].
- [73] C. Cesarotti, Q. Lu, Y. Nakai, A. Parikh and M. Reece, *Interpreting the Electron EDM Constraint*, *JHEP* **05** (2019) 059 [1810.07736].
- [74] G. Panico, A. Pomarol and M. Riembau, *EFT approach to the electron Electric Dipole Moment at the two-loop level*, *JHEP* **04** (2019) 090 [1810.09413].
- [75] J. Brod and E. Stamou, *Electric dipole moment constraints on CP-violating heavy-quark Yukawas at next-to-leading order*, *JHEP* **07** (2021) 080 [1810.12303].
- [76] J. Brod and D. Skodras, *Electric dipole moment constraints on CP-violating light-quark Yukawas*, *JHEP* **01** (2019) 233 [1811.05480].
- [77] S. Weinberg, *Larger Higgs Exchange Terms in the Neutron Electric Dipole Moment*, *Phys. Rev. Lett.* **63** (1989) 2333.
- [78] A.Y. Morozov, *MATRIX OF MIXING OF SCALAR AND VECTOR MESONS OF DIMENSION  $D \leq 8$  IN QCD. (IN RUSSIAN)*, *Sov. J. Nucl. Phys.* **40** (1984) 505.
- [79] E. Braaten, C.-S. Li and T.-C. Yuan, *The Evolution of Weinberg's Gluonic CP Violation Operator*, *Phys. Rev. Lett.* **64** (1990) 1709.
- [80] E. Braaten, C.S. Li and T.C. Yuan, *The Gluon Color - Electric Dipole Moment and Its Anomalous Dimension*, *Phys. Rev. D* **42** (1990) 276.
- [81] D. Chang, T.W. Kephart, W.-Y. Keung and T.C. Yuan, *The Chromoelectric dipole moment of the heavy quark and purely gluonic CP violating operators*, *Phys. Rev. Lett.* **68** (1992) 439.

## Bibliography

- [82] M.J. Booth, *Anomalous dimensions of Weinberg operators*, *Phys. Rev. D* **45** (1992) 2518.
- [83] J.S.M. Ginges and V.V. Flambaum, *Violations of fundamental symmetries in atoms and tests of unification theories of elementary particles*, *Phys. Rept.* **397** (2004) 63 [physics/0309054].
- [84] V.A. Dzuba and V.V. Flambaum, *Parity violation and electric dipole moments in atoms and molecules*, *Int. J. Mod. Phys. E* **21** (2012) 1230010 [1209.2200].
- [85] L.V. Skripnikov, A.N. Petrov and A.V. Titov, *Communication: Theoretical study of ThO for the electron electric dipole moment search*, *Journal of Chemical Physics* **139** (2013) .
- [86] T. Fleig and M.K. Nayak, *Electron Electric Dipole Moment and Hyperfine Interaction Constants for ThO*, *J. Molec. Spectrosc.* **300** (2014) 16 [1401.2284].
- [87] T. Bhattacharya, V. Cirigliano, R. Gupta, H.-W. Lin and B. Yoon, *Neutron Electric Dipole Moment and Tensor Charges from Lattice QCD*, *Phys. Rev. Lett.* **115** (2015) 212002 [1506.04196].
- [88] PNDME collaboration, *Iso-vector and Iso-scalar Tensor Charges of the Nucleon from Lattice QCD*, *Phys. Rev. D* **92** (2015) 094511 [1506.06411].
- [89] R. Gupta, B. Yoon, T. Bhattacharya, V. Cirigliano, Y.-C. Jang and H.-W. Lin, *Flavor diagonal tensor charges of the nucleon from (2+1+1)-flavor lattice QCD*, *Phys. Rev. D* **98** (2018) 091501 [1808.07597].
- [90] M. Pospelov and A. Ritz, *Neutron EDM from electric and chromoelectric dipole moments of quarks*, *Phys. Rev. D* **63** (2001) 073015 [hep-ph/0010037].
- [91] O. Lebedev, K.A. Olive, M. Pospelov and A. Ritz, *Probing CP violation with the deuteron electric dipole moment*, *Phys. Rev. D* **70** (2004) 016003 [hep-ph/0402023].
- [92] J. Hisano, J.Y. Lee, N. Nagata and Y. Shimizu, *Reevaluation of Neutron Electric Dipole Moment with QCD Sum Rules*, *Phys. Rev. D* **85** (2012) 114044 [1204.2653].
- [93] I.I.Y. Bigi and N.G. Uraltsev, *Induced Multi - Gluon Couplings and the Neutron Electric Dipole Moment*, *Nucl. Phys. B* **353** (1991) 321.
- [94] D.A. Demir, M. Pospelov and A. Ritz, *Hadronic EDMs, the Weinberg operator, and light gluinos*, *Phys. Rev. D* **67** (2003) 015007 [hep-ph/0208257].
- [95] T. Bhattacharya, V. Cirigliano, R. Gupta, E. Mereghetti and B. Yoon, *Dimension-5 CP-odd operators: QCD mixing and renormalization*, *Phys. Rev. D* **92** (2015) 114026 [1502.07325].
- [96] T. Bhattacharya, V. Cirigliano, R. Gupta and B. Yoon, *Quark Chromoelectric Dipole Moment Contribution to the Neutron Electric Dipole Moment*, *PoS LATTICE2016* (2016) 225 [1612.08438].

- [97] M. Abramczyk, S. Aoki, T. Blum, T. Izubuchi, H. Ohki and S. Syritsyn, *Lattice calculation of electric dipole moments and form factors of the nucleon*, *Phys. Rev. D* **96** (2017) 014501 [1701.07792].
- [98] J. Dragos, T. Luu, A. Shindler and J. de Vries, *Electric Dipole Moment Results from lattice QCD*, *EPJ Web Conf.* **175** (2018) 06018 [1711.04730].
- [99] M. Rizik, C. Monahan and A. Shindler, *Renormalization of CP-Violating Pure Gauge Operators in Perturbative QCD Using the Gradient Flow*, *PoS LATTICE2018* (2018) 215 [1810.05637].
- [100] J. Kim, J. Dragos, A. Shindler, T. Luu and J. de Vries, *Towards a determination of the nucleon EDM from the quark chromo-EDM operator with the gradient flow*, *PoS LATTICE2018* (2019) 260 [1810.10301].
- [101] T. Bhattacharya, B. Yoon, R. Gupta and V. Cirigliano, *Neutron Electric Dipole Moment from Beyond the Standard Model*, *12*, 2018 [1812.06233].
- [102] S. Syritsyn, T. Izubuchi and H. Ohki, *Calculation of Nucleon Electric Dipole Moments Induced by Quark Chromo-Electric Dipole Moments and the QCD  $\theta$ -term*, *PoS Confinement2018* (2019) 194 [1901.05455].
- [103] R. Gupta, *Present and future prospects for lattice QCD calculations of matrix elements for  $n$ EDM*, *PoS SPIN2018* (2019) 095 [1904.00323].
- [104] USQCD collaboration, *The Role of Lattice QCD in Searches for Violations of Fundamental Symmetries and Signals for New Physics*, *Eur. Phys. J. A* **55** (2019) 197 [1904.09704].
- [105] *Fundamental Physics at the Intensity Frontier*, *5*, 2012. 10.2172/1042577.
- [106] P. Schmidt-Wellenburg, *The quest to find an electric dipole moment of the neutron*, *1607.06609*.
- [107] T.M. Ito et al., *Performance of the upgraded ultracold neutron source at Los Alamos National Laboratory and its implication for a possible neutron electric dipole moment experiment*, *Phys. Rev. C* **97** (2018) 012501 [1710.05182].
- [108] H. Weyl, *Electron and Gravitation. 1. (In German)*, *Z. Phys.* **56** (1929) 330.
- [109] E.C.G. Stueckelberg, *Interaction forces in electrodynamics and in the field theory of nuclear forces*, *Helv. Phys. Acta* **11** (1938) 299.
- [110] G. 't Hooft, *Symmetry Breaking Through Bell-Jackiw Anomalies*, *Phys. Rev. Lett.* **37** (1976) 8.
- [111] H. Georgi and S.L. Glashow, *Unity of All Elementary Particle Forces*, *Phys. Rev. Lett.* **32** (1974) 438.
- [112] H. Fritzsch and P. Minkowski, *Unified Interactions of Leptons and Hadrons*, *Annals Phys.* **93** (1975) 193.

## Bibliography

- [113] H.P. Nilles, *Supersymmetry, Supergravity and Particle Physics*, *Phys. Rept.* **110** (1984) 1.
- [114] H.E. Haber and G.L. Kane, *The Search for Supersymmetry: Probing Physics Beyond the Standard Model*, *Phys. Rept.* **117** (1985) 75.
- [115] N. Chamoun, F. Domingo and H.K. Dreiner, *Nucleon decay in the R-parity violating MSSM*, 2012.11623.
- [116] T. Banks and N. Seiberg, *Symmetries and Strings in Field Theory and Gravity*, *Phys. Rev. D* **83** (2011) 084019 [1011.5120].
- [117] D. Harlow and H. Ooguri, *Constraints on Symmetries from Holography*, *Phys. Rev. Lett.* **122** (2019) 191601 [1810.05337].
- [118] P. Langacker, *Grand Unified Theories and Proton Decay*, *Phys. Rept.* **72** (1981) 185.
- [119] S. Raby, *Proton decay*, in *10th International Conference on Supersymmetry and Unification of Fundamental Interactions (SUSY02)*, pp. 421–431, 10, 2002 [hep-ph/0211024].
- [120] P. Nath and P. Fileviez Perez, *Proton stability in grand unified theories, in strings and in branes*, *Phys. Rept.* **441** (2007) 191 [hep-ph/0601023].
- [121] J. Ellis, J.L. Evans, N. Nagata, K.A. Olive and L. Velasco-Sevilla, *Supersymmetric proton decay revisited*, *Eur. Phys. J. C* **80** (2020) 332 [1912.04888].
- [122] SUPER-KAMIOKANDE collaboration, *Search for proton decay via  $p \rightarrow e^+ \pi^0$  and  $p \rightarrow \mu^+ \pi^0$  with an enlarged fiducial volume in Super-Kamiokande I-IV*, *Phys. Rev. D* **102** (2020) 112011 [2010.16098].
- [123] SUPER-KAMIOKANDE collaboration, *Review of Nucleon Decay Searches at Super-Kamiokande*, in *51st Rencontres de Moriond on EW Interactions and Unified Theories*, pp. 437–444, 2016 [1605.03235].
- [124] J. Heeck and V. Takhistov, *Inclusive Nucleon Decay Searches as a Frontier of Baryon Number Violation*, *Phys. Rev. D* **101** (2020) 015005 [1910.07647].
- [125] S. Girmohanta and R. Shrock, *Improved Lower Bounds on Partial Lifetimes for Nucleon Decay Modes*, *Phys. Rev. D* **100** (2019) 115025 [1910.08106].
- [126] SUPER-KAMIOKANDE collaboration, *Search for proton decay via  $p \rightarrow e^+ \pi^0$  and  $p \rightarrow \mu^+ \pi^0$  in 0.31 megaton-years exposure of the Super-Kamiokande water Cherenkov detector*, *Phys. Rev. D* **95** (2017) 012004 [1610.03597].
- [127] SUPER-KAMIOKANDE collaboration, *Search for Nucleon Decay into Charged Anti-lepton plus Meson in Super-Kamiokande I and II*, *Phys. Rev. D* **85** (2012) 112001 [1203.4030].
- [128] J.F. Donoghue, *General relativity as an effective field theory: The leading quantum corrections*, *Phys. Rev. D* **50** (1994) 3874 [gr-qc/9405057].

- [129] J.F. Donoghue, *Introduction to the effective field theory description of gravity*, in *Advanced School on Effective Theories*, 6, 1995 [gr-qc/9512024].
- [130] C.P. Burgess, *Quantum gravity in everyday life: General relativity as an effective field theory*, *Living Rev. Rel.* **7** (2004) 5 [gr-qc/0311082].
- [131] J.F. Donoghue, *The effective field theory treatment of quantum gravity*, *AIP Conf. Proc.* **1483** (2012) 73 [1209.3511].
- [132] J.F. Donoghue and B.R. Holstein, *Low Energy Theorems of Quantum Gravity from Effective Field Theory*, *J. Phys. G* **42** (2015) 103102 [1506.00946].
- [133] J.F. Donoghue, M.M. Ivanov and A. Shkerin, *EPFL Lectures on General Relativity as a Quantum Field Theory*, 1702.00319.
- [134] G. 't Hooft, *An algorithm for the poles at dimension four in the dimensional regularization procedure*, *Nucl. Phys. B* **62** (1973) 444.
- [135] G. 't Hooft and M.J.G. Veltman, *One loop divergencies in the theory of gravitation*, *Ann. Inst. H. Poincare Phys. Theor. A* **20** (1974) 69.
- [136] M.H. Goroff and A. Sagnotti, *QUANTUM GRAVITY AT TWO LOOPS*, *Phys. Lett. B* **160** (1985) 81.
- [137] M.H. Goroff and A. Sagnotti, *The Ultraviolet Behavior of Einstein Gravity*, *Nucl. Phys. B* **266** (1986) 709.
- [138] S. Deser and P. van Nieuwenhuizen, *One Loop Divergences of Quantized Einstein-Maxwell Fields*, *Phys. Rev. D* **10** (1974) 401.
- [139] S. Deser and P. van Nieuwenhuizen, *Nonrenormalizability of the Quantized Dirac-Einstein System*, *Phys. Rev. D* **10** (1974) 411.
- [140] S. Deser, H.-S. Tsao and P. van Nieuwenhuizen, *One Loop Divergences of the Einstein Yang-Mills System*, *Phys. Rev. D* **10** (1974) 3337.
- [141] M.A. Shifman, A.I. Vainshtein and V.I. Zakharov, *QCD and Resonance Physics. Theoretical Foundations*, *Nucl. Phys. B* **147** (1979) 385.
- [142] I.I. Balitsky, V.M. Braun and A.V. Kolesnichenko,  $\Sigma^+ \rightarrow P\gamma$  *Decay in QCD. (In Russian)*, *Sov. J. Nucl. Phys.* **44** (1986) 1028.
- [143] Y.Y. Balitsky, V.M. Braun and A.V. Kolesnichenko, *The decay  $\Sigma^+ \rightarrow p \gamma$  in QCD: Bilocal corrections in a variable magnetic field and the photon wave functions*, *Sov. J. Nucl. Phys.* **48** (1988) 348.
- [144] I.I. Balitsky, V.M. Braun and A.V. Kolesnichenko, *QCD SUM RULES FOR THE DECAY  $\Sigma^+ \rightarrow P \gamma$ . (IN RUSSIAN)*, *Sov. J. Nucl. Phys.* **48** (1988) 546.
- [145] V.M. Braun and I. Filyanov, *QCD Sum Rules in Exclusive Kinematics and Pion Wave Function*, *Sov. J. Nucl. Phys.* **50** (1989) 511.

## Bibliography

- [146] I.I. Balitsky, V.M. Braun and A.V. Kolesnichenko, *Radiative Decay  $\Sigma^+ \rightarrow p \gamma$  in Quantum Chromodynamics*, *Nucl. Phys. B* **312** (1989) 509.
- [147] V.L. Chernyak and I.R. Zhitnitsky, *B meson exclusive decays into baryons*, *Nucl. Phys. B* **345** (1990) 137.
- [148] V.L. Chernyak and A.R. Zhitnitsky, *Asymptotic Behavior of Hadron Form-Factors in Quark Model. (In Russian)*, *JETP Lett.* **25** (1977) 510.
- [149] A.V. Efremov and A.V. Radyushkin, *Asymptotical Behavior of Pion Electromagnetic Form-Factor in QCD*, *Theor. Math. Phys.* **42** (1980) 97.
- [150] A.V. Efremov and A.V. Radyushkin, *Factorization and Asymptotical Behavior of Pion Form-Factor in QCD*, *Phys. Lett. B* **94** (1980) 245.
- [151] G.P. Lepage and S.J. Brodsky, *Exclusive Processes in Quantum Chromodynamics: Evolution Equations for Hadronic Wave Functions and the Form-Factors of Mesons*, *Phys. Lett. B* **87** (1979) 359.
- [152] V.L. Chernyak and A.R. Zhitnitsky, *Asymptotics of Hadronic Form-Factors in the Quantum Chromodynamics. (In Russian)*, *Sov. J. Nucl. Phys.* **31** (1980) 544.
- [153] G.P. Lepage and S.J. Brodsky, *Exclusive Processes in Perturbative Quantum Chromodynamics*, *Phys. Rev. D* **22** (1980) 2157.
- [154] S.J. Brodsky and G.P. Lepage, *Large Angle Two Photon Exclusive Channels in Quantum Chromodynamics*, *Phys. Rev. D* **24** (1981) 1808.
- [155] B.L. Ioffe, *Calculation of Baryon Masses in Quantum Chromodynamics*, *Nucl. Phys. B* **188** (1981) 317.
- [156] S. Weinberg, *The Quantum theory of fields. Vol. 1: Foundations*, Cambridge University Press (6, 2005).
- [157] M.J.G. Veltman, *Diagrammatica: The Path to Feynman rules*, vol. 4, Cambridge University Press (5, 2012).
- [158] J.F. Nieves and P.B. Pal, *Generalized Fierz identities*, *Am. J. Phys.* **72** (2004) 1100 [[hep-ph/0306087](#)].
- [159] C.C. Nishi, *Simple derivation of general Fierz-like identities*, *Am. J. Phys.* **73** (2005) 1160 [[hep-ph/0412245](#)].
- [160] B.L. Ioffe, *ON THE CHOICE OF QUARK CURRENTS IN THE QCD SUM RULES FOR BARYON MASSES*, *Z. Phys. C* **18** (1983) 67.
- [161] K.G. Wilson, *Nonlagrangian models of current algebra*, *Phys. Rev.* **179** (1969) 1499.
- [162] V.A. Novikov, M.A. Shifman, A.I. Vainshtein and V.I. Zakharov, *Wilson's Operator Expansion: Can It Fail?*, *Nucl. Phys. B* **249** (1985) 445.

- [163] M.A. Shifman, *Snapshots of hadrons or the story of how the vacuum medium determines the properties of the classical mesons which are produced, live and die in the QCD vacuum*, *Prog. Theor. Phys. Suppl.* **131** (1998) 1 [[hep-ph/9802214](#)].
- [164] V.A. Novikov, M.A. Shifman, A.I. Vainshtein and V.I. Zakharov, *Calculations in External Fields in Quantum Chromodynamics. Technical Review*, *Fortsch. Phys.* **32** (1984) 585.
- [165] L.J. Reinders, H. Rubinstein and S. Yazaki, *Hadron Properties from QCD Sum Rules*, *Phys. Rept.* **127** (1985) 1.
- [166] P. Gubler, *A Bayesian Analysis of QCD Sum Rules*, Springer Japan, 1 ed. (2013), 10.1007/978-4-431-54318-3.
- [167] V.M. Belyaev and B.L. Ioffe, *Determination of Baryon and Baryonic Resonance Masses from QCD Sum Rules. 1. Nonstrange Baryons*, *Sov. Phys. JETP* **56** (1982) 493.
- [168] B.L. Ioffe and A.V. Smilga, *Nucleon Magnetic Moments and Magnetic Properties of Vacuum in QCD*, *Nucl. Phys. B* **232** (1984) 109.
- [169] B.L. Ioffe, V.S. Fadin and L.N. Lipatov, *Quantum Chromodynamics: Perturbative and Nonperturbative Aspects*, Cambridge Monographs on Particle Physics, Nuclear Physics and Cosmology, Cambridge University Press (2010), 10.1017/CBO9780511711817.
- [170] E.C. Poggio, H.R. Quinn and S. Weinberg, *Smearing the Quark Model*, *Phys. Rev. D* **13** (1976) 1958.
- [171] M.A. Shifman, *Quark hadron duality*, in *8th International Symposium on Heavy Flavor Physics*, vol. 3, (Singapore), pp. 1447–1494, World Scientific, 7, 2000, DOI [[hep-ph/0009131](#)].
- [172] M. Pospelov and A. Ritz, *Theta induced electric dipole moment of the neutron via QCD sum rules*, *Phys. Rev. Lett.* **83** (1999) 2526 [[hep-ph/9904483](#)].
- [173] M. Pospelov and A. Ritz, *Theta vacua, QCD sum rules, and the neutron electric dipole moment*, *Nucl. Phys. B* **573** (2000) 177 [[hep-ph/9908508](#)].
- [174] I.I. Balitsky and A.V. Yung, *Proton and Neutron Magnetic Moments from QCD Sum Rules*, *Phys. Lett. B* **129** (1983) 328.
- [175] P. Colangelo and A. Khodjamirian, *QCD sum rules, a modern perspective*, [hep-ph/0010175](#).
- [176] B.L. Ioffe, V.S. Fadin and L.N. Lipatov, *Quantum chromodynamics: Perturbative and nonperturbative aspects*, Cambridge Univ. Press (2010), 10.1017/CBO9780511711817.
- [177] C.-T. Chan, E.M. Henley and T. Meissner, *Nucleon electric dipole moments from QCD sum rules*, [hep-ph/9905317](#).
- [178] PARTICLE DATA GROUP collaboration, *Review of Particle Physics*, *Phys. Rev. D* **98** (2018) 030001.

## Bibliography

- [179] Y. Chung, H.G. Dosch, M. Kremer and D. Schall, *Chiral Symmetry Breaking Condensates for Baryonic Sum Rules*, *Z. Phys. C* **25** (1984) 151.
- [180] D.B. Leinweber, *Nucleon properties from unconventional interpolating fields*, *Phys. Rev. D* **51** (1995) 6383 [[nucl-th/9406001](#)].
- [181] D.B. Leinweber, *QCD sum rules for skeptics*, *Annals Phys.* **254** (1997) 328 [[nucl-th/9510051](#)].
- [182] P. Gubler and D. Satow, *Recent Progress in QCD Condensate Evaluations and Sum Rules*, *Prog. Part. Nucl. Phys.* **106** (2019) 1 [[1812.00385](#)].
- [183] B.L. Ioffe and A.V. Smilga, *Proton and Neutron Magnetic Moments in QCD*, *JETP Lett.* **37** (1983) 298.
- [184] M. Aw, M.K. Banerjee and H. Forkel, *Direct instantons and nucleon magnetic moments*, *Phys. Lett. B* **454** (1999) 147 [[hep-ph/9902458](#)].
- [185] V.S. Fadin and R. Fiore, *Non-forward NLO BFKL kernel*, *Phys. Rev. D* **72** (2005) 014018 [[hep-ph/0502045](#)].
- [186] A.G. Oganesian, *Vacuum expectations of the high dimensional operator and their contribution in Bjorken and Ellis-Jaffe sum rules*, *Phys. Atom. Nucl.* **61** (1998) 1359 [[hep-ph/9704435](#)].
- [187] M.V. Polyakov and C. Weiss, *Estimates of higher dimensional vacuum condensates from the instanton vacuum*, *Phys. Rev. D* **57** (1998) 4471 [[hep-ph/9710534](#)].
- [188] E.V. Shuryak, *The Role of Instantons in Quantum Chromodynamics. 1. Physical Vacuum*, *Nucl. Phys. B* **203** (1982) 93.
- [189] D. Diakonov and V.Y. Petrov, *Instanton Based Vacuum from Feynman Variational Principle*, *Nucl. Phys. B* **245** (1984) 259.
- [190] D. Diakonov and V.Y. Petrov, *A Theory of Light Quarks in the Instanton Vacuum*, *Nucl. Phys. B* **272** (1986) 457.
- [191] T. Schäfer and E.V. Shuryak, *Instantons in QCD*, *Rev. Mod. Phys.* **70** (1998) 323 [[hep-ph/9610451](#)].
- [192] M.C. Chu, J.M. Grandy, S. Huang and J.W. Negele, *Evidence for the role of instantons in hadron structure from lattice QCD*, *Phys. Rev. D* **49** (1994) 6039 [[hep-lat/9312071](#)].
- [193] J.W. Negele, *Instantons, the QCD vacuum, and hadronic physics*, *Nucl. Phys. B Proc. Suppl.* **73** (1999) 92 [[hep-lat/9810053](#)].
- [194] T.A. DeGrand, *Short distance current correlators: Comparing lattice simulations to the instanton liquid*, *Phys. Rev. D* **64** (2001) 094508 [[hep-lat/0106001](#)].
- [195] P. Faccioli and T.A. DeGrand, *Evidence for instanton induced dynamics, from lattice QCD*, *Phys. Rev. Lett.* **91** (2003) 182001 [[hep-ph/0304219](#)].

- [196] P.O. Bowman, U.M. Heller, D.B. Leinweber, A.G. Williams and J.-b. Zhang, *Infrared and ultraviolet properties of the Landau gauge quark propagator*, *Nucl. Phys. B Proc. Suppl.* **128** (2004) 23 [[hep-lat/0403002](#)].
- [197] M. Cristoforetti, P. Faccioli, M.C. Traini and J.W. Negele, *Exploring the Chiral Regime of QCD in the Interacting Instanton Liquid Model*, *Phys. Rev. D* **75** (2007) 034008 [[hep-ph/0605256](#)].
- [198] V.M. Braun, *Light cone sum rules*, in *4th International Workshop on Progress in Heavy Quark Physics*, 9, 1997 [[hep-ph/9801222](#)].
- [199] V.M. Braun and I. Filyanov, *Conformal Invariance and Pion Wave Functions of Nonleading Twist*, *Sov. J. Nucl. Phys.* **52** (1990) 126.
- [200] P. Ball, *Theoretical update of pseudoscalar meson distribution amplitudes of higher twist: The Nonsinglet case*, *JHEP* **01** (1999) 010 [[hep-ph/9812375](#)].
- [201] C. Jarlskog and F.J. Yndurain, *Matter Instability in the SU(5) Unified Model of Strong, Weak and Electromagnetic Interactions*, *Nucl. Phys. B* **149** (1979) 29.
- [202] M. Machacek, *The Decay Modes of the Proton*, *Nucl. Phys. B* **159** (1979) 37.
- [203] J.T. Goldman and D.A. Ross, *How Accurately Can We Estimate the Proton Lifetime in an SU(5) Grand Unified Model?*, *Nucl. Phys. B* **171** (1980) 273.
- [204] M.B. Gavela, A. Le Yaouanc, L. Oliver, O. Pene and J.C. Raynal, *Calculation of Proton Decay in the Nonrelativistic Quark Model*, *Phys. Rev. D* **23** (1981) 1580.
- [205] P. Salati and J.C. Wallet, *Proton and Neutron Decay Rates in Conventional and Supersymmetric {GUTs}*, *Nucl. Phys. B* **209** (1982) 389.
- [206] A.M. Din, G. Girardi and P. Sorba, *A Bag Model Calculation of the Nucleon Lifetime in Grand Unified Theories*, *Phys. Lett. B* **91** (1980) 77.
- [207] J.F. Donoghue, *Proton Lifetime and Branching Ratios in SU(5)*, *Phys. Lett. B* **92** (1980) 99.
- [208] E. Golowich, *Two-body Decays of the Nucleon*, *Phys. Rev. D* **22** (1980) 1148.
- [209] J.F. Donoghue and E. Golowich, *PROTON DECAY VIA THREE QUARK FUSION*, *Phys. Rev. D* **26** (1982) 3092.
- [210] M. Wakano, *STATIC BAG MODEL PREDICTIONS OF THE PROTON LIFETIME AND BRANCHING RATIOS IN THE SU(5) GRAND UNIFIED THEORY*, *Prog. Theor. Phys.* **67** (1982) 909.
- [211] T. Okazaki and K. Fujii, *An Extended Application of the Bag Model: The Proton Decay*, *Phys. Rev. D* **27** (1983) 188.
- [212] V.S. Berezinsky, B.L. Ioffe and Y.I. Kogan, *The Calculation of Matrix Element for Proton Decay*, *Phys. Lett. B* **105** (1981) 33.

## Bibliography

- [213] M. Claudson, M.B. Wise and L.J. Hall, *Chiral Lagrangian for Deep Mine Physics*, *Nucl. Phys. B* **195** (1982) 297.
- [214] N. Isgur and M.B. Wise, *On the Consistency of Chiral Symmetry and the Quark Model in Proton Decay*, *Phys. Lett. B* **117** (1982) 179.
- [215] S. Chadha and M. Daniel, *Chiral Lagrangian Calculation of Nucleon Decay Modes Induced by  $d = 5$  Supersymmetric Operators*, *Nucl. Phys. B* **229** (1983) 105.
- [216] O. Kaymakçalan, C.-H. Lo and K.C. Wali, *Chiral Lagrangian for Proton Decay*, *Phys. Rev. D* **29** (1984) 1962.
- [217] Y. Aoki, C. Dawson, J. Noaki and A. Soni, *Proton decay matrix elements with domain-wall fermions*, *Phys. Rev. D* **75** (2007) 014507 [[hep-lat/0607002](#)].
- [218] M.B. Gavela, S.F. King, C.T. Sachrajda, G. Martinelli, M.L. Paciello and B. Taglienti, *A Lattice Computation of Proton Decay Amplitudes*, *Nucl. Phys. B* **312** (1989) 269.
- [219] JLQCD collaboration, *Nucleon decay matrix elements from lattice QCD*, *Phys. Rev. D* **62** (2000) 014506 [[hep-lat/9911026](#)].
- [220] CP-PACS, JLQCD collaboration, *Lattice QCD calculation of the proton decay matrix element in the continuum limit*, *Phys. Rev. D* **70** (2004) 111501 [[hep-lat/0402026](#)].
- [221] QCDSF collaboration, *Nucleon distribution amplitudes and proton decay matrix elements on the lattice*, *Phys. Rev. D* **79** (2009) 034504 [[0811.2712](#)].
- [222] Y. Aoki, E. Shintani and A. Soni, *Proton decay matrix elements on the lattice*, *Phys. Rev. D* **89** (2014) 014505 [[1304.7424](#)].
- [223] Y. Aoki, T. Izubuchi, E. Shintani and A. Soni, *Improved lattice computation of proton decay matrix elements*, *Phys. Rev. D* **96** (2017) 014506 [[1705.01338](#)].
- [224] J.-S. Yoo, Y. Aoki, T. Izubuchi and S. Syritsyn, *Proton decay matrix element on lattice at physical pion mass*, *PoS LATTICE2018* (2019) 187 [[1812.09326](#)].
- [225] M.B. Wise, R. Blankenbecler and L.F. Abbott, *Three-body Decays of the Proton*, *Phys. Rev. D* **23** (1981) 1591.
- [226] I. Balitsky and V.M. Braun, *Evolution Equations for QCD String Operators*, *Nucl. Phys. B* **311** (1989) 541.
- [227] V.M. Braun, A. Khodjamirian and M. Maul, *Pion form-factor in QCD at intermediate momentum transfers*, *Phys. Rev. D* **61** (2000) 073004 [[hep-ph/9907495](#)].
- [228] S.S. Agaev, V.M. Braun, N. Offen and F.A. Porkert, *Light Cone Sum Rules for the  $\pi^0$ - $\gamma^*$ - $\gamma$  Form Factor Revisited*, *Phys. Rev. D* **83** (2011) 054020 [[1012.4671](#)].
- [229] A. Khodjamirian, B. Melić, Y.-M. Wang and Y.-B. Wei, *The  $D^*D\pi$  and  $B^*B\pi$  couplings from light-cone sum rules*, [2011.11275](#).

- [230] P. Ball and R. Zwicky, *New results on  $B \rightarrow \pi, K, \eta$  decay formfactors from light-cone sum rules*, *Phys. Rev. D* **71** (2005) 014015 [[hep-ph/0406232](#)].
- [231] FLAVOUR LATTICE AVERAGING GROUP collaboration, *FLAG Review 2019: Flavour Lattice Averaging Group (FLAG)*, *Eur. Phys. J. C* **80** (2020) 113 [[1902.08191](#)].
- [232] M. Gell-Mann, R.J. Oakes and B. Renner, *Behavior of current divergences under  $SU(3) \times SU(3)$* , *Phys. Rev.* **175** (1968) 2195.
- [233] V.M. Braun, A. Lenz, N. Mahnke and E. Stein, *Light cone sum rules for the nucleon form-factors*, *Phys. Rev. D* **65** (2002) 074011 [[hep-ph/0112085](#)].
- [234] V. Braun, A. Lenz and M. Wittmann, *Nucleon Form Factors in QCD*, *Phys. Rev. D* **73** (2006) 094019 [[hep-ph/0604050](#)].
- [235] M.C. Chu, J.M. Grandy, S. Huang and J.W. Negele, *Correlation functions of hadron currents in the QCD vacuum calculated in lattice QCD*, *Phys. Rev. D* **48** (1993) 3340 [[hep-lat/9306002](#)].
- [236] D.B. Leinweber, *Testing QCD sum rule techniques on the lattice*, *Phys. Rev. D* **51** (1995) 6369 [[nucl-th/9405002](#)].
- [237] RQCD collaboration, *Light-cone distribution amplitudes of octet baryons from lattice QCD*, *Eur. Phys. J. A* **55** (2019) 116 [[1903.12590](#)].
- [238] K.G. Chetyrkin, J.H. Kühn and M. Steinhauser, *RunDec: A Mathematica package for running and decoupling of the strong coupling and quark masses*, *Comput. Phys. Commun.* **133** (2000) 43 [[hep-ph/0004189](#)].
- [239] F. Herren and M. Steinhauser, *Version 3 of RunDec and CRunDec*, *Comput. Phys. Commun.* **224** (2018) 333 [[1703.03751](#)].
- [240] J. Bordes, C.A. Dominguez, P. Moodley, J. Penarrocha and K. Schilcher, *Chiral corrections to the  $SU(2) \times SU(2)$  Gell-Mann-Oakes-Renner relation*, *JHEP* **05** (2010) 064 [[1003.3358](#)].
- [241] B.L. Ioffe, *Condensates in quantum chromodynamics*, *Phys. Atom. Nucl.* **66** (2003) 30 [[hep-ph/0207191](#)].
- [242] T. Nihei and J. Arafune, *The Two loop long range effect on the proton decay effective Lagrangian*, *Prog. Theor. Phys.* **93** (1995) 665 [[hep-ph/9412325](#)].
- [243] P. Ball, V.M. Braun and A. Lenz, *Higher-twist distribution amplitudes of the K meson in QCD*, *JHEP* **05** (2006) 004 [[hep-ph/0603063](#)].
- [244] B. Pire and L. Szymanowski, *QCD analysis of  $\bar{p} N \rightarrow \gamma^* \pi$  in the scaling limit*, *Phys. Lett. B* **622** (2005) 83 [[hep-ph/0504255](#)].
- [245] B. Pire, K. Semenov-Tian-Shansky and L. Szymanowski, *Transition distribution amplitudes and hard exclusive reactions with baryon number transfer*, [2103.01079](#).

## Bibliography

- [246] T. Plehn, D.L. Rainwater and D. Zeppenfeld, *Determining the Structure of Higgs Couplings at the LHC*, *Phys. Rev. Lett.* **88** (2002) 051801 [[hep-ph/0105325](#)].
- [247] G. Klamke and D. Zeppenfeld, *Higgs plus two jet production via gluon fusion as a signal at the CERN LHC*, *JHEP* **04** (2007) 052 [[hep-ph/0703202](#)].
- [248] ATLAS collaboration, *Constraints on non-Standard Model Higgs boson interactions in an effective Lagrangian using differential cross sections measured in the  $H \rightarrow \gamma\gamma$  decay channel at  $\sqrt{s} = 8\text{ TeV}$  with the ATLAS detector*, *Phys. Lett. B* **753** (2016) 69 [[1508.02507](#)].
- [249] F. Ferreira, B. Fuks, V. Sanz and D. Sengupta, *Probing CP-violating Higgs and gauge-boson couplings in the Standard Model effective field theory*, *Eur. Phys. J. C* **77** (2017) 675 [[1612.01808](#)].
- [250] ATLAS collaboration, *Measurements of Higgs boson properties in the diphoton decay channel with  $36\text{ fb}^{-1}$  of  $pp$  collision data at  $\sqrt{s} = 13\text{ TeV}$  with the ATLAS detector*, *Phys. Rev. D* **98** (2018) 052005 [[1802.04146](#)].
- [251] F.U. Bernlochner, C. Englert, C. Hays, K. Lohwasser, H. Mildner, A. Pilkington et al., *Angles on CP-violation in Higgs boson interactions*, *Phys. Lett. B* **790** (2019) 372 [[1808.06577](#)].
- [252] R. Barbieri, A. Pomarol, R. Rattazzi and A. Strumia, *Electroweak symmetry breaking after LEP-1 and LEP-2*, *Nucl. Phys. B* **703** (2004) 127 [[hep-ph/0405040](#)].
- [253] B. Gripaios, A. Pomarol, F. Riva and J. Serra, *Beyond the Minimal Composite Higgs Model*, *JHEP* **04** (2009) 070 [[0902.1483](#)].
- [254] J.R. Espinosa, B. Gripaios, T. Konstandin and F. Riva, *Electroweak Baryogenesis in Non-minimal Composite Higgs Models*, *JCAP* **01** (2012) 012 [[1110.2876](#)].
- [255] G. D'Ambrosio, G.F. Giudice, G. Isidori and A. Strumia, *Minimal flavor violation: An Effective field theory approach*, *Nucl. Phys. B* **645** (2002) 155 [[hep-ph/0207036](#)].
- [256] CMS collaboration, *Observation of  $t\bar{t}H$  production*, *Phys. Rev. Lett.* **120** (2018) 231801 [[1804.02610](#)].
- [257] ATLAS collaboration, *Observation of Higgs boson production in association with a top quark pair at the LHC with the ATLAS detector*, *Phys. Lett. B* **784** (2018) 173 [[1806.00425](#)].
- [258] ATLAS collaboration, *Observation of  $H \rightarrow b\bar{b}$  decays and  $VH$  production with the ATLAS detector*, *Phys. Lett. B* **786** (2018) 59 [[1808.08238](#)].
- [259] CMS collaboration, *Observation of Higgs boson decay to bottom quarks*, *Phys. Rev. Lett.* **121** (2018) 121801 [[1808.08242](#)].
- [260] ATLAS collaboration, *Combined measurements of Higgs boson production and decay using up to  $80\text{ fb}^{-1}$  of proton–proton collision data at  $\sqrt{s} = 13\text{ TeV}$  collected with the ATLAS experiment*, Tech. Rep. ATLAS-CONF-2019-005, CERN, Geneva (Mar, 2019).

- [261] CMS collaboration, *Combined measurements of Higgs boson couplings in proton–proton collisions at  $\sqrt{s} = 13$  TeV*, *Eur. Phys. J. C* **79** (2019) 421 [1809.10733].
- [262] G.T. Bodwin, F. Petriello, S. Stoynev and M. Velasco, *Higgs boson decays to quarkonia and the  $H\bar{c}c$  coupling*, *Phys. Rev. D* **88** (2013) 053003 [1306.5770].
- [263] C. Delaunay, T. Golling, G. Perez and Y. Soreq, *Enhanced Higgs boson coupling to charm pairs*, *Phys. Rev. D* **89** (2014) 033014 [1310.7029].
- [264] A.L. Kagan, G. Perez, F. Petriello, Y. Soreq, S. Stoynev and J. Zupan, *Exclusive Window onto Higgs Yukawa Couplings*, *Phys. Rev. Lett.* **114** (2015) 101802 [1406.1722].
- [265] ATLAS collaboration, *Search for Higgs and Z Boson Decays to  $J/\psi\gamma$  and  $\Upsilon(nS)\gamma$  with the ATLAS Detector*, *Phys. Rev. Lett.* **114** (2015) 121801 [1501.03276].
- [266] G. Perez, Y. Soreq, E. Stamou and K. Tobioka, *Constraining the charm Yukawa and Higgs-quark coupling universality*, *Phys. Rev. D* **92** (2015) 033016 [1503.00290].
- [267] M. König and M. Neubert, *Exclusive Radiative Higgs Decays as Probes of Light-Quark Yukawa Couplings*, *JHEP* **08** (2015) 012 [1505.03870].
- [268] G. Perez, Y. Soreq, E. Stamou and K. Tobioka, *Prospects for measuring the Higgs boson coupling to light quarks*, *Phys. Rev. D* **93** (2016) 013001 [1505.06689].
- [269] I. Brivio, F. Goertz and G. Isidori, *Probing the Charm Quark Yukawa Coupling in Higgs+Charm Production*, *Phys. Rev. Lett.* **115** (2015) 211801 [1507.02916].
- [270] F. Bishara, U. Haisch, P.F. Monni and E. Re, *Constraining Light-Quark Yukawa Couplings from Higgs Distributions*, *Phys. Rev. Lett.* **118** (2017) 121801 [1606.09253].
- [271] Y. Soreq, H.X. Zhu and J. Zupan, *Light quark Yukawa couplings from Higgs kinematics*, *JHEP* **12** (2016) 045 [1606.09621].
- [272] F. Yu, *Phenomenology of Enhanced Light Quark Yukawa Couplings and the  $W^{\pm}h$  Charge Asymmetry*, *JHEP* **02** (2017) 083 [1609.06592].
- [273] T. Han and X. Wang, *Radiative Decays of the Higgs Boson to a Pair of Fermions*, *JHEP* **10** (2017) 036 [1704.00790].
- [274] J. Cohen, S. Bar-Shalom, G. Eilam and A. Soni, *Light-quarks Yukawa couplings and new physics in exclusive high- $p_T$  Higgs boson+jet and Higgs boson +  $b$ -jet events*, *Phys. Rev. D* **97** (2018) 055014 [1705.09295].
- [275] ATLAS collaboration, *Search for the Decay of the Higgs Boson to Charm Quarks with the ATLAS Experiment*, *Phys. Rev. Lett.* **120** (2018) 211802 [1802.04329].
- [276] CMS collaboration, *Sensitivity projections for Higgs boson properties measurements at the HL-LHC*, Tech. Rep. CMS-PAS-FTR-18-011, CERN, Geneva (2018).
- [277] CMS collaboration, *Measurement and interpretation of differential cross sections for Higgs boson production at  $\sqrt{s} = 13$  TeV*, *Phys. Lett. B* **792** (2019) 369 [1812.06504].

## Bibliography

- [278] T. Han, B. Nachman and X. Wang, *Charm-quark Yukawa Coupling in  $h \rightarrow c\bar{c}\gamma$  at LHC*, *Phys. Lett. B* **793** (2019) 90 [1812.06992].
- [279] ATLAS collaboration, *Measurements and interpretations of Higgs-boson fiducial cross sections in the diphoton decay channel using  $139\text{ fb}^{-1}$  of  $pp$  collision data at  $\sqrt{s} = 13\text{ TeV}$  with the ATLAS detector*, Tech. Rep. ATLAS-CONF-2019-029, CERN, Geneva (Jul, 2019).
- [280] CMS collaboration, *Search for the standard model Higgs boson decaying to charm quarks*, Tech. Rep. CMS-PAS-HIG-18-031, CERN, Geneva (2019).
- [281] CMS collaboration, *Search for Higgs and Z boson decays to  $J/\psi$  or Y pairs in the four-muon final state in proton-proton collisions at  $s=13\text{TeV}$* , *Phys. Lett. B* **797** (2019) 134811 [1905.10408].
- [282] L. Alasfar, R. Corral Lopez and R. Gröber, *Probing Higgs couplings to light quarks via Higgs pair production*, *JHEP* **11** (2019) 088 [1909.05279].
- [283] D. Ghosh, R.S. Gupta and G. Perez, *Is the Higgs Mechanism of Fermion Mass Generation a Fact? A Yukawa-less First-Two-Generation Model*, *Phys. Lett. B* **755** (2016) 504 [1508.01501].
- [284] V.A. Smirnov, *Applied asymptotic expansions in momenta and masses*, *Springer Tracts Mod. Phys.* **177** (2002) 1.
- [285] R. Alonso, E.E. Jenkins, A.V. Manohar and M. Trott, *Renormalization Group Evolution of the Standard Model Dimension Six Operators III: Gauge Coupling Dependence and Phenomenology*, *JHEP* **04** (2014) 159 [1312.2014].
- [286] L.F. Abbott, *The Background Field Method Beyond One Loop*, *Nucl. Phys. B* **185** (1981) 189.
- [287] L.F. Abbott, *Introduction to the Background Field Method*, *Acta Phys. Polon. B* **13** (1982) 33.
- [288] W. Bizoń, U. Haisch and L. Rottoli, *Constraints on the quartic Higgs self-coupling from double-Higgs production at future hadron colliders*, *JHEP* **10** (2019) 267 [1810.04665].
- [289] M. Gorbahn and U. Haisch, *Two-loop amplitudes for Higgs plus jet production involving a modified trilinear Higgs coupling*, *JHEP* **04** (2019) 062 [1902.05480].
- [290] H.H. Patel, *Package-X: A Mathematica package for the analytic calculation of one-loop integrals*, *Comput. Phys. Commun.* **197** (2015) 276 [1503.01469].
- [291] G. Degrandi, E. Franco, S. Marchetti and L. Silvestrini, *QCD corrections to the electric dipole moment of the neutron in the MSSM*, *JHEP* **11** (2005) 044 [hep-ph/0510137].
- [292] J. de Vries, G. Falcioni, F. Herzog and B. Ruijl, *Two- and three-loop anomalous dimensions of Weinberg’s dimension-six CP-odd gluonic operator*, *Phys. Rev. D* **102** (2020) 016010 [1907.04923].

- [293] M. Misiak and M. Munz, *Two loop mixing of dimension five flavor changing operators*, *Phys. Lett. B* **344** (1995) 308 [hep-ph/9409454].
- [294] J.A. Gracey, *Three loop  $\overline{MS}$  tensor current anomalous dimension in QCD*, *Phys. Lett. B* **488** (2000) 175 [hep-ph/0007171].
- [295] M. Gorbahn, U. Haisch and M. Misiak, *Three-loop mixing of dipole operators*, *Phys. Rev. Lett.* **95** (2005) 102004 [hep-ph/0504194].
- [296] K. Abe et al., *Letter of Intent: The Hyper-Kamiokande Experiment — Detector Design and Physics Potential —*, 1109.3262.
- [297] JUNO collaboration, *Neutrino Physics with JUNO*, *J. Phys. G* **43** (2016) 030401 [1507.05613].
- [298] DUNE collaboration, *Long-Baseline Neutrino Facility (LBNF) and Deep Underground Neutrino Experiment (DUNE): Conceptual Design Report, Volume 2: The Physics Program for DUNE at LBNF*, 1512.06148.
- [299] Y. Nambu and D. Lurie, *Chirality conservation and soft pion production*, *Phys. Rev.* **125** (1962) 1429.
- [300] S.L. Adler and R.F. Dashen, *Current algebras and applications to particle physics*, Benjamin, New York et al. (1968).
- [301] H. van Dam and M.J.G. Veltman, *Massive and massless Yang-Mills and gravitational fields*, *Nucl. Phys. B* **22** (1970) 397.
- [302] J. Learned, F. Reines and A. Soni, *Limits on Nonconservation of Baryon Number*, *Phys. Rev. Lett.* **43** (1979) 907.
- [303] SUPER-KAMIOKANDE collaboration, *Search for Trilepton Nucleon Decay via  $p \rightarrow e^+ \nu \nu$  and  $p \rightarrow \mu^+ \nu \nu$  in the Super-Kamiokande Experiment*, *Phys. Rev. Lett.* **113** (2014) 101801 [1409.1947].
- [304] V. Fock, *Proper time in classical and quantum mechanics*, *Phys. Z. Sowjetunion* **12** (1937) 404.
- [305] J.S. Schwinger, *On gauge invariance and vacuum polarization*, *Phys. Rev.* **82** (1951) 664.
- [306] A. Khodjamirian, T. Mannel, N. Offen and Y.M. Wang,  *$B \rightarrow \pi \ell \nu_l$  Width and  $|V_{ub}|$  from QCD Light-Cone Sum Rules*, *Phys. Rev. D* **83** (2011) 094031 [1103.2655].
- [307] JEFFERSON LAB collaboration, *Charged pion form-factor between  $Q^{*2} = 0.60\text{-GeV}^{*2}$  and  $2.45\text{-GeV}^{*2}$ . II. Determination of, and results for, the pion form-factor*, *Phys. Rev. C* **78** (2008) 045203 [0809.3052].



# Acknowledgements

Special thanks to Andrea, for all her support. Many thanks also to my advisor Uli Haisch for his council and for the great and interesting time at the Max Planck institute. I would also like to thank Andi Weiler and Frank Steffen for their advice as well as all my former and current office mates, all my colleagues at the institute and at TUM, my friends and family of course, and everybody else that I forgot to mention for their great support during my PhD.